Mechanosignaling through Caveolae : A New Role for the Control of JAK-STAT Signaling

Nicolas Tardif

NNT : 2018SACLS337

Mechanosignaling through caveolae : A new role for the control of JAK-STAT signaling

Thèse de doctorat de l'Université Paris-Saclay
préparée à l'université Paris Sud

École doctorale n°568 signalisations et réseaux intégratifs en biologie (Biosigne), aspect moléculaire et cellulaire de la biologie

Thèse présentée et soutenue à Paris, le 19 octobre 2018, par

Nicolas Tardif

Composition du Jury :

Marc Le Maire Professeur emerite, institut de biologie intégrative de la cellule	Président
Corinne Albiges-Rizo Directeur de recherche, institut pour l'avancée des biosciences	Rapporteur
Benjamin Nichols Directeur de recherche, MRC-LMB Cambridge	Rapporteur
Gideon Schreiber Professeur, Weizmann institute	Examinateur
Christophe Lamaze Directeur de recherche, institut Curie	Directeur de thèse
Cédric Blouin Postdoctorant, institut Curie	Invité

«Heureux qui, comme Ulysse, a fait un beau voyage»

Joachim Du Bellay

«Ici on taille pas des bambous»

Christophe Lamaze

Acknowledgements

As Ulysse, I am delighted with my amazing journey, which was as challenging as thrilling. This adventure wouldn't have been possible without the support of my supervisor and the whole team, in which I always felt very proud to be part of. Hence, in first place I would like thank my thesis supervisor, Christophe a.k.a. "the boss" for putting all his trust in me with this project. I wish all PhD students could have a supervisor as supportive as you, and I'm glad we made it possible. Then I would like to thank Cedric, the man in the shadow, you are a wise man, always of good advice and very supportive. I would like to acknowledge our collaborators from IINS Bordeaux: Grégory Giannone, Olivier Rossier and R.K. Finally, I thank Ludger Johannes for his precious feedback during joined meeting.

I would like to thank my thesis jury members, Corinne Albiges-Rizo and Ben Nichols for the time they dedicated to review my manuscript and their pertinent feedback. I couldn't be more proud having reviews by such scientists. I would like to thank Gideon Schreiber for nicely accepting my invitation and last but not least, Marc Le Maire who drove me through my university course until the wonderful world of plasma membrane and cell signaling and will now preside my jury.

I would like to thank also the team members that contributed to the everyday pleasure I had to sit at my desk/bench such as Christophe, you really contributed to strengthen my self-confidence and participated to the pleasure I had to work every single day for this project. You are a man of extremes, endearing with whom we like to share. Then the second leader of this team (and babysitter), most likely carrying the Lamaze lab legacy on his shoulders: Cédric (papy mougeot) for all his benevolence for "les grumeaux" and other "babies" of the team. Thank you for inculcating me the taste of excessively overpriced watches and other techs, which I could never afford as a PhD student. You are such a great mentor. Last but not least, thank you for allowing me to stay in the office whenever some of my worst jokes come up. I would like to thank my sidekick, wing-woman, bench-neighbor and desk-neighbor: Melissa. Thank you for your support, I'm so grateful I could share this adventure with you. Counter-thank you for deliberately ignoring that singing (or

trying) catchy songs was prohibited in the office/lab (this law should be extended to earth). Thank you for always laughing at my subtle jokes in your deep interior while harboring a poker face just to act like they were not funny although they were… (Christine would agree… and Cédric (on Fridays)). Hence, thank you Christine for sharing my humor. Thank you for your patience and your wise lab advice and mostly for all the fun we shared; *vinos vomitas*. I would like to have a special "tachacor" for Massi. Without you I wouldn't speak fluent Persian lv2. Thank you for being that supportive and for your life and lab advice. I enjoyed having highly intellectual conversations with you, now I'm pretty sure everybody knows DNA is double strand. During these four years both the Jedi and the padawan fought the general Koss. I thank Estelle for being such a good badminton partner and for all the fun she puts in the lab. Carlos our spanish sound-box – desk vibrator, thank you for your support. I thank Satish for your gaming advice and above all for your chicken. Alison for actively contributing to the nice atmosphere we have in the office and for teaching me rude Italian words. I apologize to Ewan for winning the word cup. I guess it did not come home… Xièxiè Changting. I acknowledge Manon for her patience (a key asset to work in this office). I would like to thank Christian and all other members of the Johannes team for their wise advice and feedback on this project. To finish I thank all the past members who actively contributed to my lab life: Steph, Natacha, Henri, Weiwei and Daniela.

Finally I warmly acknowledge the people who constitute the pillars of my life: my closest friends, Camille, Jérémie (la bande de Bazoches) and the team rocket Francky, Flo, Michou and Baba for their unswerving support and loyalty. I thank my whole family especially Mariette and Bernard for transmitting me the great interest I have for sciences since my early childhood. I am also grateful to Yann and Evon for their precious help starting my life in science. Behind every man success there is woman. The story does not tell whether behind small success there is a short woman. Anyway, thank you Anna for sharing my everyday life and making it a bit sweeter everyday. Thank you for your unbreakable support and for standing by my side these last months regardless how grumpy I could be. To finish, I dedicate this manuscript to my parents for their support and for believing in me since ever. They play a key role in the reach of my life goals.

Table of Contents

Abbreviations

aa: amino acid

AMFR: Autocrine Motility Factor Receptor

Bcl-xL: B cell Lymphoma-extra Large

bFGF: basic Fibroblast Growth Factor

BSCL: Berardinelli-Seip-Congenital Lipodistrophy

c-Myc: cellular Myelocytosis

Ca^{2+}: Calcium

CAF: Cancer Associated Fibroblast

Cas: Crk associated substrate

Cav1: Caveolin-1

Cav2: Caveolin-2

Cav3: Caveolin-3

CCL2: Chemokine (C-C) Ligand 2

CD: Circular Dichroism

cGAS: cyclic GMP-AMP Synthase

CKα: Casein Kinase α

CLIC: CLathrin Independent Carrier

$cPLA_2$: cytosolic PhosphoLipase A2

CRAC: Cholesterol Recognition/interaction Amino acid Consensus

CREB: cAMP Responsive Element Binding

CSD: Caveolin Scaffolding Domain

CTxB: Cholera Toxin subunit B

DPC: Dodecyl-PhosphatidylCholine

ECD: ExtraCellular Domain

ECM: ExtraCellular Matrix

EGFR: Epidermal Growth Factor Receptor

EMT: Epithelial to Mesenchymal Transition

eNOS: endothelial Nitric Oxide Synthase

ER: Endoplasmic Reticulum

ER-α: Estrogen Receptor α

ERK: Extracellular signal-Regulated protein Kinase

EV: Extracellular Vesicle

FA: Focal Adhesion

FAK: Focal Adhesion associate Kinase

FERM: Four point one Ezrin, Radixin, Moesin

FNIII: Fibronectin III

G3BP2: Ras GTPase-activating protein-binding 2

GAP: GTPase Activating Protein

GAS: IFN Gamma Activated Sequence

GEEC: GPI-AP-enriched Early Endosomal Compartment

GSL: GlycoSphingoLipid

hCR: helical Cytokine Receptor

HER2: Human Epidermal growth factor Receptor 2

HO: Heme Oxygenase

IFN: Interferon

IFNAR: InterFeroN Alpha Receptor

IFNGR: InterFeroN Gamma Receptor

IL6: InterLeukin 6

IRF2: IFN-Regulatory Factor 2

IRF9: IFN-Regulatory Factor 9

IRS-1: Insulin Response Substrate-1

ISG: IFN-Stimulated Gene

ISRE: IFN-Sensitive Response Element

JH: JAK Homology

KIR: Kinase Inhibitory Region

Klf-8: Kruppel-like factor 8

LATS: LArge Tumor Suppressor

LDL: Low-Density Lipoprotein

LINC: Linker of Nucleoskeleton and Cytoskeleton

LOX: 5-LipOXygenase

MAPK: Mitogen Activated Protein Kinase

MDR: MultiDrug Resistance

MEF2: Myocyte Enhancer Factor 2

MG53: MitsuGumin 53

MSC: Mechano-Sensitive Channel

MsC: Mensenchymal stem Cells

MT1-MMP: Membrane Type 1 Matrix MetalloProteinase

MURC: Muscie-Related Coiled coil protein

MVB: Multi Vesicular Bodies

NMR: Nuclear Magnetic Resonance

NO: Nitric Oxide

P2X7: P2X purinoreceptor 7

PDK2: Protein kinase D2

PEST: Proline glutamic acid Serine Threonine

PI(3)K: PhosphoInositide-3 Kinase

PIAS: Protein Inhibitor of Activated STAT

PiP_2: Phosphatidylinositol (4,5) bisPhosphate

PKCα: Protein Kinase C α

PKCδ: Protein Kinase C δ

POPC: PhOsPhatidylCholine

PRKCDB: PRotein Kinase C Delta-Binding protein

Ptdser: Phosphatidylserine

PTEN: Phosphatase and TENsin homologue

PTP1B: Protein Tyrosine Phosphatase 1B

PTRF: Polymerase 1 and Transcript Release Factor

Rap1: Ras-related protein 1

ROCK: Rho associate protein Kinase

SDPR: Serum Deprivation Protein Response

Ser80: Serine 80

SFK: Src Family Kinase

SHP1: Src homology region 2 domain-containing phosphatase 1

SHP2: Src homology region 2 domain-containing phosphatase 2

SOCS: Suppressor Of Cyrokine Signaling

SOX2: Sex determining region on Y box 2

SRBC: SDPR-Related gene product that Binds to C kinase

Src: Sarcoma protein kinase

STAT: Signal Transducer and Activator of Transcription

STING: STimulator of INterferon Genes

SV40: Simian Virus 40

TAZ: TAfaZzin

TEAD: TEA Domain family member

TGFBR1: Transforming Growth Factor β Receptor type 1

TMD: TransMembrane Domain

TRIM: TRI-partite Motif

TRP: Transient Receptor Potential channel

TWIST1: Twist related protein 1

Tyr14: Tyrosine 14

USP18: Ubiquitin-Specific Peptidase 18

VIP21: Vesicular Integral-membrane Protein of 21 kDa

YAP: Yes Associated Protein

β-Trcp2: β transducing repeats-containing protein 2

List of figures

Thesis summary

Caveolae are small cup-shaped plasma membrane invaginations. These multifunctional organelles play a key role in cell mechanoprotection and cell signaling. Indeed our laboratory reported that caveolae have the ability to flatten out upon membrane tension increase, protecting cells from mechanical strains (Sinha et al., 2011). Since caveolae play a key role in cell signaling we hypothesized that the mechano-dependent cycle of caveolae disassembly/reassembly may constitute a mechanical switch for signaling pathways (Nassoy and Lamaze, 2012). In this project, we elucidated the molecular mechanism underlying the control of JAK-STAT signaling by caveolae mechanics. The fate of caveolar components upon caveolae disassembly remains elusive. We showed that caveolin-1 (Cav1), the essential structural component of caveolae, is released and become highly mobile at the plasma membrane under mechanical stress. Considering that caveolae are important signaling hubs at the plasma membrane, we addressed the effects of the mechanical release of Cav1 on cell signaling. Using high throughput screening, we identified the JAK-STAT signaling pathway as a candidate. To further dissect the molecular mechanism underlying the control of JAK-STAT signaling by caveolae mechanics, we addressed the role of Cav1 in the control of JAK-STAT signaling stimulated by IFN-α. We found that Cav1 was a specific negative regulator of the JAK1 dependent STAT3 phosphorylation. Furthermore, the level of Cav1 interaction with JAK1 depended on mechanical stress. We could show that Cav1-JAK1 interaction was mediated by the Caveolin Scaffolding domain (CSD), abolishing JAK1 kinase activity, hence, interfering with STAT3 activation upon IFN-α stimulation. Interestingly, STAT1 activation by IFN-α was not affected by caveolae mechanics. Altogether our results show that caveolae are mechano-signaling organelles that disassemble under mechanical stress, releasing non-caveolar Cav1, which binds to the JAK1 tyrosine kinase and inhibits its catalytic activity, preventing thereby JAK-STAT signal transduction.

Résumé de la thèse

Les cavéoles sont des invaginations en forme de coupelle à la membrane plasmique. Ces organelles multifonctionnelles jouent entre autres, un rôle clé dans la mécanoprotection et la signalisation cellulaire. En effet, notre laboratoire a démontré que les cavéoles ont la faculté de s'aplanir en réponse à l'augmentation de la tension membranaire, afin de protéger la cellule des contraintes mécaniques (Sinha et al., 2011). Les cavéoles jouant un rôle clé dans la signalisation cellulaire, nous avions émis l'hypothèse que le cycle mécano-dépendent de désassemblage/réassemblage des cavéoles constitue un interrupteur mécanique de certaines voies de signalisation. Ce projet consiste à élucider le mécanisme moléculaire responsable du contrôle de la voie de signalisation JAK-STAT par la mécanique des cavéoles. Le devenir des constituants cavéolaires lors du désassemblage des cavéoles, reste à ce jour inconnu. Dans ces travaux, nous avons pu démontré que la cavéoline-1 (Cav1), un constituant essentiel des cavéoles, est libérée et devient hautement mobile au niveau de la membrane plasmique. Considérant les propriétés de signalisation de Cav1, nous avons testé l'effet du désassemblage des cavéoles sur la signalisation cellulaire. En effectuant un criblage à haut débit, nous avons identifié la voie de signalisation JAK-STAT stimulée par l'IFN-α comme voie modèle pour cette étude. En effet, la transduction du signal JAK-STAT induit par l'IFN-α est modulée par la mécanique des cavéoles. Afin de disséquer le mécanisme moléculaire responsable du control de la signalisation JAK-STAT par la mécanique des cavéoles, nous avons déterminé le rôle de Cav1 dans le contrôle de la signalisation JAK-STAT stimulée par l'IFN-α. Nous avons observé que Cav1 est un régulateur négatif de la phosphorylation de STAT3 dépendante de la kinase JAK1. De plus, nous avons démontré que Cav1 interagit avec JAK1 en fonction de la tension membranaire. Nous avons également démontré que cette interaction Cav1-JAK1 fait intervenir le « scaffolding domain » de Cav1 (CSD), et que celui-ci est responsable de l'abolition de l'activité kinase de JAK1. Par conséquent, l'interaction de Cav1 avec JAK1 empêche l'activation de STAT3 par la kinase JAK1. De manière surprenante, STAT1 échappe à cette régulation. En effet, l'activation de STAT1 par l'IFN-α n'est pas affectée par la mécanique des cavéoles. Ces résultats démontrent que les cavéoles sont des organelles de mécanosignalisation, qui, lors d'un stress mécanique,

libèrent de la Cav1 non cavéolaire capable d'inactiver la kinase JAK1, empêchant ainsi, la transduction du signal JAK-STAT induite par une stimulation à l'IFN-α.

- INTRODUCTION -

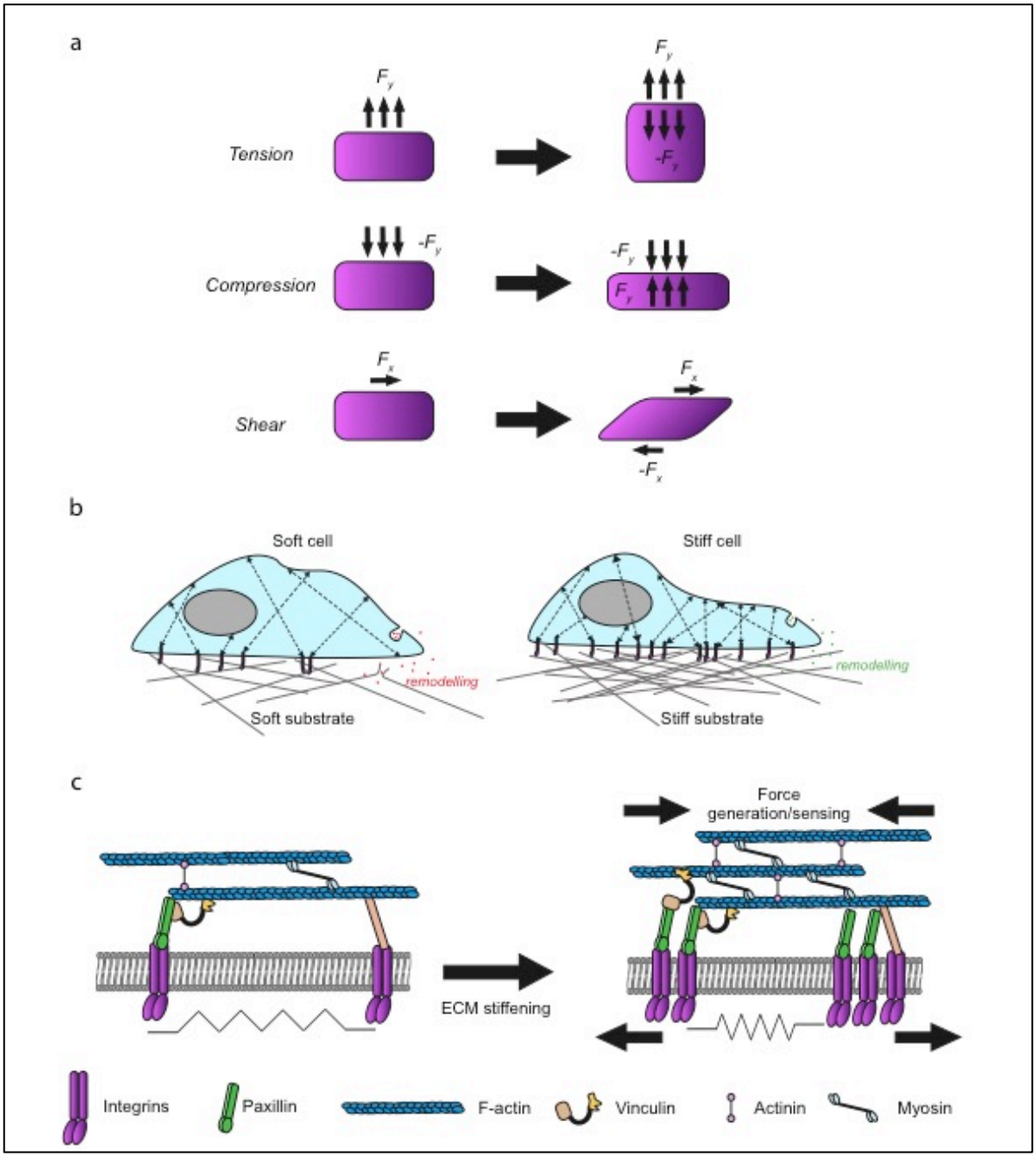

Figure 1. Mechanical forces and mechanoreciprocity

(a) Tension stress is applied perpendicular to the cell and leads to expansion. Compression stress is applied perpendicular to the cell and leads to compaction. Shear stress is applied parallel to the surface of the cell (adapted from Butcher et al., 2009). **(b)** The cell senses soft matrix and deforms the ECM by contracting. The cell has only few focal adhesions (purple sticks) and actin fibers (black arrows). It can also loosen the matrix by secreting metalloproteinases that digest the ECM (red dots) (left). The same cell on stiff matrix that cannot be deformed, the number of focal adhesions increases. The secretion of crosslinking factors (green dots) can mediate ECM stiffening. Substrate stiffening results in more and thicker actin stress fibers (black arrows) leadind to cell spreading and stiffening (right). **(c)** The basic machinery that senses and responds to ECM-generated mechanical signal. The cell surveys its mechanical environment with periodic contractions of stress fibers, which are attached to integrins that pull against matrix. Immature focal adhesions cannot sense matrix stiffness or exert strong mechanical forces on the ECM (left). While mature focal adhesions recruits myosin that allows force generation in response to matrix stiffening and recruits vinculin and actinin that increase F-actin number and crosslink the filaments to enlarge and strengthen focal adhesions and generates more contraction force (right) (based on Janmey et al., 2011).

Introduction

1 Cell mechanics and mechanotransduction

1.1 Cell and tissue mechanics

Of course, as every element of our universe, cells are subjected to the laws of physics and the renewal of the study of mechanics applied to the cell with the emergence of a mechanobiology field has already changed our understanding of most of fundamental biological processes.

1.1.1 Force generation (may the force be with you)

Cells are continuously subjected to mechanical forces including tensile force, compression, shear stress or hydrostatic pressure. Cells accommodate them by modifying their behavior and remodeling their microenvironment (Fig. 1). The interplay between cells and their microenvironment contribute through the resulting mechanical strains to fundamental biological processes but also to the development of pathologies (Egeblad et al., 2010; Kai et al., 2016). Tissues are composed of multiple constituents, among those; one can find different cell types and the extra cellular matrix (ECM). Each of these components can be characterized by several mechanical properties such as elasticity, viscosity, plasticity and stiffness (Janmey and Miller, 2011). All these physical properties govern how a tissue senses, transmits and responds to mechanical cues. For example, ECM stiffness can modulate essential biological processes at the level of individual cell such as differentiation, motility and morphology (Weaver et al., 1997; Engler et al., 2006; Vogel and Sheetz, 2009). Pelman and Wang, who used collagen-coated beads embedded in substrate with different stiffness, demonstrated that increasing substrate stiffness leads to the modulation of the size and dynamics of focal adhesion and therefore cell locomotion (Pelham and Wang, 1998). On the other hand, cells can generate mechanical strains

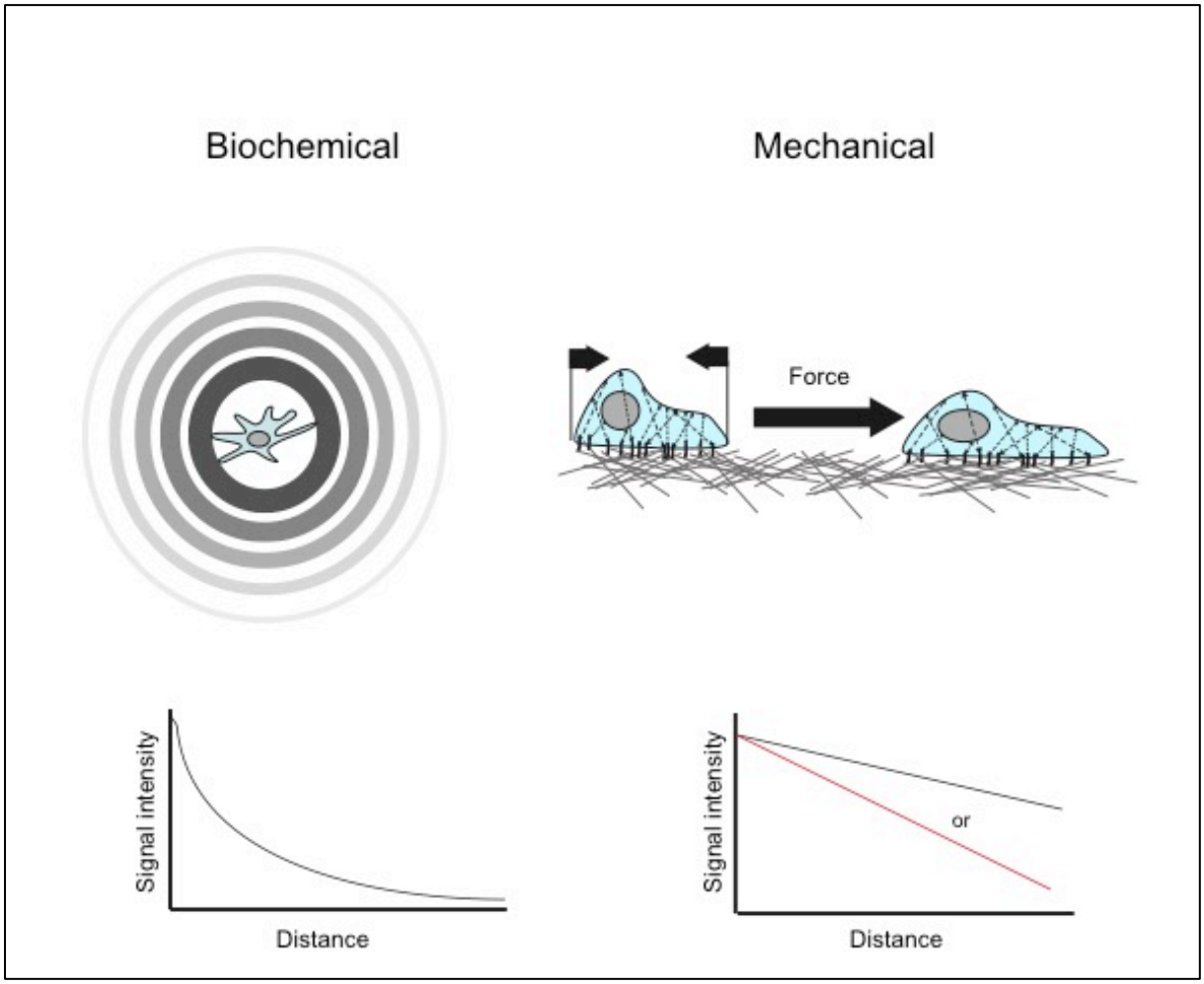

Figure 2. Biochemical versus mechanical signal

Biochemical signal diffuses and form a gradient from a point of source and can be re released into the circulation (upper left). The strength of the signal decreases with the distance from its origin at a rate of $1/r^2$ (bottom left). Mechanical signals are transmitted through forces directionally applied to a target cell, directly or indirectly (through cell-cell contacts or matrix deformation) (upper right). Mechanical signals do not significantly decrease with the distance (bottom right, black). How ever signal intensity might be altered by the physical properties of the transmitting substance (cell or ECM) such as elasticity. Therefore the full force of the initial deformation might not be transmitted (red) (adapted from Janmey et al., 2011).

on the ECM and surrounding cells (Fig. 1b, c). Indeed, cells could wrinkle a soft rubber sheet on which they were cultured (Harris et al., 2008). This phenomenon occurs through active processes including actin assembly and ROCK dependent actomyosin contraction. The cytoskeleton appears to play a central role in the mechanobiology of the cell. It allows the cells to exert forces in the nanoNewton range on their surrounding environment and sense the mechanics of cells or substrate around them (du Roure et al., 2005). The overall cytoskeletal organization of cells, including actin filaments, intermediate filaments and microtubules, in interplay with the ECM components dictate the viscoelastic property of a tissue and the resulting forces. ECM is highly dynamic since cells constantly remodel their microenvironment with the secretion of either metalloproteinases leading to ECM degradation (Mrkonjic et al., 2017), or in contrast, of ECM components (Lu et al., 2011) and crosslinking enzymes such as lysyl oxidases and transglutaminases that stiffen the ECM (Lee et al., 2015). By using inner active processes such as cytoskeletal reorganization together with the secretion of ECM degrading/crosslinking enzymes, cells are able to adapt to their physical microenvironment to reach the mechanical equilibrium. Thus, all cells respond to mechanical forces by a mechanism called “mechanoreciprocity” (Fig. 1) (Ding et al., 2013).

1.1.2 Biochemical *versus* mechanical signal

The major difference between these two types of signal is their way of spreading. Indeed, chemical messengers passively diffuse from the source of production to the target receptor (Fig. 2). This implies that the signal is not directed and equally irradiates to all directions from the production site. However, in the context of chemotaxis, the interpretation of the signal by the target is directed but limited in terms of distances. The diffusion of first messengers upon paracrine and autocrine signaling occurs through the microenvironment, therefore, it is subjected to environmental forces such as flow. Thus, it rapidly decays over time (at the rate of $1/\text{radius}^2$) and depends on the rate of production over the rate of neutralization (Fig. 2). Moreover, chemical molecules can only signal across few tens of micrometers. On the contrary, mechanical forces can be directed in a specific direction through fibers within the cells or the ECM (Janmey and Miller, 2011). A meshwork of

filaments such as those composing the ECM or the cytoskeleton can align in the direction of the stress to convert filament bending into filament stretching (Onck et al., 2005). Unlike chemical signals, mechanical signals decay linearly and therefore can rapidly propagate up to hundreds of micrometers away from its point of generation (Winer et al., 2009). Transduction of mechanical signals is a rapid process generated from the perturbation of the mechanical equilibrium between cells and their microenvironment. While biochemical signaling is generally a slower process with timescales of seconds or minutes, (except for processes such as synaptic transduction), mechanotransduction is believed to be a fast process. For example, Sarcoma kinase (Src) activation by mechanical cues occurs in less than 0.3s while chemokine mediated activation of Src requires more than 12s (Na et al., 2008).

1.1.3 The dark side of the force

As discussed above, the cell microenvironment and its mechanical properties govern a wide range of biological processes. For example, substrate stiffness can control cell fate (Fig. 3a). Mesenchymal stem cells (MsCs) can differentiate into three cell types depending on their substrate stiffness. MsCs cultured on substrates mimicking brain (0.15-0.30 kPa), muscle (8-14 kPa) or bone stiffness (25-45 kPa) respectively differentiate into neuronal, muscle-like or bone cells (Engler et al., 2006). Therefore, any abnormality in the ECM that could modify its mechanical properties such as stiffness can perturb essential biological events by generating abnormal mechanical signal. These processes may trigger non-physiological conditions where tissue mechanics alter programmed cell functions leading to pathologies. Indeed, mechanical stress is involved in a myriad of diseases such as liver, renal, muscular diseases and cancer. The relationship between mechanical deregulation and pathological behavior in the context of cardiovascular, muscular pathologies and cancer are described below.

1.1.3.1 Cardiovascular and muscular pathologies

Myocytes, by their function of contraction – relaxation are constantly subjected to mechanical stress. Any mechanical dysfunction of the cell itself or its

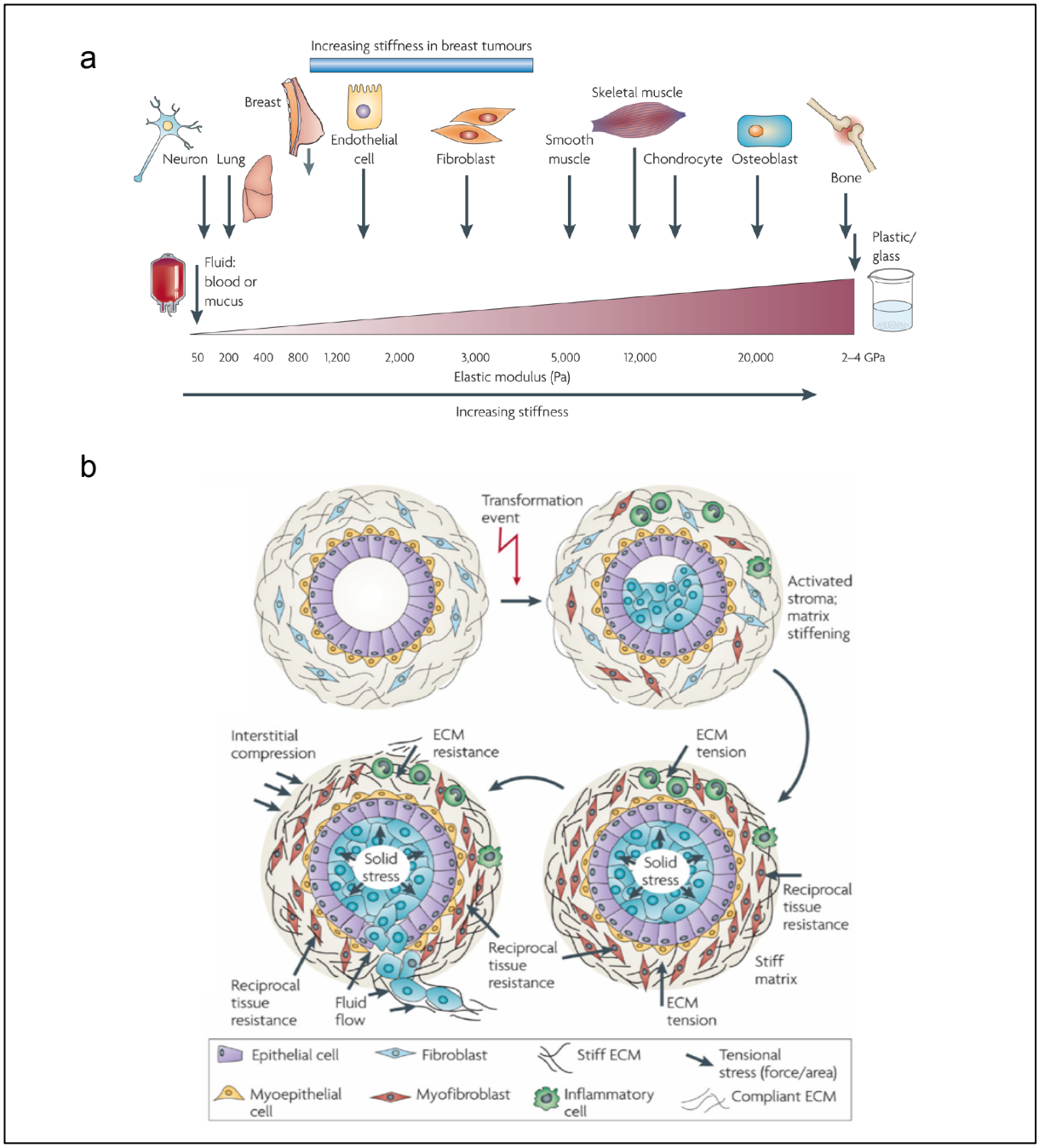

Figure 3. Tissue rheology and pathological development

(a) All cells are exposed to mechanical forces that are generated by cell-cell or cell-ECM interactions. These mechanical forces influence cell function. Each cell type is specifically tuned to the specific tissue in which it resides. Following transformation, breast tissue becomes progressively stiffer and tumor cells become significantly more contractile and hyper-responsive to mechanical cues. **(b)** Transformation (blue cells) resulting from accumulation of genetic and epigenetic alterations in the epithelium along with an altered stromal matrix leads to unchecked proliferation and enhanced survival of luminal epithelial cells, which compromises normal ductal structure. The abnormal pre-neoplastic luminal mammary epithelial cells eventually expand to fill the breast ducts exerting outwards projecting compression forces on the basement membrane and adjacent myoepithelium. The damaged pre-neoplastic tissue produces soluble factors that stimulate cell infiltration and activation of fibroblast to induce a dramatic reorganization and stiffening of the ECM over time. The rigid parenchyma exerts a progressively greater inward projecting resistance force on the expanding pre-neoplastic duct. Over time, the number of myoepithelial cells surrounding the pre-neoplastic mass decreases and the basement membrane thins, probably owing to increased matrix metalloproteinases (from Butcher et al., 2009).

microenvironment preventing the myocyte normal functions is highly deleterious. For example, myocardial infarct leads to fibrotic stiffening that impairs cardiac output (Cecelja and Chowienczyk, 2009). Indeed, embryogenic myocytes grown on a heart-like substrate stiffness of approximately 11 kPa normally beat, while those grown on a myocardial scar-like substrate stiffness (35-70 kPa) exhibit a drastic decrease of beat frequency (Engler et al., 2008).

An increased stiffness of muscle fibers most likely due to ECM stiffening by collagen crosslinking, is responsible for diastole in the context of congenital heart disease (Chaturvedi et al., 2010). Similarly, aortic stiffness increases the risk of heart failure and strokes (DeLoach and Townsend, 2008).

More recently our lab discovered that caveolin-3 mutations involved in muscular dystrophies prevent caveolae formation at the plasma membrane. Hence myotubes carrying these mutations are more prone to plasma membrane disruption under mechanical stress due to a defect of caveolae mechanoprotection (developed in 2.3.3). It also exhibits a defect of IL6/STAT3 mechanosignaling (Dewulf et al., 2018 under revision, see annex 3).

1.1.3.2 Cancer

1.1.3.2.1 Mechanical forces in the context of tumor progression

Some cancer clinical diagnoses rely on the detection of abnormal mechanical properties of the tissue. Indeed, detection of stiffen tissues is proceeded by palpation, X-ray, and ultrasound techniques. Most of the solid tumors are stiffer than surrounding healthy tissues. For example, normal breast tissue stiffness is around 0.2 kPa while breast tumors stiffness is increased by approximately 20 folds (Levental et al., 2007; Baker et al., 2009). Similar stiffness increase is found for pancreatic and colorectal cancer (Butcher et al., 2009; Kai et al., 2016). Abnormal tissue stiffness most likely originates from the imbalance between ECM deposition and its degradation increasing the total ECM quantity. Tissue stiffening is not only the result of pathological processes; it also promotes their establishment (Fig. 3b). Collagen crosslinking and stiffening induce the invasiveness of oncogene activated

epithelial cells by generating larger focal adhesion sites (Levental et al., 2009). Secretion of several metalloproteinases at the level of the invadosome such as MT1-MMP loosen and reduce matrix stiffness to counteract this crosslinking process (Willis et al., 2013) in response to mechanical cues (Mrkonjic et al., 2017). Stromal cells also exert considerable forces on the ECM. Cancer associated fibroblasts (CAFs) deform the extracellular matrix via strong actomyosin contractions, contributing to ECM stiffening (Laklai et al., 2016). The increase of cell density also promotes tissue stiffening. Cancer cells are usually stiffer than healthy cells (Fabry et al., 2001). Moreover "jamming" of cancer cells prevents their spatial reorganization to adapt to mechanical strains therefore contributing to tissue stiffening. Ultimately, in the context of metastasis, tumor cells have to squeeze through matrix fibers, travel through the organism and establish in a new tissue with different mechanical properties, which are as many processes that subject the cells to different mechanical stresses with a variety of biological consequences on tumor cells.

1.1.3.2.2 Tumor physical microenvironment influences cancer progression

Tissue stiffening is not only symptomatic of cancer development; it also actively drives tumor progression. As discussed above mechanical forces influence a wide range of biological processes. Hence, throughout evolution, devices named mechanotransducers have been conserved to convert mechanical cues into interpretable biochemical information (detailed in 1.2). Most of pathological situations emerge from altered signal transduction such as irrelevant pathway activation or inactivation. Similarly to aberrant biochemical signaling such as growth hormone signaling, aberrant mechanical signaling also promotes tumor progression. For example abnormally stiff ECM drives epithelial to mesenchymal transition (EMT) and metastasis through the TWIST1-G3BP2 mechanotransduction pathway (Wei et al., 2015a). The most well-known mechanosignaling hubs are focal adhesions. The direct anchorage to the ECM and their link with the cytoskeleton, place these structures at the perfect place to integrate mechanical cues provided by ECM deformation. Several focal adhesion components such as integrins, talin, paxillin and Cas are sensitive to mechanical strains. Focal adhesions regulate a myriad of signaling molecules of major cancer pathways such as Src, FAK, Rho, ERK, PTEN (Kandoth et al., 2013; Mouw et al., 2014). Together with filamentous actin, integrins

also control the mechanical activation of the YAP/TAZ oncogenes (Dupont et al., 2011; Lamar et al., 2012). In three dimensional situation, studies have emphasized the role of integrins clustering in the transduction of mechanical cues (Harunaga and Yamada, 2011). Tumor cells are subjected to mechanical stretch at the periphery of the tumor but cells in the deep interior of the tumor are subjected to compressive forces (Fig. 3b). Mechanical forces are known to control cell cycle and apoptosis therefore promoting growth heterogeneity within the tumor (Chang et al., 2008; Lien et al., 2013). Cells sense and adapt to the microenvironment physical strains through the reorganization of their cytoskeleton, however such a process also implies plasma membrane topological reorganization to achieve mechanoadaptation and mechanosensation. Indeed, some mechanoreceptors engaged in cancer evolution reside inside the lipid bilayer. For example, stretch sensitive channel Piezo 1 and 2 that triggers calcium signaling and other TRP ion channels are involved in tumor pogression (Li et al., 2015; Wu et al., 2017; Pardo-Pastor et al., 2018).

1.2 Signal mechanotransduction

Cells can generate precise three-dimensional structure through morphogenic movements and ensure the cell/organism structural stability. As gravity and muscle contraction shape bones, shear stress from flowing blood influences the heart vasculature and many other examples show that the ability of cells to convert mechanical cues into biochemical signal is essential. Failure of these mechanisms contributes to a wide breadth of pathologies (Janmey and Miller, 2011) as discussed in 1.1.3. Therefore, considerable efforts are currently directed toward determining how a variety of mechanical stimuli lead to the regulation of gene expression.

Mechanotransduction is achieved through a rich set of mechanisms. In this introduction, only a few of them will be presented as examples. One of the best-studied mechanisms of signal mechanotransduction is the conversion of physical forces into biochemical signal through protein structural refolding. In general, proteins adopt the conformation that favors the lowest free energy. Therefore, changes in the energy landscape induced by physical strains lead to the reshaping of the protein (Orr et al., 2006). This process is comparable to other post-translational modifications

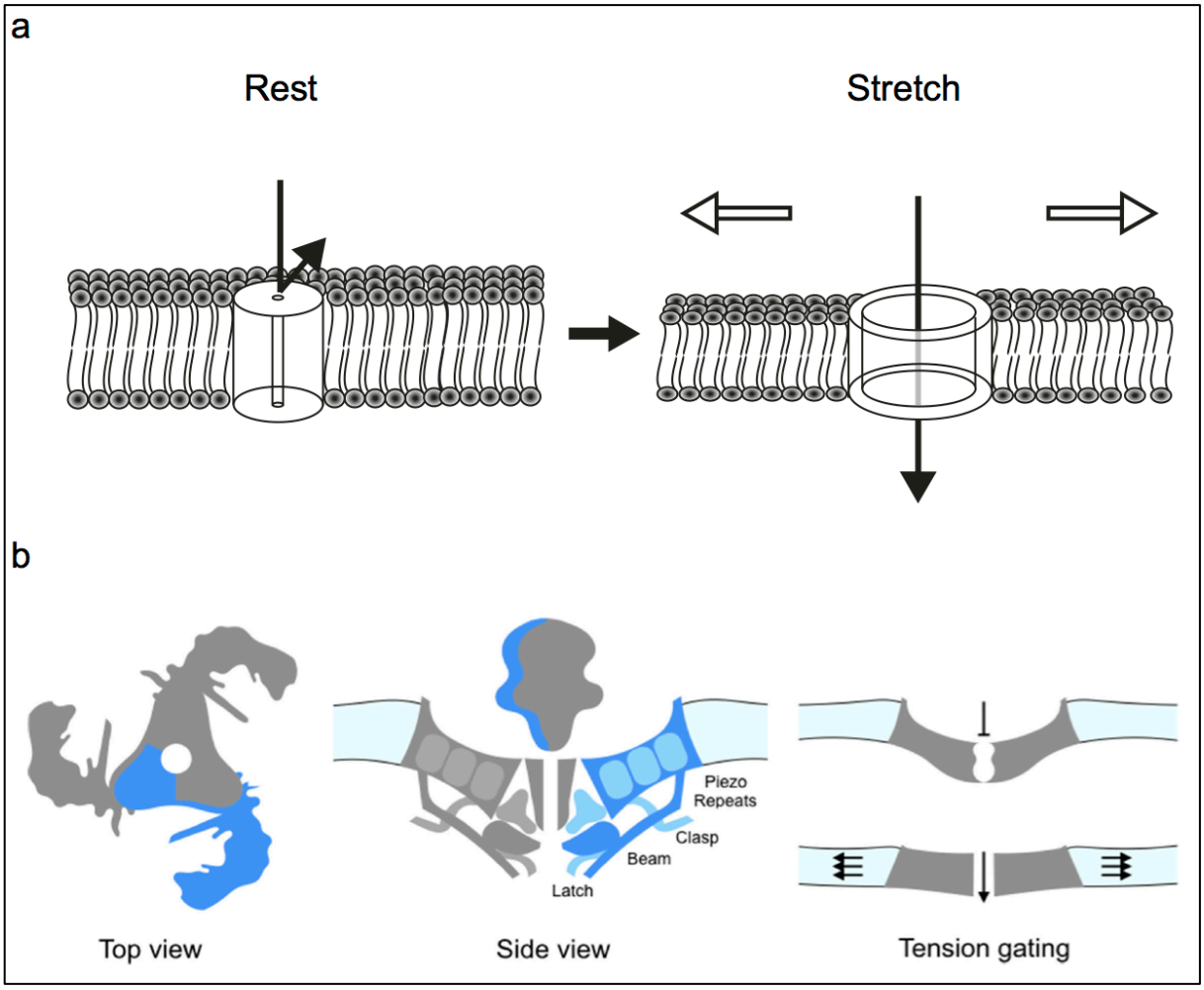

Figure 4. Mechanosensitive channels

(a) Mechanism of activation of mechanosensitive channels (MSCs). The channel occupies a restricted area in resting, while proceeding to rearrangement into open conformation to decrease energy cost due to membrane tension and exposition of its hydrophobic part induced by membrane thinning. **(b)** Schematic structure of Piezo1 viewed from above, showing the three “propeller blades” surrounding a centrale pore (left). Side view of the structure of Piezo1 (center). When the cell is not submitted to to pressure, Piezo1 bends to make a dome-like structure pointing inside the cell, and the channel is closed. When the membrane is stretched the complex flattens, openning the channel (Chesler et al., 2018).

such as phosphorylation. Phosphorylation introduces a negatively charged phosphate group, inducing protein refolding due to charge repulsion in the inner structure of the protein. These modifications will then induce structural changes that will modulate the catalytic activity or the interaction ability to transduce a signal.

1.2.1 Mechanosignaling at the plasma membrane

The best example of plasma membrane mechanotransducers are mechanosensitive channels (MSCs) such as voltage gating mechanochannels (Martinac, 2004). These channels can sense membrane stretch and curvature. Pressure sensitive channels such as Piezo 1 and 2 are also an emerging important category of MSCs (Coste et al., 2011). Increasing the membrane tension, increases the probability to open the channel (Martinac and Hamill, 2002). In this context, MSCs opened conformation occupies a greater space in the stretched lipid bilayer, favoring lower free energy. Hence the opening of this gate induces membrane permeability to ions (Fig. 4). The inner leaflet of the plasma membrane is negatively charged therefore the arrival of positively charged ions into the cytoplasm leads to membrane depolarization and generates an electrical signal. Moreover Ca^{2+} entry through MSCs also leads to the activation of Ca^{2+} sensitive molecules such as calmodulin domain-containing proteins. Piezo and the other MSCs are involved in many biological processes such as hearing, touch, nociception and proprioception.

1.2.2 Mechanosignaling in the cytosol

On the other hand, direct application of a stalling force against a molecular motor or an enzyme inhibits its catalytic activity, most likely by unfolding its catalytic domain (Finer et al., 1994; Yin et al., 1995; Ingber, 2006). Similarly, some proteins unfold in a stepwise manner when they are mechanically extended. This unfolding may lead to the exposure of cryptic binding or phosphorylation sites for potential signaling downstream effectors (Ingber, 2006) (Fig. 5a). In addition, mechanical strains can also influence signal transduction by strengthening or weakening protein-protein interaction (Evans and Calderwood, 2007).

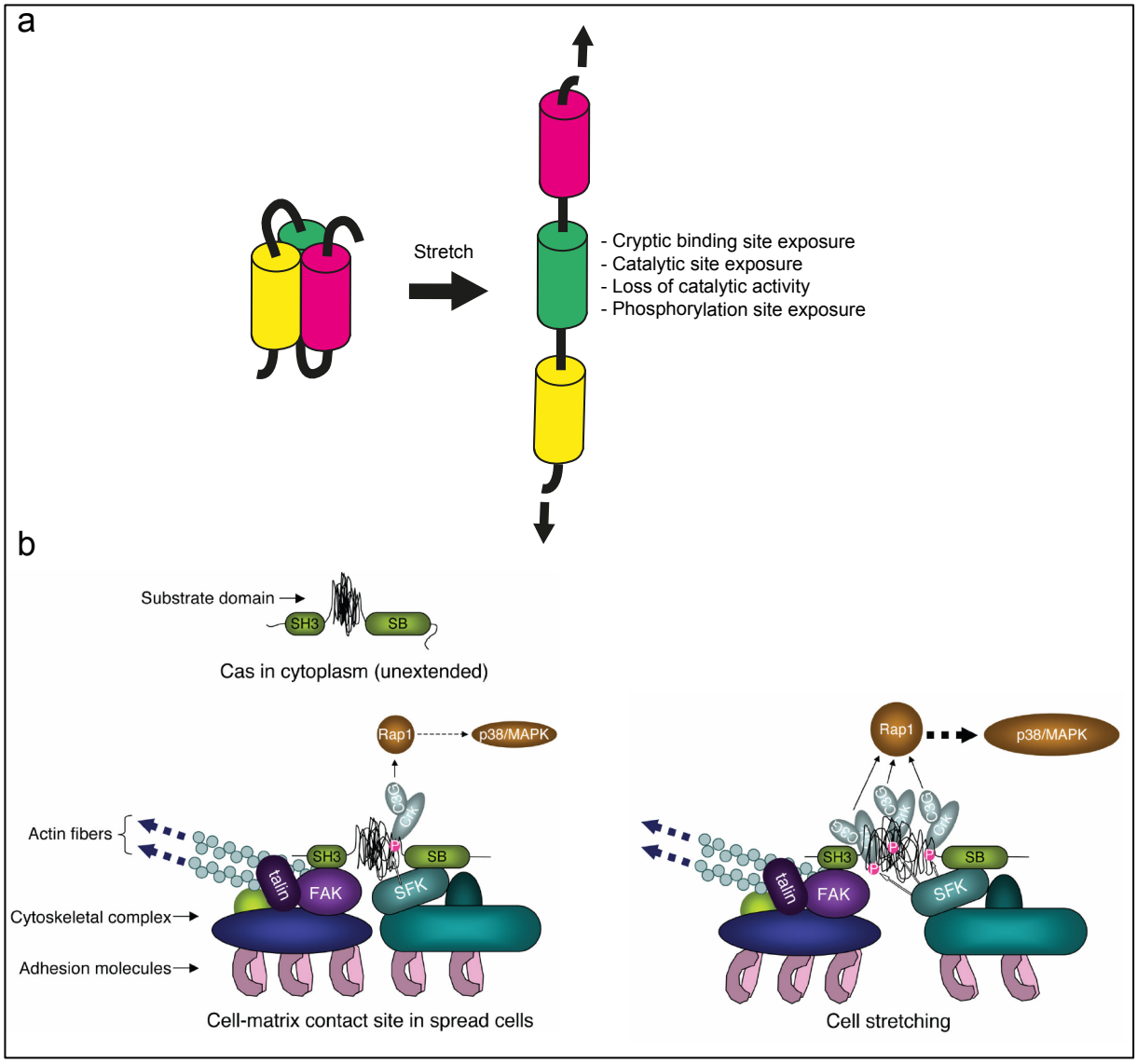

Figure 5. Mechanotransduction at the level of the protein and protein complex

(a) Stress on mechanosensors can induce conformational changes generating a biochemical signal (based on Ding et al., 2013). **(b)** Cas molecule with unextended configuration of substrate domain and with moderate extension of substrate domain at the cell-matrix contact site of spread cells, respectively (left). Extension-dependent phosphorylation of Cas substrate domain by SFK and enhancement of its downstream signaling. SH3 and SB represent the SH3 and Src-binding domain of Cas, respectively (right) (Sawada et al., 2006).

Focal adhesion sites (FA) are probably the most studied mechanosignaling platforms. Its direct link with the cell cytoskeleton and the ECM put this structure in perfect position to transduce mechanical signals. Mechanical forces directly control the shape, size and dynamics of FA (Galbraith et al., 2002). Indeed, clusters of integrins (focal adhesion) can generate forces on the overall cell through the cytoskeleton. Nevertheless, focal adhesion can sense mechanical forces (Grashoff et al., 2011). For example shear stress-induced cytoskeletal reorganization is controlled by integrins activation balance (Macek Jilkova et al., 2014). Integrins are connected to the cytoskeleton through several adaptor proteins such as talin, vinculin, zyxin, Cas etc., which are as many components susceptible to transduce mechanical cues.

For example, talin directly links integrins to the actin filaments. Upon ECM deformation or actomyosin contractions, talin rods are stretched and deformed by the mechanical strain. The unfolding of talin unveils cryptic binding sites for vinculin interaction (Fig 5a). Hence, talin unfolding leads to the recruitment of vinculin that strengthen the link with filamentous actin and cluster the integrins into focal adhesion sites (del Rio et al., 2009).

Similarly, p130Cas (Crk associated substrate) binds to the focal adhesion kinase (FAK) and the Src family of protein kinase (SFK). Upon cell stretch, Cas substrate domain unfolds exposing phosphorylation sites (Fig. 5b). Their phosphorylation by the SFK kinase triggers the recruitment of signaling partners and the activation of the p38/MAPK pathway through Ras associated protein 1 (Rap1) activation (Sawada et al., 2006).

Another example of cytosolic mechanotransduction is the yes associated protein/taffazin (YAP/TAZ) pathway that controls processes such as proliferation and differenciation (Dupont et al., 2011; Mosqueira et al., 2014). YAP/TAZ is an emerging mechanotransduction pathway. It transduces mechanical signals from the cytoskeleton to the nucleus. YAP/TAZ are transcriptional co-factors that are well studied in the context of the Hippo signaling, where upstream large tumor suppressor kinases (LATS) phosphorylate YAP and TAZ leading to their cytosolic retention (Low et al., 2014). There are clear evidences linking YAP/TAZ regulation to cell mechanics. Indeed, the subcellular distribution of YAP/TAZ is highly dependent on

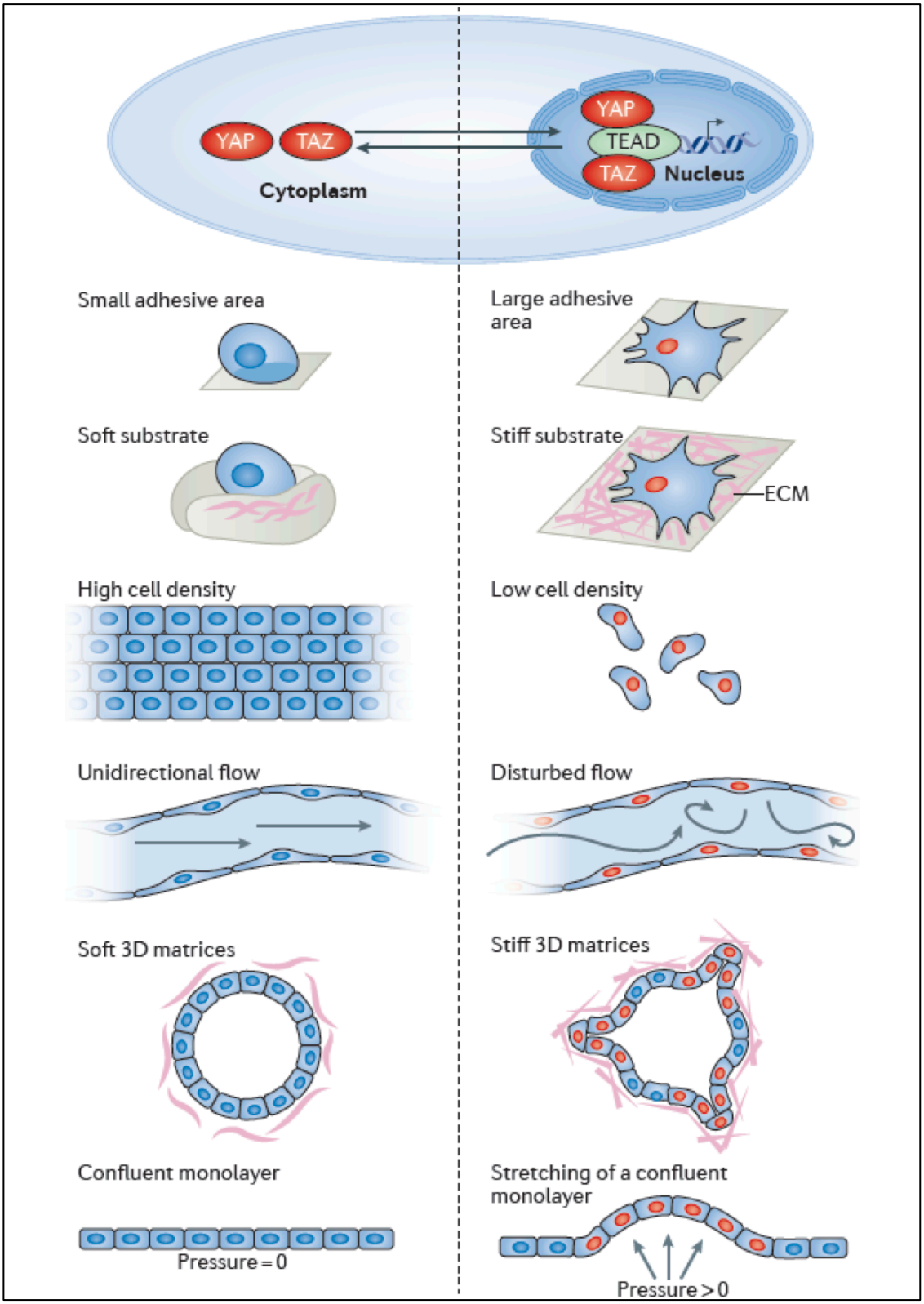

Figure 6. Schematic representations of mechanical stimuli influencing YAP and TAZ subcellular localization and activity

When YAP and TAZ are mechanically activated (red), they translocate to the nucleus, where they interact with TEA domain family factors (TEAD) to regulate gene expression (top). Schematics illustrating how different matrix, geometry and physical conditions influence YAP and TAZ localization and activity: the left panels show conditions in which YAP and TAZ are inhibited and localized to the cytoplasm, whereas the right panels show conditions that promote YAP and TAZ nuclear localization (indicated by red coloring of cell nuclei) (Panciera et al., 2017).

cell mechanics and matrix physical properties (Fig. 6). For example cells cultured on soft substrate exhibit a cytosolic YAP/TAZ distribution, while those grown on stiff microenvironment exhibit a nuclear YAP/TAZ localization and those residing in an “in-between” microenvironment stiffness possess an evenly distributed YAP/TAZ localization. Therefore, substrate stiffness but also cell shape controls YAP/TAZ distribution (Dupont et al., 2011). Yet, how mechanical cues regulate YAP/TAZ localization and activity is still unknown, however it is tightly dependent on the F-actin organization, contraction and cytoskeletal mechanics (Dupont et al., 2011; Aragona et al., 2013). Propagation of tensile forces through the cytoskeleton induced by actomyosin network contraction or ECM deformation pulling on cytoskeleton-linked integrins leads to YAP and TAZ activation (Taniguchi et al., 2015; Hu et al., 2017). The cytoskeleton is also connected to the nucleus; therefore, force propagation through the cytoskeleton may also reach the nucleus thereby directly affecting nuclear mechanics and the regulation of YAP/TAZ nuclear translocation as detailed in the next chapter.

1.2.3 Nuclear mechanotransduction

Mechanotransduction is not a process only restricted to “surface” receptors. An array of biological processes such as cell migration, programmed necrosis or infection trigger nucleus deformation (swelling, squeezing and stretching). For example, a transient decrease of extracellular osmotic pressure promotes nuclear swelling (Irianto et al., 2013). External mechanical strains can also exert direct mechanical forces on the nucleus since it is connected to the cell surface through the cytoskeleton via the linker of nucleoskeleton and cytoskeleton (LINK) complex. In a metastatic context, tumor cells have to squeeze through the extracellular matrix fibers subjecting their nucleus to deformations. Interestingly, the nucleus appears to be a good mechanotransduction organelle. Indeed, the nuclear envelope participate less to cell trafficking, therefore its overall area fluctuates less. Moreover its membrane is more loose and easy to stretch, thus it is more prone to detect external strains (Bigay and Antonny, 2012). The nuclear envelope possesses a dynamic structure that can rapidly adapt to tensile force by adjusting its stiffness via the phosphorylation of proteins of the nuclear envelope such as emerin (Guilluy et al.,

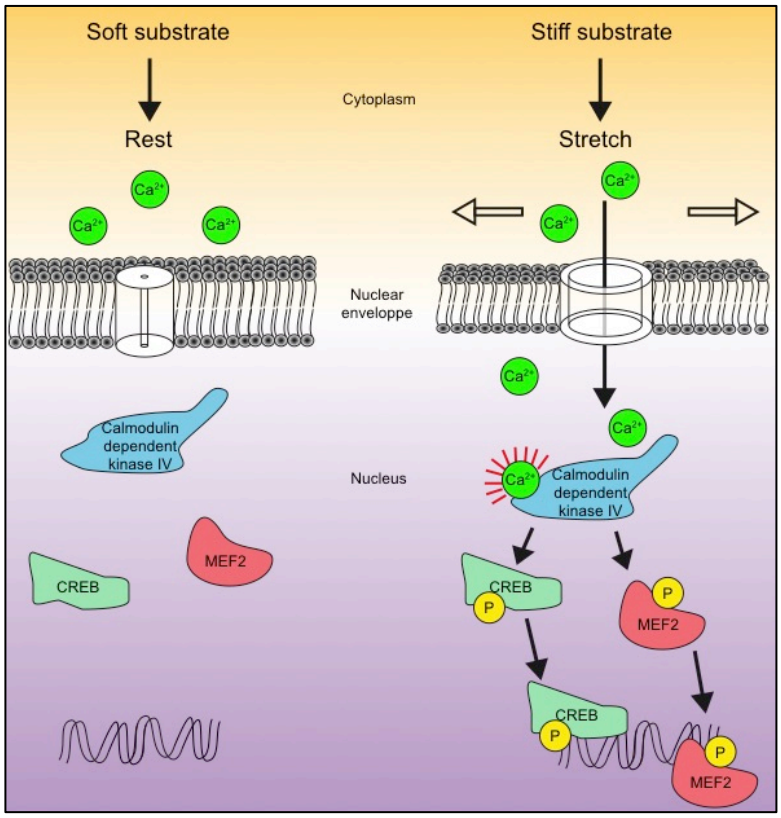

Figure 7. Mechanosensitive calcium signaling in the nucleus

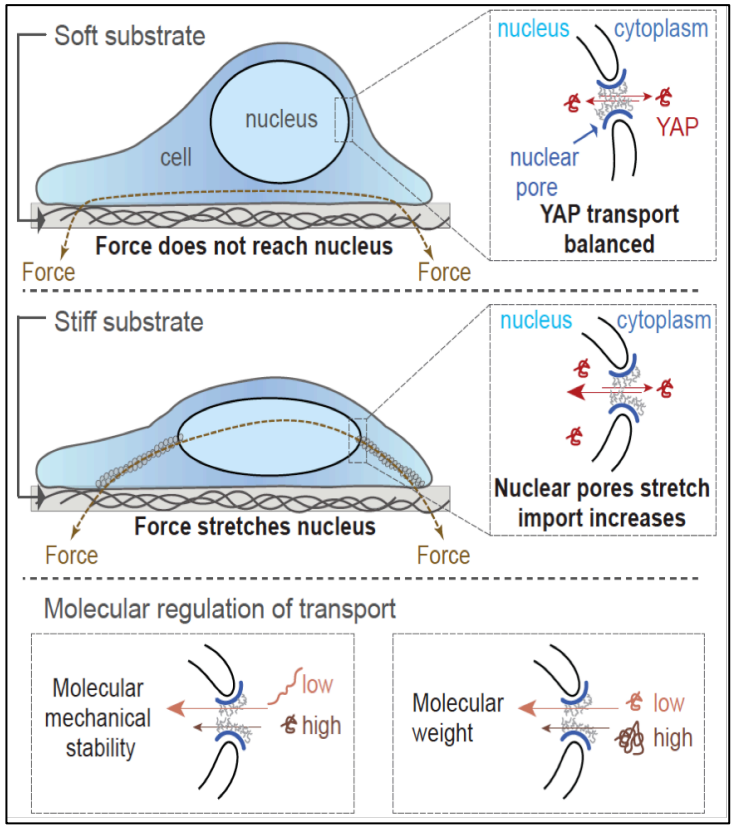

Figure 8. Proposed model of mechanosensitive nucleoplasmic shuttling (Elosegui-Artola et al., 2017)

2014). The nuclear envelope serves as scaffold for the activation of important peripheral proteins. Hence, nuclear expansion induced by cell swelling leads to the recruitment of the phospholipase enzyme $cPLA_2$ and the 5-lipoxygenase (LOX) at the inner face of the nuclear membrane. This promotes LOX-dependent generation of pro-inflammatory eicosanoids such as leukotrienes, which are key factors in inflammatory diseases such as asthma (Peters-Golden and Brock, 2001). Nuclear mechanics can also directly control gene expression. Indeed, some MSCs are found in the nuclear envelope and mediate Ca^{2+} release in response to nuclear and endoplasmic reticulum stretch induced by cell spreading. For example, the nuclear mechanical release of Ca^{2+} regulates gene expression through the cAMP responsive element binding (CREB) and myocyte enhancer factor 2 (MEF2) transcription factor phosphorylation by the calmodulin dependent kinase IV (Itano et al., 2003) (Fig. 7). Nucleus deformation also alters the integrity of the nuclear pores. Indeed, the crossing of molecules through the nuclear envelope via these nuclear pores is a key and tightly regulated step of many signaling cascades to achieve the regulation of gene expression and by extension the cellular responses. The nucleus deformation stretches the nuclear pores thereby decreasing the energy requirement for molecular transport through these structures. Nuclear deformation and the consecutive nuclear pores stretch have been shown to trigger YAP nuclear translocation and might be a more general mechanism for other signaling molecules (Elosegui-Artola et al., 2017) (Fig. 8). Finally, harsh nuclear deformation induced by nuclear squeezing during cell migration, can result in nuclear membrane damages releasing DNA in the cytoplasm. This situation promotes the activation of damage-sensing pathways including cyclic GMP-AMP synthase and stimulator of interferon genes (cGAS-STING) pathway and triggers the expression of immunomodulatory genes such as interferons (Raab et al., 2016).

To summarize, mechanical forces generated by external strains can modify protein folding and larger complex organization inside the cell, thereby changing their biochemical properties and therefore transforming mechanical cues into biochemical signals. Nevertheless, studies demonstrated that larger structure such as plasma membrane nanodomains called caveolae can also respond to mechanical strains applied to the plasma membrane (Sinha et al., 2011).

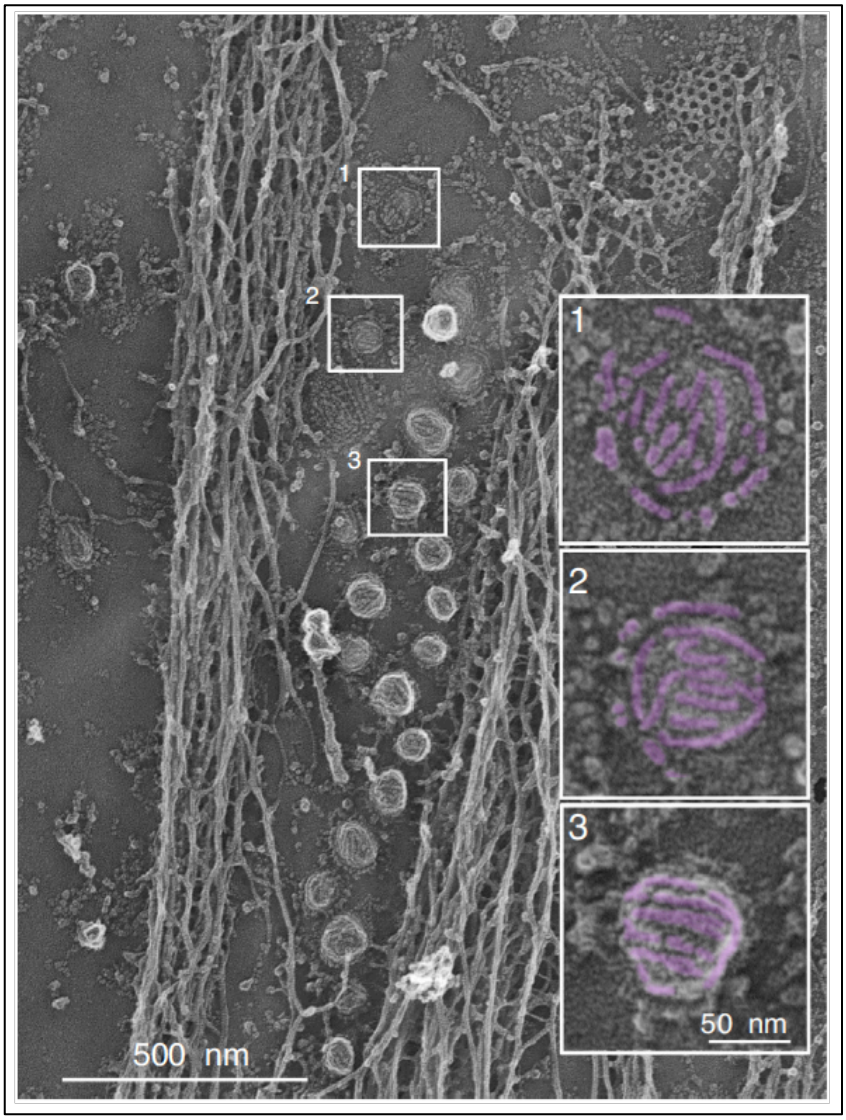

Figure 9. Visualization of the caveolar coat at the plasma membrane of myotubes

Survey view of the cytoplasmic surface of an unroofed myotube presenting caveolae at the plasma membrane. Different types of caveolae structures are apparent, ranging from flat (1), circular (2), to fully budded (3). Scale 500 nm. Scale bar in insets: 50 nm (from Lamaze et al., 2017)

2 The caveolae: specialized plasma membrane structures

More than sixty years ago, fine plasma membrane structures identified by electron microscopy as “caves” or “cave-like indentation of the plasma membrane” thereby named caveolae, were first visualized in blood capillaries and mouse gall bladder by George E. Palade and Eichi Yamada (Palade, 1953; Yamada, 1955). These plasma membrane invaginations are smaller than clathrin coated pits since their diameter varies between 50 and 80 nm and they present a striated coat (Rothberg et al., 1992) (Fig. 9). Caveolae are also found as interconnected caveolar structures named “rosette” (Pelkmans and Zerial, 2005). Adipocytes, endothelial and muscle cells are particularly enriched in caveolae, yet almost all mammalian cell types possess caveolae except neurons and lymphocytes despite their expression of caveolin-1.

2.1 Structure and composition

The first step to fully understand the function of these “cave-like” plasma membrane structures was to elucidate their molecular composition. Therefore, since the discovery of caveolae, a lot of effort has been put toward the identification of their molecular composition and organization.

2.1.1 Caveolar proteins

2.1.1.1 Caveolins

Almost forty years after the first visualization of caveolae, structural studies of the caveolae inner face (facing the cytoplasm) revealed a striated coat composed of “filaments”. These filaments have been first identified as a 22 kDa substrate for v-src tyrosine kinase in virus-transformed chick embryo fibroblasts and therefore called caveolin (Rothberg et al., 1992). The same year, a vesicular integral-membrane protein of 21 kDa (VIP21) was also found by another team to be an important component of the caveolar coat (Kurzchalia et al., 1992). Actually, these two newly

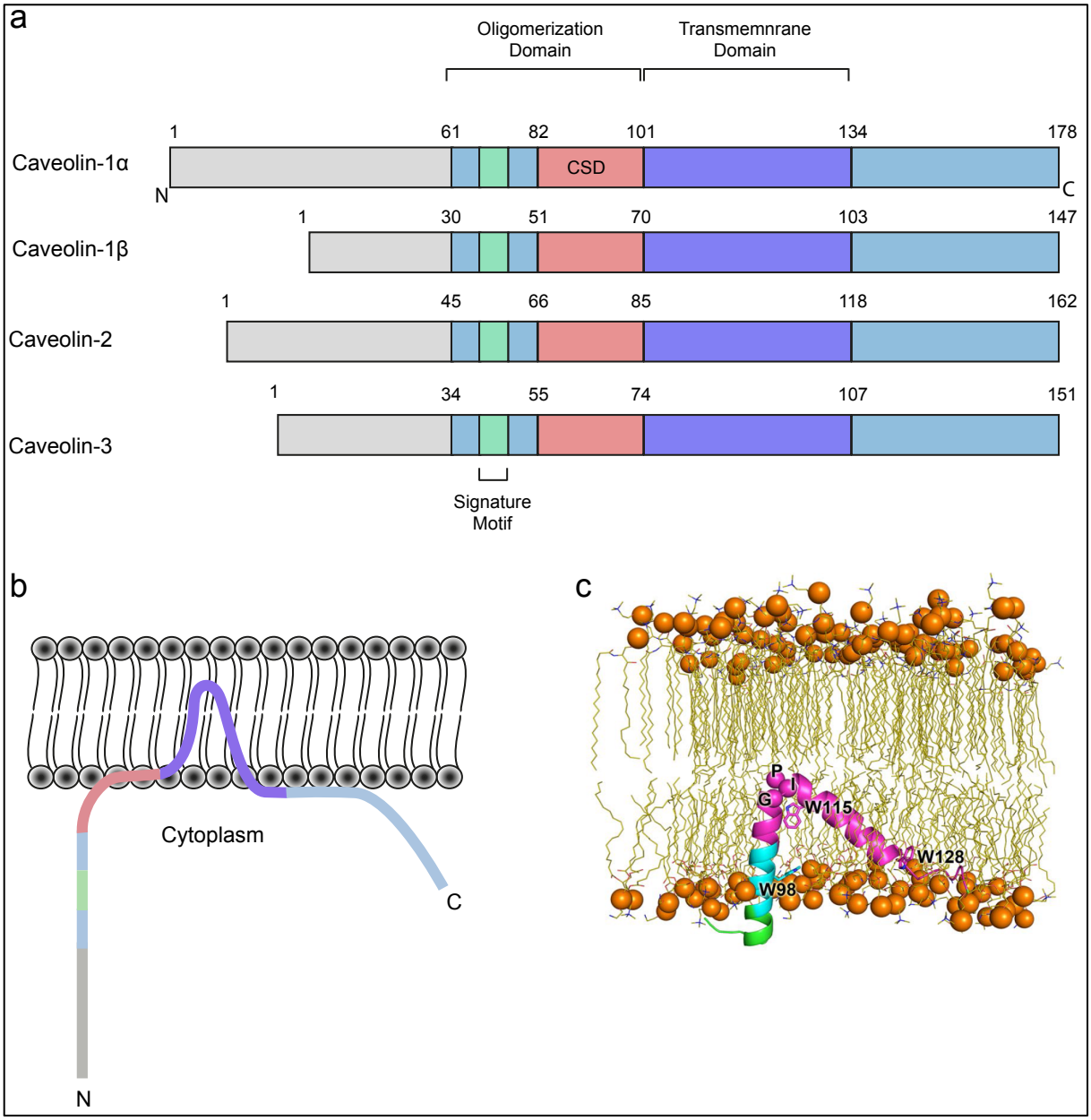

Figure 10. Caveolins domains and insertion in the plasma membrane

(a) Conserved domains of the caveolin protein family. An oligmerization domain encompassing an 8 amino acids stretch signature motif (FEDVIAEP) and the caveolin scaffolding domain followed by the transmembrane domain. Length variability of caveolins -1β, -2 and -3 is the consequence of truncated N-terminal part. **(b)** Proposed model of caveolin-1 (Cav1) topology within the lipid bilayer. Cav1 is inserted in the plasma membrane inner leaflet via its TMD conferring a hairpin-shaped topology. Both N- and C-termini are facing the cytoplasm (based on Parton and del Pozo, 2013). **(c)** Computational analysis of Cav1 insertion within the plasma membrane. Snapshot of the insertion of $Cav1^{82-136}$ is shown in the illustration with the CRAC motif in cyan and putative TMD in magenta as well as the N-terminus in green. The C_{α}atoms of G108-P110 are shown in spheres. W98, W115 and W128 are shown in sticks. Cholesterol molecules and, ions and water are hidden for clarity (Liu et al., 2016).

discovered caveolar proteins appeared to be the same (Glenney and Soppet, 1992). Hence, it has been decided that both v-src substrate in Rous sarcoma virus-transformed fibroblasts and VIP21 would be renamed as caveolin. This is how the first member of the caveolin family has been identified thus named as caveolin-1 (Cav1), shortly followed, by the identification of two homologues: caveolin-2 (Cav2) and the muscle restricted isoform: caveolin-3 (Cav3) (Way and Parton, 1995).

Cav1 molecules (and Cav3 in muscle cells) are essential components of caveolae. Indeed, these two proteins are required for caveolae biogenesis. Lack of Cav1 or Cav3 leads to mis-invagination of the caveolae. Caveolins can form structures of higher complexity by homo and hetero-oligomerization into 300 kDa complexes (Sargiacomo et al., 1995). All the caveolin isoforms share a signature motif of eight amino acids ^{68}FEDVIAEP^{75} localized in their oligomerization domain (Fig. 10a).

Cav1 is the most studied member of the caveolin family. Cav1 is an integral plasma membrane protein of 178 amino acids with both N- and C-termini facing the cytoplasm (Monier et al., 1995; Aoki et al., 2010) (Fig. 10b). Its structure remains debated and mainly relies on predictions based on circular dichroism (CD), nuclear magnetic resonance (NMR) and computational analysis. From these studies, we know that Cav1 crosses only the inner leaflet of the plasma membrane through a putative hairpin-shaped transmembrane domain (TMD) predicted to be from L102 to I134 (Razani et al., 2002a). The TMD adopts a helix-break-helix topology (Lee and Glover, 2012) (Fig. 10c). Indeed the two α-helices are separated by three residues linker regions containing a proline 110 that induces a 50° angle between those two helices (Root et al., 2015). The TMD adopts a U-shaped conformation (Aoki et al., 2010) and plays a key role in the oligomerization ability of Cav1 and Cav2 (Das et al., 1999). The insertion of the TMD within the inner leaflet of the plasma membrane thereby displacing lipids of the inner layer has been proposed to induce membrane curvature (McMahon and Gallop, 2005). The Cav1 C-terminal end (K135-I178) is involved in plasma membrane attachment, trans-Golgi localization and oligomer-oligomer interaction (Song et al., 1997; Schlegel and Lisanti, 2000) . Moreover, it presents three palmitoylation sites on C133, C153 and C156, which are not required

for Cav1 anchorage to the plasma membrane but may influence Cav1 oligomerization (Dietzen et al., 1995; Monier et al., 1996).

The most prominent domain of Cav1 is the caveolin scaffolding domain (CSD) (Fig. 10a). Indeed this domain is involved in Cav1 oligomerization, protein-protein interaction, and cholesterol recognition/binding (Li et al., 1996; Couet et al., 1997; Schlegel et al., 1999). However, the role of the CSD in the control of biological processes such as signaling remains somehow controversial (developed in 2.3.4.4 and discussion)(Collins et al., 2012). The CSD topology is not clear, and was first proposed to be a fully amphipathic α-helix that partially lies inside the plasma membrane inner leaflet (Le Lan et al., 2006), then later appeared to be a mixture of β and α structures (Hoop et al., 2012). More recently, the CSD was proposed to adopt a dynamic structure that can be either fully helical or partially unstructured (Liu et al., 2016). Interestingly, Cav1 also exhibits a high affinity for cholesterol (Murata et al., 1995). Cholesterol recognition is achieved through the cholesterol recognition/interaction amino acid consensus (CRAC) motif within the CSD. Since Cav1 has been first discovered as a tyrosine kinase substrate, it was later shown that Cav1 can be phosphorylated on its tyrosine 14. More recently, serine 80 has been found to be phosphorylated. Yet, the precise function of these two post-translational modifications is not well understood. Tyr14 phosphorylation has been recently proposed to mediate signaling (Joshi et al., 2012) and Cav1 conformation changes (further developed in the discussion) to regulate the CSD accessibility (Shajahan et al., 2012; Meng et al., 2017). The Ser80 phosphorylation is required for proper caveolae formation (Ariotti et al., 2015) and triggers its binding to the endoplasmic reticulum (ER) membrane in the context of regulated secretion of pancreatic cells (Schlegel et al., 2001). Finally, Cav1 can be ubiquitinated, a process that mediates Cav1 lysosomal degradation (Hayer et al., 2010a).

Cav1 encompasses two isoforms: a full-length α isoform (α-Cav1) and a truncated β-isoform (β-Cav1). The β-isoform lack the first thirty-three amino acids, hence it cannot be phosphorylated on Tyr14.

Few years after the identification of Cav1, a homologue of α-Cav1 was discovered by nucleotide sequence alignment. Cav3 shares common features with

Cav1 such as the caveolin signature motif, an oligomerization domain, an hydrophobic 102-134 TMD, a CSD and palmitoylation sites (Way and Parton, 1995; Tang et al., 1996) (Fig. 10a). Moreover, Cav1 and Cav3 can form hetero-oligomeric complexes with Cav1 in cardiac myocytes (Volonte et al., 2008). Cav3 also lacks the first twenty-seven aa, hence, neither Cav3 undergoes Tyr14 phosphorylation.

The purification of membrane fractions enriched in caveolae revealed the existence of a last member of the caveolin family: caveolin-2 (Cav2). Indeed, this isoform shares the common signature motif in its N-terminal part. It has been first described to differ from Cav1 from its inability to interact with the heterotrimeric G protein (Scherer et al., 1996). Moreover, Cav2 colocalizes with Cav1 indicating that Cav2 is a component of the caveolar coat (Scherer et al., 1996; Tang et al., 1996). There are two Cav2 isoforms: α-Cav2 and β-Cav2 that are respectively shortened by 16 and 29 aa compared to α-Cav1 (Fig. 10a). Likewise, Cav2 is not phosphorylated on its Tyr14. Unlike the other members of the caveolin family, Cav2 cannot homo-oligomerize, but it can dimerize and hetero-oligomerize with other caveolins (Scherer et al., 1996, 1997). α-Cav2 can be tyrosine phosphorylated on its residues 19 and 27 and serine phosphorylated on its residues 23 and 36. In addition Cav2 can be fatty acylated. However, the function of these post-translational modifications remains poorly understood. Cav2 serine phosphorylation participates to caveolae morphogenesis (Sowa et al., 2003). On another hand both Cav2 fatty acylation and phosphorylation have been reported to play a role in insulin signaling (Kwon et al., 2009; Kwon and Pak, 2010; Kwon et al., 2015). For example Cav2 phosphorylation prevent the interaction between the insulin receptor and a signal terminator (Kwon and Pak, 2010).

To conclude, caveolins are integral plasma membrane proteins possessing a characteristic hairpin shaped topology with both N- and C-termini facing the cytoplasm. They all share a common signature motif in their N-terminal part and an oligomerization domain allowing the formation of complex oligomerized structures that compose an essential part of the caveolar coat.

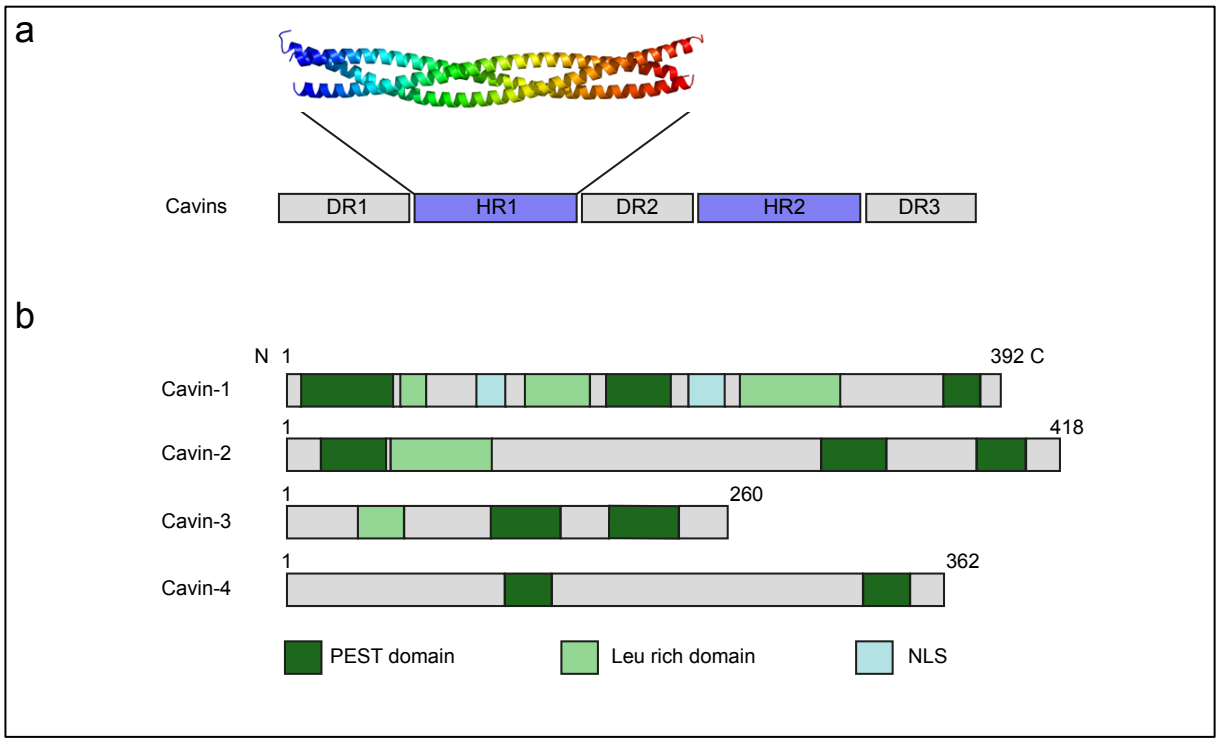

Figure 11. Cavins structure and caveolae morphogenesis

(a) General structural organization of cavins. Three disordered regions (DR) are separated by two coiled coil (ordered) regions (HR) (adapted from Kovtun et al., 2014). **(b)** Cavins domains. PEST domain mediates cavins degradation and Leu-rich domain mediates protein-protein interaction (based on Bastiani et al., 2009). Cavin sizes are heterogenous. Cavin-1 is the only member possessing nuclear localization sequences.

2.1.1.2 Cavins

Cavins are a family of cytosolic proteins which comprises four members: PTRF, SDPR, SRBC and MURC. Their caveolar localization and function pushed the scientists to gather these proteins under the name of “cavins” and rename them from cavin-1 to cavin-4 (Vinten et al., 2005; Bastiani et al., 2009; McMahon et al., 2009). As the caveolin family, the last member of the cavin family (cavin-4) is restricted to muscle cells (Ogata et al., 2008). Initially, polymerase 1 and transcript release factor (PTRF) was first identified as a regulator of RNA polymerase 1 (Jansa et al., 2001). Vinten and colleagues identified a 60 kDa protein associated with the caveolar coat in adipocytes. The protein was therefore called cavP60 (Vinten et al., 2001). Three years later PTRF has been reported to be enriched at the caveolar coat (Aboulaich et al., 2004), shortly after, PTRF and cavP60 appeared to be the same protein and thus were renamed cavin (Vinten et al., 2005).

SDPR was first described as a phosphatidylserine binding protein thus named PS-p68 (Burgener et al., 1990). When it was involved in serum deprivation response, it was renamed serum deprivation-response protein (SDPR) (Gustincich and Schneider, 1993). SDPR was shown to associate together with the protein kinase C α (PKCα) to the caveolar coat (Mineo et al., 1998). The SDPR-related gene product that binds to c-kinase (SRBC) was also involved in the serum deprivation response and first identified as a binding partner of PKCδ and thus named protein kinase C delta-binding protein (PRKCDBP) (Izumi et al., 1997). Both SRBC and SDPR were found in the mass spectrometry analysis that identified cavin-1 (Aboulaich et al., 2004).

Cavin-1 is required for caveolae formation (Hill et al., 2008; Liu et al., 2008). Cavins are proteins from 31 to 47 kDa with 261 to 425 amino acids. The four proteins share the same topology (Hansen et al., 2009). *In silico* analysis revealed that cavins possess two conserved α helical regions (HR) that are basic and positively charged. These HR regions are separated by acidic and negatively charged disordered regions (DR) (Fig. 11a). The HR1 region mediates cavin trimeric oligomerization (Kovtun et al., 2014). Indeed, cavin-1 can form trimers with either two cavin-1 or with cavin-1 and cavin-2 or with cavin-1 and cavin-3 (Fig. 14). All members of the cavin

family except cavin-4 carry a leucine zipper motif in the HR1 region that mediates protein-protein interaction (Fig. 11b). These leucine zipper domains are required for cavin recruitment at the plasma membrane (Wei et al., 2015b). Moreover all four cavins exhibit a short half-life due to the presence of PEST motifs that mediate proteasomal degradation (Fig 11b). Cavins have a basic C-terminal domain that participates to their membrane anchorage (Parton and del Pozo, 2013). Finally cavin-1 possesses two nuclear localization signals (Hansen and Nichols, 2010).

All cavins exhibit multiple phosphorylation sites. For example cavin-1 possesses more than twenty tyrosine and serine phosphorylation sites (Kovtun et al., 2014). Cavin-1 phosphorylation has been linked to Cav1 phosphorylation in the context of insulin signaling (Kruger et al., 2008) and have been suggested to participate to the control of cavin-1 fragmentation at the caveolar coat (Aboulaich et al., 2004). Cavins binds to phosphatidylserine (Ptdser) (Burgener et al., 1990). In addition cavin-1 and cavin-2 exhibit a high affinity for phosphatidyl 4,5 bisphosphate (PiP_2) (Kovtun et al., 2014).

In summary, cavins are cytosolic proteins associated to the caveolar coat. All four cavins present a similar strucuture with a first coiled coil helical region that mediates trimeric association and a second coiled coil helical region that mediates hetero-association of cavin trimers.

2.1.1.3 Accessory proteins

Several non-essential caveolar components have been also identified since then. The F-BAR protein PACSIN2 (Protein Kinase C and Casein Substrate In Neurons) also called syndapin 2, which regulates and senses membrane curvature and participates to caveolae morphogenesis (Hansen et al., 2011; Senju et al., 2011). The dynamin2 GTPase and the dynamin-like ATPase Eps15 homology-domain containing protein 2 (EHD2) oligomers localize at the caveolar neck (Oh et al., 1998; Stoeber et al., 2012; Ludwig et al., 2013). While dynamin2 is involved in caveolae internalization, EHD2 controls caveolar dynamics and stability at the plasma membrane (Morén et al., 2012). In addition EHD2 and other EHDs (1 and 4)

are responsible for caveolae clustering into membrane ultrastructure during mechanical stress (Yeow et al., 2017). More recently, our laboratory also demonstrated that EHD2 links caveolar dynamics to gene transcription, since mechanical release of EHD2 in the cytosol leads to its nuclear translocation and initiation of transcriptional programs (Torrino et al., 2018, submitted).

2.1.2 Lipid composition

Very early, it was shown that caveolae are plasma membrane nanodomains enriched in sphingolipids (Tran et al., 1987) and cholesterol (Rothberg et al., 1990). Moreover their resistance to detergent treatment (Sargiacomo et al., 1993) primarily led the scientists to classify caveolae as “lipid raft” and later as caveolin-enriched nanodomains (Simons and Ikonen, 1997; Simons and Sampaio, 2011). The lipid composition of caveolae may be explained by the affinity of the caveolar components such as Cav1 or cavin-1 for specific lipids. As mentioned in the chapter 2.1.1.1 Cav1 exhibit a high affinity for cholesterol mediated by its CRAC motif (Murata et al., 1995; Thiele et al., 2000; Epand et al., 2005). Cholesterol is an essential caveolar component required for *bona fide* caveolae biogenesis. Indeed, drugs removing cholesterol lead to caveolae flattening and disassembly (Rothberg et al., 1992). Likewise, cavins binds to Ptdser with high affinity and specificity (Burgener et al., 1990; Hill et al., 2008), which is a key element of the plasma membrane that influences caveolae assembly and dynamics. Indeed, decreased Ptdser induced by cavin-1 loss impairs caveolae stability/formation (Hirama et al., 2017). In addition Cav1 has been shown to bind *in vitro* to Ptdser and phosphatidylinositol 4,5 bisphosphate (PiP_2) through its scaffolding domain (Arbuzova et al., 2000; Wanaski et al., 2003) which most likely constitute a common binding site for cholesterol, Ptdser and PiP_2. In addition, caveolae lipid composition not only consists of Ptdser and PiP_2 but also of sphingolmyelin, glycerophopholipids, and gangliosids such as GM1 (Iwabuchi et al., 1998; Ortegren et al., 2004; Sonnino and Prinetti, 2009).

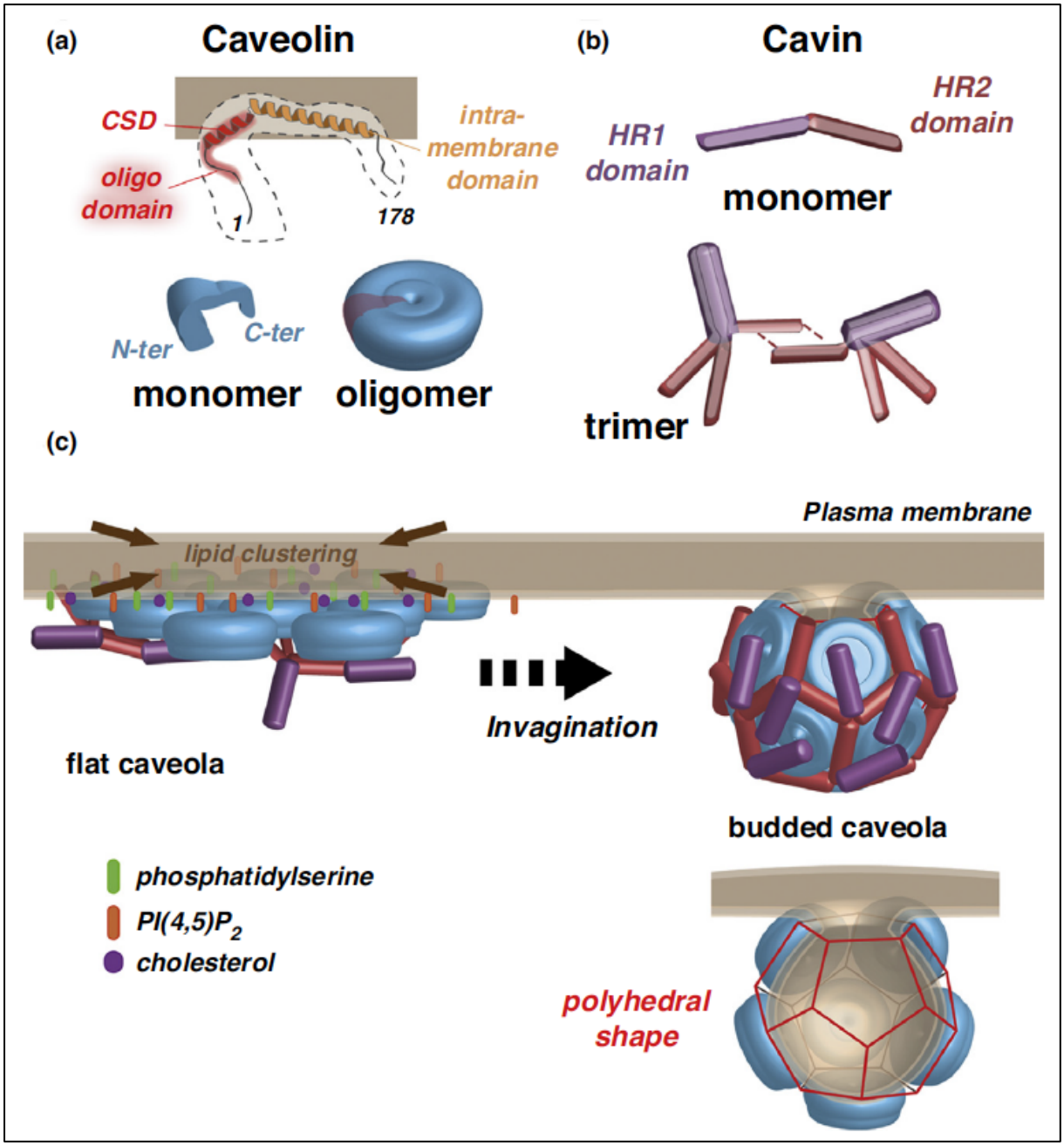

Figure 12. Putative model of caveolar coat assembly and organization

(a) Schematic model of Cav1 topology. Cav1 is inserted into the plasma membrane through the caveolin scaffolding domain (CSD; red), an amphipathic helix part of the oligomerization domain (diffuse red), and through a second amphipathic helix, the intra-membrane domain (orange). Based on Cav3 ternary structure, Cav1 monomers may assemble as a disk-shaped oligomer with the C-terminal part oriented toward the center. **(b)** Cavin monomers exhibit two helical rich domains, HR1 and HR2, that may form coil-coiled structures. Cavins, through interaction with the HR1 domain, can form trimers consisting of either three cavin-1 or two cavin-1 associated with one cavin-2 or one cavin-3 protein. The cavin-1 isoform could be responsible for a more complex assembly through the coiled-coil domain 2 (cc2) sequence in the HR2 domain. **(c)** At the plasma membrane, Cav1 oligomers cluster specific lipids such as cholesterol, $PI(4,5)P_2$ and phosphatidyl serine involved in the recruitment of cavin trimers. This is followed by caveola invagination, a process not completely understood. It has been recently suggested that the overall architecture of the caveolar coat made of caveolins and cavins would best fit with a polyhedron structure. In this model, Cav1 oligomers position on each pentagonal face and cavin complexes align with the vertices and cover the Cav1 oligomers. (from Lamaze et al., 2017)

2.1.3 Caveolar ultrastructure

For many years not much was known on caveolae ultrastucture. Only very recent data allowed the scientists to glimpse the caveolar coat structure. Approximately 150 to 200 Cav1 monomers associate with 15-20 cavins trimers to form a caveola. It was proposed that the caveolins oligomerize and organize as “discs” where N-ter ends are at the periphery of the discs, mediating oligomerization and C-ter at the center of the discs. Each disc constitutes a pentagonal face of the caveolar dodecahedron. The net of cavins stabilizes the caveolin discs within the caveolae (Pelkmans and Zerial, 2005; Ludwig et al., 2013; Gambin et al., 2014; Ludwig et al., 2016; Stoeber et al., 2016; Lamaze et al., 2017) (Fig. 12). But still, this hypothesis does not perfectly match the organization of the caveolar coat when observed with deep-etch EM.

2.2 Caveolae biogenesis: from protein synthesis to the caveolar bulb

Caveolae biogenesis requires the recruitment of several essential elements (Fig. 12). Cav1 and Cav3 are essential for caveolae biogenesis since their depletion causes a complete loss of caveolae in their respective tissues (Drab et al., 2001; Galbiati et al., 2001). In contrast Cav2 is not essential for caveolae formation (Razani et al., 2002b), however it may participate to caveolae formation in some cell types (Lahtinen et al., 2003; Sowa et al., 2003). For several years, Cav1 was believed to be sufficient for caveolae biogenesis since exogenous expression of Cav1 generated caveolae-like structures at the plasma membrane of lymphocyte and bacteria (Fra et al., 1995; Walser et al., 2012). Nevertheless, cavin-1 identification brought to light a new essential component for *bona fide* caveolae formation. Indeed cavin-1 ablation leads also to a loss of caveolae. Yet, due to transcriptional co-regulation of cavin-1 and all three caveolins, cavin-1 knocked out mice exhibit a markedly decreased caveolins expression (Liu et al., 2008). Therefore it was not clear whether this phenotype was attributable to cavin-1 loss. By using prostate cancer cells (PC3) and notochord cells of zebrafish that have the particularity to express caveolins despite the lack of cavin-1 expression, Hill and colleagues observed in the absence of cavin-1, caveolins remaining in “flat” caveolae (Hill et al., 2008). From these studies, it

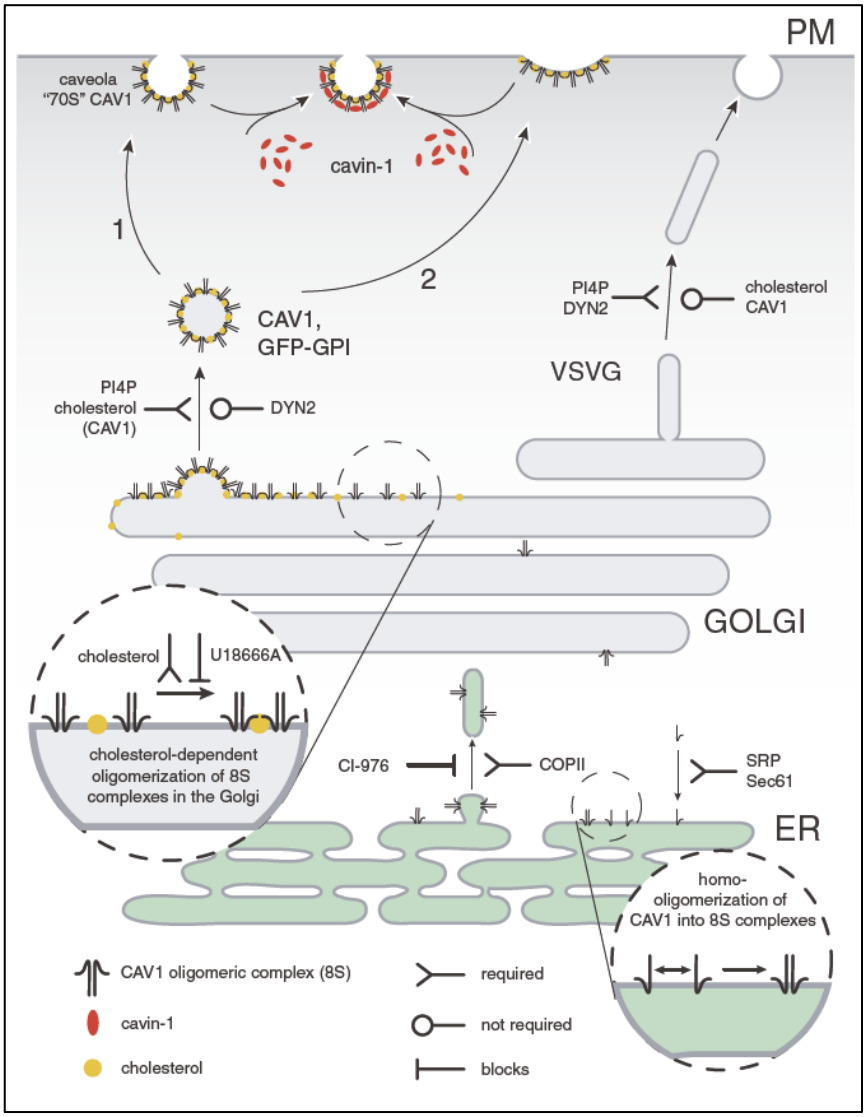

Figure13. Model of caveolae assembly and biosynthetic trafficking of Cav1 (Hayer et al., 2010b)

clearly appeared that both Cav1/3 and cavin-1 are necessary for *de novo* caveolae formation. Evolutionary studies revealed that caveolins are conserved among vertebrates and invertebrates. Nevertheless there are no evidences supporting the ability of CeCav1 to form caveolae in *C.elegans* (Kirkham et al., 2008). In addition the absence of orthologues of cavin gene family in invertebrate suggests that this family is restricted to vertebrate and that caveolae morphogenesis appeared with cavins evolution (Hansen and Nichols, 2010). Furthermore it suggests that caveolins may have biological functions independently from caveolae.

2.2.1 Caveolin-1: Tale of a journey from the ER to the plasma membrane

During Cav1 mRNA traduction, the signal recognition motif of the newly synthetized N-ter protein is recognized by SRP (Signal Recognition Particle), allowing Cav1 concomitant ribosomal synthesis and integration into the ER membrane (Monier et al., 1995). After its synthesis, Cav1 undergoes a first stage of homo-oligomerization of 7-14 Cav1 into 8S complexes in the ER (Monier et al., 1996; Hayer et al., 2010b). Caveolins are then transported through COPII vesicles to the cis-Golgi apparatus, a process requiring the specific DXE export motif. In the median Golgi apparatus, Cav1 further oligomerizes into 140-160 Cav1 complexes of 70S and associates with cholesterol and specific lipids generating higher ordered nanodomains (Epand et al., 2005; Pelkmans and Zerial, 2005; Pol et al., 2005; Hayer et al., 2010b) (Fig. 13). The Cav1-dependent clustering of specific lipids will contribute to the recruitment of other caveolar coat components such as cytosolic cavins which have high affinity for Ptdser (Kovtun et al., 2014).

2.2.2 Cavin recruitment and caveolae morphogenesis

As mentioned above, cavins are cytosolic proteins identified as components of the caveolar coat. The striated structure observed in the caveolae cytosolic face has been recently proposed to be due to the presence of cavins rather than caveolin oligomers (Gambin et al., 2014; Kovtun et al., 2014; Ludwig et al., 2016; Stoeber et al., 2016). Cavins are recruited at the very last steps of caveolae morphogenesis; only after preassembled Cav1 oligomers are exported to the plasma membrane.

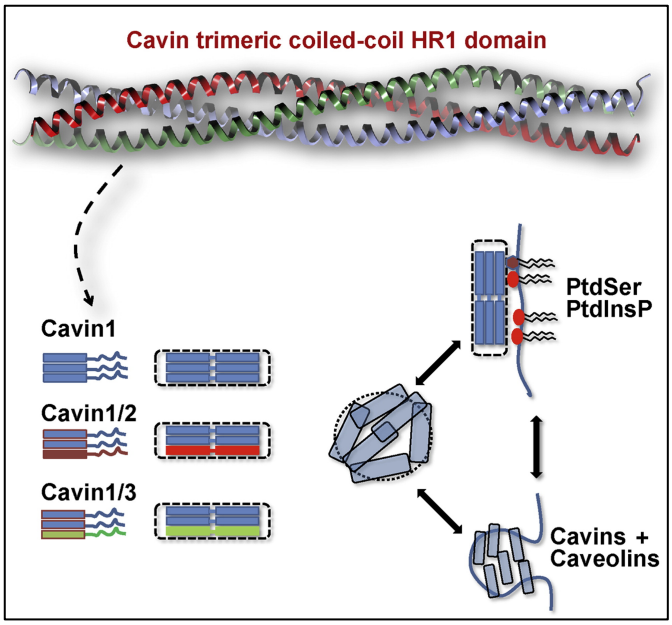

Figure 14. Model for the assembly of the cavin coat (Kovtun et al., 2014)

Cavins were first believed to be recruited through interaction with Cav1 (Bastiani et al., 2009). However recent studies suggest that cavins are rather recruited by Ptdser and PiP_2 at the caveolar nanodomains at the plasma membrane through electrostatic-based interactions between the negatively charged headgroups and the HR1 and HR2 cavin domains (Burgener et al., 1990; Hill et al., 2008; McMahon et al., 2009; Hirama et al., 2017) (Fig. 12 and 14). Cavin-1 is necessary for the recruitment of other cavins and plays a key role for caveolae morphogenesis. Recently, cavin-1 recruitment at caveolae have been suggested to play the role of a “net” that traps caveolin discs together and further invaginates the plasma membrane (Stoeber et al., 2016) (Fig. 12). Cavin-2 is essential for caveolae biogenesis in specific tissues such as lung and adipose (Hansen et al., 2013). Cavin-2 recruits cavin-1 and regulates membrane curvature as cavin-2 overexpression generates membrane tubulations (Hansen et al., 2009). Together with cavin-3; it controls the budding and dynamics of caveolae (Nabi, 2009; Mohan et al., 2015). However, cavin-3 is not essential for caveolae biogenesis as cavin-3 knock out does not impair caveolae formation in mouse model (Liu et al., 2014). In contrast the role of cavin-4 in caveolae morphogenesis remains elusive (Bastiani et al., 2009; Hansen and Nichols, 2010).

2.2.3 Recruitment of accessory proteins

In addition to essential proteins, a set of accessory proteins is recruited to the caveolar coat to control caveolae dynamics. The dynamin-like ATPase EHD2 is recruited at the level of the caveolar neck in an ATP binding dependent manner and requires its homo-oligomerization. EHD2 is involved in caveolae dynamics since it is associated to the static population of caveolae. Indeed, EHD2 depletion leads to an increase of caveolar dynamics while EHD2 overexpression induces caveolar retention at the plasma membrane (Morén et al., 2012; Stoeber et al., 2012). Moreover dynamin 2 is also localized at the caveolar neck and mediates caveolae budding and fission (Pelkmans et al., 2002). Caveolar retention by EHD2 is mediated by preventing dynamin2 recruitment by both EHD2 and PACSIN2 (Senju and Suetsugu, 2015). PACSIN (Syndapin) family members PACSIN2 and the muscle-restricted isoform PACSIN3 are also localized at the caveolar structures. Their mechanism of recruitment remains unknown. However, PACSIN2 phosphorylation

modulates its binding to the plasma membrane. Moreover PACSIN2 depletion decreases caveolae population and increases caveolins and cavins complexes at the plasma membrane (Hansen et al., 2011; Senju et al., 2015).

2.3 Caveolae functions

Caveolar accessory proteins participate to the tight regulation of caveolae dynamics and mechanics. Moreover, caveolae constitute a large fraction of the plasma membrane. Therefore it is not surprising that caveolae play critical roles in highly regulated cellular processes. Indeed, as it has been emphasized in the literature, many functions have been ascribed to caveolae (Cheng and Nichols, 2016). New caveolar functions are regularly unveiled and many others remain to be discovered.

2.3.1 Caveolae mediated endocytosis and trafficking

Due to their resemblance with other vesicular shaped endocytic structures, the role of caveolae in cargo internalization has been questioned early (Montesano et al., 1982). However, studies on caveolae-mediated endocytosis are curbed by the lack of caveolae specific cargo and the inaccessibility from the outside of standard reagents such as antibodies to caveolar proteins. The simian virus 40 (SV40) has been described to enter the host cell through caveolae dependent endocytosis (Pelkmans et al., 2001). Nevertheless the specificity of this process has been later challenged as new studies suggesting that overexpressed exogenous Cav1 is degraded in the late endosome earlier misidentified as “caveosome” and SV40 would rather use another clathrin-independent endocytic pathway to enter the host cell (Engel et al., 2011; Hayer et al., 2010a). Cholera toxin subunit B (CTxB) and the autocrine motility factor receptor (AMFR) can be internalized through caveolae mediated endocytosis (Benlimame et al., 1998; Orlandi and Fishman, 1998). However both CTxB and AMFR are also internalized through other endocytic pathways therefore complicating the studies on their internalization through caveolae (Torgersen et al., 2001; Nichols, 2002). Moreover, lipids such as lactoceramide and cholesterol can also trigger caveolae endocytosis (Pagano, 2003; Sharma et al., 2003; Le Lay et al., 2006). A

subpopulation of caveolae also undergoes a “kiss and run” process of cyclic rapid appearance/disappearance at the plasma membrane (Pelkmans and Zerial, 2005). In addition, like clathrin-coated pits, some caveolae can scission from the plasma membrane, a process depending most likely from the dynamin 2 GTPase, which is present at the neck of some caveolae (Oh et al., 1998). In contrast to clathrin-coated pits, caveolae are less dynamic and their budding frequency is more variable (Thomsen et al., 2002; Pelkmans and Zerial, 2005). After caveolae scission from the plasma membrane, caveolin enriched vesicles fuse with the early endosome or multivesicular bodies (MVBs) (Shvets et al., 2015). The presence of Cav1 in MVBs may generate extracellular vesicules (EVs) containing Cav1. Indeed, Cav1 has been found in EVs produced by prostate cancer cells (Llorente et al., 2004) and in the plasma of melanoma patients (Logozzi et al., 2009). Nevertheless, the role of caveolin secretion remains unknown. In addition, a crosstalk between caveolae and other endocytic pathways exists: caveolar component such as Cav1, Cav3 and cavin-1 can impact clathrin independent carriers (CLIC) and GPI-AP enriched compartment (GEEC), independently from the caveolae structure. The inhibition of CLIC/GEEC pathway by Cav1 and Cav3 is mediated by their CSD (Chaudhary et al., 2014). Finally, caveolae have been found to mediate the transcytosis of several molecules such as low-density lipoprotein (LDL), albumin and insulin (Vasile et al., 1983; Ghitescu et al., 1986; Bendayan and Rasio, 1996).

2.3.2 Lipid homeostasis

Caveolae sense and regulate plasma membrane composition. Indeed the affinity of caveolar components for certain lipid species contributes to the spatial organization of lipids within the plasma membrane. For example, the loss of caveolae impairs the distribution of Ptdser within the lipid bilayer therefore perturbing Ras spatial nano-organization (Ariotti et al., 2014). Moreover caveolae also regulate the plasma membrane lipid composition through internalization of lipids such as sphingolipids (Shvets et al., 2015). Cav1 has been shown to be essential for fatty acids flip-flop (Meshulam et al., 2006). Fatty acids have been proposed to be transformed into triacylglycerol, another lipid of caveolae in adipocytes (Ost et al., 2005). In addition, the loss of caveolae leads to less abundant glycosphingolipids

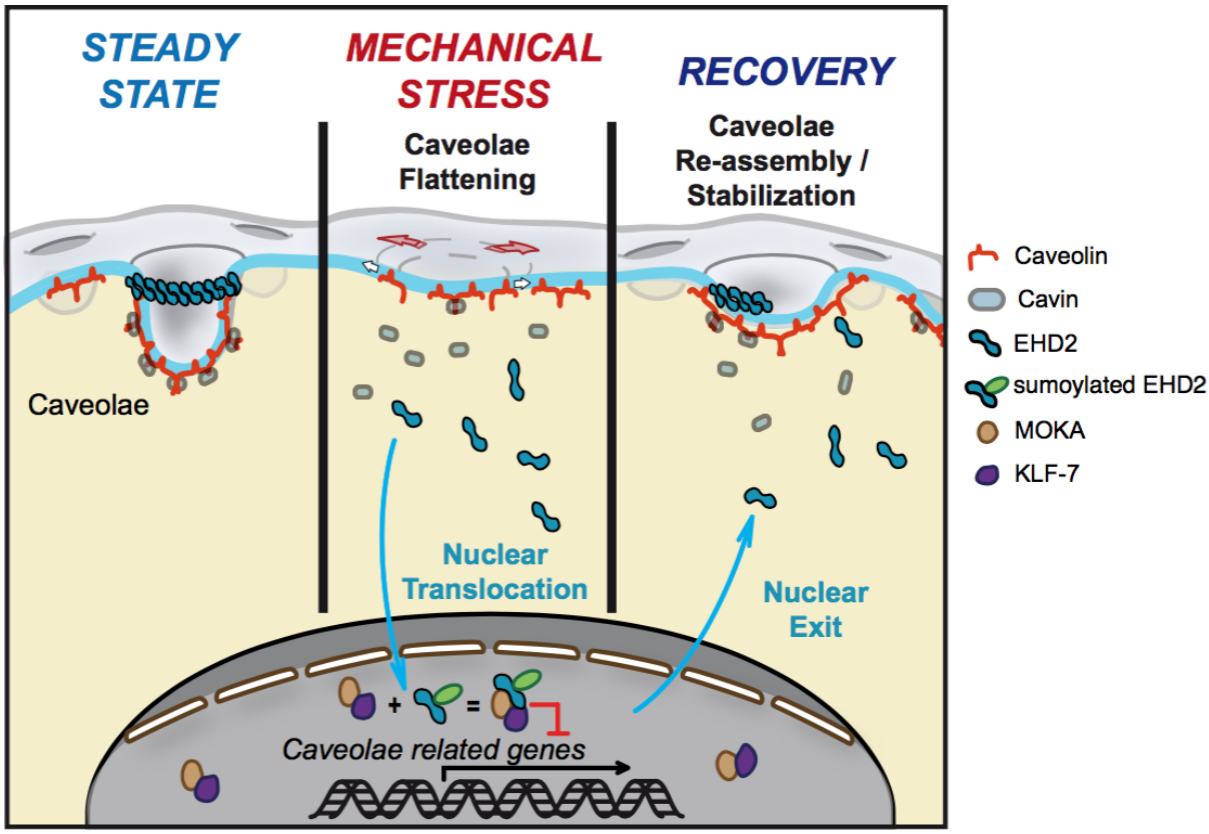

Figure 15. Caveolae mechanical disassembly

At steady state, caveolae remain invaginated and the integrity of the caveolar coat is intact (left). In contrast, upon membrane tension increase induced by a mechanical stress, the caveolar coat disassembles. Caveolins are released, cavins are released in the cytoplasm and EHD2 is translocated in the nucleus to form a complex with KLF-7 and MOKA cofactors to induce transcriptional programs (middle). In recovery, the caveolar coat reform, EHD2 is exported from the nucleus. (from Torrino et al., 2018, submitted)

(GSL) GM3 and phospholipids such as Ptdser, phosphatidylcholine and phophatidylethanolamine due to marked decreased expression of their synthetic enzymes (Ariotti et al., 2014). Cav1 has been involved in cholesterol trafficking from the lysosome (Mundy et al., 2012). Finally, Cav1 and Cav2 can be associated with lipid droplets in adipocytes and other cell types, (Fujimoto et al., 2001; Ostermeyer et al., 2001; Pol et al., 2001; Blouin et al., 2008).

2.3.3 Mechanoprotection

More than forty years ago Dulhunty and Franzini-Armstrong proposed that caveolae might function as a membrane reservoir which functions as a safety valve to prevent membrane rupture in muscle cells subjected to mechanical stress. Using muscle cells of *Rana Pipiens* frogs, which are constantly subjected to contraction/stretch cycles, the authors observed the opening of the caveolar neck upon cell stretch up to non-physiological levels thereby increasing the surface area of the cell (Dulhunty and Franzini-Armstrong, 1975; Prescott and Brightman, 1976). Thirty-six years later, using “home-made” tools combined with advanced physics and biochemical techniques to study caveolae dynamics and mechanics, our laboratory definitely established the mechanoprotective role of caveolae and its underlying mechanism. Indeed, we demonstrated that upon membrane tension increase induced by mechanical stresses such as osmotic cell swelling or cell stretching, caveolae rapidly flatten out and disassemble to release the additional excess of membrane stored in their invagination thereby “buffering” the membrane tension increase (Fig. 15). This process is passive, *i.e.* it is ATP and actin independent. In contrast, caveolae reassembly is reversible and requires both ATP and actin (Sinha et al., 2011). Taking this newly discovered caveolar function into account, it is not surprising that most of cells within tissue subjected to mechanical stress generated by forces such as blood flow, muscular contraction/relaxation, bladder/lung swelling *etc.*, have a large amount of caveolae. Interestingly, the mechanoprotective function of caveolae has been confirmed *in vitro* and *in vivo* as the lack of caveolae induced susceptibility to plasma membrane damages, impaired function of muscle cells in zebrafish and impaired notochord integrity during zebrafish development and endothelial cells integrity during increased cardiac output (Lo et al., 2015; Cheng et

al., 2015; Garcia et al., 2017; Lim et al., 2017). Considering the wide breadth of biological processes controlled by caveolae, the rapid disappearance of those structures and the release of caveolar components in the cell may have critical consequences by associating these processes to mechanosensing. Based on this observation our laboratory hypothesized that caveolae may constitute mechanosignaling hubs as these scaffolding structures have been involved in cellular signaling (detailed below) (Nassoy and Lamaze, 2012). The first observed consequence of the stretch-induced caveolae disassembly was a redistribution of Cav1 and a spatial reorganization of GSLs within the lipid bilayer together with c-Src activation (Gervasio et al., 2011). More recently, we could show that upon caveolae disassembly, the caveolar accessory protein EHD2 accumulates in the nucleus where it acts as transcription cofactor (Torrino et al., 2018, submitted) (Fig. 15).

2.3.4 Cell signaling

Numerous studies have long associated caveolae to the regulation of cellular signaling. Indeed, Cav1 was primarily described as a substrate of the Src kinase and heterotrimeric G protein found in Cav1 rich domains. It has been therefore proposed early that caveolae might be involved in cell signaling (Lisanti et al., 1994). It is now clear that caveolae function as signaling scaffolds for a wide range of signaling proteins which are found associated with the caveolar coat or to directly interact with caveolar components (Cheng and Nichols, 2016; Lamaze et al., 2017 see annex 2). The role of Cav1 in the regulation of intracellular signaling remains however poorly understood.

2.3.4.1 Indirect regulation of signaling

As mentioned earlier, caveolae play a key role in lipid sorting and GSL/cholesterol organization at the plasma membrane. Lipid nanoscale organization is a prominent parameter for the dynamics and structural integrity of transmembrane proteins such as plasma membrane receptors activation (Rao and Mayor, 2014; Blouin et al., 2016). Caveolae dynamics and mechanics could therefore actively modulate the activation of some plasma membrane signaling proteins (Nassoy and

Lamaze, 2012) (Fig. 17). For example, Cav1 depletion induces a redistribution of Ptdser and lipid composition changes within the plasma membrane resulting in the spatial reorganization of the lipid anchored Ras GTPase that control cell growth, proliferation and differentiation (Ariotti et al., 2014). In addition, stretch-induced caveolae disassembly leads to the redistribution of sphingolipids and Cav1 together with c-Src activation (Gervasio et al., 2011). On another hand, calcium pumps have been localized in caveolae (Fujimoto, 1993), and the mechanical disassembly of caveolae led to reduced Ca^{2+} through changes in Gαq/Cav1 association (Guo et al., 2015). Since caveolae also mediate endocytosis and cell trafficking, they might also modulate the endosomal control of signaling by delivering signaling proteins to this compartment (Gonnord et al., 2012).

2.3.4.2 Cavins-mediated signaling

The recently identified cavins such as cavin-1 may also play a role in caveolar signaling, as it is required for proper caveolae morphogenesis and functions. Indeed cavin-1 control the number of functional caveolae and therefore is a key element for the proper targeting of receptors in these structures (Moon et al., 2013; Li et al., 2014). For example, cavin-3 mediates ERK and Akt signaling by anchoring the caveolae at the plasma membrane through the myosin-1c (Hernandez et al., 2013) and regulates their dynamics (Mohan et al., 2015).

2.3.4.3 Signaling through Cav2

Cav2 remains the least studied caveolar component; hence its functions are poorly understood. However, Cav2 has been reported to play important roles in signaling pathways. Indeed Cav2 is required for proper estrogen receptor α (ER-α) activation by 17β estradiol (Totta et al., 2016). Moreover, Cav2 phosphorylation and fatty acylation seem to regulate insulin signaling. These two post-translational modifications prevent the interaction of the signal terminator SOCS3 with the insulin receptor thereby allowing the activation of IRS-1 and STAT3 (Kwon and Pak, 2010; Kwon et al., 2009, 2015). Surprisingly, Cav2 has been reported to control the nuclear

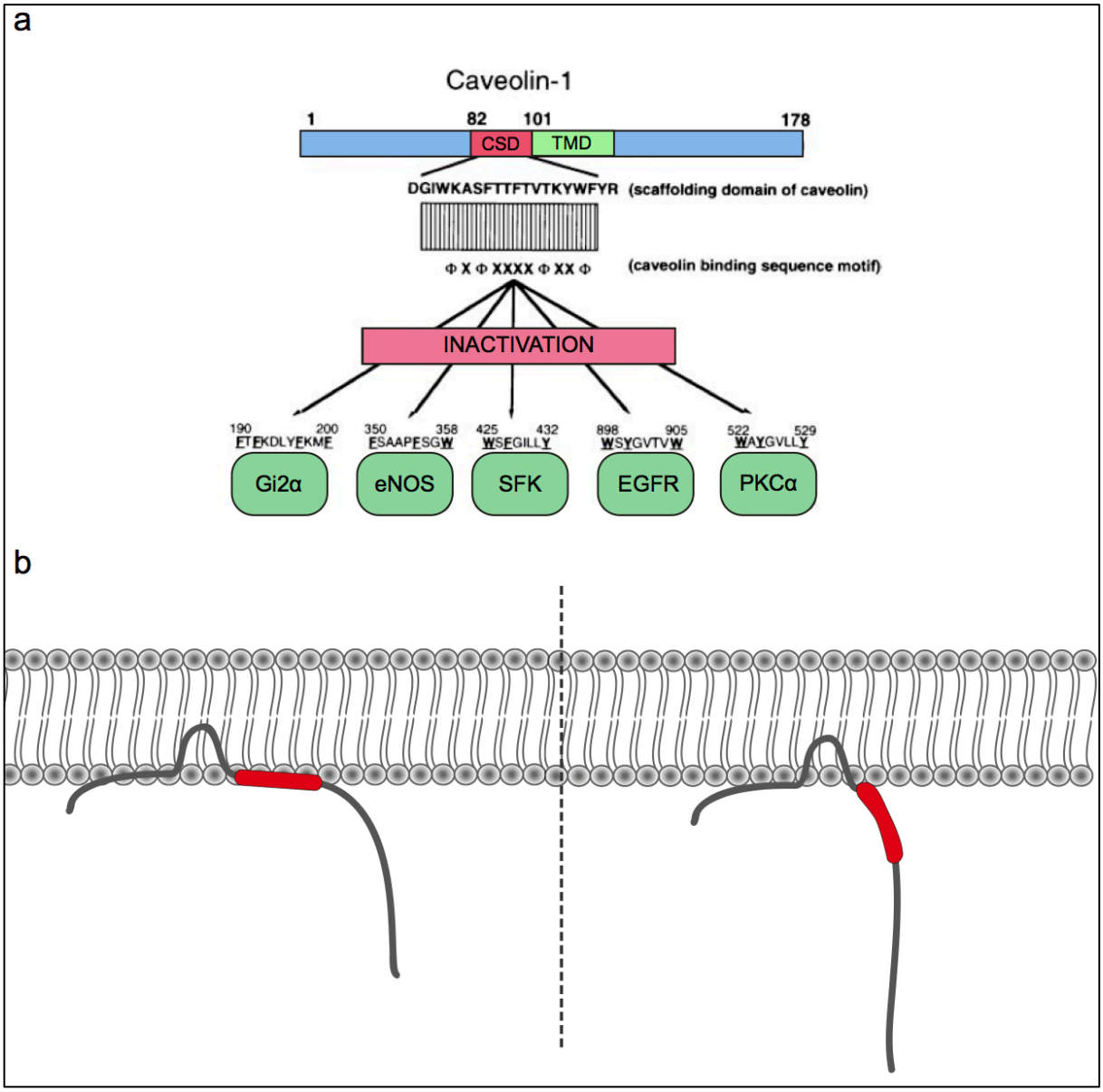

Figure 16. Cav1 signaling hypothesis

(a) Schematic of the caveolin signaling as originally proposed by Okamoto and colleagues (Okamoto et al., 1998) (based on Collins et al., 2012; Okamoto et al., 1998). **(b)** Two models of the association of Cav1 with the plasma membrane. A first model where the CSD is embedded inside the membrane inner leaflet thus poorly accessible as proposed by Kirkham and colleagues (Kirkham et al., 2008) (left). A second model where the N-terminus of Cav1 is extended thereby exposing the CSD (right).

targeting of signaling proteins such as phosphoERK whose nuclear translocation relies on Cav2 motif ^{154}SSV^{156} (Kwon et al., 2011).

2.3.4.4 Remaining controversies on Cav1 signaling

Cav1 has been extensively reported to interact with signaling proteins including endothelial nitric oxide synthase (eNOS), P2X purinoreceptor 7 (P2X7), epidermal growth factor receptor (EGFR), transforming growth factor β receptor type 1 (TGFBR1), heme oxygenase (HO) and many others, (reviewed in Lamaze et al., 2017). The interaction of Cav1 with these molecules and the modulation of their signaling have been suggested to occur through a specific Cav1 domain named caveolin scaffolding domain (CSD) (further detailed in 2.1.1.1) (Fig. 16a).

This domain has been first identified for the interaction and regulation of heterotrimeric G proteins, H-Ras and Src (Li et al., 1995, 1996). The role of this domain for Cav1 interaction has been confirmed for eNOS, H-Ras and HO (Garcia-Cardena, 1997; Song et al., 1997; Taira et al., 2011). Furthermore, a caveolin binding motif (CBM) has been identified by phage display and found in several Cav1 binding partners (Couet et al., 1997a; Garcia-Cardena, 1997; Song et al., 1997; Taira et al., 2011; Bernatchez et al., 2005; Kirkham et al., 2008) (Fig. 16a). Extensive studies on eNOS regulation by Cav1 brought deeper insight on the underlying molecular mechanism. These studies revealed that upon eNOS interaction with the Cav1 CSD, the lateral chain of phenylalanine 92 (F92) located in the CSD, reaches eNOS hydrophobic pocket resulting in an inhibition of its catalytic activity (Bernatchez et al., 2005; Trane et al., 2014). More recently a similar regulatory mechanism by CBM-CSD interaction resulting in catalytic inhibition of the target effector has been unveiled for HO regulation (Taira et al., 2011). Moreover, the CSD might directly mediate the Cav1 inhibitory effect, as peptides that mimic the CSD are sufficient to exert a negative effect on the effectors. In contrast, mutated CSD peptides release this inhibition most likely by competing with endogenous Cav1 (Bernatchez et al., 2011). Interestingly, only Cav1-mediated inhibitory effects have been reported across the literature, suggesting that Cav1 represses the effector catalytic activities.

However the only exception is the positive stimulation of insulin receptor kinase activity by Cav1 and Cav3 CSD (Yamamoto et al., 1998). It is possible however that this positive effect of the CSD on insulin signaling might be mediated by the inhibition of a regulatory intermediate.

Recent studies have questioned this regulatory model. The debate arised from Cav1 structural features (further detailed in the discussion). As mentioned in 2.1.1.1, the CSD is located from residue 82 to 101, next to the Cav1 TMD thus in close proximity with the plasma membrane. In addition, the CSD has been first predicted as an amphipathic helix that is partially embedded inside the plasma membrane thereby accessible with difficulty to potential binding partners (Kirkham et al., 2008) (Fig. 16b). However recent studies suggest that the CSD possesses a dynamic topology which is either partially unstructured or fully helical (Liu et al., 2016). Considering that the CSD undergoes structural transitions one could assume that CSD conformational changes may regulate its accessibility (Fig. 16b). FRAP experiments suggest that Cav1 is released from the caveolae upon mechanical disassembly (Sinha et al., 2011). It is therefore likely that the CSD conformation and thereby its accessibility within non-caveolar Cav1 may also differ from caveolar Cav1. In addition, alternative mechanisms may influence the dynamics of CSD accessibility to promote interactions with the CSD and their reversibility. Indeed Cav1 undergoes several post-translational modifications. Ser80 phosphorylation may results to the spreading of the N-ter part of Cav1 away from the plasma membrane due to charge repulsion thereby further exposing the CSD (Fig. 16b) (Ariotti et al., 2015; Jung et al., 2018). Similarly Tyr14 phosphorylation would facilitate CSD binding (Shajahan et al., 2012; Jung et al., 2018).

Likewise, the functional role of the CBM is also a subject of controversy as structural analysis of Cav1 binding partners revealed that this motif is buried in the deep interior of their ternary structure, and thus would not be available for protein interaction. Moreover the CBM encompasses three putative motifs that only consist in (ΦXΦXXXXΦ, ΦXXXXΦXXΦ, or ΦXΦXXXXΦXXΦ; Φ=aromatic residue (Trp, Phe, or Tyr); X=any residue) (Couet et al., 1997a) and therefore poorly discriminative and largely found across organism proteomes, including those devoid of caveolins.

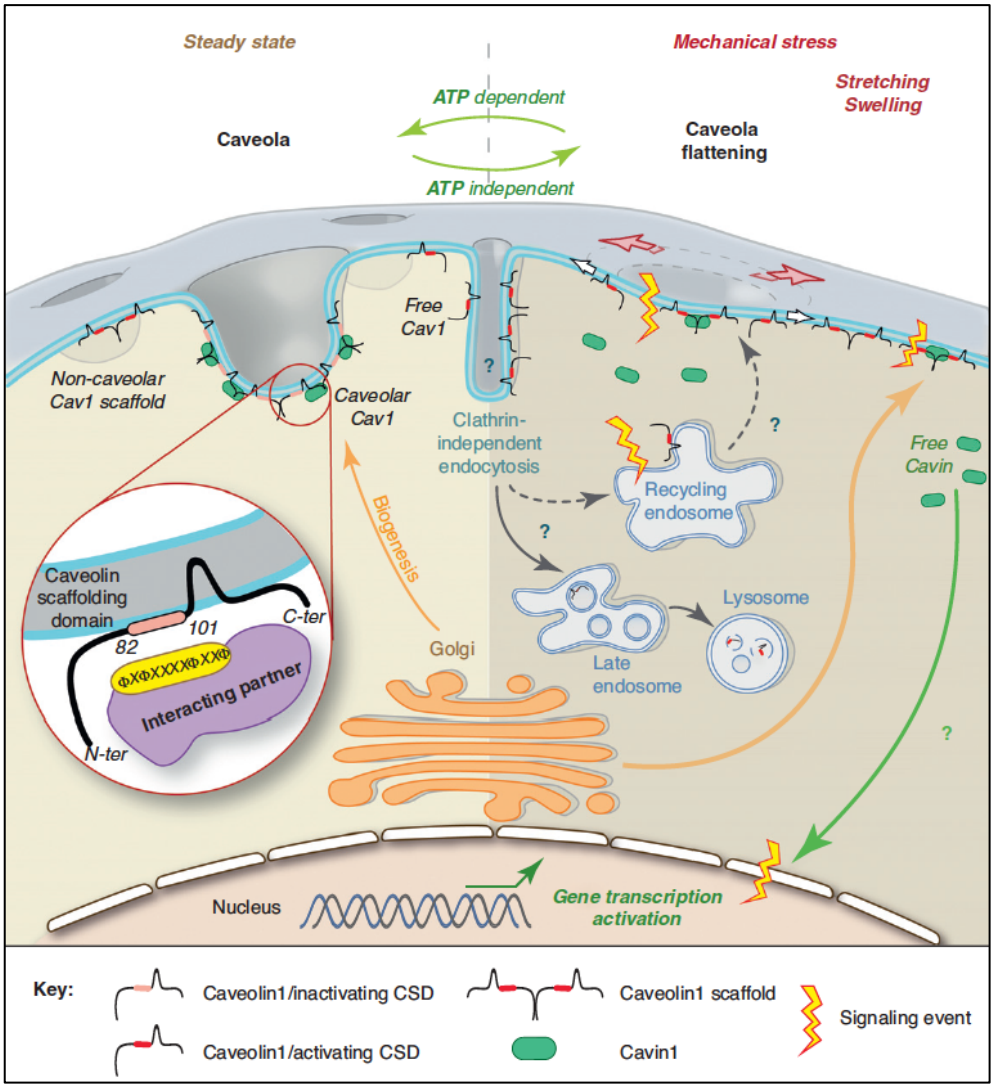

Figure 17. Molecular and cellular consequences of caveolar flattening induced by mechanical stress

Upon acute mechanical stress (hypo-osmotic swelling or stretching), caveolae flatten out in the plasma membrane to provide additional membrane and buffer membrane tension. Caveolar flattening releases Cav1 and Cavin-1 from the caveolar structure, increasing the amount of freely diffusing Cav1 and Cavin-1 at the plasma membrane. On the removal of the force, Cavin-1 and Cav1 rapidly reassemble into caveolae in an ATP-dependent process. This cycle represents the primary cell response to acute mechanical stress. Non-caveolar Cav1 is likely to be internalized by a clathrin-independent pathway that remains to be characterized. Endocytosed Cav1 becomes detectable in late endosomes (LE) and lysosomes, where it is degraded. It can also accumulate in the recycling endosome. Whether Cav1 and Cavin-1 follow identical intracellular routes after their release from caveolae by mechanical stress is unknown. It is possible that the endosomal (black arrows) and Golgi (orange arrow) pools of Cav1 are solicited during prolonged shear stress when the caveolar density is increased several-fold at the plasma membrane. Another possibility is that the released Cavins (green arrow) activate cellular processes to induce caveolar biogenesis, thereby increasing membrane reservoir size. Caveolar flattening can modulate mechanosignaling by several non-mutually exclusive mechanisms (lightning arrows). Released Cav1 and Cavins may interfere with the organization and dynamics of membrane microdomains and associated signaling molecules at the plasma membrane and endosomes. Gene transcription may be activated as a result of the nuclear translocation of released cavins. Magnification shows insertion of Cav1 and the Cav1 scaffolding domain (CSD) into the caveolar structure. The Cav1 CSD would form an in-plane amphipathic helix buried within the membrane in assembled caveolae. Many signaling molecules including several receptors and non-receptor tyrosine kinases and their downstream effectors, have been shown to interact with the Cav1 CSD in vitro (from Nassoy and Lamaze, 2012).

Moreover no particular CBM-containing protein enrichment has been found in Cav1 interactome (Byrne et al., 2012; Collins et al., 2012).

To conclude, considering the mechanoprotective role of caveolae. Our laboratory hypothesized that signaling through the multiple caveolar components could be coupled to caveolae mechanics. Therefore, the mechanical cycle of caveolae disassembly/reassembly would constitute a mechanical switch for several signaling pathways (Fig. 17).

2.4 Caveolae pathophysiology

Considering the multiple functions of caveolae, it is not surprising that any physical, biochemical and genetic perturbations impairing caveolar integrity, mechanics or dynamics would result in pathological situations. Indeed, there is a large literature on the pleiotropic phenotypes induced by deficient caveolar components. In the context of this work, it is interesting that the alteration of caveolae integrity mostly affects cell types chronically subjected to mechanical stress such as adipocytes, endothelial cells and myocytes. Deletion or mutation of caveolar components have been associated with multiple caveolinopathies such as lipodystrophy, vascular dysfunction, musculopathies (Ariotti and Parton, 2013) and cancer (Goetz et al., 2008).

2.4.1 Lipodystrophy

Cav1 or cavin-1 deficiency results in a lipodystrophic phenotype. Caveolae loss induced by cavin-1 deletion results in glucose intolerance and markedly decreased fat mass. Cavin-1 null mice have normal weight but exhibit hypertriglyceridemia and hyperinsulinemia which are characteristic of the lipodystrophic phenotype (Liu et al., 2008). Similarly Cav1 null mice have problems with lipid metabolism and adipocytes functions. These mice are small and lean. They show a resistance to diet-induced obesity with elevated triglycerides and free fatty acid levels. Moreover, these mice are insulin resistant which is consistent with the role of Cav1 and Cav3 as activators of insulin signaling (Yamamoto et al., 1998). In

agreement with Yamamoto and colleagues, Cav2 deletion in mice did not impair insulin signaling (Cohen et al., 2003). In addition Cav1 is found at the plasma membrane of key lipid storage organelles: adipocytes and lipid droplets (Blouin et al., 2008). Since insulin stimulation induces lipid uptake within the adipocytes, it is not surprising that Cav1 null mice have adipose atrophy (Londos et al., 1999). In humans, a rare case of homozygous nonsense mutation of *Cav1* (p.Glu38X) results in Berardinelli-Seip-Congenital Lipodistrophy (BSCL) (Kim et al., 2008). Likewise, a homozygous frame shift mutation (c.696_697insC) of *cavin-1* has been identified in another human lipodystrophy example (Hayashi et al., 2009). Other heterozygous frame shift mutations of *Cav1* have been later found in patients with lipodystrophy c.88delC and p.I134fsdel1-X137 (Cao et al., 2008) and p.Phe160X (Schrauwen et al., 2015). Similarly, another heterozygous *cavin-1* frame shift mutation consisting in a deletion in *cavin-1* gene c.947delA in a child with myopathy results in congenital lipodistrophy (Ardissone et al., 2013). Altogether these studies emphasize the prominent role of caveolae in lipid homeostasis and the maintenance of physiological processes (Lamaze et al., 2017).

2.4.2 Vascular dysfunction

As caveolae are important structures for the control of NO and calcium signaling (Isshiki and Anderson, 2003) (2.3.4) it is not unexpected that Cav1 disruption in mice leads to impaired NO and Ca^{2+} signaling in the cardiovascular system. This impairment results in altered contraction/relaxation and maintenance of the myogenic tone of the endothelium (Drab et al., 2001). Accordingly, eNOS activity is upregulated in Cav1 null mice, consistent with the inhibitory role of Cav1. In addition, loss of Cav1 caused endothelial cell proliferation and fibrosis (Razani et al., 2001). Cav1 ablation in mice also results in decreased angiogenic response to basic fibroblast growth factor (bFGF) (Woodman et al., 2003). *In vivo* treatment with CSD mimicking peptides decreased acetylcholine-induced vasodilatation and NO production. CSD peptides treatment also markedly decreases inflammation and vascular leak at the same extent as glucocorticoids. These results emphasize the prominent role of this Cav1 domain in the control of cell signaling and its potential therapeutic targeting (Bucci et al., 2000). Moreover high level of Cav1 expression has

been involved in atherosclerosis development (Fernandez-Hernando et al., 2010). Endothelial cells experience shear stress within the vessels due to blood flow. Loss of Cav1 in mice vascular endothelial cells induces susceptibility to acute rupture under high cardiac output (Cheng et al., 2015). Caveolae are mechanosensitive organelles that regulate vascular functions, therefore with a key role in vessels remodeling induced by shear stress (Yu et al., 2006).

2.4.3 Muscular dystrophies and cardiomyopathies

Mutations of Cav3, cavin-1 and cavin-4 have been associated with multiple musculopathies from dystrophies to cardiomyopathies (Hayashi et al., 2009). Thirty Cav3 mutations have been identified. These mutations lead to skeletal muscle dysfunction resulting in several musculopathies: limb-girdle muscular dystrophy, rippling muscle disease, distal myopathy and hyperCKemia. Cav3 mutations have been associated with sarcolemmal membrane alterations, disorganization of T-tubule network and cell signaling deregulation (Galbiati et al., 2001; Gazzerro et al., 2010). Since caveolae play a key role in membrane protection and lipid homeostasis, lack of caveolae would directly impair the cell response to mechanical stress (Cheng et al., 2015; Lo et al., 2015; Sinha et al., 2011). More recently our lab discovered that two mutations of Cav3 P28L and R26Q lead to Cav3 Golgi retention preventing caveolae formation at the plasma membrane. Hence myotubes with these Cav3 mutations are more prone to membrane rupture under mechanical strains. In addition, the central muscle signaling pathway IL-6/STAT3 is impaired in this context (Dewulf et al., 2018 under revision, see annex 3). Other muscle related signaling pathways such as those involving Ca^{2+}, p38MAPK and Akt might be affected by the absence of caveolae (Capanni et al., 2003; Weiss et al., 2008; Stoppani et al., 2011). Finally, Cav3 mutations alter the expression and trafficking of proteins participating to membrane integrity or membrane repair such as dysferlin and the Tri-partite motif (TRIM) protein mitsugumin 53 (MG53) (Capanni et al., 2003; Hernandez-Deviez et al., 2006; Cai et al., 2009).

2.4.4 Cancer

Caveolae have pleiotropic functions that have been implicated in multiple essential cancer processes such as cell migration, cell cycle progression, cell death/survival, cell transformation, angiogenesis and multidrug resistance (MDR). Hence, several studies have involved caveolae and caveolar processes in tumor development. In particular, Cav1 have received a lot of attention as it plays an important but complex role in tumor progression. Indeed, no consensus has been reached so far on the role of Cav1 in cancer. Dual and contradictory roles have been ascribed to Cav1 as it acts both as oncogene and tumor suppressor depending on the pathological context (Goetz et al., 2008; Lamaze and Torrino, 2015). The ability of Cav1 to control cell signaling (as described in 2.3.4.4) may play an important role in the regulation of oncogenic processes. The first evidence of the tumor suppressor effect came from the inhibition of anchorage-independent cell growth of transformed cells by recombinant Cav1 expression (Engelman et al., 1997). The tumor suppressor effect was then further confirmed by the ability of fibroblasts depleted for Cav1 to form tumors in mouse model through p42/44MAPK hyper activation (Galbiati et al., 1998). Similarly, pancreatic carcinoma cells overexpressing Cav1 had reduced tumor formation due to MAPK inhibition and decreased anchorage-independent growth (Han et al., 2009). Moreover, consistently with the tumor suppressor role of Cav1, decreased Cav1 levels have been reported in breast, lung, ovary, thyroid and mesenchymal cancers. Nevertheless, Cav1 can also play an opposite role depending on cancer types. Indeed, Cav1 has oncogenic effects as it promotes tumor progression in prostate cancer in mouse models (Williams et al., 2005). In addition, clinicopathological analysis of human bladder, breast, renal, brain, lung and prostate cancers revealed that Cav1 upregulation is correlated with reduced survival (reviewed in Williams and Lisanti, 2005; Goetz et al., 2008)). Therefore, Cav1 expression has been proposed as reliable prognosis and diagnosis marker. On another hand, as Cav3 mutation P104L leading to musculopathies, Cav1 mutation P132L has been identified in some human breast cancers. This mutation is involved in cell transformation and MAPK activation, promoting cell invasion (Hayashi et al., 2001). Six other Cav1 mutations have been identified and associated with ER-α positive breast cancers (Li et al., 2006). Cav1 play also a key role in the tumor microenvironment. Indeed loss of Cav1 expression in stromal cells has been

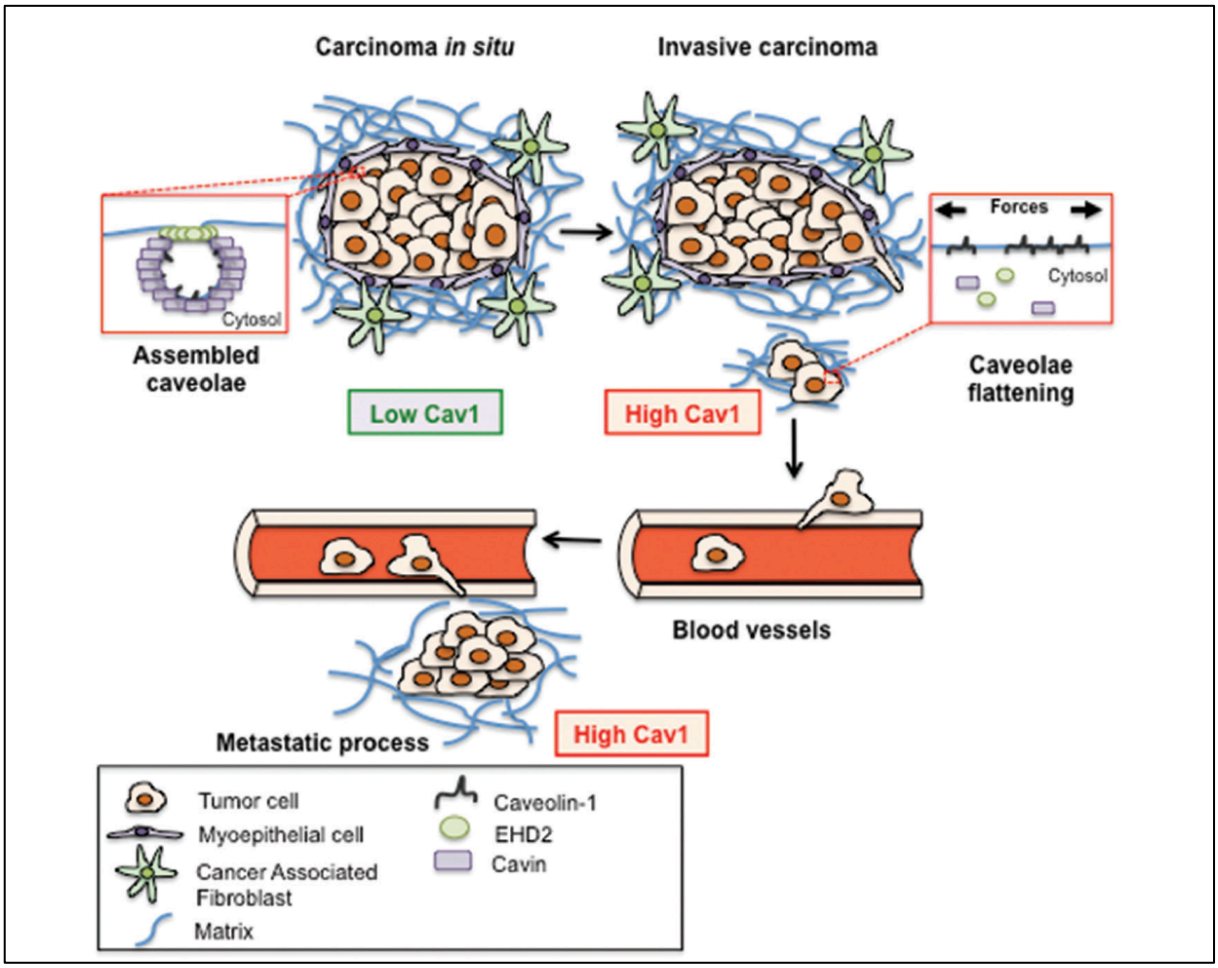

Figure 18. Potential role of caveolae in tumor progression

Potential role of caveolae in tumor progression. Tumors are often characterized by enhanced rigidity and stiffness and recent evidence shows that tumor progression is associated with alterations in tissue and cell mechanics. Caveolin-1 (Cav1), the main constituent of caveolae, is clearly involved in tumor progression. A biphasic expression pattern could be correlated with distinct Cav1 functions. It was shown that Cav1 expression is low during the first stage of tumor progression. However, Cav1 is overexpressed during the advanced cancer phases, including metastatic process. Thus, Cav1 would act as a tumor suppressor at early stage of transformation and tumor progression while it would play an oncogenic role inducing migration and metastasis at later stages. Our hypothesis is that the dual role of Cav1 in tumor progression may be explained by their recently discovered new function as mechanosensors that adapt the cell response to mechanical forces. Thus, in *in situ* carcinoma, when proliferative tumor cells become confined by the basal membrane, functional caveolae respond as mechanosensors with cycles of caveolae disassembly/reassembly induced by external forces. In invasive carcinoma, tumor cells break down the basal membrane and invade the extracellular matrix. Tumor cells are thus exposed to mechanical forces generated by the extracellular matrix and tissue stiffness. Increased mechanical environment may overwhelm and alter the functional cycle of caveolae disassembly/reassembly. This in turn may impair the caveolae mechanical response and Cav1 dependent mechanosignaling thereby promoting migration and metastasis formation. (Lamaze and Torrino, 2015)

associated with poor prognosis in breast cancer and correlates with the upregulation of ECM components in the tumor microenvironment (Witkiewicz et al., 2009; Trimmer et al., 2011). In addition, stromal expression of Cav1 contributes to the remodeling of the microenvironment, which facilitates tumor invasion and metastasis (Goetz et al., 2011). However, the mechanism underlying the role of Cav1 in tumor development might be more complex than a matter of level and pattern of expression. Indeed, recent studies emphasize the prominent role of mechanical strains generated by the microenvironment of the tumor (Kai et al., 2016). Therefore, considering the essential role of caveolae in cell mechanoresponse, how caveolae dynamics and mechanics are affected by these mechanical strains should be investigated as well as the biological processes they mediate in the context of tumor progression, such as signaling (Fig. 18) (Lamaze and Torrino, 2015).

3 Type I interferon-induced JAK-STAT signaling

JAK-STAT is one of the most studied signaling cascades of the cell. This pathway is used by a wide array of cytokines and growth factors to transduce a multitude of signals and generate accurate gene responses. JAK-STAT signaling is involved in a wide breadth of biological processes such as hematopoiesis, innate and adaptive immunity, cell proliferation, differentiation, migration and apoptosis (Igaz et al., 2001; O'Shea et al., 2002; Villarino et al., 2017).

3.1 Interferons

Among the different cytokines that activate the JAK-STAT cascade, interferons (IFNs) are among the most studied. They represent the prototypical example of JAK-STAT signaling. Most cell types bind IFNs with a large variability in binding affinity and numbers of binding sites (200-10^3/cell) (Langer and Pestka, 1988). IFNs are secreted cytokines with a broad range of biological activities such as antiviral, antibacterial, cytotoxic and antiproliferative effects. Hence, these molecules constitute an essential element of the line of defense against viral infections and of

the immunosurveillance for cancer cells (Gresser and Belardelli, 2002; Santini et al., 2002). Thus, over the last three decades, recombinant IFNs have been used for clinical applications. Indeed, IFN-α2 used to be administrated in treatment of hepatitis C virus infection (Pfeffer et al., 1998) and IFN-β has been shown to be effective in multiple sclerosis (Paty and Li, 1993; Prosperini et al., 2014). Recombinant human IFNs have shown effectiveness for cancer treatment for the first time with hairy cell leukemia and for Kaposi's sarcoma. Since then, human IFNs have been approved for the treatment of a wide breadth of cancers such as metastatic malignant melanoma (Di Trolio et al., 2015).

3.1.1 Classification

More than 60 years ago, Isaac and Lindenmann discovered a secreted factor that prevents viral replication in chicken embryonic cells (Isaac and Lindenmann, 1957). Indeed, this factor was described as a "product of influenza viral interference" therefore named interferon, giving rise to the first member of the interferon family. On the basis of their structural, biological properties and their cognate receptors, IFNs are divided into three subfamilies: IFNs type I (IFN-α/-β), type II (IFN-γ) and type III (IFN-λ) (Platanias, 2005; Davidson et al., 2016). Indeed, IFNs type I share a common receptor named interferon alpha receptor (IFNAR), type II binds to interferon gamma receptor (IFNGR) and type III to IL28RA/IL-10Rβ. The first family of IFNs encompasses sixteen members: twelve IFN-α subtypes and IFN-β, -ε -κ, -ω. IFN-δ and IFN-τ have been described only in pigs and cattle and do not have human homologues (Pestka et al., 2004).

3.1.2 Specificity

IFNs type I perfectly illustrate the paradox of signaling, as they all possess similar structures and bind to the same receptor, yet result in distinct biological outcomes (Brierley and Fish, 2002). In addition to cellular mechanisms such as clathrin-dependent endocytosis that mediates signal specificity between type I and type II IFNs (Marchetti et al., 2006), signal specificity can also be achieved within the type I subfamily through the binding strength of the cytokine to one of the IFNAR

chains (Lamken et al., 2004). Indeed, an engineered IFN-α2 mutant with 30 fold higher affinity for IFNAR1 (in the range of IFN-β affinity) induces an IFN-β-like cellular response (Jaitin et al., 2006). In addition, this specificity can be also mediated through IFNAR endosomal sorting (Ng et al., 2015; Chmiest et al., 2016; Zanin et al., 2018).

3.2 Interferons receptors

IFNAR belongs to the family of helical cytokine receptors (hCR) class II, which thereby includes IFNGR and IL-10Rβ. IFNAR is a non-tyrosine kinase receptor. Indeed IFNAR1 and IFNAR2 do not possess intrinsic kinase activity and must be associated with cytosolic kinases to transduce signals.

3.2.1 IFNAR1, IFNAR2 and their isoforms

The IFNAR chains were first discovered in 1990 with the emergence of cloning techniques. Indeed, Uzé and colleagues identified one of the IFNAR chains as the receptor of human IFN-α8 (Uze et al., 1990). Four years later, another IFNAR chain (IFNAR2), that physically associates with a tyrosine kinase and later identified as IFNAR2c was described as a universal ligand-binding receptor to human IFN-α/-β (Novick et al., 1994). Finally, two truncated isoforms of IFNAR2 generated by alternative splicing, exon skipping or different polyadenylation sites were characterized: IFNAR2a and a secreted, thus soluble isoform IFNAR2b (Lutfalla et al., 1995). Due to the truncation of the cytosolic part, thereby isolating the receptor from downstream effectors, both isoforms do not process signal transduction (de Weerd et al., 2007). These non-functional IFNAR2 isoforms may serve to negatively regulate the signaling pathway (Gazziola et al., 2005). Another IFNAR1 isoform has been reported in cancer cells, however, it results most likely from an artifact or aberrant mRNA (Abramovich et al., 1994).

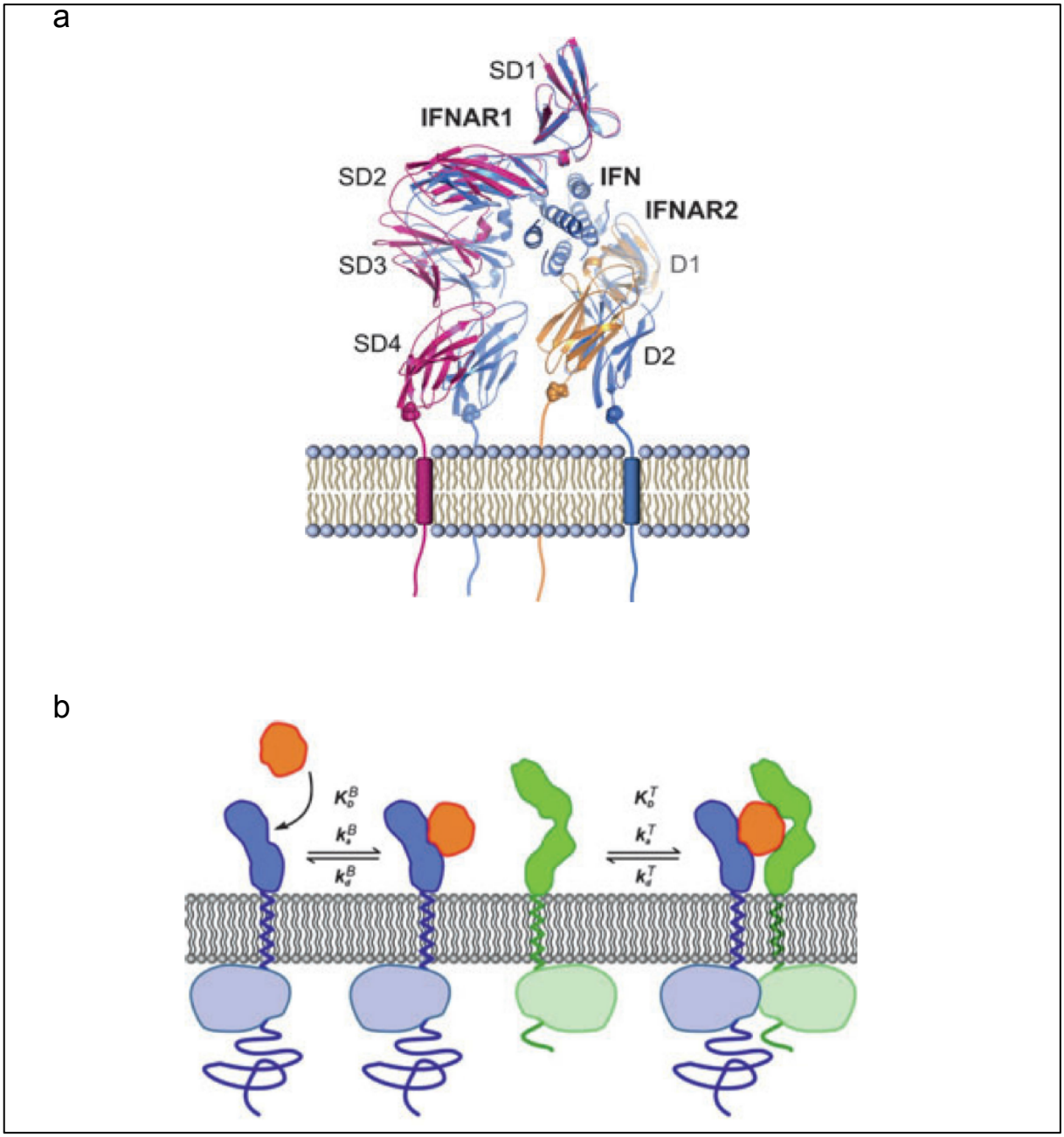

Figure 19. Structure and dynamics of IFN-IFNAR ternary complex formation
(a) Ligand-induced conformational changes in IFNAR (based on a comparison of unbound and bound structures). The bound conformation is in blue. (Piehler et al., 2012) **(b)** Two-step assembly of the ternary IFN-receptor complex in the plasma membrane (orange, IFN; blue, IFNAR2; green, IFNAR1): rapid and high-affinity binding of IFN to IFNAR2 is followed by recruitment of IFNAR1 into the ternary complex. (Piehler et al., 2012)

3.2.2 Structure and mechanism of activation

IFNAR is composed of two transmembrane proteins IFNAR1 and IFNAR2 with a structure similar to the immunoglobulin constant domain (Bazan, 1990). Both chains are heavily glycosylated resulting in a high molecular weight (120-130 kDa) despite their relatively short amino acid sequence length: IFNAR1 (557 aa) and IFNAR2c (515 aa) (Ling et al., 1995). Under no stimulation, IFNAR1 and IFNAR2 remain separated at the plasma membrane. IFNAR1 and IFNAR2 clustering requires binding of IFN (Cohen et al., 1995). The binding affinity of IFNs to IFNAR1 differs from IFNAR2. Indeed, Scatchard analysis revealed that IFNAR possess two binding sites: a low affinity site (of micromolar range) corresponding to IFNAR1 and a high affinity site (nanomolar range) corresponding to IFNAR2. The IFNAR1 extracellular domain (ECD) of 409 aa is subdivided into four domains named SD1 to SD4, each one harboring a fibronectin type III (FNIII)-like domain. SD1 contains residues responsible for plasma membrane glycosphingolipid binding (Ghislain et al., 1994). SD1-3 are essential for the cytokine binding and SD4 is essential for the ternary complex (IFNAR1-ligand-IFNAR2) formation (Lamken et al., 2005). According to a proposed model, upon IFN binding the N-terminal SD1 folds to form a lid above the bound IFN (Cajean-Feroldi et al., 2004; de Weerd et al., 2007; Piehler et al., 2012; Schreiber, 2017) (Fig. 19a). On the other hand, IFNAR2 ECD is composed of only two FNIII-like domains referred as D1 and D2 that are both involved in IFN binding. Finally, a two step assembly mechanism has been proposed for the formation of the ternary complex (Lamken et al., 2004; Gavutis et al., 2005; Piehler et al., 2012): A first step of ligand binding to IFNAR2 chain and a consecutive association of IFNAR1 chain to the preformed IFNAR2-ligand complex (Fig. 19b). Since IFNAR1 and IFNAR2 bind on the opposite sides of IFN, the newly formed ternary complex adopts a unique orthogonal shape (Piehler et al., 2012) (Fig. 19a). For type 1 IFN, studies suggest that the initiation of the signal transduction is rather induced by IFNAR dimerization than IFN-binding-induced rearrangement of ECD propagating to the cytosolic tail (Wilmes et al., 2015).

As mentioned earlier, IFNARs lack intrinsic kinase activity and thus their cytosolic tails need to be constitutively associated with cytosolic kinases to transduce the signal subsequently to formation of the ternary complex.

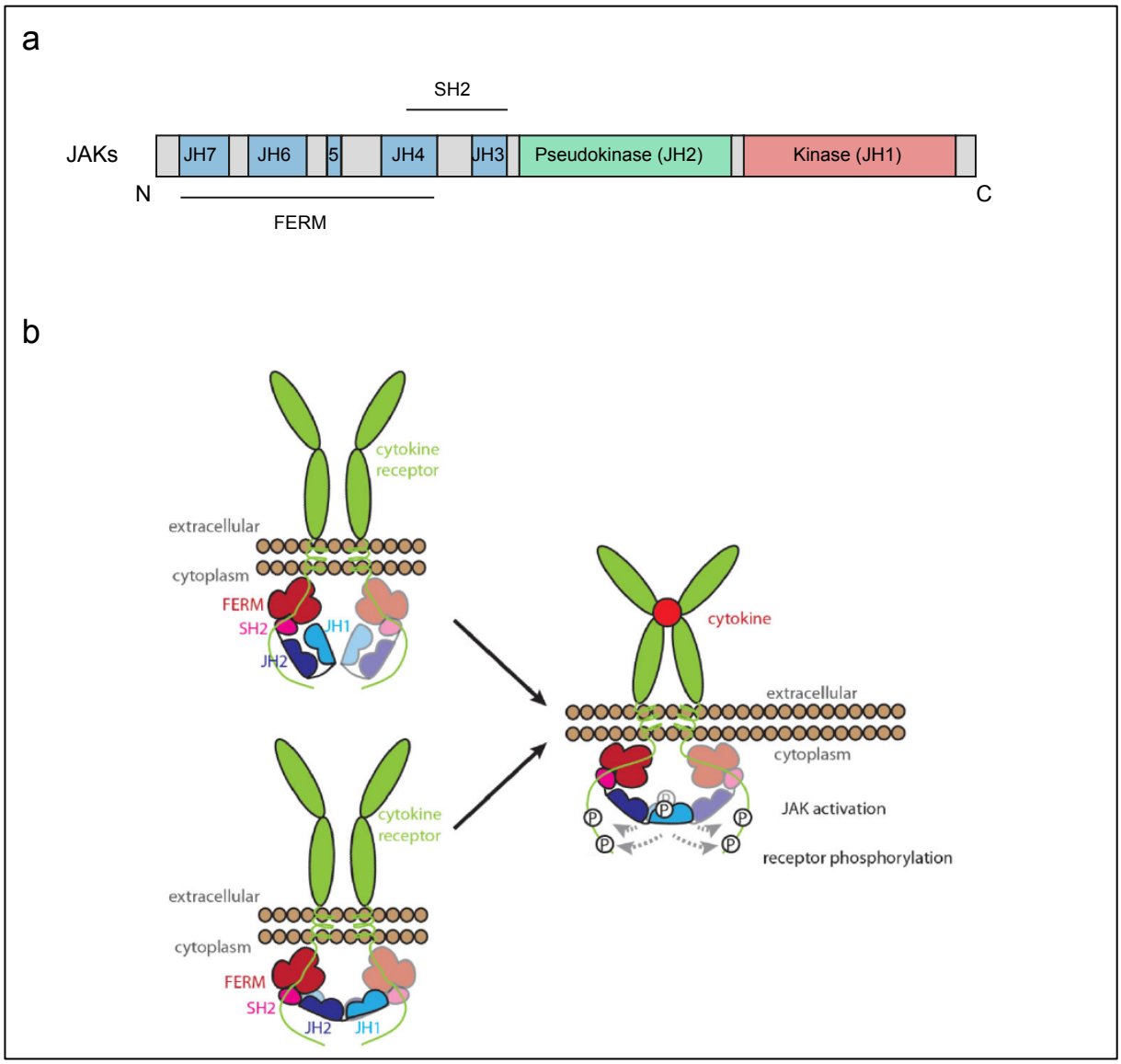

Figure 20. JAKs general structure and regulation

(a) JAK1 domains organization (based on Haan et al., 2006). **(b)** The two prevailing models for regulation of JAK kinase domain catalytic activity by the pseudokinase domain: (top) *in cis*; (bottom) *in trans*. In the *in cis* inhibition model (top), the pseudokinase domain binds the kinase domain within the same JAK monomer, leading to a suppression in catalytic activity. The *in trans* model for inhibition (bottom) involves the binding of the pseudokinase domain from one JAK to the kinase domain of another within a receptor-assembled JAK dimer to suppress the kinase domain's catalytic activity. Activation of JAK in either model involves reorientation of the JAKs to facilitate mutual trans-phosphorylation and thus activation of the JAK kinase domains. (from Babon et al., 2014)

3.3 JAK: Just another kinase...

JAK kinases are members of the large family of protein tyrosine kinases (PTK). The first two members of the JAK family (JAK1 and JAK2) were first discovered by Andrew Wilks from a PCR-based screen, aiming at identifying new PTKs. Therefore, these two proteins were initially termed “Just Another Kinase” (Wilks, 1989). These kinases have the particularity to carry both a functional kinase domain and a non-functional (pseudo) kinase domain, defining a new class of PTKs (Wilks et al., 1991). This singularity, prompted A. Wilks to rename this family “Janus Kinase” referring to the two-faced roman god of Gates (Wilks, 2008). In the meantime another member of the JAK family: TYK2 was identified (Krolewski et al., 1990; Firmbach-Kraft et al., 1990; David et al., 1995). JAK3 was later identified due to its restriction to hematopoietic cells (Kawamura et al., 1994).

3.3.1 Structural features

JAK kinases exhibit a high molecular weight (130-140 kDa). All four members share seven characteristic domains (Wilks et al., 1991), which are named JAK homology (JH) domains (Haan et al., 2006). In addition, the N-terminal part (JH3-JH7) comprises a Src homology domain-2 (SH2), and a 4.1, Ezrin, Radixin, Moesin (FERM) domain that targets JAKs to the membrane-proximal region of cytokine receptors (Fig. 20a). Both mediate their non-covalent association with the cytosolic tail of the receptor (Wallweber et al., 2014). Indeed, JAKs have been reported to be predominantly found at the plasma membrane, pre-associated to different cytokine receptors (Behrmann et al., 2004; Haan et al., 2006), which are required for JAK targeting at the plasma membrane.

The non-functional kinase domain JH2 is critical for the modulation of the catalytic domain (JH1) and are both positioned at the C-terminal part of the protein. The pseudokinase domain presents high structural similarities with the tyrosine kinase domain JH1 (Toms et al., 2013), yet it lacks essential residues involved in catalytic activity and substrate binding (Wilks et al., 1991; Saharinen et al., 2000). Hence, it has been hypothesized that the pseudokinase domain has a regulatory role

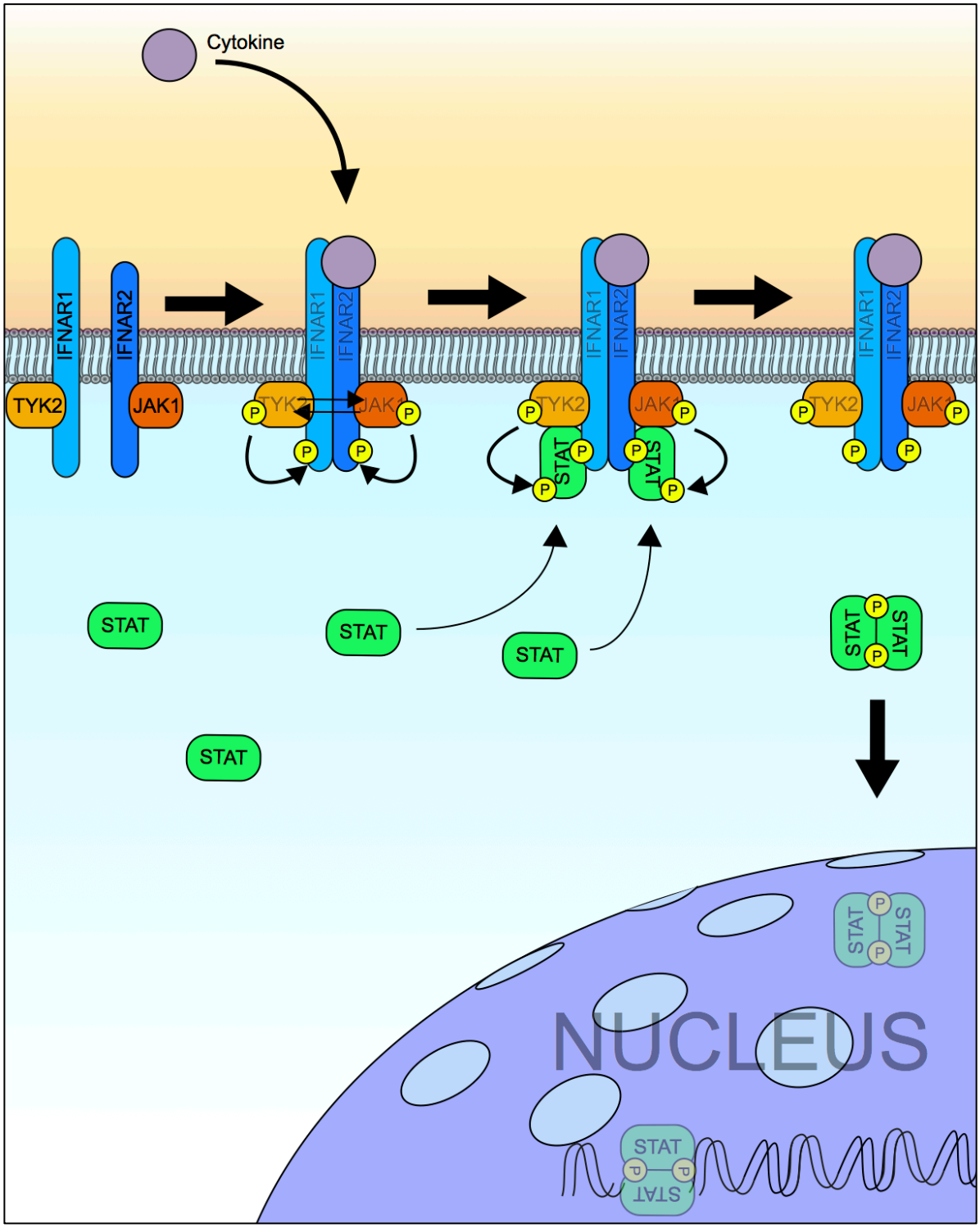

Figure 21. JAK-STAT signal transduction

At steady state IFNAR1 and IFNAR2 remain separated within the plasma membrane. Upon cytokine binding to IFNAR2, IFNAR1 is recruited to form the ternary complex resulting in JAK1 and TYK2 juxtaposition, which leads to their reciprocal transphosphorylation inducing their full activation. Fully activated JAKs phosphorylate IFNARs that become a docking platform for latent cytosolic STATs. IFNAR-docked STATs are thereby phosphorylated by JAKs and released in the cytosol where they dimerize to be imported into the nucleus and initiate specific transcriptional programs.

within the JAKs. Indeed, JH2 deletion from TYK2 impaired IFN signaling (Velazquez et al., 1995). Multiple studies support the regulatory role of the pseudokinase domain, showing that JH2-deleted JAK2 and JAK3 exhibit an increased basal activity (Saharinen and Silvennoinen, 2002).

3.3.2 Mechanism of activation

The precise molecular mechanism of JAKs activation remains unclear. However it is clear that the pseudokinase domain acts as a protein interaction module that inhibits the tyrosine kinase activity of the JH1 domain. Two models have been proposed where autoinhibition occurs either *in cis* (within the same JAK protein) or *in trans* where both JAKs mutually inhibit their JH1 domain with their JH2 domain (Babon et al., 2014) (Fig. 20b). Nevertheless, considering that IFNAR chains remain separated in absence of ligand, it is unlikely that *trans* inhibition occurs in this context. Moreover, crystal structure analysis of the pseudokinase-kinase tandem of TYK2 support the model of *cis* inhibition (Lupardus et al., 2014).

The mechanism triggering the dissociation between JH2 and JH1 (JAK activation) is unknown and may result from conformational changes induced by JAKs juxtaposition and/or transphosphorylation on their kinase domain activation loop (Yamaoka et al., 2004). On the other hand, autoinhibition of JAK2 slightly differs from the other JAKs. Indeed, the JAK2 pseudokinase domain possesses a weak catalytic activity that autophosphorylates itself on two autoinhibitory residues (Ser523 and Tyr570) (Ungureanu et al., 2011). These two autoinhibitory residues are not conserved among the other JAKs.

Upon ligand binding to IFNAR, both chains associate within the ternary complex and undergo conformational changes that propagate to their respective cytosolic tail. These events lead to JAKs juxtaposition and repositioning of their respective pseudokinase domain, relieving autoinhibition (Babon et al., 2014). This repositioning may be triggered by reciprocal transphosphorylation on both kinase domain activation loop (Feng et al., 1997). These last steps drastically enhance the kinase catalytic activity leading to IFNAR tyrosine phosphorylation (IFNAR1 Y466 and

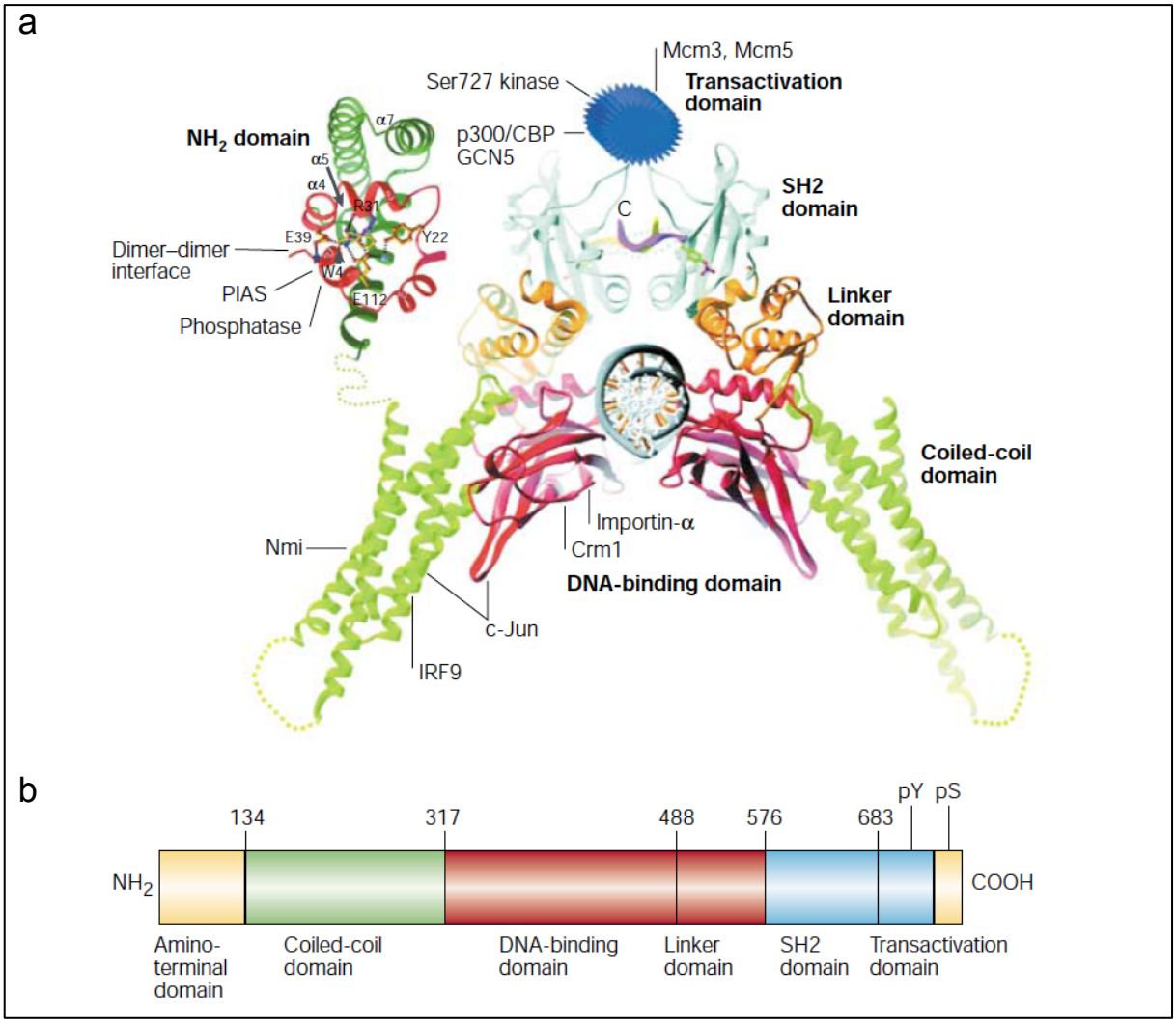

Figure 22. STAT domains structure and protein binding sites

(a) The core structure (amino acids ~130–712) shows binding of a STAT1 dimer to DNA and the location of binding sites of various proteins in various domains. The amino-terminal structure, the placement of which in the intact structure is undefined, also interacts with various partners, as does the carboxy-terminal transactivation domain, the structure of which is unknown. CBP, CREB binding protein; IRF, interferon regulatory factor; Mcm, minichromosome maintenance; Nmi, N-Myc interactor; PIAS, protein inhibitor of activated STAT. **(b)** STAT structure. STAT, signal transducer and activator of transcription. SH2, Src- homology-2 domain (from Levy and Darnell, 2002).

IFNAR2 Y337/542) (Abramovich et al., 1994; Constantinescu et al., 1994; Platanias et al., 1994). Therefore, the new motifs constituted by phosphorylated tyrosines harbored by IFNAR become docking sites for the latent cytosolic signal transducers and activators of transcription (STATs) (Zhong et al., 1994) (Fig. 21).

3.4 Signal Transducers and Activators of Transcription

The family of cytosolic STAT proteins encompasses seven members: STAT1, 2, 3, 4, 5a, 5b and 6. The STATs have been characterized based on their sequence homology and their functional ability to activate distinct sets of genes in response to growth factor and cytokine stimulation (Leaman et al., 1996). The STAT family shares conserved domains: a N-terminal part which is involved in the regulation of STAT activity, a coiled coil domain involved in receptor and regulatory proteins interaction, an SH2 domain that mediates STATs interaction with the tyrosine phosphorylated receptor, a DNA binding domain and a variable C-ter transactivation domain involved in the modulation of gene transcription (Kisseleva et al., 2002) (Fig. 22). In addition, STATs are substrates of JAKs and undergo phosphorylation on a conserved tyrosine residue. This tyrosine phosphorylation triggers STAT homo or heterodimerization (through reciprocal SH2-phosphotyrosine interactions) and their subsequent nuclear translocation relying on the importin-α_5 and the Ran import pathway (Kisseleva et al., 2002). STAT phosphorylation promotes their nuclear retention. Inside the nucleus, depending on the composition of STAT dimers, it eventually form complexes with other co-trancritption factors such as the IFN regulatory factor 9 (IRF9) and binds to DNA consensus sequences such as the IFN response elements (ISREs) or IFN-γ activated sequence (GAS) elements in the promoter of IFN-stimulated genes (ISGs) to initiate transcriptional programs (Darnell et al., 1994; Schreiber and Piehler, 2015). Signal termination is mediated by STAT dephosphorylation and their subsequent nuclear export (Mertens and Darnell, 2007). DNA bound STATs are protected from phosphatases and thereby remain in the nucleus to process the transcriptional program (Meyer et al., 2003) (Fig. 22).

a

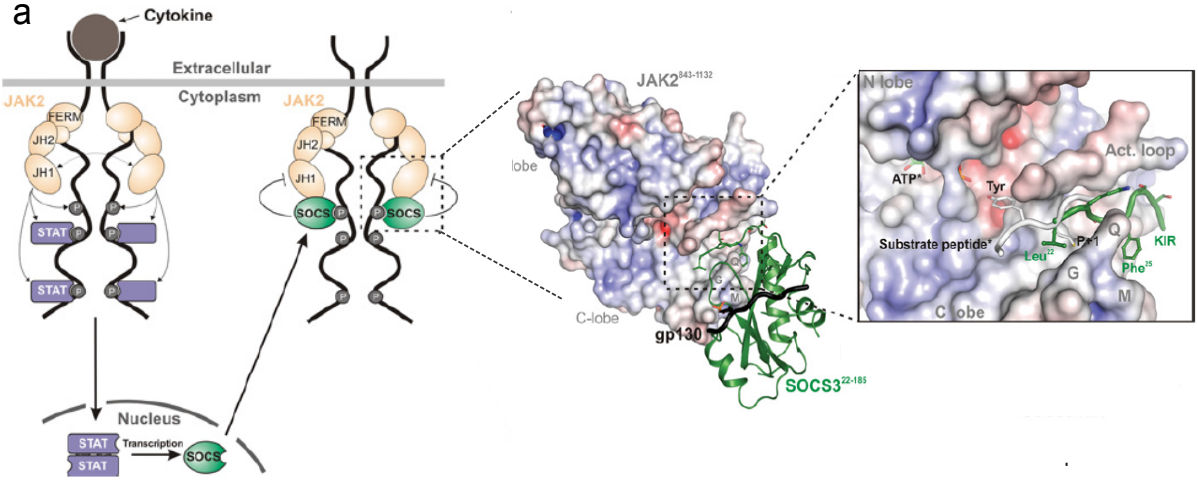

b

Negative regulator	Target	Mechanism
DCST1	STAT2	Ubiquitination
IRF2	IRFs	Binding
PIAS1	STAT1	Binding
PIASy	STAT1	Inhibition of STAT1-dependent transcription
PKD2	IFNAR1	Ubiquitination
PTP1B	TYK2	Dephospholyration
RNF2	STAT1	Ubiquitination
S1PR1	IFNAR1	Lysosomal degradation
SHP1	JAK1, STAT1	Dephospholyration
SHP2	JAK1, STAT1, STAT2	Dephospholyration
SMAD2, SMAD3	STAT1	Binding
SMURF1	STAT1	Ubiquitination
SOCS1	TYK2	Binding
SOCS3	JAK1	Binding
SPRY1, SPRY2, SPRY4	ERK1/2	Dephospholyration
TC-PTP	JAK1	Dephospholyration
USP18	IFNAR2	Binding

Figure 23. Negative regulation of JAK-STAT signaling

(a) Schematic diagram of cytokine-induced JAK-STAT signaling. SOCS proteins are targets for STAT-induced up-regulation, whereupon they inhibit signaling, forming a negative-feedback loop. The two most potent members of the SOCS family, SOCS1 and SOCS3, act by directly inhibiting the catalytic domain (JH1 domain) of JAK2 (left). SOCS3 (green, cartoon representation) docks on to the GQM motif of JAK (electrostatic surface representation) and places its KIR in the substrate-binding groove. The numbering indicates the exact fragments present in the crystal structure of PDB code 4GL9 (left). Close-up of the JAK–KIR interaction with a substrate peptide (white) modeled. The asterisk (*) indicates that ATP and substrate are modeled on the basis of the IRK–substrate–ATP structure (PDB code 1IR3). The KIR of SOCS3 (green) blocks substrate binding, the first residue of the KIR, Leu22, is located where the P+1 residue would reside; this is indicated schematically in (boxed) (adapted from Kershaw et al., 2013b). **(b)** Negative regulators of IFN-induced JAK-STAT signaling (from Arimoto et al., 2018)

3.5 JAK-STAT regulation

As mentioned above, JAK-STAT is a key signaling pathway that allows the control of major cellular processes in response to extracellular stimuli. Therefore, a tight regulation is essential to avoid any undesirable responses that would give rise to dramatic consequences at the whole organism scale. Hence, a multitude of regulatory mechanisms have been setup at each milestone of the signaling pathway to ensure correct activation, signal termination and desensitization.

3.5.1 Upstream regulation

JAK-STAT can be regulated at the level of the cytokine receptors. Indeed, serine phosphorylation on IFNAR1 residue 535 by different sets of kinases such as protein kinase D2 (PDK2) or casein kinase α (CKα) induces the recruitment of F-box protein E3 ubiquitin ligase subunit β transducing repeats-containing protein 2 (β-Trcp2) resulting in IFNAR1 ubiquitination and its subsequent degradation (Marijanovic et al., 2006; Bhattacharya et al., 2010; Zheng et al., 2011). Similarly, ubiquitin-specific peptidase 18 (USP18) interacts with IFNAR2 displacing the associated JAK1 (Malakhova et al., 2006). This interaction results in a destabilization of IFN-α binding to IFNAR2 (Francois-Newton et al., 2011, 2012).

3.5.2 Downstream regulation

JAK kinases are key effectors of the JAK-STAT signal transduction. Therefore, JAKs catalytic activity or activation (*i.e*. phosphorylation) is naturally targeted by regulatory mechanisms. Hence, the JAK-STAT regulatory toolbox includes a wide range of inhibitory proteins including phosphatases (Arimoto et al., 2018).

One of the most well known families of JAK-STAT regulatory proteins is the SOCS family. They were identified on the basis of their ability to bind JAKs and inhibit cytokine signaling. SOCS are part of a negative feedback loop induced by JAK-STAT signaling (Endo et al., 1997; Naka et al., 1997; Starr et al., 1997). There are eight members of the SOCS family. They all contain an SH2 domain and a SOCS

JAK/STAT	Important for signaling by	Knockout mouse phenotype	Genetic links to human disease
JAK1	IFNα/β, IFNγ, IL-2, IL-4, IL-7, IL-9, IL-21, IL-6 family cytokines, IL-10 family cytokines	Perinatally lethal	GOF somatic mutations cause ALL, AML, solid organ malignancies
JAK2	IFNγ, IL-3, IL-5, GM-CSF, EPO, TPO, G-CSF, GH, leptin	Embryonically lethal due to absence of erythropoiesis	GOF mutations cause PCV, MF, ET, hypercoagulable STATe; somatic mutations associated with acute and chronic hematologic malignancies
JAK3	IL-2, IL-4, IL-7, IL-15, IL-21	Defective T and B cell maturation	Loss of function mutation causes severe combined immunodeficiency (SCID), Jacobsen syndrome
TYK2	IFNα/β, IFNγ, IL-12, IL-23	Reduced responses to Type I IFN and IL12, and defective Stat3 activation.	Loss-of function mutation causes primary immunodeficiency
STAT1	All IFNs	Impaired responses to Type I and Type II IFN	LOF mutations confer susceptibility to mycobacterial and viral infections; GOF mutations cause chronic mucocutaneous candidiasis
STAT2	Type I IFNs	Impaired response to Type I IFN and susceptibility to viral infections	Deficiency causes increased susceptibility to viral mutations
STAT3	Il-6 and other gp130 cytokines	Embryonically lethal	LOF mutations cause AD-HIES; GOF somatic mutations strongly associated with LGL
STAT4	IL-12, IL-23, type I interferons	Mutations in mouse inhibit Th1 differentiation	Polymorphisms associated with RA, SLE
STAT5a/STAT5b	IL-2, EPO, TPO, GM-CSF, GH, IL-7	Defective hematopoietic cell lines	Deficiency causes autoimmunity, bleeding diathesis, immunodeficiency and dwarfism; somatic mutations associated with LGL
STAT6	IL-4, IL-13	Mutations in mouse inhibit T helper 2 differentiation	Polymorphisms associated with asthma, atopy, increased levels of IgE

Figure 24. JAKs and STATs with associated cytokines and phenotypes (O'Shea et al., 2015)

box domain. They function as E3 ubiquitin ligase that promotes cytokine receptors and their associated JAKs ubiquitination and their subsequent degradation. However SOCS1 and SOC3 mechanism differ from other SOCS as they directly inhibit JAKs catalytic activity (Yasukawa et al., 1999). Indeed SOCS1 and SOCS3 carry a kinase inhibitory region (KIR) that sits on and occludes JAK substrate-binding sites upon receptor-SOCS1/3-JAK interaction (Kershaw et al., 2013a) (Fig. 23a).

Protein tyrosine phosphatases are also important regulators of JAK-STAT. For example, PTP1B is an SH3 and phosphatase containing protein that dephosphorylates both JAK2 and TYK2 (Myers et al., 2001). PTP1B inhibits IFN-α and IFN-γ signaling by dephosphorylating the activation loop of JAK2 and TYK2. A similar protein named T-cell protein phosphatase (TCPTP) has been reported to dephosphorylate JAK1 and JAK3 (Simoncic et al., 2002). In addition Src homology region 2 domain-containing phosphatase 1 and 2 (SHP1 and SHP2) are phosphatases that directly bind to and dephosphorylate JAK1, JAK2 and TYK2 (David et al., 1995; Yetter et al., 1995; Jiao et al., 1996). Their SH2 domain allows to specifically target activated JAKs by binding to the phophotyrosine of their activation loop.

Finally, STAT-induced transcription can be inhibited by the interaction with a protein inhibitor of activated STAT (PIAS) (Fig. 22a). PIAS are composed of four members: PIAS1, 3, x and y. For example, PIAS1 inhibits STAT1 binding to DNA, thus it prevents STAT1-induced gene transcription (Liu et al., 2004). In addition, the IFN-regulatory factor 2 competes with other IRFs such as IRF9 for ISRE binding thereby preventing ISRE-mediated genes induction (Taki, 2002).

3.6 JAK-STAT in tumor progression

Due to the wide array of physiological processes mediated by JAK-STAT, gain or loss of function mutations in genes encoding for JAKs, STATs and their regulatory proteins are associated with a broad range of human diseases (reviewed in O'Shea et al., 2015) (Fig. 24). For example inactivating mutations of JAK kinases have been reported in patients with immunodeficiencies (Casanova et al., 2012). On the other

hand, mutations resulting in constitutively active JAKs were early involved in myeloproliferative diseases and tumor development such as leukemia/lymphoma and solid tumor development including breast cancer (Leonard and O'Shea, 1998). In this chapter, I will further develop how non-functional JAK-STAT signaling may drive breast cancer development.

All members of the STAT family have important role in mammary gland development. For example, STAT3 is a prominent factor for self-renewal of pluripotent stem cells (Niwa et al., 1998). Moreover, STAT3 mediates inflammatory signaling, tissue remodeling and triggers apoptosis by regulating the expression of phosphoinositide-3 kinase (PI(3)K) regulatory subunits during mammary gland development. STAT6 induces expression of cytokines and important factors for the maintenance of luminal alveolar cells. STAT5 mediates lactation and STAT1 has been reported to be phosphorylated during tissue remodeling of the gland (Abell et al., 2005; Hughes and Watson, 2012). As JAKs and STATs regulate cell proliferation and survival in the mammary gland, it is not surprising that those proteins are involved in breast tumor progression, with either oncogenic or tumor suppressor roles. Somatic mutations of JAK1, JAK2 and JAK3 have been reported in patients with breast cancer (Jeong et al., 2008; Caffarel et al., 2012). Moreover STAT3 and STAT5 are well-known oncogenic factors of the mammary gland that are found to be hyperactivated in a high proportion of breast tumors (Cotarla et al., 2004; Diaz et al., 2006). Indeed, gain of function V617F mutation of JAK2 leads to constitutive STAT5 activation and increased survival and cell proliferation (Caffarel et al., 2012). However, unlike many other oncogenes, mutations in JAKs or STATs are very rare and the mechanisms leading to JAK-STAT subversion are not well understood. In most cancers, STAT1 has paradoxical activities as it is either considered as a tumor suppressor or oncogene depending on the context. For example, in postmenopausal breast cancer, STAT1 acts as a tumor suppressor while it promotes malignancy in premenopausal breast tumors (Haricharan and Li, 2014). Indeed, STAT1 is repressed during breast cancer progression, while highly expressed in surrounding tissues of benign breast tumors (Chan et al., 2012). In addition, STAT1 expression in ER^-/human epidermal growth factor receptor 2-positive ($HER2^+$) and $HER2^-$ breast cancer is correlated with better prognosis (Desmedt et al., 2008). In contrast, in some cases, high STAT1 expression is associated with metastasis and drug resistance

Drug	Target	Status	Diseases
Ruxolitinib (INC424)	JAK1, JAK2	*FDA approved* Phase II Phase 2b	Polycythemia, Myelofibrosis, Various cancers Psoriasis (topical)
Tofacitinib	JAK3>JAK1≫ (JAK2)	*FDA approved* Phase III Phase II	RA Psoriasis, Ulcerative colitis spondyloarthropathy, JIA Transplant rejection
Oclacitinib	JAK1	*FDA approved*	Canine allergic dermatitis
ABT494	JAK1	Phase II	RA, Crohn's
Baricitinib	JAK1, JAK2	Phase II	RA, Psoriasis, Diabetic nephropathy, autoinflammatory disease
Momelitinib	JAK1, JAK2	Phase III	Myelofibrosis
GLPG0634(filgotinib)	JAK1	Phase II	RA, Crohn's
INCB047986	JAK inhibitor	Phase I	Lymphoma, solid tumors
INCB039110	JAK1, JAK2	Phase II	Psoriasis, RA
CYT387	JAK1, JAK2	Phase II	Myelofibrosis
ASP015K	JAK 3/JAK1≫ JAK2/TYK2	Phase II	Psoriasis, RA
R333	JAK/SYK	Phase II	Discoid lupus (topical)
PF-04965842	JAK1	Phase I	healthy adults
GLG0778	JAK1	Phase II	SLE
GSK2586184	JAK1	Phase II	SLE, Psoriasis
VX-509 (decernotinib)	JAK3	Phase IIb	RA
Lestaurtinib	FLT3, JAK2, TRKs	Phase II	AML, PCV/ET, myelofibrosis
Pacritinib	JAK2	Phase II	Myelofibrosis, myeloid leukemias, MDS
LY2784544	JAK2	Phase II Phase I	myelofibrosis various cancers
AZD1480	JAK1, JAK2	Phase I	myeloproliferative diseases, various cancers
XL019	JAK2	Phase I, terminated	Myelofibrosis, PCV
BMS-911543	JAK2	Phase II	Myelofibrosis
NS-108	JAK2, SRC	Phase II	Myelofibrosis
PF-06263276	pan-JAK	Phase I	healthy (topical)
SV1578	JAK2, Flt3	Phase I	healthy adults
ISIS-STAT3Rx (AZD9150)	STAT3	Phase II	various cancers
OPB-51602	STAT3	Phase I	nasopharyngeal carcinoma
OPB-31121	STAT3	Phase I	various cancers

Figure 25. Therapeutic inhibitors of JAKs and STATs (O'Shea et al., 2015)

(Weichselbaum et al., 2008). On the other hand, STAT3 is an oncogene that is constitutively activated in a wide array of cancers. Indeed, STAT3 hyperactivation is often reported in primary breast cancers and is associated with poor prognosis (Charpin et al., 2009). Aberrant STAT3 activation leads to tumor formation as phosphoSTAT3 transactivates a large numbers of oncogenes such as c-Myc, Cyclin D1, prosurvival factors Bcl-xL and survivin together with angiogenesis and invasion factors v-EGF and klf-8 (Bromberg et al., 1999; Diaz et al., 2006). Therefore, transcriptional program initiated by STAT3 results in highly metastatic tumors. Mice with constitutively activated STAT3 exhibit significantly more aggressive tumors (Barbieri et al., 2010). In addition STAT3 also regulates miR-21 and miR-181-b1 transcription via PTEN generating inflammatory signaling, which results in cell transformation through epigenetic mechanisms (Iliopoulos et al., 2010). STAT3 activation also induces stem-cell like phenotype by activating *Sox2* expression or CCL2 production that in turn activates NOTCH1 signaling in tumor cells (Tsuyada et al., 2012; Yang et al., 2013). Moreover, STAT3 activation affects the tumor microenvironment by stimulating the secretion of various cytokines that recruits T-helper and tumor associated macrophages promoting growth and differentiation of tumor cells and inhibition of antitumor immunity (Hynes and Watson, 2010).

The clear role of JAK-STAT signaling in tumor progression makes this pathway an attractive therapeutic target for antitumor treatment. Indeed clinical targeting of JAK-STAT has been proven to be efficient in clinical trials in patients with solid tumors. For example, Ruxolitinib, developed by Novartis, which targets JAK1 and JAK2 is used for a wide range of solid tumors. Other JAKs inhibitors such as INCB39110 and INCB047986 (InCyte corp.) that blocks JAK1 phosphorylation are currently in advanced clinical trials (Buchert et al., 2016) (Fig. 25). Similarly STATs inhibitors are being developed, yet STATs blockade is much more challenging than blocking kinases and may not be as efficient due to STATs redundancy (O'Shea et al., 2015). However small-molecules and oligonucleotide based inhibitor targeting STAT3 and STAT5 are promising (Furqan et al., 2013).

- RESULTS -

Results

4 Caveolae Mechanics Control JAK-STAT signaling

4.1 Objectives and summary

Mechanoprotection is the last function ascribed to cavolae. Indeed, our laboratory demonstrated that caveolae have the ability to flatten out upon membrane tension increase induced by a mechanical stress, thereby providing additional plasma membrane surface in order to prevent cell damages. On another hand it has been established that caveolae are key signaling organelles. Therefore our lab hypothesized that the mechano-dependent cycle of caveolae disassembly/reassembly constitutes a mechanical switch for signaling pathways (Nassoy & Lamaze 2012). In the present work, we hypothesized that the caveolae mechanical disassembly leads to the release of non-caveolar Cav1 in the plasma membrane. Considering the ability of Cav1 to modulate the activity of signaling molecules, we further hypothesized that the mechanical release of non-caveolar Cav1 modulates major signaling pathways. Indeed, using high throughput screening we identified JAK-STAT as a signaling pathway that is modulated by caveolae mechanics. Hence, the aim of this work is to identify the molecular mechanisms underlying the control of JAK-STAT signaling by caveolae mechanics.

Single molecule localization revealed that “free” Cav1 is released in the lipid bilayer upon membrane tension increase induced by osmotic cell swelling. Moreover, consistently with high throughput screening results, biochemical assay and cell imaging confirmed that IFN-α-induced STAT3 activation is decreased upon cell stretch. Study of STAT3 activation profile in mouse endothelial cells WT (WT MLEC) and knock out for Cav1 (*Cav1*$^{-/-}$ MLEC), revealed that caveolae/Cav1 are negative regulators of STAT3 activation. Using mouse embryonic fibroblast (MEF) lacking cavin-1 expression (*cavin-1*$^{-/-}$ MEF) we could demonstrate that non-caveolar Cav1

negatively regulates JAK-STAT signaling. Immunoprecipitation and pulldown experiments revealed that Cav1 interacts with JAK1, which is a key effector of the JAK-STAT signaling pathway. In addition, Cav1-JAK1 interaction depended on membrane tension. It has been proposed that Cav1 modulates signaling events via direct binding and inhibition of signaling molecules through its caveolin scaffolding domain (CSD). Nevertheless, this model remains debated. In the present work, we definitely show that Cav1 CSD has a prominent role in the Cav1-mediated JAK-STAT control. Indeed, mutation of this domain on amino acids F92 and V94 prevents Cav1 interaction with JAK1 resulting in the abolishment of Cav1 negative effect on JAK-STAT. Furthermore, the CSD is sufficient to mimic Cav1 negative effect on STAT3 activation and directly impairs JAK1 catalytic activity as JAK1-mediated ATP conversion *in-vitro* could be decreased by CSD mimicking peptide.

The detailed results of this work are presented below, under the form of an article in preparation for submission.

4.2 Article

Caveolae Mechanics Control JAK-STAT signaling

Nicolas Tardif[1], Richard Ruez[2], Melissa Dewulf[1], Ludger Johannes[3]*, Olivier Rossier[4,5], Grégory Gianonne[4,5], Cédric M. Blouin[1]*§ and Christophe Lamaze[1]*§

[1] Institut Curie - Centre de Recherche, PSL Research University, Membrane Dynamics and Mechanics of Intracellular Signaling Laboratory, 75248 Paris cedex 05, France

[2] Department of Pediatrics, Cell Physiology, and Metabolism, Geneva University Hospitals, University of Geneva, Geneva, Switzerland

[3]Institut Curie - Centre de Recherche, PSL Research University, Endocytic Trafficking and Intracellular Delivery Laboratory, 75248 Paris cedex 05, France

[4] Interdisciplinary Institute for Neuroscience, UMR 5297, University of Bordeaux, Bordeaux, France.

[5] Interdisciplinary Institute for Neuroscience, UMR 5297, CNRS, Bordeaux, France.

* Corresponding authors: christophe.lamaze@curie.fr, cedric.blouin@curie.fr

§ equal contribution

Abstract

Caveolae are small invaginations of the plasma membrane that have been classically involved in membrane trafficking and signaling. These multifunctional organelles were recently shown to play a key role as mechanosensors that adapt the cell response to mechanical stress. Here, we investigated the role of caveolae mechanics in the control of the JAK-STAT signaling pathway. Single molecule imaging experiments revealed that caveolae disassembly induced by mechanical stress led to a drastic increase of caveolin-1 diffusion at the plasma membrane. This promoted the direct interaction of the caveolin-1 scaffolding domain with the tyrosine kinase JAK1, inhibiting its catalytic activity and thereby the activation by IFN-α of the JAK1 downstream effector STAT3. These results therefore establish caveolae as mechanosignaling hubs that couple the sensing of mechanical stress to the

regulation of intracellular signaling through the release of free caveolin-1 at the plasma membrane.

Introduction

Since their first visualization by electron microscopy more than 60 years ago (Palade, 1953; Yamada, 1955) the small cup-shaped plasma membrane invaginations named caveolae have been extensively investigated. Caveolae are shaped by a protein complex composed of caveolin and cavin proteins. Among the three mammalian caveolins, caveolin-1 (Cav1) is the only isoform required for the assembly of caveolae in non-muscle cells. (Parton et al., 2006; Rothberg et al., 1992; Scherer et al., 1996). The second group of caveolae proteins is represented by a family of four cytosolic proteins named cavins (cavin-1 to -4) (Aboulaich et al., 2004). Cavin-1 is essential for caveolae morphogenesis in all cell types whereas Cav3 and cavin-4 are strictly restricted to muscle cells (Bastiani et al., 2009; Way and Parton, 1995). Recent electron microscopy and X-ray crystallography studies gave a further insight into the stoichiometric organization of the characteristic striated coat observed on the outer cytoplasmic side of caveolae. It has been calculated that 150-200 Cav1 monomers associate with 50-60 cavins organized as trimers to form a caveola (Gambin et al., 2014; Ludwig et al., 2013; Stoeber et al., 2016). Several proteins, albeit less well characterized, have also been localized at the neck of caveolae, including dynamin 2, PACSIN2 (syndapin 2) and the ATPase EHD2 (Hansen et al., 2011; Morén et al., 2012).

Caveolae, which are particularly abundant in adipocytes, endothelial cells and muscle cells, are multifunctional organelles that have been classically involved in membrane trafficking and cell signaling (Cheng and Nichols, 2016; Lamaze et al., 2017). Mutations or impaired expression of caveolins and cavins have been associated with several human diseases including lipodystrophy, vascular dysfunction, cancer and muscle dystrophies (Lamaze et al., 2017). If caveolae have long been associated with the control of intracellular signaling, the mechanisms underlying this control remain poorly understood and often debated (Collins et al., 2012). Caveolae are likely to regulate the activation of signaling effectors by several non-mutually exclusive means (Lamaze et al., 2017). Owing to the strong affinity of Cav1 for cholesterol and sphingolipids, caveolae can locally modulate the lipid

composition and thereby the nanoscale organization of the plasma membrane, a key parameter for the activation of transmembrane receptors and associated signaling molecules (Blouin et al., 2016). This process was recently illustrated for the control of Ras signaling (Ariotti et al., 2014). Caveolae can also function as nanodomains themselves to confine signaling effectors locally at the plasma membrane as shown for the regulation of calcium signaling through the localization of the Ca^{2+} pump into caveolae (Fujimoto, 1993). Finally, caveolae can regulate cell signaling through direct interaction of Cav1 with its signaling partners. In this context, it was shown that Cav1 carries a specific caveolin scaffolding domain (CSD), which is able to interact with and regulate the activity of several signaling molecules bearing a corresponding caveolin binding motif (CBM), a consensus signature motif found in several Cav1 binding proteins (Couet et al., 1997a; Lisanti et al., 1995; Okamoto et al., 1998). If this interaction has been described in several studies, more recent structure- and sequence-based data on Cav1-CSD and CBMs have questioned the direct regulation of cell signaling by caveolae through protein-protein interaction with Cav1 (Byrne et al., 2012; Collins et al., 2012)

We established a new function of caveolae as mechanosensing organelles that protect cells from rupture of the plasma membrane under mechanical stress (Sinha et al., 2011). Under various conditions where membrane tension is increased, caveolae immediately flatten out and disassemble to release the membrane stored in their invagination and buffer membrane tension variations. The essential role of caveolae in cell mechanoprotection was confirmed in several cell types *in vitro* and *in vivo* (Cheng et al., 2015; Lim et al., 2017; Lo et al., 2015). It has been proposed that the classical functions of caveolae should be reconsidered through their new function in cell mechanics (Cheng and Nichols, 2016; Nassoy and Lamaze, 2012). Here we revisited the role of caveolae on intracellular signaling by investigating the effects of the mechano-dependent cycle of caveolae disassembly/reassembly on cell signaling. We identified the Janus kinase/signal transducers and activators of transcription (JAK-STAT) signaling pathway to be directly regulated by caveolae mechanics. Upon mechanical stress, we found that Cav1 was rapidly released from caveolae into the plasma membrane. The pool of released Cav1 was able to directly interact via its CSD with the JAK1 tyrosine kinase, leading to the inhibition of its catalytic activity and preventing thereby the activation of JAK-STAT signaling by interferon-α (IFN-α).

Our study unveils a new mechanism by which caveolae couple mechanosensing with the control of cell signaling under mechanical stress.

Results

Mechanical stress drastically increases the diffusion of Cav1 at the plasma membrane.

We previously demonstrated that caveolae have the ability to flatten out and disassemble in response to increased membrane tension (Sinha et al., 2011). Yet, the fate of the caveolar components following the disassembly of caveolae under mechanical stress remains unclear. Single-molecule fluorescence analysis revealed that changes in membrane tension led to the release of the cavin coat from flattened caveolae as two distinct cavin-1/cavin-2 and cavin-1/cavin-3 cytosolic subcomplexes (Gambin et al., 2014). Less is known about the topology of Cav1 oligomers after caveolae flattening. Caveolins could remain organized as a flat caveolar structure, as observed by deep-etch electron microscopy (Sinha et al., 2011), or released as non-caveolar Cav1 oligomers. Indeed, FRAP experiments showed that the mobile fraction of Cav1 was increased upon mechanical stress, suggesting a higher number of Cav1 molecules freely diffusing outside of caveolae (Sinha et al., 2011). We performed high-resolution single particle tracking (sptPALM) together with total internal reflection fluorescence microscopy (TIRF) to monitor with higher spatiotemporal resolution the fate of Cav1 molecules that are released from disassembled caveolae. This allowed us to measure the diffusion coefficient (D) of Cav1 fused to phospho-switchable mEOS3.2 after photoactivation in mouse lung endothelial cells (MLEC). At steady state, the Cav1-mEos trajectories remain confined around static Cav1-mEOS objects, whose characteristics indicate that they are most likely confined within caveolae. Under membrane tension increase induced by hypo-osmolarity, we observed dramatic changes in the diffusion parameters of Cav1-mEOS with Cav1-mEOS trajectories increasing in length and exploring a wider area (Fig. 1a). The D coefficient of Cav1-mEOS is redistributed as well, and translated a faster diffusion of Cav1-mEOS (Fig. 1b). Importantly, the logarithmic value of the diffusion coefficient increased with the time of exposure to hypo-osmolarity (Fig. 1c). In contrast, the D coefficient of Cav1-mEOS3.2 returns to a iso-osmotic-like distribution in shocked cells back to iso-osmolarity, which translate a return to a confined state for Cav1-

mEOS (Fig. 1d). Altogether, these results clearly indicate that after caveolae disassembly by mechanical stress, Cav1 molecules are released from the caveolar coat and freely diffuse at the plasma membrane. This process is dynamic and reversible.

Caveolae can control several signaling pathways under mechanical stress

We have hypothesized that the mechano-dependent cycle of caveolae disassembly/reassembly may constitute a mechanical switch by which caveolae and /or caveolins could control intracellular signaling (Nassoy and Lamaze, 2012). We therefore investigated whether the pool of freely diffusing Cav1 released under mechanical stress could impact the activation of some signaling pathways. To identify some of these signaling pathways, we ran a screening experiment based on the reverse phase protein assay (RPPA), a miniaturized high throughput dot-blot technology for proteomic analysis allowing the analysis of protein expression, post-translational modifications and identification of activated or altered signaling pathways. The RPPA was performed on MLEC cells having (WT) or not caveolae (*Cav1*$^{-/-}$), in resting condition or under uniaxial stretching. We also stimulated the cells by IFN-α so as to analyze the JAK/STAT signaling pathway. Results from the RPPA screening revealed several signaling pathways that were affected by cell uniaxial stretching as exemplified by the stretch dependent activation of MAPK and Akt pathways. As expected, IFN-α stimulation led to the tyrosine phosphorylation of STAT3 and STAT1 (Fig. 2a). Interestingly, the level of STAT3 phosphorylation was strongly decreased upon cell stretching, in a Cav1 dependent manner, whereas STAT1 activation was not affected. Other signaling pathways such as MAPK are activated by stretch independently from caveolae (Fig. 2a).

Mechanical stress impairs the JAK/STAT signaling pathway

We further investigated the role of caveolae mechanics on the JAK/STAT signaling pathway activated by IFN-α. JAK-STAT signaling represents one of the major signaling pathways of the cell. It is used by a wide array of cytokines and growth factors to transduce signal and generate accurate gene responses. It governs multiple biological processes as diverse as hematopoiesis, innate and adaptive immune function, cell proliferation, differentiation, migration and apoptosis (Villarino et al., 2017). The activation of JAK-STAT signaling by IFN-α relies on the ubiquitous

IFNAR receptor composed of two non-tyrosine kinase receptor subunits IFNAR1 and IFNAR2. IFN-α binding to IFNAR2 allows the formation of a ternary complex with IFNAR1, where the two IFNAR-associated JAK1 and TYK2 tyrosine kinases are mutually activated by trans-phosphorylation. These conformational changes trigger the full activation of JAK1 and TYK2, which in turn create tyrosine phosphorylated docking sites on IFNAR1 and IFNAR2 subunits where cytosolic STAT molecules (STAT1, STAT2 or STAT3) are recruited. The tyrosine phosphorylation by JAK1 and TYK2 allows the release of STATs in the cytosol and their dimerization before their translocation to the nucleus where they induce a transcriptional program specific to IFN-α (Schreiber and Piehler, 2015).

We confirmed the data obtained through RPPA screening by monitoring STAT3 activation by IFN-α that is, phosphorylation at tyrosine 705, a key step required for the formation of active transcriptional complexes (Kaptein et al., 1996). We measured by immunoblotting the level of STAT3 phosphorylation and its consecutive nuclear translocation in WT MLEC or *Cav1*$^{-/-}$ MLEC cells stimulated with IFN-α under 25% uniaxial stretching. We found that the level of STAT3 tyrosine phosphorylation was decreased by about 43% in stretched WT MLEC cells (Fig. 3a). The decrease of STAT3 activation translated into a defect of STAT3 nuclear translocation in stretched cells (Fig. 3b). As observed above in the RRPA screening, the level of STAT3 tyrosine phosphorylation remained unchanged when *Cav1*$^{-/-}$ MLEC cells were stretched, indicating that this regulation requires functional caveolae (Fig. 3a). Again, we found that STAT1 activation by IFN-α was insensitive to mechanical stress since pSTAT1 nuclear translocation occurred normally in stretched cells (Fig. 3b).

Non-caveolar Cav1 mediates STAT3 inhibition

Our data indicate that caveolae and mechanical stress can control the activation of STAT3 by IFN-α. We next asked whether this control could occur in unstimulated cells. As expected, in the absence of stimulation by IFN-α, no activation of STAT1 and STAT3 were detected in WT MLEC (Fig. 4a, b). In contrast, we observed a strong activation of STAT3 in unstimulated *Cav1*$^{-/-}$ MLECs. The absence of caveolae had no effect on the level of phosphorylated STAT1 at steady state in agreement with the RPPA and nuclear translocation data (Fig. 4b). The constitutive activation of STAT3 was dependent on the activity of the JAK1 tyrosine kinase since siRNA-

mediated JAK1 depletion completely abolished STAT3 activation in stimulated and unstimulated *Cav1*$^{-/-}$ MLEC cells (Fig. 4c, d). These data indicate that caveolae and/or caveolins are negative regulators of STAT3 activation at steady state.

A key question in the field of caveolae is to distinguish the role of caveolae from the role of caveolins (Lamaze et al., 2017). Since we showed that mechanical stress released a pool of freely diffusing Cav1 at the plasma membrane (Fig. 1), we sought to investigate the role of non-caveolar Cav1 on STAT3 activation. To do so, we took advantage of mouse embryonic fibroblasts (MEF) knocked out for *cavin-1*. Indeed, in the absence of cavin-1, Cav1 is unable to assemble into morphologically distinguishable caveolae and remains as a pool of non-caveolar Cav1 with increased lateral mobility at the plasma membrane (Hill et al., 2008). We therefore measured the level of STAT3 phosphorylation in unstimulated and IFN-α-stimulated *cavin-1*$^{-/-}$ MEF cells. As expected, STAT3 was not activated in unstimulated *cavin-1*$^{-/-}$ MEF cells (Fig. 5a). However, the stimulation of *cavin-1*$^{-/-}$ MEF cells by IFN-α failed to activate STAT3. The rescue of cavin-1 expression in *cavin-1*$^{-/-}$ cells (*cavin-1*$^{-/-}$ + cavin-1) allowed again the activation of STAT3 by IFN-α (Fig. 5b). These results suggest that the pool of non-caveolar Cav1 is responsible for the lack of STAT3 activation by IFN-α. Indeed, the treatment of WT MLEC cells with methyl-β-cyclodextrin, which disrupts caveolae by removing cholesterol at the plasma membrane, led also to a significant decrease of the level of STAT3 activation by IFN-α (Supplementary fig. 1). Finally, we measured the level of STAT3 activation in *cavin-1*$^{-/-}$ MEF expressing increasing amounts of non-caveolar Cav1 and found a dose dependent inhibition of IFN-α-induced STAT3 activation (Fig. 5c). Altogether these data indicate that an excess of non-caveolar Cav1 inhibits the activation of STAT3 by IFN-α.

The level of Cav1 and JAK1 interaction is tuned by mechanical stress

STAT3 is the direct downstream effector of JAK1 and TYK2 kinases that are associated to the IFNAR complex (Platanias, 2005). It is therefore likely that the inhibition of IFN-α-induced STAT3 tyrosine phosphorylation by non-caveolar Cav1 occurs through interaction with the JAK kinases. We found indeed that Cav1 could interact with JAK1 in pull-down experiments performed in *Cav1*$^{-/-}$ MLECs cells expressing Cav1-RFP (Fig. 6a). Our data showing on one hand that mechanical stress both releases non-caveolar Cav1 from caveolae and prevents the activation of

STAT3 by IFN-α, and on the other hand that non-caveolar Cav1 prevents the activation of STAT3 by IFN-α, led us to postulate that mechanical stress could regulate the interaction between Cav1 and JAK1. We thus applied a 30 mOsm hypo-osomotic shock for 5 min so as to disassemble caveolae and promote the release of non-caveolar Cav1 at the plasma membrane. Under this condition, we observed an increase by about 65% of the amount of JAK1 co-immunoprecipitated with Cav1 (Fig. 6b). Furthermore, the increase of Cav1 and JAK1 interaction under mechanical stress, was correlated with a concomitant 80% decrease of STAT3 activation by IFN-α (Fig. 6c). Importantly, upon return to iso-osmotic conditions, when caveolae have been reassembled to initial numbers (recovery) (Sinha et al., 2011), both the levels of Cav1 interaction with JAK1 and STAT3 activation by IFN-α resumed to the levels measured before hypo-osmotic shock. These data indicate that the level of Cav1-JAK1 interaction is tuned by the amount of Cav1 released from caveolae that are disassembled to buffer the increase of membrane tension induced by hypo-osmotic shock. Moreover, it shows that the inhibition of STAT3 activation by IFN-α is correlated with the level of Cav1 interaction with JAK1 suggesting that JAK1 inhibition is tuned by the amount of Cav1 that binds to JAK1.

JAK1 inhibition is mediated by the caveolin scaffolding domain

Early studies have identified a so-called caveolin scaffolding domain that was involved in the direct regulation, mostly inhibitory, of several signaling molecules by Cav1 including eNOS or heterotrimeric G proteins and lastly heme oxygenase (Couet et al., 1997b; Garcia-Cardena, 1997; Taira et al., 2011). Interestingly, we found that the tyrosine kinase JAK1 carries several CBMs, the caveolin binding motifs that may be involved in the recognition by the Cav1 CSD. One is localized in the pseudokinase domain, one putative CBM is in the kinase domain (Jasmin et al., 2006) and another CBM can be found in the FERM domain of JAK1. The phenylalanine 92 and valine 94 residues play a key role in the CSD/CBM interaction (Nystrom et al., 1999; Trane et al., 2014). To test whether the interaction between Cav1 and JAK1 was mediated by the Cav1 CSD, we expressed a Cav1 CSD construct mutated for the F92 and V94 residues (F92A/V94A Cav1) in *Cav1*$^{-/-}$ MLEC cells. In agreement with previous experiments, we found JAK1 in pulled-down lysates from WT Cav1 expressing cells. In contrast, no JAK1 could be detected in pulled-down fraction from lysates of F92A/V94A Cav1 expressing cells (Fig. 7a), which indicates that the interaction

between Cav1 and JAK1 requires the CSD phenylalanine 92 and valine 94 residues. In addition the CSD shares primary sequence similarities with the pseudosubstrate domain of SOCS1 and SOCS3, which is the domain that mediates JAKs inhibition by SOCS1 and SOCS3 (Jasmin et al., 2006; Kershaw et al., 2013).

To test whether the inhibitory role of Cav1 on JAK1 activity was mediated by the CSD, we examined the level of pSTAT3 nuclear translocation induced by IFN-α stimulation in *Cav1*$^{-/-}$ MLEC cells expressing either WT or F92A/V94A Cav1 (Bernatchez et al., 2011; Meng et al., 2017; Nystrom et al., 1999). While the nuclear translocation of pSTAT3 occurred normally in non-transfected cells, cells overexpressing Cav1 WT showed a defect of pSTAT3 nuclear translocation in agreement with the inhibitory role of Cav1 on JAK1 activity. It was reported indeed that the overexpression of Cav1 generates a pool of non-caveolar Cav1 at the plasma membrane, which is likely due to a stoichiometric imbalance between the number of Cav1 molecules and the other caveolar components required for caveolae assembly (Hayer et al., 2010; Moon et al., 2013). On the contrary, in cells expressing the F92A/V94A mutated Cav1 CSD, we observed a normal nuclear translocation of pSTAT3 induced by IFN-α stimulation, indicating that F92A/V94A Cav1 lost the ability to negatively regulate STAT3 activation, most likely through its inability to interact with JAK1 (Fig. 7b). In agreement with the lack of regulation of STAT1 activation by mechanical stress and caveolae, the nuclear translocation of pSTAT1 induced by IFN-α was not affected whether cells express WT Cav1, F92A/V94A Cav1 or none (Supplementary fig. 2).

We further established the role of the Cav1 CSD using two CSD mimicking peptides, a peptide named CavTratin corresponding to the Cav1 CSD (Cav1 ^{82}DGIWKASF**TTF**TVTKYWFYR^{101}) and a dominant negative peptide named CavNoxin (Cav1 ^{82}DGIWKASF**AAA**TVTKYWFYR^{101}) where key amino acids have been replaced by alanines thereby abolishing its inhibitory effect (Bernatchez et al., 2011). WT MLEC cells treated with CavTratin showed a significant decrease of STAT3 tyrosine phosphorylation upon IFN-α stimulation, indicating that the caveolin domain CSD is sufficient to mimic the negative regulation of STAT3 activation by Cav1. Conversely, cells treated with CavNoxin showed a significant increase of STAT3 tyrosine phosphorylation upon IFN-α stimulation (Fig. 7c). These data confirm that increasing the amount of Cav1 that is able to interact with the JAK1 kinase inhibit STAT3 activation whereas the mutated Cav1 CSD peptide relieves the JAK1

inhibition, most likely by competing with endogenous Cav1. We could definitely establish the direct role of the Cav1 CSD on JAK1 catalytic activity by assessing in a cell free assay, the effect of CSD binding on the ability of JAK1 to catalyze ATP hydrolysis. We measured *in vitro* the catalytic activity of a human recombinant JAK1 by measuring the conversion of ATP to ADP. We found that increasing concentrations of a control peptide did not affect the catalytic activity of JAK1 as ADP production was maintained. In contrast, JAK1 dependent ADP production significantly decreased in a dose dependent manner when CavTratin was added to the reactional mix (Fig. 7d). These data therefore demonstrate that the negative regulation of STAT3 activation by Cav1 results from direct binding of the Cav1 CSD to JAK1, which inhibits JAK1 catalytic activity.

Discussion

Over the past decades, many functions have been ascribed to caveolae (other reviewed here: Lamaze et al., 2017). The discovery of the role of caveolae in cell mechanics in 2011 (Sinha et al., 2011) led the field to revisit the classical functions of caveolae in this new context (Cheng and Nichols, 2016). In this study, we investigated the fate of Cav1 upon caveolae mechanical disassembly and its impact on caveolae dependent signaling. Upon membrane tension increase, we could visualize by single molecule microscopy the appearance of a highly mobile pool of non-caveolar Cav1 at the plasma membrane. Considering the established role of caveolae in signaling (Parton and Simons, 2007; Patel et al., 2008), we exanimated the effect of non-caveolar Cav1 release on cell signaling pathways. High throughput screening revealed that the JAK-STAT signaling pathway was modulated by cell stretching in a caveolae dependent manner. We could demonstrate that non-caveolar Cav1 generated by caveolae mechanical disassembly, binds directly to the JAK1 tyrosine kinase and inhibits its catalytic activity in a CSD-dependent manner. Cav1 binding to JAK1 results in impaired activation of STAT3 by IFN-α. Importantly, we further show that the level of Cav1-JAK1 interaction and thereby the downregulation of IFNα-induced STAT3 activation, is modulated by mechanical stress. Finally, based on CSD mimicking peptides and CSD-mutated Cav1, we could demonstrate that the Cav1 CSD domain is required for the interaction of Cav1 with JAK1 and directly mediates the inhibitory effect of Cav1 on JAK1 catalytic activity.

Numerous studies have involved Cav1 as an essential component of the signal transduction function of caveolae, based on its ability to interact with many signaling proteins (Couet et al., 1997b; Gangadharan et al., 2015; Garcia-Cardena, 1997; Li et al., 1996; Nystrom et al., 1999; Taira et al., 2011). The mechanisms by which caveolae control signaling remains poorly understood and some aspects are still debated (Lamaze et al., 2017). Early work has involved the Cav1 CSD domain in the control of Cav1 interaction with signaling effectors (Li et al., 1995; Li et al., 1996). The corresponding CBM domains have been found in many downstream signaling effectors that bind to Cav1 (Couet et al., 1997a). Indeed, sequence analysis showed that JAK1 displays three domains that could correspond to putative CBMs: one in the FERM domain (^{157}YLFAQGQY^{164}), one in the pseudokinase domain (^{777}WSFGTTLW^{784}) and a last one in the kinase domain (^{1065}WSFGVTLH^{1072}) (Supplementary fig. 3). While the role of these motifs has not been investigated in this work, our data involve most likely the CBM2 or CBM3 since it is the only CBMs present in the recombinant JAK1 kinase used in the cell free assay. Although the CSD-CBM interaction has been extensively investigated for the interaction of Cav1 with signaling proteins such as insulin and trimeric G protein receptors, eNOS or Heme Oxygenase (Bernatchez et al., 2005; Nystrom et al., 1999; Taira et al., 2011; Trane et al., 2014), its role in signaling has been regularly questioned. The debate on the CSD-CBM interaction has been fueled by the recent structural features of Cav1 (Lamaze et al., 2017). The CSD consists in an amphipathic helix that is partially embedded in the inner leaflet of the plasma membrane, which would make it not suitable to mediate interaction (Byrne et al., 2012; Collins et al., 2012; Kirkham et al., 2008).

In this study, we show nevertheless that the Cav1-JAK1 interaction is directly mediated by the CSD and that this interaction is tuned by mechanical stress. One could therefore hypothesize that the mechanical release of Cav1 from caveolae triggers the exposition of the CSD by Cav1 conformation changes induced by the mechanical release of Cav1. In this context, it is interesting that previous studies reported that the CSD is not static and presents instead a dynamic structure, that is either fully helical or partially unstructured and could determine CSD accessibility (Liu et al., 2016). In addition, one or the other conformation would be favored by the lipid environment (Hoop et al., 2012; Le Lan et al., 2006). It is therefore possible that non-caveolar Cav1 may experience a different lipid environment, hence its increased

mobility, resulting in a different CSD conformation. Finally, it cannot be excluded that Cav1 and/or JAK1 post-translational modifications induced by the mechanical release of Cav1 could mediate this interaction. Indeed, Cav1 is phosphorylated on Tyr 14 and Ser 80 by different sets of kinases. The introduction of negative charges in the N-terminal part of Cav1, may induce a kink in Cav1 structure by further pushing away the N-ter end from the plasma membrane due to charge repulsion (Ariotti et al., 2015; Meng et al., 2017; Shajahan et al., 2012).

An unresolved question in the field is the role of caveolae *versus* non-caveolar Cav1 in signaling (Cheng and Nichols, 2016; Lamaze et al., 2017). Our study unveils a regulatory role of caveolae in JAK-STAT signaling based on the mechanical control of the balance between non-caveolar Cav1 (high stress) and caveolar Cav1 (low stress). This process allows the fine mechanical tuning of JAK-STAT signaling as the level of non-caveolar Cav1 is below detection under resting conditions (Hill et al., 2008; Sinha et al., 2011). We have identified here and elucidated the molecular mechanism underlying the selective control of JAK-STAT signal transduction by caveolae mechanics. Interestingly, this mechanism selectively targets JAK1 dependent STAT3 activation, while at steady state, IFN-α indifferently induces both STAT1 and STAT3 activation (Platanias, 2005). The molecular basis driving this signal specificity needs to be further investigated. Our data showing that STAT3 was activated in *Cav1* knocked out cells in the absence of IFN-α and that the Cav1 CSD interacted directly with JAK1 and inhibited its catalytic in the absence of IFN-α indicate that this control is not restricted to IFN-α and could be extended to other cytokines activating JAK1. Williams and colleagues, recently revealed that proper JAK-STAT signal suppression through SOCS3 requires *bona fide* caveolae and stable cavin-1 (Williams et al., 2018). Hence one could hypothesize that mechanical disassembly of caveolae and the destabilization of cavin complexes, would result in impaired SOCS3 mediated JAK-STAT signal termination. Therefore, under mechanical stress, the release of free Cav1 might lock the JAK-STAT signaling pathway to prevent aberrant JAK-STAT signaling.

The physiological role of JAK-STAT signaling control by caveolae mechanics remains unclear. The deregulation of STAT3 activation has been involved in many human pathologies including Crohn's disease, psoriasis, Hyerglobulin E syndrome and cancer (O'Shea et al., 2015). This process could be involved in tumor development and may partially explain the ambivalent role that Cav1 plays in tumor

growth (Goetz et al., 2008; Lamaze and Torrino, 2015). On one hand, STAT3 is a well-known oncogene targeted by many anti-cancer therapies (Beebe et al., 2018). On the other hand, STAT1 is a tumor suppressor (Koromilas and Sexl, 2013). This new aspect of caveolae functioning as mechanosignaling hubs may play a critical role during tumor growth. Indeed the mechanical forces encountered by cancer cells during tumor progression (Kai et al., 2016), may perturb caveolar dynamics that in turn would impair the fine tuning of the STAT3/STAT1 activation balance through caveolae mechanics.

Figures

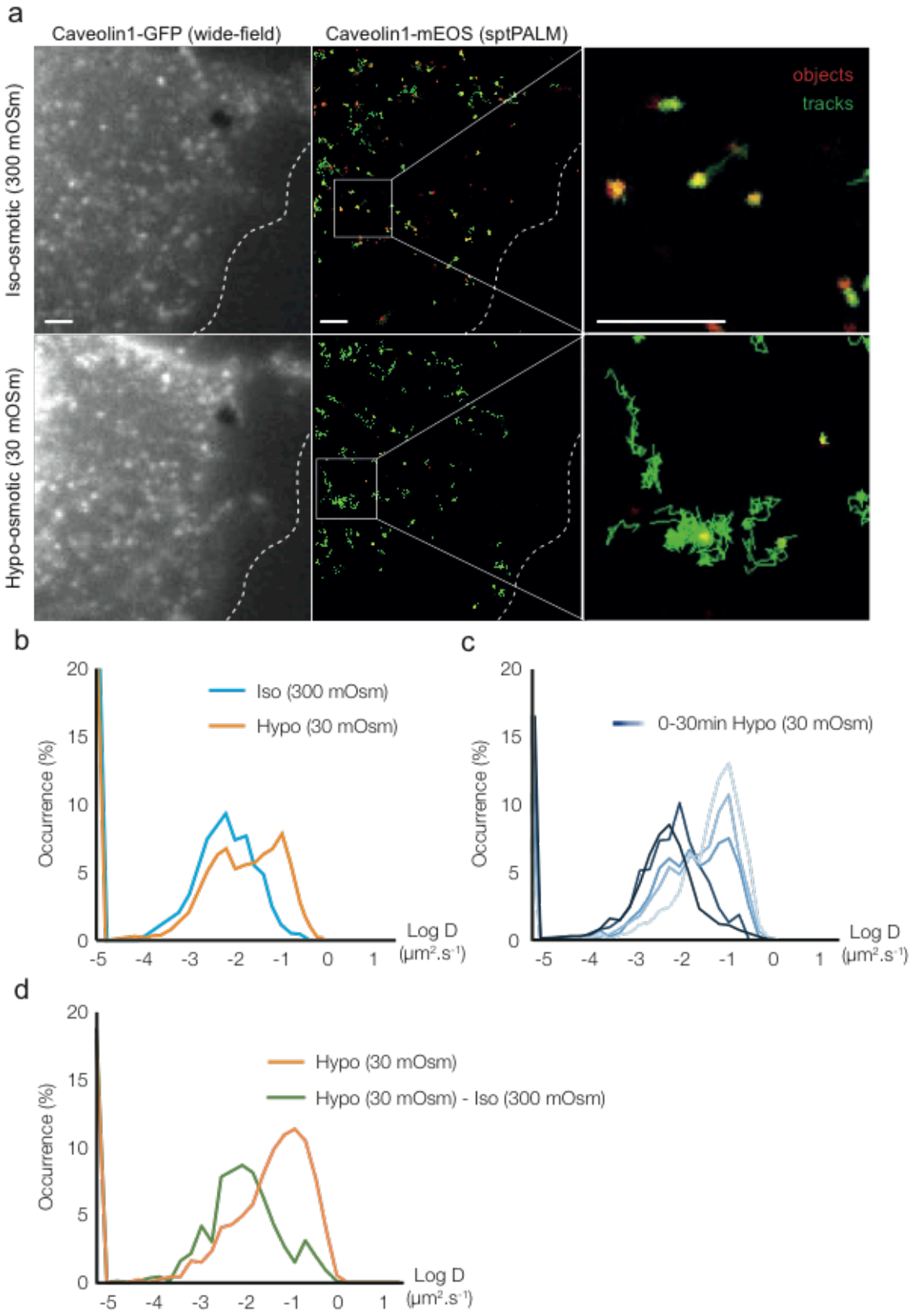
a
Caveolin1-GFP (wide-field)
Caveolin1-mEOS (sptPALM)
objects
tracks
Iso-osmotic (300 mOSm)
Hypo-osmotic (30 mOSm)
b
Iso (300 mOsm)
Hypo (30 mOsm)
Occurrence (%)
Log D (µm².s⁻¹)
c
0-30min Hypo (30 mOsm)
Occurrence (%)
Log D (µm².s⁻¹)
d
Hypo (30 mOsm)
Hypo (30 mOsm) - Iso (300 mOsm)
Occurrence (%)
Log D (µm².s⁻¹)

Figure 1. **High resolution analysis of Cav1 diffusion under mechanical stress**
(a) Left panel, wide field images of Cav1-GFP under iso-osmolarity (300 mOsm) and hypo-osmolarity (30 mOsm) in MLEC cells. Right panel, Cav1-mEOS3.2 trajectories (green) and Cav1-mEOS3.2 objects (red) acquired using TIRF-sptPALM. **(b)** Distribution of log(D) for Cav1-mEOS3.2 in iso-osmotic condition (blue) and hypo-osmotic condition (orange). **(c)** Distribution of log(D) for Cav1-mEOS3.2 in hypo-osmotic from 0 minute (deep blue) to 30 minutes (light blue). **(d)** Distribution of log(D) for Cav1-mEOS3.2 in hypo-osmotic condition (orange) and recovery condition (green).

a

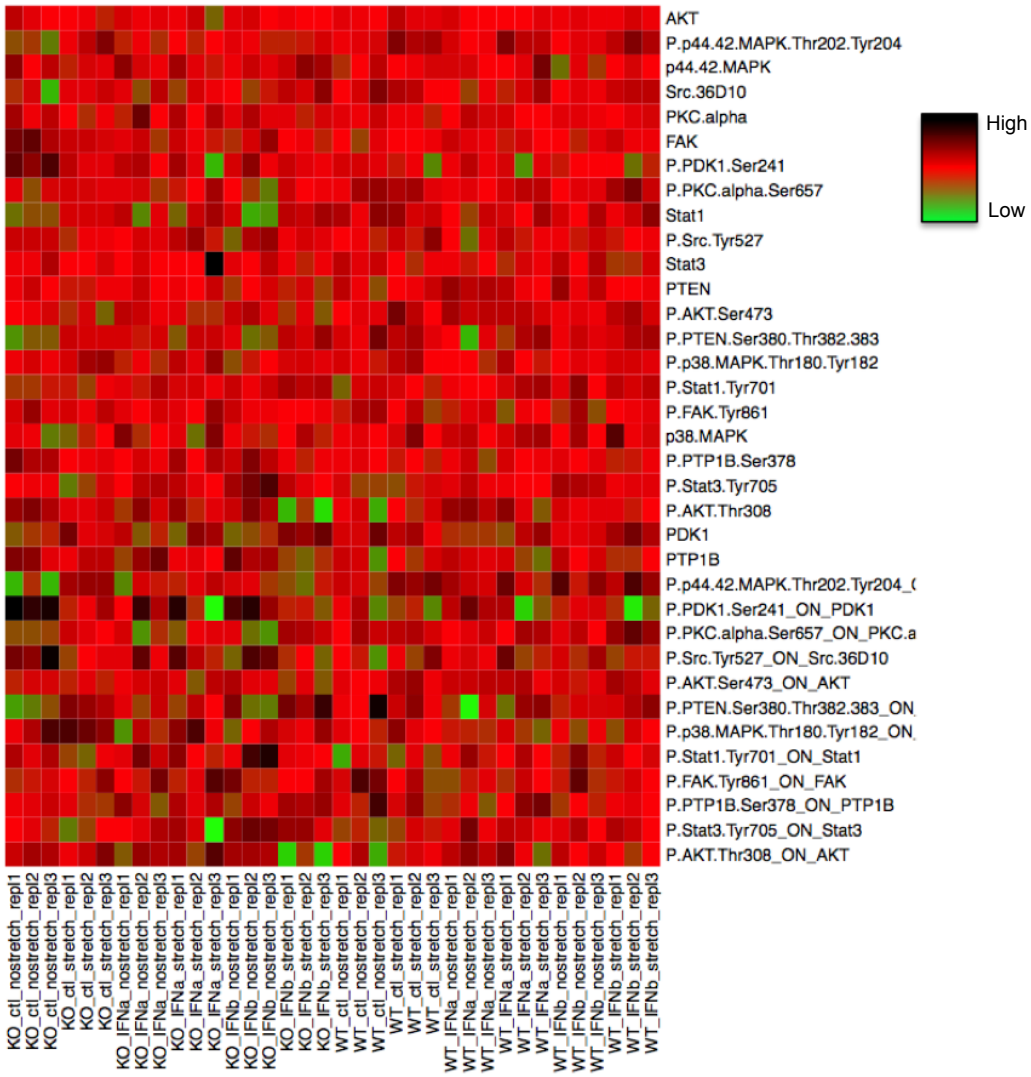
AKT
P.p44.42.MAPK.Thr202.Tyr204
p44.42.MAPK
Src.36D10
PKC.alpha
FAK
P.PDK1.Ser241
P.PKC.alpha.Ser657
Stat1
P.Src.Tyr527
Stat3
PTEN
P.AKT.Ser473
P.PTEN.Ser380.Thr382.383
P.p38.MAPK.Thr180.Tyr182
P.Stat1.Tyr701
P.FAK.Tyr861
p38.MAPK
P.PTP1B.Ser378
P.Stat3.Tyr705
P.AKT.Thr308
PDK1
PTP1B
P.PDK1.Ser241_ON_PDK1
P.Src.Tyr527_ON_Src.36D10
P.AKT.Ser473_ON_AKT
P.FAK.Tyr861_ON_FAK
P.PTP1B.Ser378_ON_PTP1B
P.Stat3.Tyr705_ON_Stat3
P.AKT.Thr308_ON_AKT
High
Low
KO_ctl_nostretch_repl1
KO_ctl_nostretch_repl2
KO_ctl_nostretch_repl3
KO_ctl_stretch_repl1
KO_ctl_stretch_repl2
KO_ctl_stretch_repl3
KO_IFNa_nostretch_repl1
KO_IFNa_nostretch_repl2
KO_IFNa_nostretch_repl3
KO_IFNa_stretch_repl1
KO_IFNa_stretch_repl2
KO_IFNa_stretch_repl3
KO_IFNb_nostretch_repl1
KO_IFNb_nostretch_repl2
KO_IFNb_nostretch_repl3
KO_IFNb_stretch_repl1
KO_IFNb_stretch_repl2
KO_IFNb_stretch_repl3
WT_ctl_nostretch_repl1
WT_ctl_nostretch_repl2
WT_ctl_nostretch_repl3
WT_ctl_stretch_repl1
WT_ctl_stretch_repl2
WT_ctl_stretch_repl3
WT_IFNa_nostretch_repl1
WT_IFNa_nostretch_repl2
WT_IFNa_nostretch_repl3
WT_IFNa_stretch_repl1
WT_IFNa_stretch_repl2
WT_IFNa_stretch_repl3
WT_IFNb_nostretch_repl1
WT_IFNb_nostretch_repl2
WT_IFNb_nostretch_repl3
WT_IFNb_stretch_repl1
WT_IFNb_stretch_repl2
WT_IFNb_stretch_repl3

b

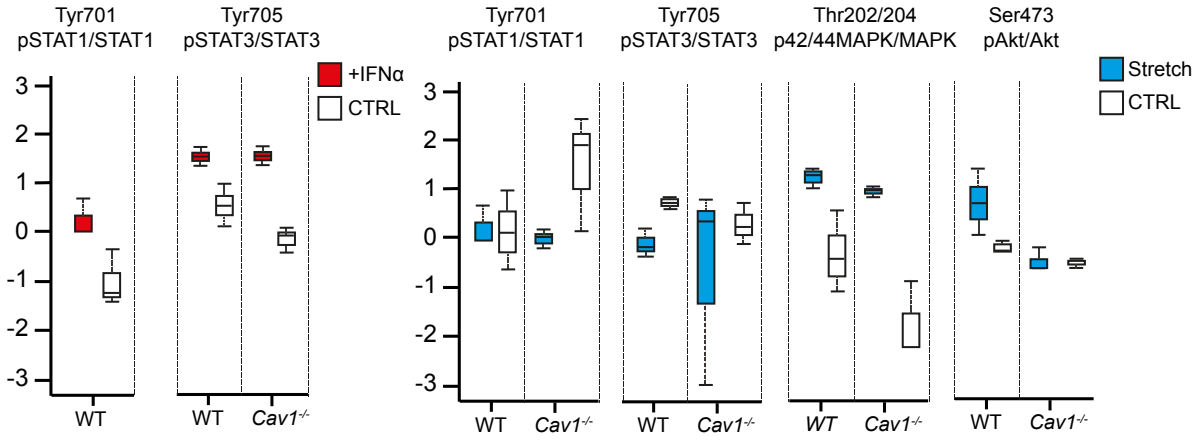
Tyr701
pSTAT1/STAT1
Tyr705
pSTAT3/STAT3
+IFNα
CTRL
WT
WT
Cav1-/-
Tyr701
pSTAT1/STAT1
Tyr705
pSTAT3/STAT3
Thr202/204
p42/44MAPK/MAPK
Ser473
pAkt/Akt
Stretch
CTRL
WT
Cav1-/-
WT
Cav1-/-
WT
Cav1-/-
WT
Cav1-/-

Figure 2. High throughput screening of signaling pathways modulated by caveolae mechanics

(a) Heat map of signaling effectors activation in WT and *Cav1*$^{-/-}$ MLEC cells under resting condition or uniaxial stretch and with type I IFN stimulation or not. **(b)** STAT1 and STAT3 activation under type I IFN stimulation (left). STAT1, STAT3, p42/44 MAPK and Akt phosphorylation level under uniaxial stretch.

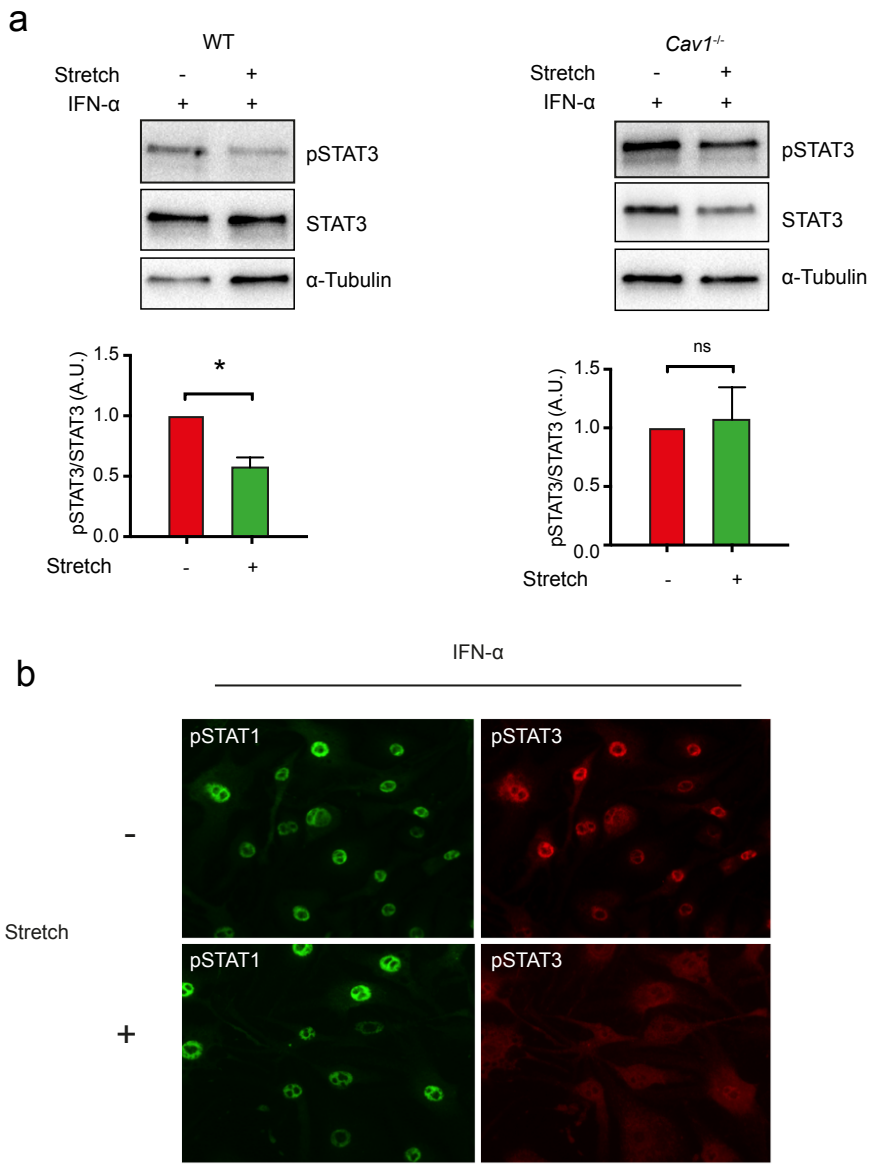
a
WT
Stretch - +
IFN-α + +
pSTAT3
STAT3
α-Tubulin
pSTAT3/STAT3 (A.U.)
1.5
1.0
0.5
0.0
*
Stretch - +
Cav1-/-
Stretch - +
IFN-α + +
pSTAT3
STAT3
α-Tubulin
ns
pSTAT3/STAT3 (A.U.)
1.5
1.0
0.5
0.0
Stretch - +
b
IFN-α
Stretch
-
+
pSTAT1
pSTAT3
pSTAT1
pSTAT3

Figure 3. Uniaxial stretching controls IFN-α induced STAT3 activation

(a) STAT3 phosphorylation level induced by IFNα stimulation in *Cav1*$^{-/-}$ MLEC cells submitted or not to stretch. Representative immunoblot. Immunoblot quantification of signal ratio relative to "No stretch" condition. Mean value ± SEM. Statistic were processed using two tailored unpaired t test. *P<0,05. **(b)** Analysis of the nuclear translocation of pSTAT1 (green) and pSTAT3 (red). WT MLEC were stretched or not and prior to stimulation with IFNα for 20min. After fixation the nuclear distribution of pSTAT1 and pSTAT3 was detected by immunofluorescence.

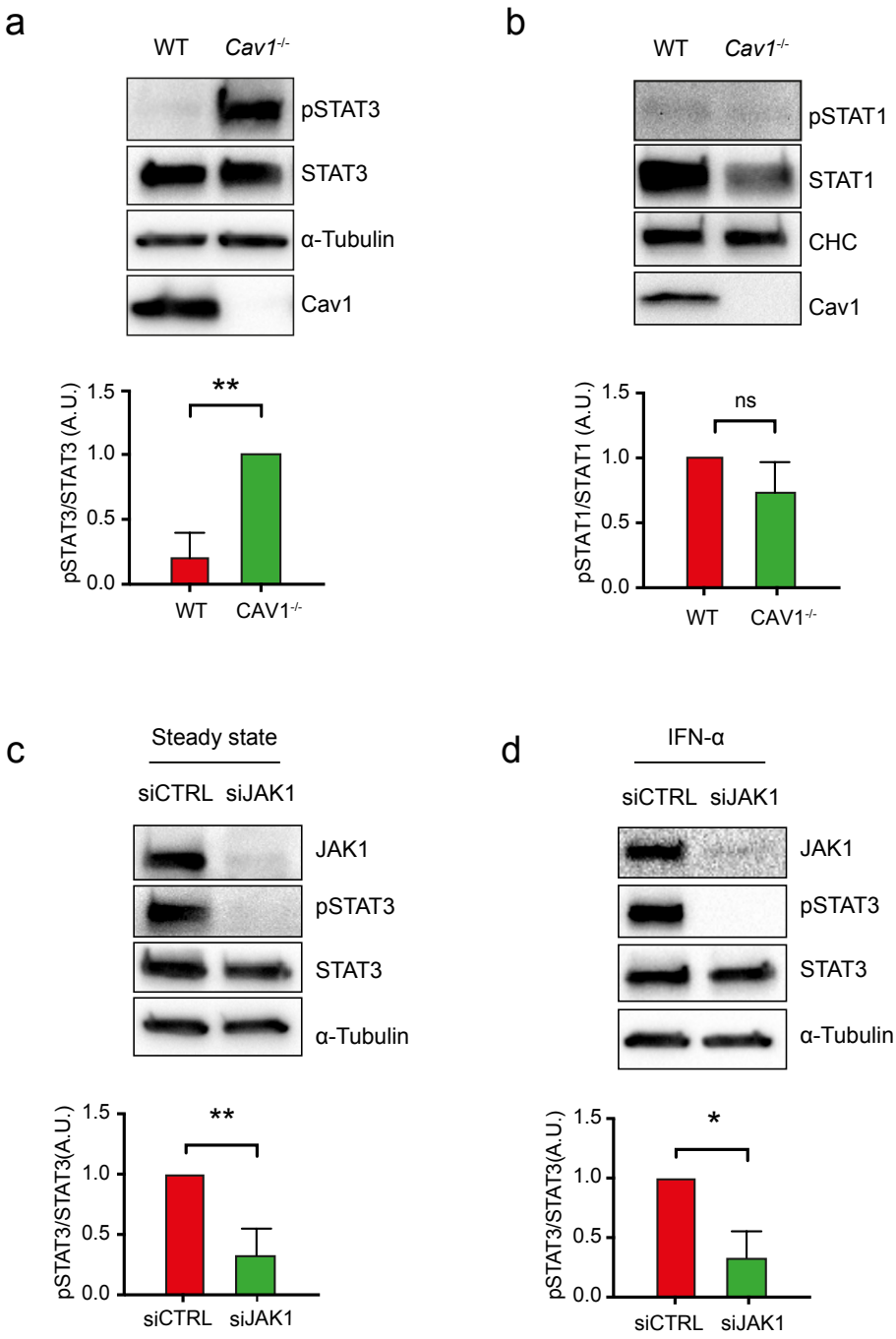
a
WT
Cav1-/-
pSTAT3
STAT3
α-Tubulin
Cav1
pSTAT3/STAT3 (A.U.)
1.5
1.0
0.5
0.0
**
WT
CAV1-/-
b
WT
Cav1-/-
pSTAT1
STAT1
CHC
Cav1
pSTAT1/STAT1 (A.U.)
ns
c
Steady state
siCTRL
siJAK1
JAK1
pSTAT3
STAT3
α-Tubulin
pSTAT3/STAT3(A.U.)
**
d
IFN-α
*

Figure 4. Cav1 negatively regulates the JAK1-dependent STAT3 activation

(a) STAT3 basal phosphorylation level in WT MLEC compared to *Cav1*$^{-/-}$ MLEC. Representative immunoblot. **(b)** STAT1 basal phosphorylation level in WT MLEC compared to *Cav1*$^{-/-}$ MLEC. Representative immunoblot. **(c)** STAT3 basal phosphorylation level in *Cav1*-/- MLEC upon control (CTRL) or JAK1 siRNA treatment. Reprensentative immunoblot. **(d)** IFNα induced STAT3 phosphorylation level in *Cav1*-/- MLEC upon CTRL or JAK1 siRNA treatment. Representative immunoblot. Immunoblot quantification of (pSTAT/Tubulin)/(STAT/Tubulin) signal ratio relative to control condition. Mean value ± SEM. Statistics was performed using two tailored unpaired t test. *P<0,05; **P<0,01.

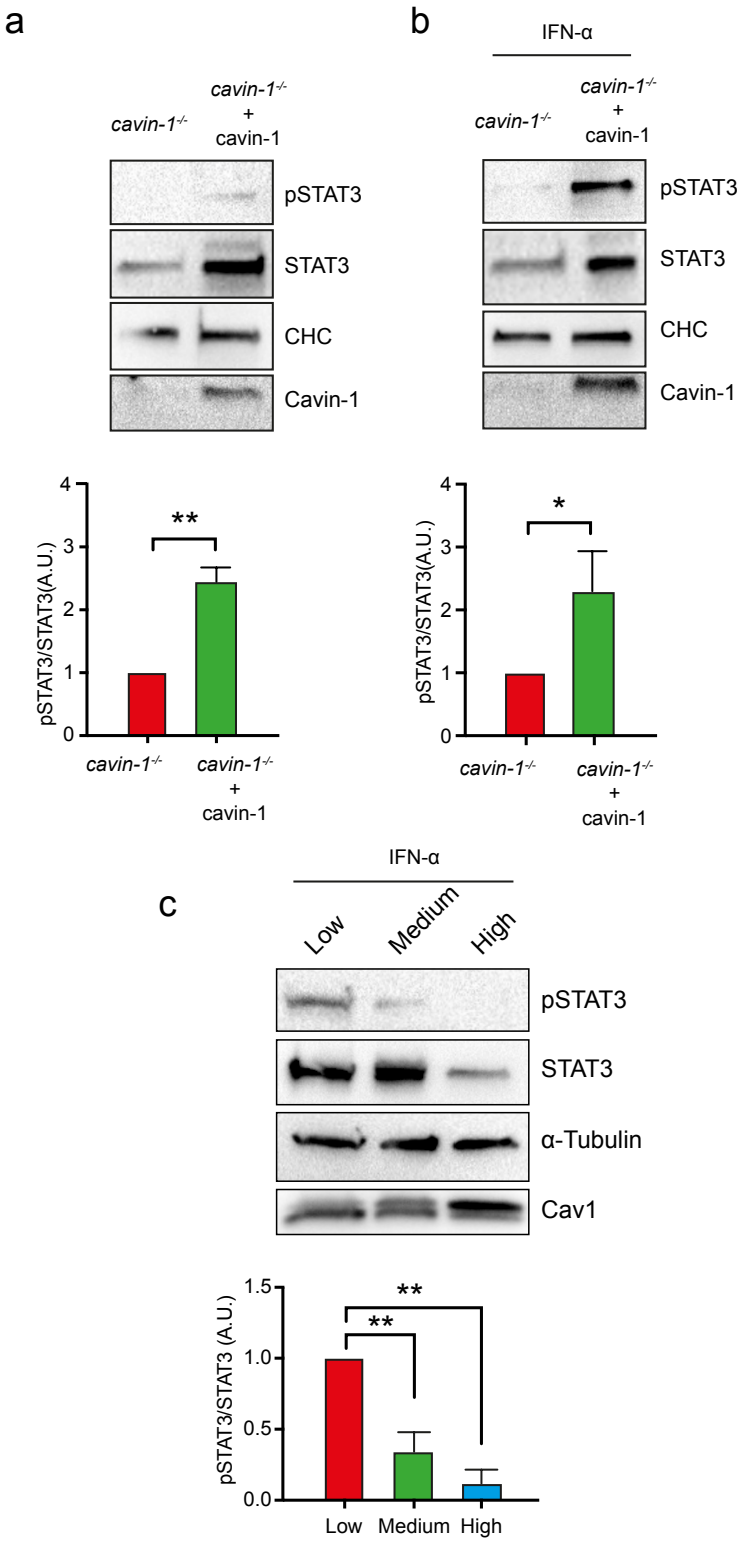
a
b
IFN-α
cavin-1-/-
cavin-1-/- + cavin-1
pSTAT3
STAT3
CHC
Cavin-1
pSTAT3/STAT3(A.U.)
**
*
c
Low
Medium
High
α-Tubulin
Cav1
pSTAT3/STAT3 (A.U.)

Figure 5. Non-caveolar Cav1 inhibits IFN-α-induced STAT3 phosphorylation in a concentration dependent manner

(a) STAT3 basal level of activation of *cavin-1*$^{-/-}$ MEF cells and *cavin-1*$^{-/-}$ MEF cells transfected with cavin-1 (+ cavin-1). Quantification of signal ratio relative to "*cavin-1*$^{-/-}$ " condition. Representative immunoblot. **(b)** IFN-α-induced STAT3 level of activation in *cavin-1*$^{-/-}$ MEF cells and *cavin-1*$^{-/-}$ MEF cells + cavin-1. Representative immunoblot. Quantification signal ratio relative to "*cavin-1*$^{-/-}$" condition. **(c)** IFN-α-induced STAT3 phosphorylation level in *cavin-1*$^{-/-}$ MEF cells with either low, medium or high Cav1 expression. Representative immunoblot. Quantification of signal ratio relative to "low" condition. (a, b, c) mean values ± SEM. Statistics were processed using unpaired t test (a, b) and multi-comparison one-way ANOVA (c). *P<0,05; **P<0,01

a

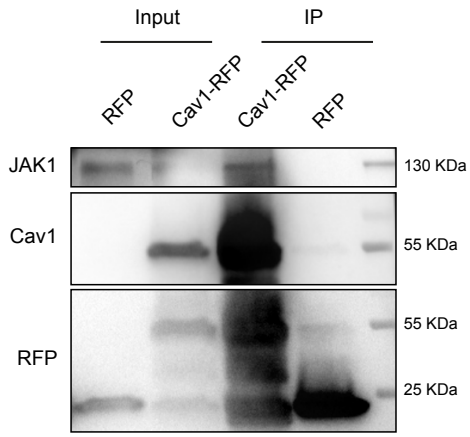
Input
IP
RFP
Cav1-RFP
Cav1-RFP
RFP
JAK1
Cav1
RFP
130 KDa
55 KDa
55 KDa
25 KDa

b

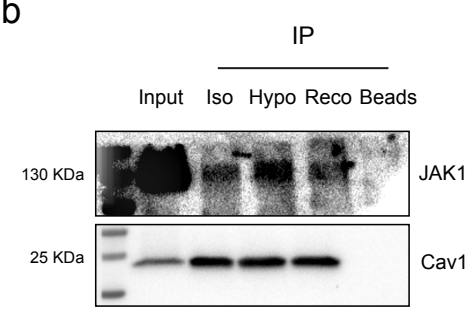
IP
Input
Iso
Hypo
Reco
Beads
130 KDa
25 KDa
JAK1
Cav1

c

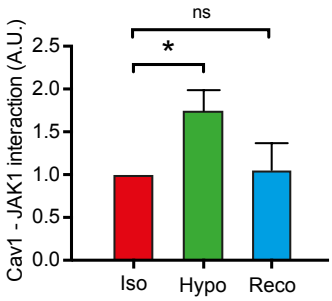
ns
*
Cav1 - JAK1 interaction (A.U.)
2.5
2.0
1.5
1.0
0.5
0.0
Iso
Hypo
Reco

d

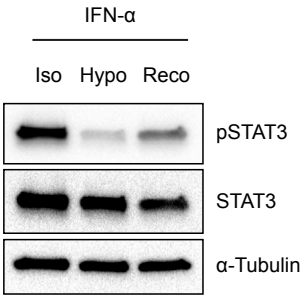
IFN-α
Iso
Hypo
Reco
pSTAT3
STAT3
α-Tubulin

e

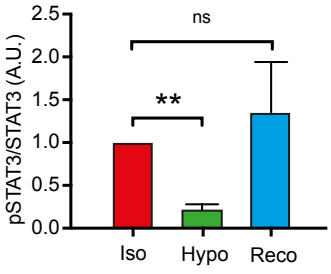
ns
**
pSTAT3/STAT3 (A.U.)
2.5
2.0
1.5
1.0
0.5
0.0
Iso
Hypo
Reco

Figure 6. **Mechanical stress determines Cav1 interaction with JAK1**

(a) RFP-trap pull down experiment in Cav1-RFP expressing *Cav1*$^{-/-}$ MLEC cells. Representative immunoblot. **(b)** Immunoprecipitation experiment of endogenous Cav1 in iso-osmotic (Iso), hypo-osmotic (Hypo) and successive hypo-osmotic shock and iso-osmotic condition (Rec). Representative immunoblot. Quantification of (JAK1/Cav1) signal ratio relative to “Iso” condition. **(c)** STAT3 phosphorylation level in WT MLEC upon IFNα stimulation under iso-osmotic (Iso), hypo-osmotic (Hypo) and successive iso and hypo-osmotic shock (Rec). Representative immunoblot. Quantification of immuno-staining upon Iso-, Hypo- and Recovery osmotic shock. (b, c) mean value ± SEM, statistics were processed using multi-comparison one-way ANOVA. *P<0,05; **P<0,01.

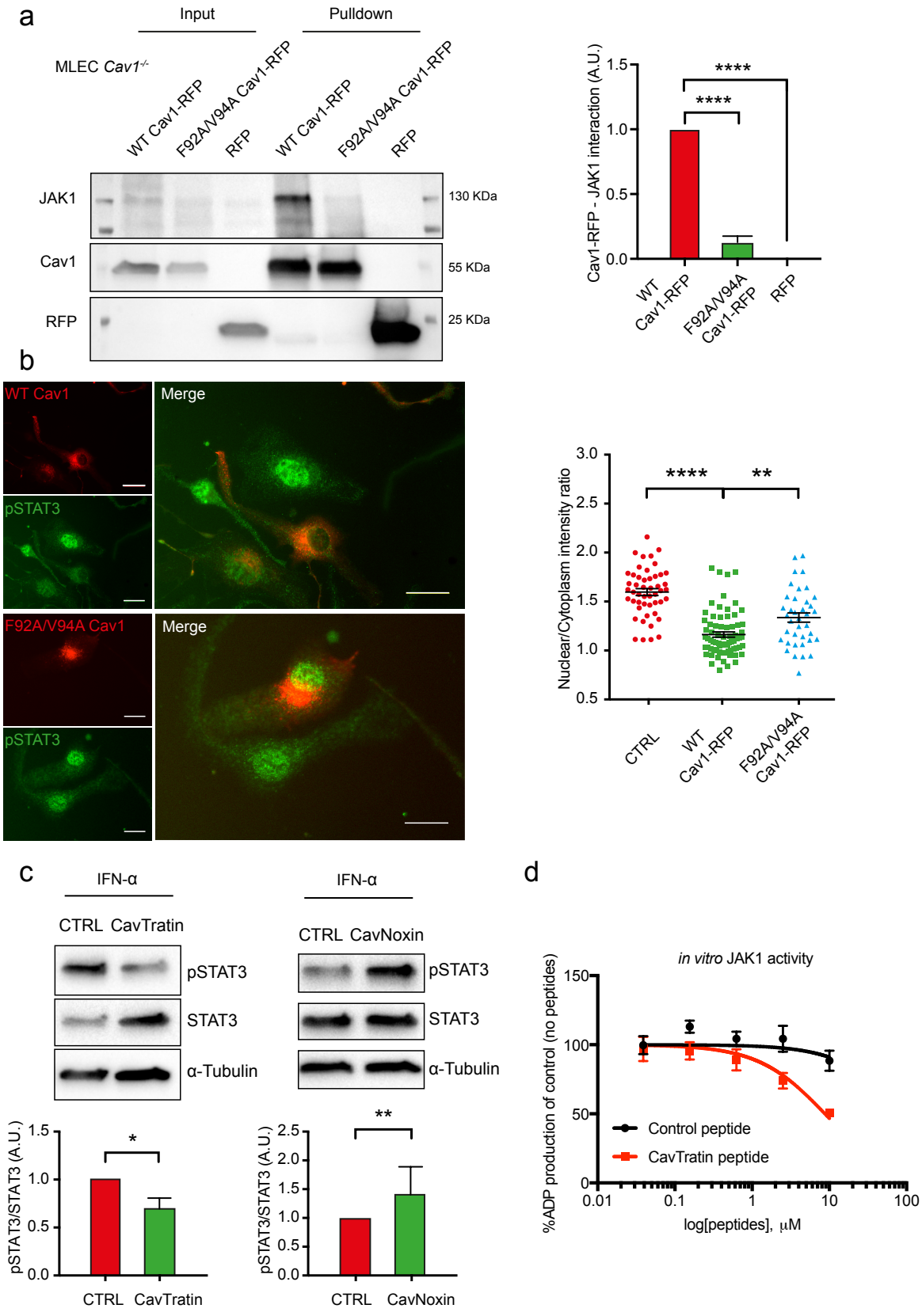
a
Input
Pulldown
MLEC Cav1-/-
WT Cav1-RFP
F92A/V94A Cav1-RFP
RFP
WT Cav1-RFP
F92A/V94A Cav1-RFP
RFP
JAK1
Cav1
RFP
130 KDa
55 KDa
25 KDa
Cav1-RFP - JAK1 interaction (A.U.)
1.5
1.0
0.5
0.0
****
****
WT Cav1-RFP
F92A/V94A Cav1-RFP
RFP
b
WT Cav1
Merge
pSTAT3
F92A/V94A Cav1
Merge
pSTAT3
Nuclear/Cytoplasm intensity ratio
3.0
2.5
2.0
1.5
1.0
0.5
****
**
CTRL
WT Cav1-RFP
F92A/V94A Cav1-RFP
c
IFN-α
CTRL CavTratin
pSTAT3
STAT3
α-Tubulin
IFN-α
CTRL CavNoxin
pSTAT3
STAT3
α-Tubulin
pSTAT3/STAT3 (A.U.)
1.5
1.0
0.5
0.0
*
CTRL CavTratin
pSTAT3/STAT3 (A.U.)
2.5
2.0
1.5
1.0
0.5
0.0
**
CTRL CavNoxin
d
in vitro JAK1 activity
%ADP production of control (no peptides)
150
100
50
0
Control peptide
CavTratin peptide
0.01
0.1
1
10
100
log[peptides], μM

Figure 7. The caveolin scaffolding domain is required for Cav1-JAK1 interaction and Cav1 negative effect

(a) immunoblot of RFP-trap pulldown experiment performed on *Cav1*$^{-/-}$ MLEC cells expressing either WT Cav1-RFP or F92A/V94A Cav1-RFP or RFP (left). Quantification of JAK1/Cav1 signal ratio relative to "WT Cav1-RFP" condition (right). **(b)** Analysis of nuclear translocation of pSTAT3 (green) of IFN-α stimulated *Cav1*$^{-/-}$ MLEC expressing either exogenous WT Cav1-RFP or F92A/V94A Cav1-RFP (red) (left). Quantification of nuclear/cytosol pSTAT3 signal ratio in CTRL, WT Cav1 and F92A/V94A Cav1 (right). After fixation, the nuclear distribution of pSTAT3 was detected by immunofluorescence. **(c)** IFN-α-induced STAT3 phosphorylation level of WT MLEC cells upon either control peptide and CavTratin treatment (left) or control peptide and CavNoxin treatment (right). Representative immunoblots. **(d)** Graph representing in vitro JAK1 ADP production relative to peptide log concentration (μM), control peptide (black curve) or CavTratin (red curve). (a, b, c) mean values ± SEM. Statical analysis were processed using one-way ANOVA (a, b) and two tailored unpaired t test (c). *P<0,05; **P<0,01; ***P<0,001; ****P<0,0001.

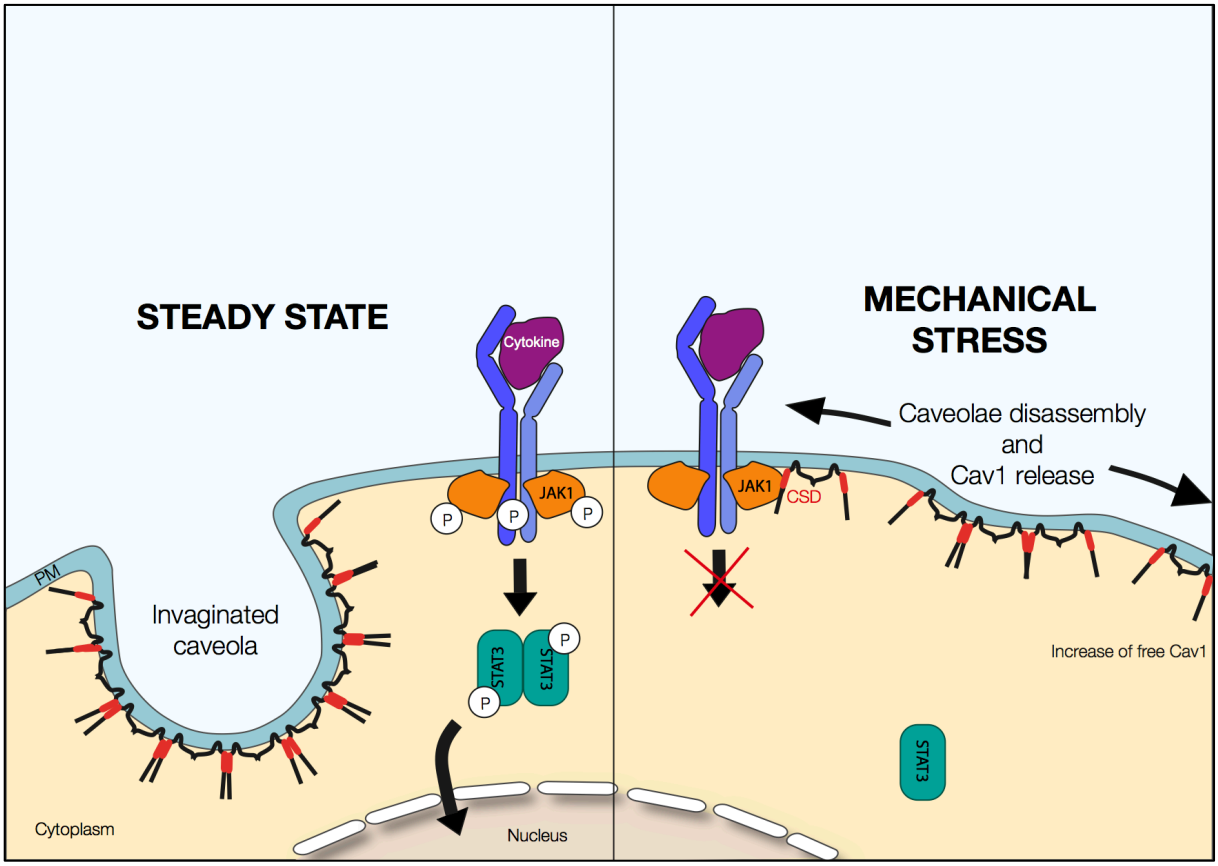
STEADY STATE
Cytokine
JAK1
P
P
P
PM
Invaginated
caveola
STAT3
STAT3
P
P
Cytoplasm
Nucleus
MECHANICAL
STRESS
Caveolae disassembly
and
Cav1 release
JAK1
CSD
Increase of free Cav1
STAT3

Figure 8. Molecular model of the control of JAK-STAT signaling by caveolae mechanics

Left panel: At steady state, Cav1 is entirely caveolar and its localization is restricted to invaginated caveolae. Upon IFN-α stimulation, signal transduction occurs through the JAK-STAT pathway, activating STAT3 phosphorylation and its consecutive nuclear translocation. **Right panel:** Upon mechanical stress, membrane tension increases, which leads to rapid caveolae flattening and disassembly. Caveolae disassembly dramatically increases the diffusion of non-caveolar Cav1 oligomers that are able to bind to JAK1 via its CSD. This results in the direct inhibition of the tyrosine kinase catalytic activity. JAK1 inhibition mediated by Cav1 interaction prevents signal transduction of JAK-STAT pathway when stimulated by IFN-α.

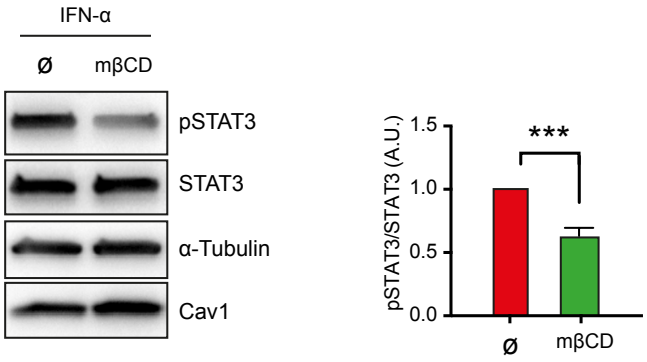

Supplementary figure 1. Caveolae disruption by cyclodextrin treatment decreased IFN-α-induced STAT3 phosphorylation

STAT3 phosphorylation level of WT MLEC stimulated by IFN-α upon mβCD treatment. Representative immunoblot. Quantification of (PSTAT3/Tub)/(STAT3/Tub) signal ratio relative to control condition. Mean values ± SEM. Statical analysis were processed using two tailored unpaired t test, ***P<0,001.

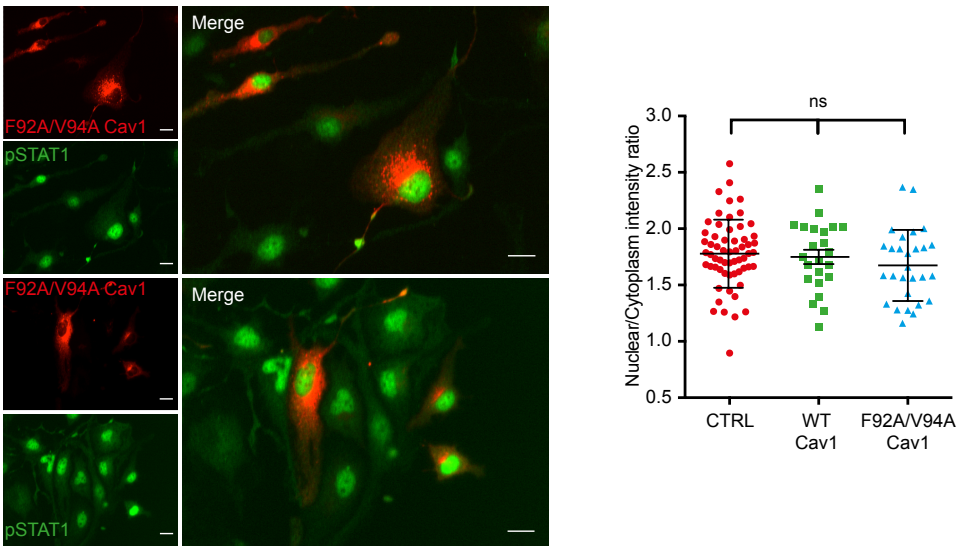

Supplementary figure 2. IFN-α induced STAT1 nuclear translocation.

Analysis of the nuclear translocation of pSTAT1 (green) of IFN-α stimulated *Cav1*$^{-/-}$ MLEC expressing either exogenous WT Cav1-RFP or F92A/V94A Cav1-RFP (red). After fixation the nuclear distribution of pSTAT1 (green) was detected by immunofluorescence. Quantification of nuclear/cytosol pSTAT3 signal ratio in CTRL, WT Cav1 and F92A/V94A Cav1. Statistics were processed using standard one-way ANOVA.

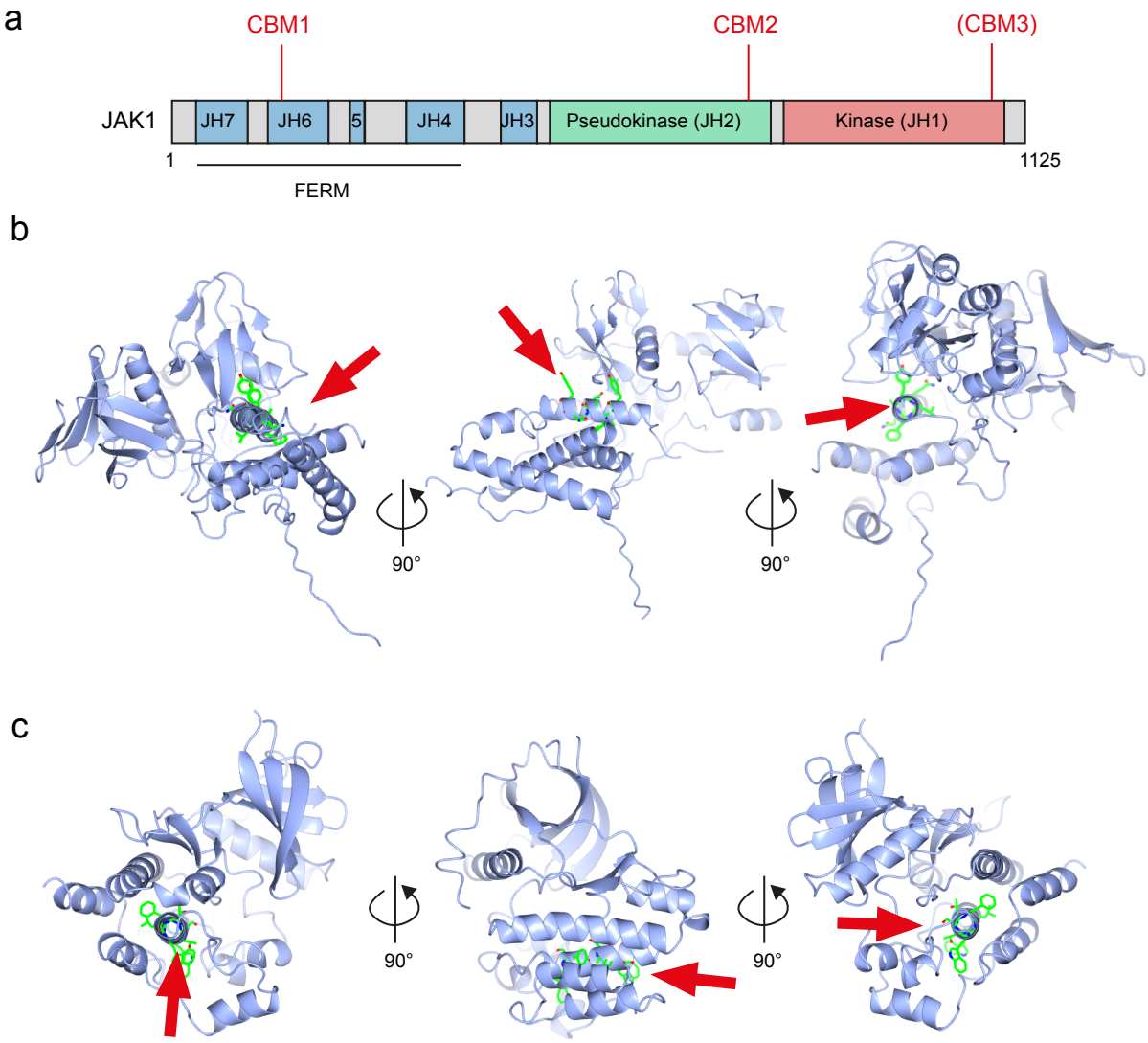

Supplementary figure 3. CBM localization on JAK1 structure

(a) Putative CBM localization in JAK1 primary structure. **(b)** CBM1 (highlighted lateral chains, red arrow) localization in the tridimensional structure of the FERM domain of JAK1 (PDB 5IXI). **(c)** CBM2 (highlighted lateral chains, red arrow) localization in JAK1 pseudokinase tridimensional structure (PDB 4L00). Pseudokinase and kinase domains are structurally identical. The putative CBM3 has a localization similar to the CBM2 but within the kinase domain.

Materials & Methods

Cell lines.

WT MLEC and *Cav1*$^{-/-}$ cell lines were characterized by Sessa's team (Murata et al., 2007) and kindly provided by Radu V.Stan (Darthmouth Mediac School, NH, USA). These mice lung endothelial cells were immortalized using polyomavirus T antigen and selected according to CD31, VE-Cadherin and PV1 expression.

Cell culture.

All cells were grown at 37°C under 5% of CO2. WT MLEC and *Cav1*$^{-/-}$ MLEC cell lines were cultured in Enothelial Balal Medium (EBM2) from Lonza supplemented with 15% Hyclone FCS, 4mM glutamine, 5mM sodium pyruvate, 0,01 % penicillin streptomycin (v/v), 0.04% hydrocortisone (v/v), 0.4% hEGF-B (v/v), 0.1% VEGF (v/v), 0.1% R3-IGF-1 (v/v), 0.1% ascorbic acid (v/v), 0.1% hEGF (v/v), 0.1% GA-1000 (v/v), 0.1% heparin (v/v) (EGM2 singlequote, Lonza). MEF cells were cultured in DMEM high-glucose glutamax (Gibco, Life Technologies), supplemented with 10% SVF (v/v), 0.01% penicillin streptomycin (v/v) and 5mM sodium pyruvate.

Antibodies and reagents.

Mouse anti-αTubulin (Sigma-Aldrich, clone B512, T5168, 1/1000 for WB); mouse anti-chlatrin heavy chain (BD Transduction, 610500, 1/5000 for WB) rabbit anti-caveolin-1 (Cell Signaling 3238S, 1/1000 for WB); mouse anti-caveolin-1 (BD Transduction, 610407, 10µg/condition for IP); mouse anti-PTRF (BD Biosciendes 611258, 1/1000 for WB); mouse anti-STAT3 (Cell signaling, clone 124H6, 9139, 1/1000 for WB); rabbit anti-pSTAT3 (Cell signaling, clone D3A7 9145, 1/1000 for WB, 1/100 for IF); rabbit anti-STAT1 (Cell signaling, 9172, 1/1000 for WB); mouse anti-pSTAT1 (Cell Signaling, 9167, 1/1000 for WB, 1/100 for IF); rabbit anti-JAK1 (Cell Signaling, 3332S, 1/1000 for WB); Secondary antibodies conjugated to Alexa 488, Cy3 or horse radish peroxidase (Beckman Coulter or Invitrogen).

RNA interference-mediated silencing.

WT MLEC cells were transfected with small interfering RNAs (siRNAs) using using HiPerFect (Qiagen) according to manufacturer's protocol. Experiments were performed 24 hours after transfection, on validation of silencing efficiency by

immunoclot analysis using specific antibodies and normalizing to the total level of α-tubulin used as loading control. 20 nM SMART pool siRNA targeting JAK1 mRNA (GE healthcare/Dharmacon, L-040117-00-0005) was used for JAK1 knock down. Control siRNA (QIAGEN, 1022076) was used at the same concentration and served as reference point.

Immunoblotting.

Cells were lysed in sample buffer (62.5 mM Tris/HCl ph 6.0, 2% SDS (v/v), 10% glycerol (v/v), 40 mM dithiothreitol and 0.03% phenol red (w/v)). Lysates were analyzed by SDS-PAGE and Western blot analysis and immunoblotted with the indicated primary antibodies and horseradish peroxydase-conjugated secondary antibodies. Chemiluminescence signal was revealed using Pierce™ ECL Western Blotting Substrate, SuperSignal West Dura Extended Duration Substrate or SuperSignal West Femto Substrate (Thermo Scientific Life Technologies). Acquisitions were performed with the ChemiDoc MP Imaging System (BioRad). Samples for the detection of phospho and non-phospho proteins were loaded on two different gels. The ratio of the signal detection for targeted protein/loading control was determined for each membrane. The overall ratio of (phosphoprotein/loading control)/(protein/loading control) was determined.

Immunofluorescence.

Transfected *Cav1*$^{-/-}$ MLEC cells were seeded on 12 mm coverslips 24h before the pSTAT nuclear translocation assay. After IFNα stimulation, cells are fixed and permeabilized with cold methanol for 15 min at -20°C. Cells are washed with PBS 0.2% BSA (v/v) then sequentially incubated with idicated promary antibody and fluorescence-conjugated secondary antibody in PBS 0.2% BSA (v/v) for 1h at room temperature. Coverslips are mounted in Fluoromount-G mounting medium (eBioscience) supplemented with 2 µg/mL DAPI (Sigma-Aldrich). Pictures were acquired on a Leica DM 6000B inverted epifluoresence microscope equipped with a HCX PL Apo 63X NA 1.40 oil immersion objective and an EMCCD camera (Photometrics CoolSMAP HQ); Camera: CCD 1392x1040; objective 40x or 63x. Quantification of pSTATs nuclear translocation by calculating the nucleocytoplasmic

ratio of phospho-STAT1-3 signal (nuclei masks were realized with the DAPI staining) with image J software 1.49a (NIH) and plugins bundle proposed by the McMaster Biophotonics Faclity (http://www.macbiohotonics.ca).

Single particle tracking.

WT MLEC cells were transfected using the AMAXA electroporation setup with Cav1-mEOS3.2 and Cav1-GFP 24h prior experiment. Cells were grown in Ringer media and 30mOsm hypo-osmotic shock was applied during acquisition. Images were acquired using sensitive EMCCD and Nikon CFI Apo TIRF 100x oil, NA 1.49 objective.

Transfection.

For single particle tracking experiment WT MLEC and *Cav1*$^{-/-}$ were transfected using Lonza AMAXA. Adapted settings for mice cells (MEF) were provided in the AMAXA setup. Lonza provided specific reagent for AMAXA mice cells transfection. Double transfection of 5ug of Cav1 mEOS3.2 and 1ug of Cav1 GFP on 1 million cells was performed 24h prior experiment. For pSTATs nuclear translocation upon Cav1 expression, cells were electroporated using a pulse of 220 V and 975 µF with a Gene Pulser® the BioRad setup.

IFN-α stimulation.

Cells were treated with or without 1000 U/ml IFNα at 37°C for the indicated times. For biochemical analysis, cells were washed with PBS and lysed in SDS Sample Buffer 1X. Total lysates were analyzed by SDS-PAGE and Western blot analysis and immunoblotted with the indicated antibodies. Chemiluminescence detection was performed with SuperSignal West Dura Extended Duration Substrate or with SuperSignal West Femto Substrate (Thermo Scientific Life Technologies). Phosphorylated and total forms of the proteins are quantified and normalized to clathrin heavy chain or tubulin levels in the same lysate. Phosphorylated protein over total ratio is determined for each condition.

High throughput screening.

25 µg/mL fibronectine diluted in NaOH 100 mM pH 8.6 is incubated on a PDMS layer at 37°C. 70k WT MLEC or *Cav1*$^{-/-}$ MLEC cells were seeded and incubated for 4 hours at 37°C in complete MLEC media. Cells were stretched by 25% for 2 minutes then while stretch is maintained, cells media is replaced by stimulation media (EBM-2 no SVF with IFNα 1000 U/ml) for 20min at 37°C. Cells were washed with PBS and lysed with hot laemmli 1X sample buffer (50 mM Tris pH=6.8, 2% SDS, 5% glycerol, 2mM DTT, 2,5 mM EDTA, 2.5mM/EGTA, 2.5mM/EGTA, 2x Phosphatase inhibitors (Halt Phosphatase inhibitor cocktail 100x, Perbio, Ref. 78420), Protease inhibitors (Protease inhibitor cocktail, complete MINI EDTA-free, Roche, Ref. 1836170), 1 tablet/5mL (or by RR : 1/1000 PIC), 4 mM Sodium Orthovanadate, 20 mM Sodium Fluoride).

Co-immunoprecipitations.

Cells were lysed in 1% NP-40 in TNE (10 mM Tris/HCl pH 7.5, 150 mM NaCl, 0.5 mM EDTA) with protease inhibitors cocktail (Roche) for 30 min at 4°C. Cleared lysates (16,000g, 10 min, 4°C) were incubated overnight at 4°C under rotation with 1 µg/ml of the indicated antibody followed by incubation for 1 hour with 25 µl of protein A/G magnetic beads (Thermo Scientific) in the case of endogenous proteins. In the case of tagged proteins, 25 µl GFP-Trap or RFP-Trap beads (Chromotek) were used. After 3 washes in TNE, immunoprecipitated beads were eluted following the manufacturers' instructions.

Osmotic shock and uni-axial stretch.

For osmotic shock, cells were seeded 24h before experiment, then complete media was replaced by 30 mOsm media (10% media and 90% H_2O) for 5 minutes, cells were immediately lysed or hypo-osmmotic media was replaced by normal iso-osmotic media (recovery) before lysis. For cell stretch, cells were seeded on a 100 um thick PDM sheet (12x7 mm) coated with fibronectin 4 hours prior experiment. The PDMS sheet was linearly stretched using a homemade setup motorized (P1, Karlsruhe, Germany). Cells were pre-stretched by 25% for 2 minutes and stretch was maintained during IFNα stimulation.

CSD mimicking peptides

CSD mimicking peptides were synthetized from biomatik. Control peptide HHHHHH-RQIKIWFQNRRMKWKKWGIDKASFTTFTVTKYWFRY; CavTratin HHHHHH-QIKIWFQNRRMKWKKDGIWKASFTTFTVTKY; CavNoxin HHHHHH-RQIKIWFQNRRMKWKKDGIWKASFAAATVTKWYFYR. Cells were treated for 6 hours with 1µM CSD mimicking peptide resuspended in endothelial basal medium 0,2% PBS/BSA (v/v)

Invitro Kinase activity measurement.

Invitro kinase assay was performed using purified JAK1 (ProQinase 1480-0000-1 JAK1 aa583-1154), RBER-IRStide (ProQinase 0863-0000-1). Kinase reaction was performed in Kinase reaction buffer ([ATP] 100 µM, RBER-IRStide 80 µg/ml, DMSO according to peptide concentration) at 30°C for 1h. Measurement of ADP production was performed using Promega ADP-Glo™ Kinase Assay. Luminescence measurement was performed using BMG Labtech FLUOstar Omega plate reader.

Drug treatment

WT MLEC cells were treated 1% with methyl β cyclodextrin (w/v) (sigma aldrich C4555) for 20 minutes and stimulated with 1000 U/ml IFNα at 37°C for 10 minutes.

References

Aboulaich, N., Vainonen, J.P., Stralfors, P., and Vener, A. V (2004). Vectorial proteomics reveal targeting, phosphorylation and specific fragmentation of polymerase I and transcript release factor (PTRF) at the surface of caveolae in human adipocytes. Biochem. J. *383*, 237–248.

Ariotti, N., Fernández-Rojo, M.A., Zhou, Y., Hill, M.M., Rodkey, T.L., Inder, K.L., Tanner, L.B., Wenk, M.R., Hancock, J.F., and Parton, R.G. (2014). Caveolae regulate the nanoscale organization of the plasma membrane to remotely control Ras signaling. J. Cell Biol. *204*, 777–792.

Ariotti, N., Rae, J., Leneva, N., Ferguson, C., Loo, D., Okano, S., Hill, M.M., Walser, P., Collins, B.M., and Parton, R.G. (2015). Molecular characterization of caveolin-induced membrane curvature. J. Biol. Chem. *290*, 24875–24890.

Bastiani, M., Liu, L., Hill, M.M., Jedrychowski, M.P., Nixon, S.J., Lo, H.P., Abankwa, D., Luetterforst, R., Fernandez-Rojo, M., Breen, M.R., et al. (2009). MURC/Cavin-4 and cavin family members form tissue-specific caveolar complexes. J. Cell Biol. *185*, 1259–1273.

Beebe, J., Liu, J.-Y., and Zhang, J.-T. (2018). Two decades of research in discovery of anticancer drugs targeting STAT3, how close are we? Pharmacol. Ther.

Bernatchez, P., Sharma, A., Bauer, P.M., Marin, E., and Sessa, W.C. (2011). A noninhbitory mutant of the caveolin1 scaffolding domain enhances eNOS-derived NO synthesis and vasodilation in mice. *121*.

Bernatchez, P.N., Bauer, P.M., Yu, J., Prendergast, J.S., He, P., and Sessa, W.C. (2005). Dissecting the molecular control of endothelial NO synthase by caveolin-1 using cell-permeable peptides. Proc. Natl. Acad. Sci. U. S. A. *102*, 761–766.

Blouin, C.M., Hamon, Y., Gonnord, P., Boularan, C., Kagan, J., Viaris de Lesegno, C., Ruez, R., Mailfert, S., Bertaux, N., Loew, D., et al. (2016). Glycosylation-Dependent IFN-??R Partitioning in Lipid and Actin Nanodomains Is Critical for JAK Activation. Cell *166*, 920–934.

Byrne, D.P., Dart, C., and Rigden, D.J. (2012). Evaluating Caveolin Interactions: Do Proteins Interact with the Caveolin Scaffolding Domain through a Widespread Aromatic Residue-Rich Motif? PLoS One *7*.

Cheng, J.P.X., and Nichols, B.J. (2016). Caveolae: One Function or Many? Trends Cell Biol. *26*, 177–189.

Cheng, J.P.X., Mendoza-Topaz, C., Howard, G., Chadwick, J., Shvets, E., Cowburn, A.S., Dunmore, B.J., Crosby, A., Morrell, N.W., and Nichols, B.J. (2015). Caveolae protect endothelial cells from membrane rupture during increased cardiac output. J. Cell Biol. *211*, 53–61.

Collins, B.M., Davis, M.J., Hancock, J.F., and Parton, R.G. (2012). Structure-Based Reassessment of the Caveolin Signaling Model: Do Caveolae Regulate Signaling through Caveolin-Protein Interactions? Dev. Cell *23*, 11–20.

Couet, J., Li, S., Okamoto, T., Ikezu, T., and Lisanti, M.P. (1997a). Identification of peptide and protein ligands for the caveolin- scaffolding domain. Implications for the interaction of caveolin with caveolae-associated proteins. J. Biol. Chem. *272*, 6525–6533.

Couet, J., Sargiacomo, M., and Lisanti, M.P. (1997b). Interaction of a receptor tyrosine kinase, EGF-R, with caveolins. Caveolin binding negatively regulates tyrosine and serine/threonine kinase activities. J. Biol. Chem. *272*, 30429–30438.

Fujimoto, T. (1993). Calcium pump of the plasma membrane is localized in caveolae. J. Cell Biol. *120*, 1147–1157.

Gambin, Y., Ariotti, N., McMahon, K.A., Bastiani, M., Sierecki, E., Kovtun, O., Polinkovsky, M.E., Magenau, A., Jung, W., Okano, S., et al. (2014). Single-molecule analysis reveals self assembly and nanoscale segregation of two distinct cavin subcomplexes on caveolae. Elife *3*, e01434.

Gangadharan, V., Nohe, A., Caplan, J., Czymmek, K., and Duncan, R.L. (2015). Caveolin-1 regulates P2X7 receptor signaling in osteoblasts. Am. J. Physiol. Cell Physiol. *308*, C41-50.

Garcia-Cardena, G. (1997). Dissecting the Interaction between Nitric Oxide Synthase (NOS) and Caveolin. functional significance of the nos caveolin binding domain in vivo. J. Biol. Chem. *272*, 25437–25440.

Goetz, J.G., Lajoie, P., Wiseman, S.M., and Nabi, I.R. (2008). Caveolin-1 in tumor progression: The good, the bad and the ugly. Cancer Metastasis Rev. *27*, 715–735.

Hansen, C.G., Howard, G., and Nichols, B.J. (2011). Pacsin 2 is recruited to caveolae and functions in caveolar biogenesis. J. Cell Sci. *124*, 2777–2785.

Hayer, A., Stoeber, M., Bissig, C., and Helenius, A. (2010). Biogenesis of caveolae: stepwise assembly of large caveolin and cavin complexes. Traffic *11*, 361–382.

Hill, M.M., Bastiani, M., Luetterforst, R., Kirkham, M., Kirkham, A., Nixon, S.J., Walser, P., Abankwa, D., Oorschot, V.M.J., Martin, S., et al. (2008). PTRF-Cavin, a Conserved Cytoplasmic Protein Required for Caveola Formation and Function. Cell *132*, 113–124.

Hoop, C.L., Sivanandam, V.N., Kodali, R., Srnec, M.N., and van der Wel, P.C.A. (2012). structural characterizationof the caveolin scaffolding domain in association with cholesterol-rich membranes. *51*, 90–99.

Jasmin, J.F., Mercier, I., Sotgia, F., and Lisanti, M.P. (2006). SOCS proteins and caveolin-1 as negative regulators of endocrine signaling. Trends Endocrinol. Metab. *17*, 150–158.

Kai, F., Laklai, H., and Weaver, V. (2016). Force Matters: Biomechanical Regulation of Cell Invasion and Migration in Disease. Trends Cell Biol. *xx*, 1–12.

Kaptein, A., Paillard, V., and Saunders, M. (1996). Dominant negative stat3 mutant inhibits interleukin-6-induced Jak-STAT signal transduction. J. Biol. Chem. *271*, 5961–5964.

Kershaw, N.J., Murphy, J.M., Lucet, I.S., Nicola, N.A., and Babon, J.J. (2013). Regulation of Janus kinases by SOCS proteins. Biochem. Soc. Trans. *41*, 1042–1047.

Kirkham, M., Nixon, S.J., Howes, M.T., Abi-Rached, L., Wakeham, D.E., Hanzal-Bayer, M., Ferguson, C., Hill, M.M., Fernandez-Rojo, M., Brown, D. a, et al. (2008).

Evolutionary analysis and molecular dissection of caveola biogenesis. J. Cell Sci. *121*, 2075–2086.

Koromilas, A.E., and Sexl, V. (2013). The tumor suppressor function of STAT1 in breast cancer. Jak-Stat *2*, e23353.

Lamaze, C., and Torrino, S. (2015). Caveolae and cancer: A new mechanical perspective. Biomed. J. *38*, 367–379.

Lamaze, C., Tardif, N., Dewulf, M., Vassilopoulos, S., and Blouin, C.M. (2017). The caveolae dress code: structure and signaling. Curr. Opin. Cell Biol. *47*, 117–125.

Le Lan, C., Neumann, J.-M., and Jamin, N. (2006). Role of the membrane interface on the conformation of the caveolin scaffolding domain: a CD and NMR study. FEBS Lett. *580*, 5301–5305.

Li, S., Okamoto, T., Chun, M., Sargiacomo, M., Casanova, J.E., Hansen, S.H., Nishimoto, I., and Lisanti, M.P. (1995). Evidence for a regulated interaction between heterotrimeric G proteins and caveolin. J. Biol. Chem. *270*, 15693–15701.

Li, S., Couet, J., and Lisanti, M.P. (1996). Src tyrosine kinases, Galpha subunits, and H-Ras share a common membrane-anchored scaffolding protein, caveolin. Caveolin binding negatively regulates the auto-activation of Src tyrosine kinases. J. Biol. Chem. *271*, 29182–29190.

Lim, Y.W., Lo, H.P., Ferguson, C., Martel, N., Giacomotto, J., Gomez, G.A., Yap, A.S., Hall, T.E., and Parton, R.G. (2017). Caveolae Protect Notochord Cells against Catastrophic Mechanical Failure during Development. Curr. Biol. *27*, 1968–1981.e7.

Lisanti, M.P., Tang, Z., Scherer, P.E., Kubler, E., Koleske, A.J., and Sargiacomo, M. (1995). Caveolae, transmembrane signalling and cellular transformation. Mol. Membr. Biol. *12*, 121–124.

Liu, H., Yang, L., Zhang, Q., Mao, L., Jiang, H., and Yang, H. (2016). Probing the structure and dynamics of caveolin-1 in a caveolae-mimicking asymmetric lipid

Lo, H.P., Nixon, S.J., Hall, T.E., Cowling, B.S., Ferguson, C., Morgan, G.P., Schieber, N.L., Fernandez-Rojo, M.A., Bastiani, M., Floetenmeyer, M., et al. (2015). The caveolin-Cavin system plays a conserved and critical role in mechanoprotection of skeletal muscle. J. Cell Biol. *210*, 833–849.

Ludwig, A., Howard, G., Mendoza-Topaz, C., Deerinck, T., Mackey, M., Sandin, S., Ellisman, M.H., and Nichols, B.J. (2013). Molecular composition and ultrastructure of the caveolar coat complex. PLoS Biol. *11*, e1001640.

Meng, F., Saxena, S., Liu, Y., Joshi, B., Wong, T.H., Shankar, J., Foster, L.J., Bernatchez, P., and Nabi, I.R. (2017). The phospho–caveolin-1 scaffolding domain dampens force fluctuations in focal adhesions and promotes cancer cell migration. Mol. Biol. Cell *28*, 2190–2201.

Moon, H., Lee, C.S., Inder, K.L., Sharma, S., Choi, E., Black, D.M., Lê Cao, K., Winterford, C., Coward, J.I., Ling, M.T., et al. (2013). PTRF/cavin-1 neutralizes non-caveolar caveolin-1 microdomains in prostate cancer. Oncogene 1–10.

Morén, B., Shah, C., Howes, M.T., Schieber, N.L., McMahon, H.T., Parton, R.G., Daumke, O., and Lundmark, R. (2012). EHD2 regulates caveolar dynamics via ATP-driven targeting and oligomerization. Mol. Biol. Cell *23*, 1316–1329.

Murata, T., Lin, M.I., Stan, R. V., Bauer, P.M., Yu, J., and Sessa, W.C. (2007). Genetic evidence supporting caveolae microdomain regulation of calcium entry in endothelial cells. J. Biol. Chem. *282*, 16631–16643.

Nassoy, P., and Lamaze, C. (2012). Stressing caveolae new role in cell mechanics. Trends Cell Biol. *22*, 381–389.

Nystrom, F.H., Chen, H., Cong, L.N., Li, Y., and Quon, M.J. (1999). Caveolin-1 interacts with the insulin receptor and can differentially modulate insulin signaling in transfected Cos-7 cells and rat adipose cells. Mol. Endocrinol. *13*, 2013–2024.

O'Shea, J.J., Schwartz, D.M., Villarino, A. V, Gadina, M., Iain, B., and Laurence, A. (2015). The JAK-STAT Pathway: Impact on Human Disease and Therapeutic Intervention. 311–328.

Okamoto, T., Schlegel, a, Scherer, P.E., and Lisanti, M.P. (1998). Caveolins, a family of scaffolding proteins for organizing "preassembled signaling complexes" at the plasma membrane. J Biol Chem *273*, 5419–5422.

Palade, G.E. (1953). The fine structure of blood capillaries. J. Appl. Phys. *24*, 1424.

Parton, R.G., and Simons, K. (2007). The multiple faces of caveolae. Nat. Rev. Mol. Cell Biol. *8*, 185–194.

Parton, R.G., Hanzal-Bayer, M., and Hancock, J.F. (2006). Biogenesis of caveolae: a structural model for caveolin-induced domain formation. J. Cell Sci. *119*, 787–796.

Patel, H.H., Murray, F., and Insel, P.A. (2008). Caveolae as organizers of pharmacologically relevant signal transduction molecules. Annu. Rev. Pharmacol. Toxicol. *48*, 359–391.

Platanias, L.C. (2005). Mechanisms of type-I- and type-II-interferon-mediated signalling. Nat. Rev. Immunol. *5*, 375–386.

Rothberg, K.G., Heuser, J.E., Donzell, W.C., Ying, Y.S., Glenney, J.R., and Anderson, R.G. (1992). Caveolin, a protein component of caveolae membrane coats. Cell *68*, 673–682.

Scherer, P.E., Okamoto, T., Chun, M., Nishimoto, I., Lodish, H.F., and Lisanti, M.P. (1996). Identification, sequence, and expression of caveolin-2 defines a caveolin gene family. Proc. Natl. Acad. Sci. U. S. A. *93*, 131–135.

Schreiber, G., and Piehler, J. (2015). The molecular basis for functional plasticity in type I interferon signaling. Trends Immunol. *36*, 139–149.

Shajahan, A.N., Dobbin, Z.C., Hickman, F.E., Dakshanamurthy, S., and Clarke, R. (2012). Tyrosine-phosphorylated caveolin-1 (Tyr-14) increases sensitivity to paclitaxel by inhibiting BCL2 and BCLxL proteins via c-Jun N-terminal Kinase (JNK). J. Biol. Chem. *287*, 17682–17692.

Sinha, B., Köster, D., Ruez, R., Gonnord, P., Bastiani, M., Abankwa, D., Stan, R. V., Butler-Browne, G., Vedie, B., Johannes, L., et al. (2011). Cells respond to mechanical stress by rapid disassembly of caveolae. Cell *144*, 402–413.

Stoeber, M., Schellenberger, P., Siebert, C.A., Leyrat, C., Helenius, A., and Grünewald, K. (2016). Model for the architecture of caveolae based on a flexible, net-like assembly of Cavin1 and Caveolin discs. Proc. Natl. Acad. Sci. U. S. A. 201616838.

Taira, J., Sugishima, M., Kida, Y., Oda, E., Noguchi, M., and Higashimoto, Y. (2011). Caveolin-1 is a competitive inhibitor of heme oxygenase-1 (HO-1) with heme: identification of a minimum sequence in caveolin-1 for binding to HO-1. Biochemistry *50*, 6824–6831.

Trane, A.E., Pavlov, D., Sharma, A., Saqib, U., Lau, K., Van Petegem, F., Minshall, R.D., Roman, L.J., and Bernatchez, P.N. (2014). Deciphering the binding of Caveolin-1 to client protein endothelial nitric-oxide synthase (eNOS): Scaffolding subdomain identification, interaction modeling, and biological significance. J. Biol. Chem. *289*, 13273–13283.

Villarino, A. V, Kanno, Y., and Shea, J.J.O. (2017). Mechanisms and consequences of Jak – STAT signaling in the immune system. *18*.

Way, M., and Parton, R.G. (1995). M-caveolin, a muscle-specific caveolin-related protein. FEBS Lett. *376*, 108–112.

Williams, J.J.L., Alotaiq, N., Mullen, W., Burchmore, R., Liu, L., Baillie, G.S., Schaper,

F., Pilch, P.F., and Palmer, T.M. (2018). Interaction of suppressor of cytokine signalling 3 with cavin-1 links SOCS3 function and cavin-1 stability. Nat. Commun. *9*, 168.

Yamada, E. (1955). The fine structure of the gall bladder epithelium of the mouse. J. Biophys. Biochem. Cytol. *1*, 445–458.

DISCUSSION
- & -
PERSPECTIVES

5 Discussion and perspectives

5.1 Caveolar Cav1 versus “free” Cav1

My laboratory previously demonstrated that upon mechanical stress resulting in membrane tension increase, caveolae rapidly flatten out to “buffer” the membrane tension increase in order to conserve the plasma membrane integrity (Sinha et al., 2011). However, the precise molecular aspect of the caveolar disassembly has remained unclear until now. In this study, super resolution imaging clearly shows that upon mechanical disassembly of caveolae, Cav1 diffusion drastically increases indicating the release of “free” *i.e.* non-caveolar Cav1 oligomers at the plasma membrane. We further demonstrate that upon caveolar mechanical disassembly, Cav1 interacts with JAK1 and thereby negatively regulates its catalytic activity. In the present work, based on the applied mechanical stress, cholesterol depletion, Cav1 overexpression and *cavin-1* knocked out cells, we hypothesized that the free Cav1 released from the disassembling caveolae is the one that interacts with JAK1. However, caveolae may not totally disassemble and some Cav1 oligomers may remain within the flat Cav1-enriched nanodomain of the former curved caveolae (Hill et al., 2008; Tachikawa et al., 2017; Yang and Scarlata, 2017; Khater et al., 2018). One can hypothesize that among the many possible mechanisms that mediate CSD accessibility; caveolae flattening may be one possible mechanism to induce Cav1 conformation changes and CSD exposure for protein-protein interaction (detailed below). Therefore, IFNAR2-JAK1 complexes would be recruited and immobilized into flat confined Cav1-enriched domains. To verify this hypothesis, we generated JAK1-mEOS3.2 to assess the diffusion rate of JAK1 upon membrane tension increase. Confined JAK1 in Cav1-enriched plasma membrane domain would be a good indicator of JAK1 recruitment at the flat caveolae. On the contrary, high diffusion of JAK1 together with Cav1 or confinement outside the caveolae upon membrane tension increase would favor the hypothesis of JAK1 interacting with “free” Cav1.

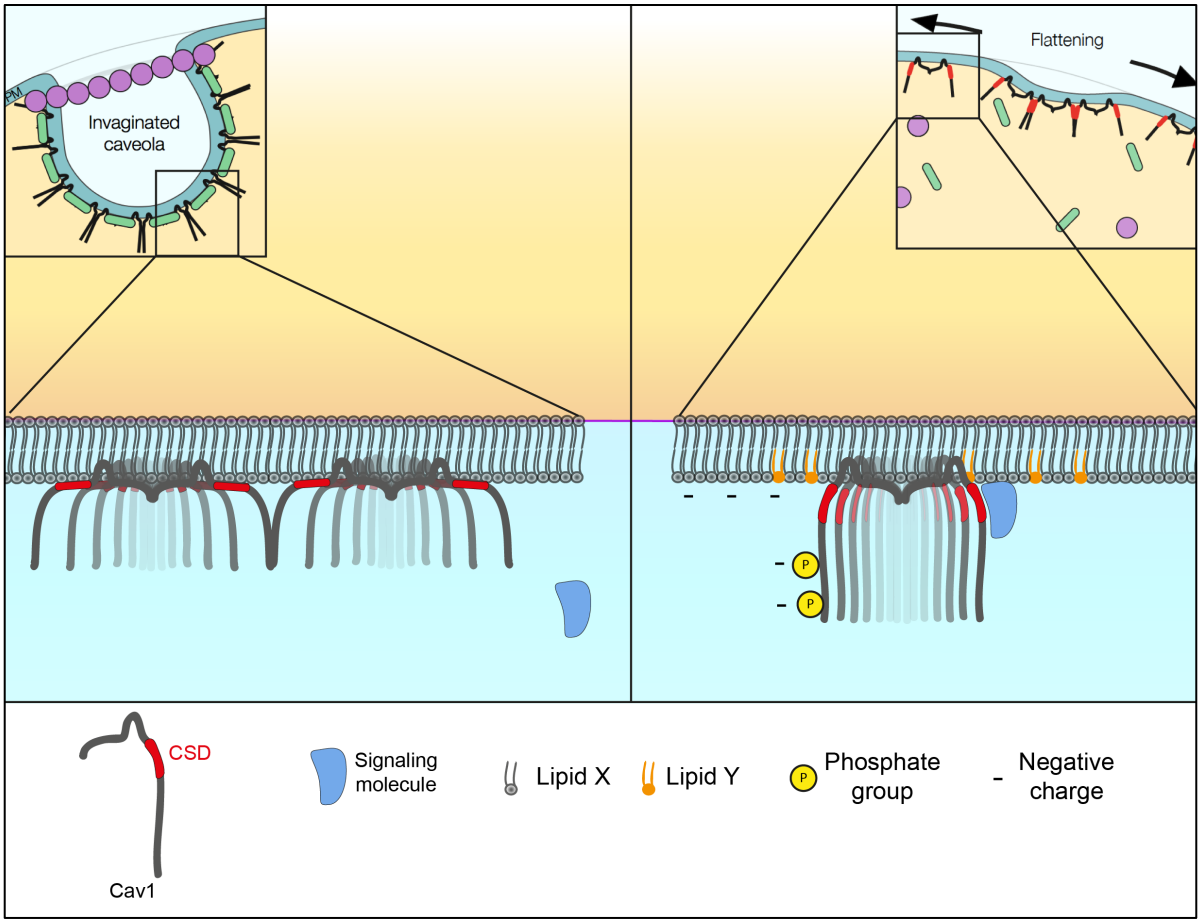

Figure 26. Proposed topology of free Cav1

At steady state Cav1 oligomers within the caveolar coat: Cav1 topology as proposed by Kirkham and colleagues (Kirkham et al., 2008). The CSD is not available for protein interaction (left). Upon caveolae flattening, Cav1 oligomers are released in the plasma membrane and encounter different membrane curvatures, lipid environment; lipid X or Y and/or might undergo posttranslational modifications such Tyr14 and Ser80 phosphorylation leading to Cav1 conformational changes that trigger CSD exposure allowing interactions with Cav1 partners (right).

5.2 CSD dependent regulation of JAK1

Cav1 CSD mutants, CSD mimicking peptides and *in vi*tro kinase assay clearly demonstrate the prominent and direct role of the CSD in Cav1-JAK1 interaction and the resulting inhibitory effect by Cav1. These new results strengthen the line of evidences that support a regulatory mechanism exerted by Cav1 on some signaling molecules. As discussed in 2.3.4.4, the regulation of signal transduction through CSD-mediated direct Cav1 interaction with signaling proteins is controverted. The keystone of this controversy relies on the Cav1 predicted ternary structure. Indeed, the CSD has a predicted structure of α-helix that is amphipathic and therefore, it is partially embedded in the inner lipid layer of the plasma membrane. Thus, this configuration would not favor the CSD interaction with the Cav1 putative binding partners (Collins et al., 2012; Ariotti et al., 2015). Interestingly, the CSD should not be considered static within the Cav1 structure. Indeed recent computational analysis of Cav1 structure within the lipid bilayer, revealed that the CSD possesses a dynamic secondary structure either partially unstructured or fully helical (Liu et al., 2016). Hence, one could hypothesize that this dynamic secondary structure may control the relative position of the CSD to the plasma membrane. Whether parameters such as Cav1 lipid environment influence the structural dynamics of the CSD should be investigated. Indeed the CSD inserted in POPC/Cholesterol adopts a mixture of β-stranded and α-helical structure while the CSD inserted in DPC micelles adopts a fully helical structure (Le Lan et al., 2006; Hoop et al., 2012). Therefore, the conformation of Cav1 within a flat caveolae or non-caveolar Cav1 oligomers diffusing in the lipid bilayer, thus experiencing different membrane curvatures and lipid environments, may differ from Cav1 within fully a budded caveola, where the CSD is poorly accessible (Fig. 26). Alternative mechanisms have also been proposed to mediate CSD exposure. Indeed, N-ter phosphorylation on Tyr14 and/or Ser80 may push away the whole N-ter end including the CSD from the plasma membrane because of charge repulsion within the inner leaflet of the lipid bilayer (Shajahan et al., 2012) (Fig. 26). This mechanism may also mediate Cav1-JAK1 interaction reversibility, which is a key parameter in cell signaling. However, variations of Cav1 Tyr14 phosphorylation upon membrane tension increase could not be detected, suggesting that this Cav1 post-translational modification is not involved in this mechanism (Fig. 27). Nevertheless, our laboratory observed a similar control of

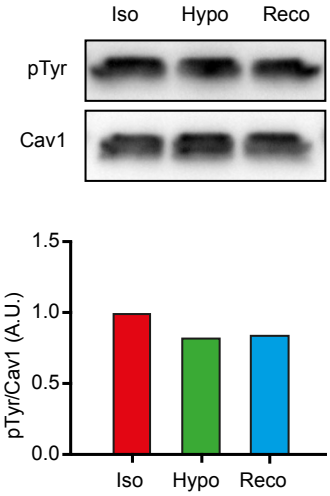

Figure 27. Cav1 tyrosine phosphorylation upon hypo osmotic shock

Western blot analysis of tyrosine phosphorylation of immunoprecipitated endogenous Cav1 in iso-osmotic, hypo-osmotic and successive hypo-osmotic shock and iso-osmotic condition (Recovery) from WT MLEC cells lysate.

IL6/STAT3 pathway in muscle cells only expressing Cav3 (see annex 3). Considering that Cav3 cannot be phosphorylated on Tyr14, it is unlikely that Tyr14 phosphorylation is involved in this mechanism. However, variations of Cav1 Ser80 phosphorylation upon mechanical stress still need to be investigated. For example, immunoprecipitation of non-phosphorylable or phosphomimetic mutants of Cav1 should be performed to assess whether S80 phosphorylation is involved in Cav1-JAK1 interaction.

On another hand, in the context of Cav1-JAK1 interaction triggering and reversibility, JAK1 post-translational modifications such as tyrosine S-nitrosylation should be investigated. Indeed, it has been reported that another member of the JAK family; JAK2 can be S-nitrosylated on two tyrosine residues. Nitrosylated JAK2 interacts with Cav1 and eNOS (Elsasser et al., 2007). JAK2 nitrosylation is performed through NO generation by proteins such as eNOS. Interstingly, Cav1 regulates eNOS activity. Similarly a regulatory mechanism of RhoA activation via S-nitrosylation of its GTPase activating protein (GAP) mediated by the Cav1-regulated eNOS-dependent NO production has been described (Rizwan Siddiqui et al., 2011). It would be therefore important to assess JAK1 nitrosylation upon mechanical stress by western blot using anti-nitrosylated tyrosine antibodies. Moreover, the effect of mechanical stress on NO production using NO probes and whether NO treatment triggers or prevents Cav1-JAK1 interaction would be interesting questions to address.

Finally, another aspect of the regulatory mechanism via the CSD-mediated Cav1 inhibition of signaling proteins largely contributed to the rise of the controversy. Indeed, the CBM, a putative CSD interaction motif has been early identified by phage screening (Couet et al., 1997a). However, structural analysis of Cav1 binding partners, revealed that most of them carry a CBM in their core thereby poorly available for interaction with the CSD (Collins et al., 2012). In addition, this motif encompasses three highly degenerated motifs. Hence, CBM containing proteins are largely found through the proteome of different organisms, even those devoid of caveolins. Therefore, the presence of CBMs in proteins primary structure might not be predictive of Cav1 interaction. Nevertheless, a CBM is found in most of Cav1 binding partners and although being non-predictive, some of them may still mediate

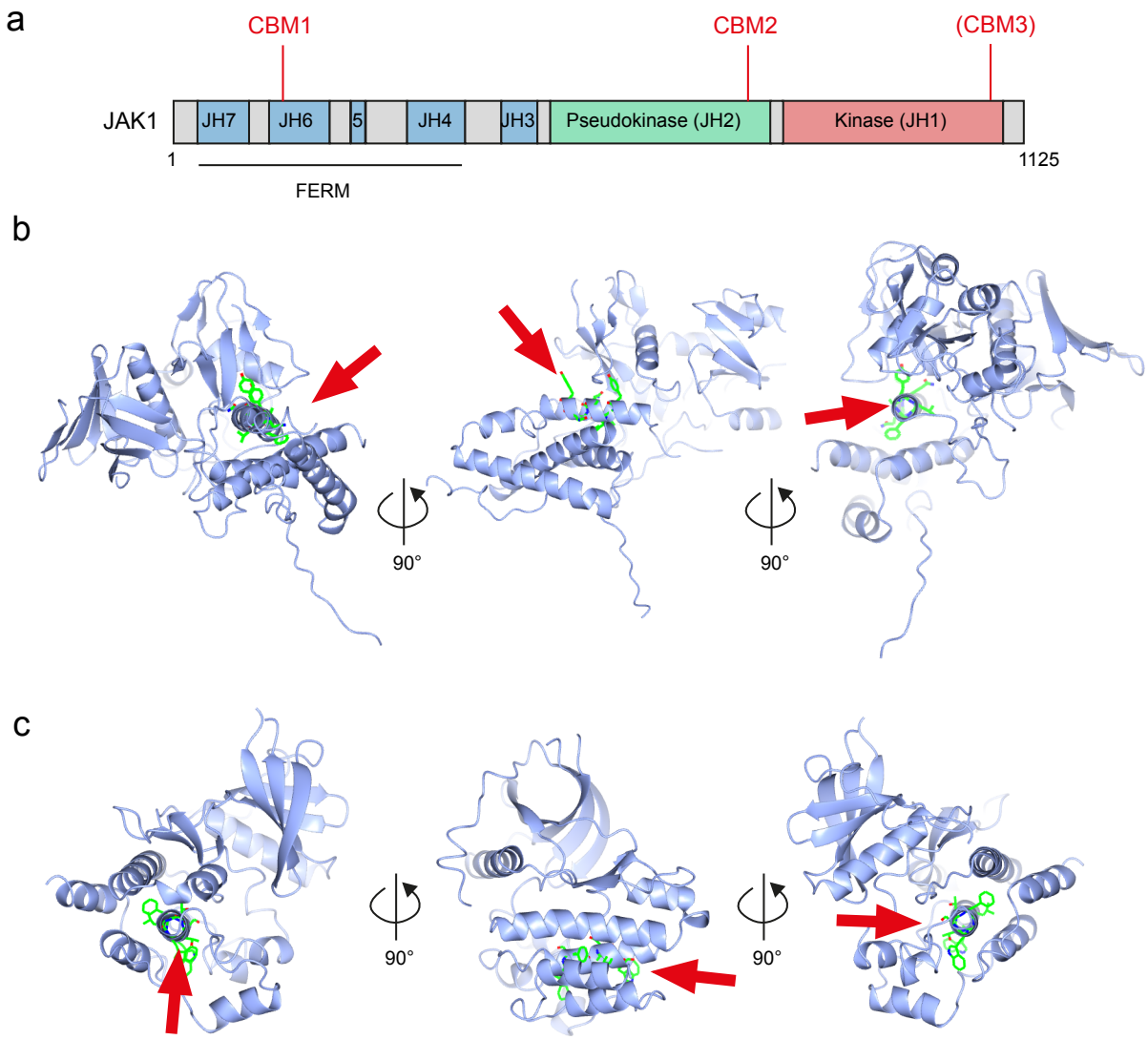

Figure 28: CBM localization on JAK1 structure

(a) localization of the putative CBMs in JAK1 primary structure. **(b)** CBM1 (highlighted lateral chains, red arrow) localization in the tridimensional structure of the FERM domain of JAK1 (PDB 5IXI). **(c)** CBM2 (highlighted lateral chains, red arrow) localization in JAK1 pseudokinase tridimensional structure (PDB 4L00). Pseudokinase and kinase domains are structurally identical. The putative CBM3 has a localization similar to the CBM2 but within the kinase domain.

the interaction with Cav1. All JAKs carry several CBMs. JAK1 has three putative CBMs: a first one is located in the JH6 region corresponding to the FERM domain (^{157}YLFAQGQY^{164}), another in the JH2 pseudokinase domain (^{777}WSFGTTLW^{784}) and a last one in the JH1 kinase domain (^{1065}WSFGVTLH^{1072}) (Fig. 28a). JAK1 CBMs are located on three α-helices that are buried inside JAK1 ternary structure. Hence, all motifs seem to be poorly accessible (Fig. 28b, c). However, to address whether one of these CBMs are required for JAK1 interaction with Cav1, we generated three JAK1 mutants with alanine replacement of each CBM (JAK1-CBM1, JAK1-CBM2 and JAK1-CBM3). Preliminary pulldown experiments of JAK1-CBM1 in HeLa cells overexpressing Cav1 (to generate an excess of non-caveolar Cav1) revealed that mutations in the CBM located in the FERM domain did not affect its ability to interact with Cav1. These data suggest therefore that the first CBM is not required for Cav1-JAK1 interaction (Fig. 29). In addition, *in vitro* kinase assay has been performed using recombinant JAK1 containing only the pseudokinase-kinase tandem, therefore it only contains the CBMs located in the pseudokinase and kinase domain (CBM2 and CBM3). These two domains are sufficient to undergo inhibition of catalytic activity by the CSD mimicking peptide. Experiments to definitely establish the role of CBM2 and CBM3 in Cav1-JAK1 interaction are currently ongoing.

To conclude, the precise molecular mechanism underlying the CSD-mediated inhibition of JAK1 remains unknown. However, our results emphasize the prominent role of Cav1 F92 and V94, since their Ala replacement relieves Cav1 inhibitory effect. Moreover the pulldown experiment clearly demonstrates that F92 and V94 are required for Cav1-JAK1 interaction. Whether F92 or V94 lateral chain sit in an important domain of JAK1 such as the regulation model established for eNOS is unknown. However, Cav1 interaction with JAK1 may also results in the stabilization of JAK1 inactive conformation, by preventing JH1 (pseudokinase domain) extension. Structural studies of the Cav1-JAK1 complex or at least, CSD-JAK1 would bring deeper insight on the molecular mechanism mediating the resulting inhibition. Interestingly, it has been suggested that caveolins may have a SOCS role in JAK-STAT signaling. Indeed sequence alignment revealed that the CSD shares a common motif with the KIR domain of SOCS1 and SOCS3 (Jasmin et al., 2006) (Fig. 30). Therefore, one could hypothesize that upon Cav1-JAK1 interaction the CSD

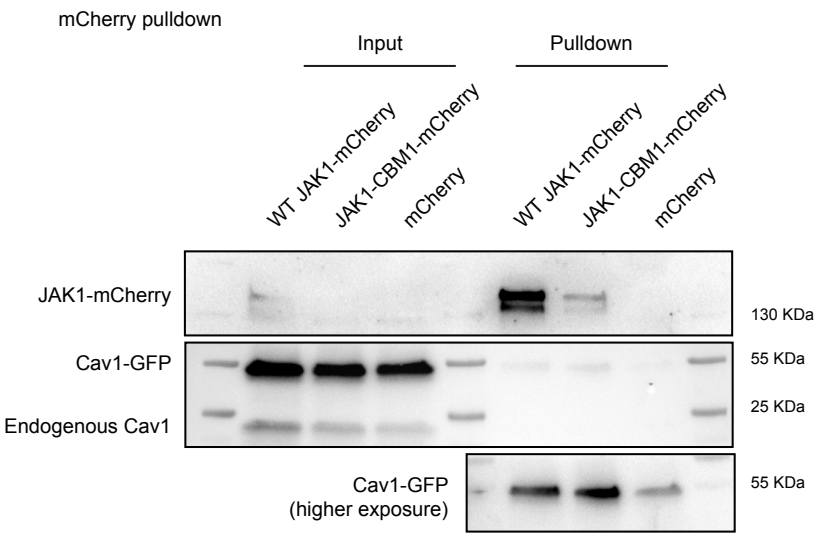

Figure 29: CBM1-mutated JAK1 pulldown
Immunoblot of JAK1-mCherry pulldown of HeLa cells expressing exogenous Cav1 and either WT-JAK1 or CBM1-mutated JAK1 (JAK1-CBM1).

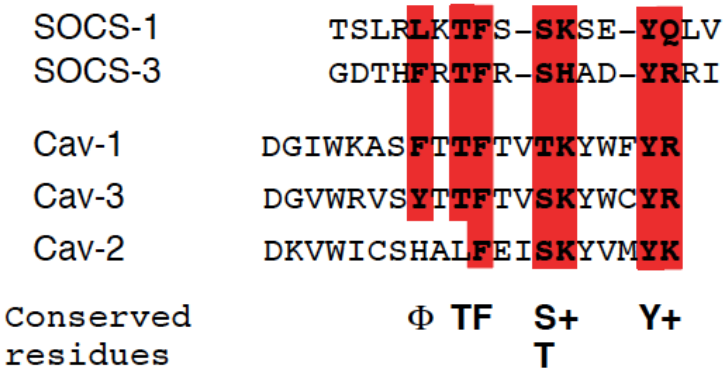

Figure 30. Sequence alignment of SOCS1 and SOCS3 KIR domains with caveolins
The Cav1 scaffolding domain shares primary sequence similarities with the SOCS-1 pseudosubstrate domain. The conserved domains are identified by the consensus sequence Φ xTFxxS/T(+) xxxY(+), where Φ is a hydrophobic or aromatic amino acid and (+) is a positively charged residue (from Jasmin et al., 2006).

would occlude the substrate binding site of JAK1, the same way SOCS inhibit JAK1 (as detailed in 3.5.1) preventing thereby JAK1 catalytic activity.

5.3 Signal specificity

An intriguing aspect of this work is that caveolae disassembly induced by a mechanical stress results in the specific inhibition of IFN-α-induced STAT3 activation. Surprisingly STAT1 activation by IFN-α is not affected by the caveolar mechanics. The molecular mechanism driving this specificity still needs to be addressed. Indeed, IFN-α stimulation normally induces both STAT1 and STAT3 activation. IFN-α binding to IFNAR leads to JAK1 and TYK2 cross-activation, which result in both STAT1 and STAT3 activation. A logical hypothesis would consist in the selective targeting of JAK1 by Cav1 that would result in STAT3 inhibition. In the meantime, TYK2 would remain activated and would mediate STAT1 activation. Nevertheless, there are no evidences of such JAK specificity for STAT activation. In addition, JAKs are activated by mutual transphophorylation, therefore, there is a reciprocal interdependency between JAK1 and TYK2. Thus, according to the consensus mechanism of JAKs activation, the targeting of one of the two kinases would inevitably prevents the activation of the other one. However, it has been reported that TYK2 plays a restricted role in IFN-α signaling. Moreover lack of TYK2 does not prevent JAK1 activation (Shimoda et al., 2000).

On another hand, caveolar mechanotransduction is not restricted to IFN-α induced JAK-STAT signal transduction. This process may constitute a general regulatory mechanism for JAK-STAT signaling, disregarding the receptors or the ligands. Indeed, basal STAT3 activation in *Cav1*$^{-/-}$ MLEC cells and *in vitro* kinase assay revealed that this mechanism directly targets JAK1 regardless of upstream signaling molecules. Hence, it is not unexpected that it can be extended to other cytokines and receptors that use JAK-STAT such as the IL6 pathway. My laboratory found that caveolae mechanics also control the IL6/STAT3 pathway through a similar Cav3 release in the context of muscle physiology (Dewulf et al., 2018 under revision see annex 3). It suggests that the muscle specific isoform of Cav3 that also carries a

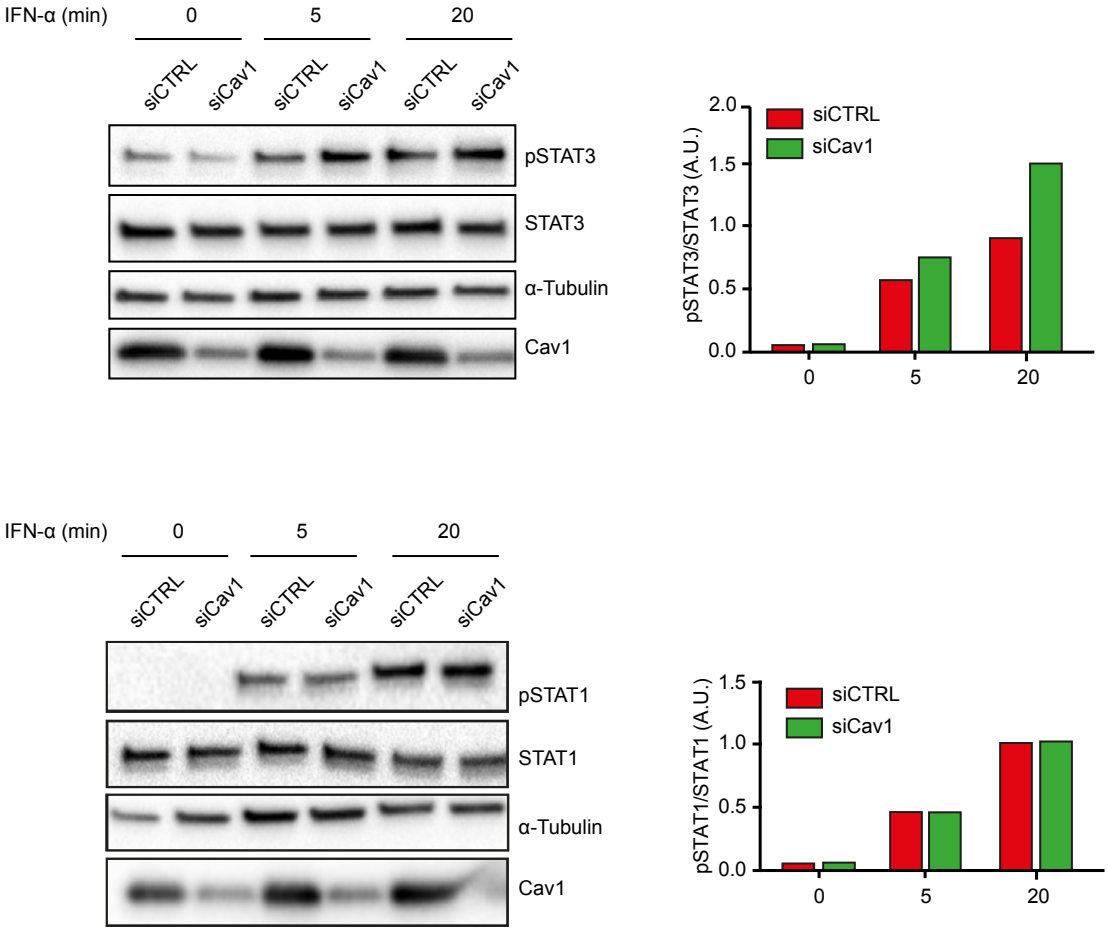

Figure 31. Specific inhibition of STAT3 by Cav1 in human breast cancer cells
Immunoblot of kinetics of IFN-α-induced STAT3 and STAT1 activation in MCF10A cells upon siCTRL or siCav1 treatment (left). Immunoblot quatification (right).

CSD, may compensate the absence of Cav1 and play a similar signaling role in muscular tissues.

5.4 Caveolae mechanotransduction: role in tumor progression

Our results clearly demonstrate that caveolae mechanics exert a control over JAK-STAT signaling. As discussed above, only STAT3 activation is affected by caveolae mechanics. As described in the introduction, STAT3 has oncogenic activities while STAT1 has, in most of situations, tumor suppressor activities. Therefore, mechanical forces encountered by cancer cells during tumor progression may regulate signal interpretation and modulate STAT3/STAT1 activation balance through caveolae mechanics. This mechanism may partially explain the ambivalent role of Cav1 during tumor progression. Moreover, any perturbations affecting the integrity of caveolae mechanotransduction may result in STAT3/STAT1 activation imbalance. For example, Cav1 knock down in breast cancer cells also induces STAT3 activation in response to IFN-α most likely because of the lack of negative regulation of JAK1 by non-caveolar Cav1 (Fig. 31). In addition, tumor cells submitted to hypo-osmotic shock exhibit this characteristic pSTAT3 inhibition (Fig. 32). Non-aggressive tumor cells HS578T grown as multicellular spheroids in agarose and submitted to tumor-like compressive forces by compressing them with an hyperosmotic solution also exhibit the characteristic decrease of IFN-α-induced STAT3 activation (Fig. 33). It would be tempting to propose that the caveolae-dependent mechanical control of JAK-STAT constitutes a physiological regulatory mechanism of cell proliferation in response mechanical strains generated by situation such as space limitation found in the tumor mass. Hence, impaired caveolar mechano-response would result in cell growth and other caveolae-related processes.

To conclude, considering the wide breadth of Cav1 binding partners, it is likely that caveolae mechanotransduction plays a key role during tumor progression by tuning several major cell signaling pathways. Moreover the release of non-caveolar Cav1 may modulate signaling cascades through other mechanism than CSD interaction. For example, non-caveolar Cav1 mechanically released from caveolae disassembly can regulate the lipid composition of receptors microenvironment, which

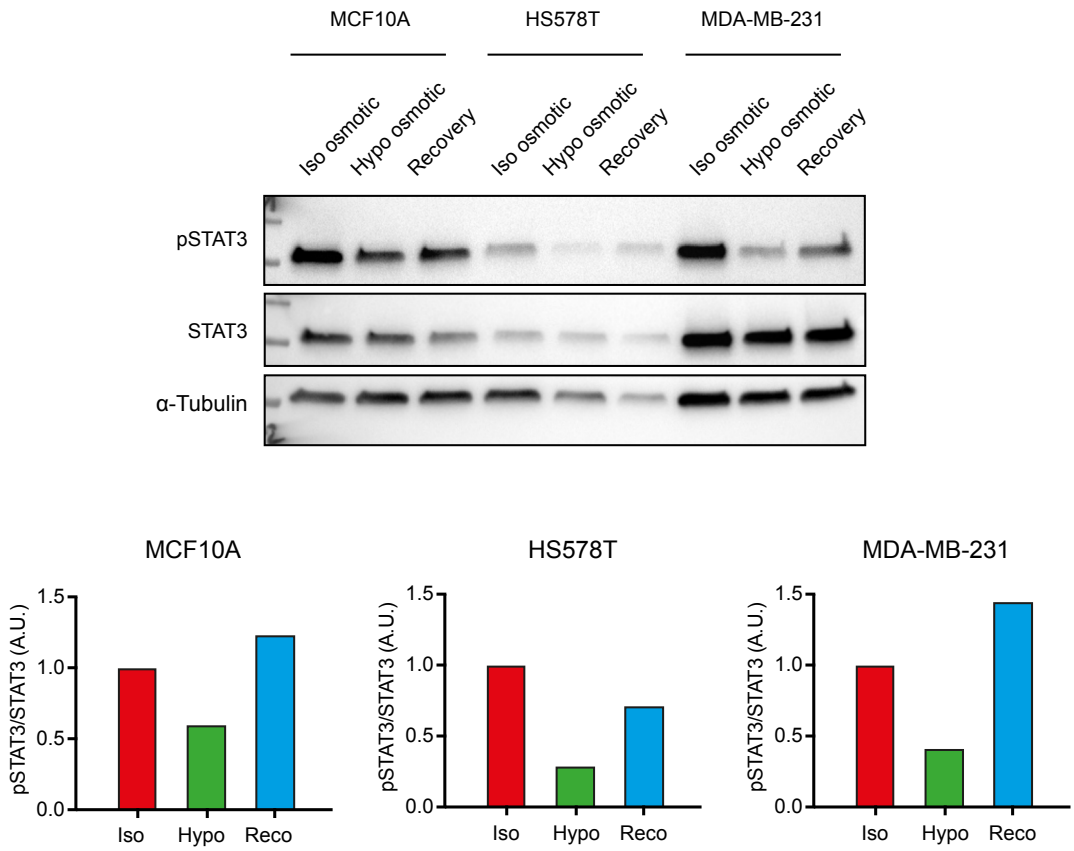

Figure 32: IFN-α-induced STAT3 activation of breast cancer cells upon hypo-osmotic shock

Immunoblot of IFNα-induced STAT3 phosphorylation in breast cancer cell lines (MCF10A, HS578T and MDA-MB-231) upon either steady-state, hypo-osmotic shock or recovery.

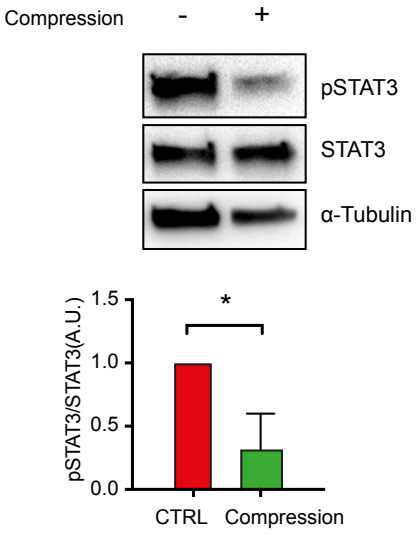

Figure 33: IFN-α-induced STAT3 activation of breast cancer cell under compression

Immunoblot of IFNα-induced STAT3 phosphorylation of encapsulated breast tumor cells HS578T.

is a key parameter for their activation (Rao and Mayor, 2014; Blouin et al., 2016). Indeed, high throughput screening revealed that other signaling pathways seem to be modulated by caveolae mechanics. Therefore, defective caveolae such as those found in many tumor cell lines like prostate cancer cells PC3 that exhibit constitutive non-caveolar Cav1 due to a lack of cavin-1 expression may lead to impaired mechanoresponse and signaling. Nevertheless, the physiological role of such mechanisms remains elusive. Williams and colleagues, recently revealed that proper JAK-STAT signal suppression through SOCS3 requires *bona fide* caveolae and plasma membrane associated cavin-1 (Williams et al., 2018). Hence one could hypothesize that mechanical disassembly of caveolae and the destabilization of cavin complexes, would result in impaired SOCS3 mediated JAK-STAT signal termination. Therefore, under mechanical stress, the release of free Cav1 might lock the JAK-STAT signaling pathway to avoid aberrant JAK-STAT signaling. On another hand, as presented in the introduction, wide breadths of biological processes are governed by the interplay between cell mechanics and the physical properties of the microenvironment. Mechanoreciprocity and establishment of mechanically regulated cell processes are achieved thanks to conserved tools such as mechanotransducers. Considering the multitude of Cav1 binding partners, caveolae mechanotransduction may therefore constitute a general mechanism. It may tunes the overall cell signaling upon mechanical stress induced by external physiological or pathological strains such as those experienced by cells within the tumor mass. Alternatively, it could locally regulate signaling events depending on local plasma membrane tension variations generated by membrane deformation during processes such as cell migration through the ECM.

References

Abell, K., Bilancio, A., Clarkson, R.W.E., Tiffen, P.G., Altaparmakov, A.I., Burdon, T.G., Asano, T., Vanhaesebroeck, B., and Watson, C.J. (2005). Stat3-induced apoptosis requires a molecular switch in PI(3)K subunit composition. Nat. Cell Biol. *7*, 392–398.

Aboulaich, N., Vainonen, J.P., Stralfors, P., and Vener, A. V (2004). Vectorial proteomics reveal targeting, phosphorylation and specific fragmentation of polymerase I and transcript release factor (PTRF) at the surface of caveolae in human adipocytes. Biochem. J. *383*, 237–248.

Abramovich, C., Shulman, L.M., Ratovitski, E., Harroch, S., Tovey, M., Eid, P., and Revel, M. (1994). Differential tyrosine phosphorylation of the IFNAR chain of the type I interferon receptor and of an associated surface protein in response to IFN-alpha and IFN-beta. EMBO J. *13*, 5871–5877.

Aoki, S., Thomas, A., Decaffmeyer, M., Brasseur, R., and Epand, R.M. (2010). The role of proline in the membrane re-entrant helix of caveolin-1. J. Biol. Chem. *285*, 33371–33380.

Aragona, M., Panciera, T., Manfrin, A., Giulitti, S., Michielin, F., Elvassore, N., Dupont, S., and Piccolo, S. (2013). A mechanical checkpoint controls multicellular growth through YAP/TAZ regulation by actin-processing factors. Cell *154*, 1047–1059.

Arbuzova, A., Wang, L., Wang, J., Hangyas-Mihalyne, G., Murray, D., Honig, B., and McLaughlin, S. (2000). Membrane binding of peptides containing both basic and aromatic residues. Experimental studies with peptides corresponding to the scaffolding region of caveolin and the effector region of MARCKS. Biochemistry *39*, 10330–10339.

Ardissone, A., Bragato, C., Caffi, L., Blasevich, F., Maestrini, S., Bianchi, M.L., Morandi, L., Moroni, I., and Mora, M. (2013). Novel PTRF mutation in a child with mild myopathy and very mild congenital lipodystrophy. BMC Med. Genet. *14*, 89.

Arimoto, K.-I., Miyauchi, S., Stoner, S.A., Fan, J.-B., and Zhang, D.-E. (2018). Negative regulation of type I IFN signaling. J. Leukoc. Biol.
Ariotti, N., and Parton, R.G. (2013). SnapShot: caveolae, caveolins, and cavins. Cell *154*, 704–704.e1.

Ariotti, N., Fernández-Rojo, M.A., Zhou, Y., Hill, M.M., Rodkey, T.L., Inder, K.L., Tanner, L.B., Wenk, M.R., Hancock, J.F., and Parton, R.G. (2014). Caveolae regulate the nanoscale organization of the plasma membrane to remotely control Ras signaling. J. Cell Biol. *204*, 777–792.

Ariotti, N., Rae, J., Leneva, N., Ferguson, C., Loo, D., Okano, S., Hill, M.M., Walser, P., Collins, B.M., and Parton, R.G. (2015). Molecular characterization of caveolin-induced membrane curvature. J. Biol. Chem. *290*, 24875–24890.

Babon, J.J., Lucet, I.S., Murphy, J.M., Nicola, N. a, and Varghese, L.N. (2014). The molecular regulation of Janus kinase (JAK) activation. Biochem. J. *462*, 1–13.

Baker, E.L., Bonnecaze, R.T., and Zaman, M.H. (2009). Extracellular matrix stiffness and architecture govern intracellular rheology in cancer. Biophys. J. *97*, 1013–1021.

Barbieri, I., Pensa, S., Pannellini, T., Quaglino, E., Maritano, D., Demaria, M., Voster, A., Turkson, J., Cavallo, F., Watson, C.J., et al. (2010). Constitutively active Stat3 enhances neu-mediated migration and metastasis in mammary tumors via upregulation of Cten. Cancer Res. *70*, 2558–2567.

Bastiani, M., Liu, L., Hill, M.M., Jedrychowski, M.P., Nixon, S.J., Lo, H.P., Abankwa, D., Luetterforst, R., Fernandez-Rojo, M., Breen, M.R., et al. (2009). MURC/Cavin-4 and cavin family members form tissue-specific caveolar complexes. J. Cell Biol. *185*, 1259–1273.

Bazan, J.F. (1990). Shared architecture of hormone binding domains in type I and II interferon receptors. Cell *61*, 753–754.

Beebe, J., Liu, J.-Y., and Zhang, J.-T. (2018). Two decades of research in discovery of anticancer drugs targeting STAT3, how close are we? Pharmacol. Ther.

Behrmann, I., Smyczek, T., Heinrich, P.C., Schmitz-Van de Leur, H., Komyod, W., Giese, B., Muller-Newen, G., Haan, S., and Haan, C. (2004). Janus kinase (Jak) subcellular localization revisited: the exclusive membrane localization of endogenous Janus kinase 1 by cytokine receptor interaction uncovers the Jak.receptor complex to be equivalent to a receptor tyrosine kinase. J. Biol. Chem. *279*, 35486–35493.

Bendayan, M., and Rasio, E.A. (1996). Transport of insulin and albumin by the microvascular endothelium of the rete mirabile. J. Cell Sci. *109 (Pt 7*, 1857–1864.

Benlimame, N., Le, P.U., and Nabi, I.R. (1998). Localization of autocrine motility factor receptor to caveolae and clathrin-independent internalization of its ligand to smooth endoplasmic reticulum. Mol. Biol. Cell *9*, 1773–1786.

Bernatchez, P., Sharma, A., Bauer, P.M., Marin, E., and Sessa, W.C. (2011). A noninhbitory mutant of the caveolin1 scaffolding domain enhances eNOS-derived NO synthesis and vasodilation in mice. *121*.

Bernatchez, P.N., Bauer, P.M., Yu, J., Prendergast, J.S., He, P., and Sessa, W.C. (2005). Dissecting the molecular control of endothelial NO synthase by caveolin-1 using cell-permeable peptides. Proc. Natl. Acad. Sci. U. S. A. *102*, 761–766.

Bhattacharya, S., HuangFu, W.-C., Liu, J., Veeranki, S., Baker, D.P., Koumenis, C., Diehl, J.A., and Fuchs, S.Y. (2010). Inducible priming phosphorylation promotes ligand-independent degradation of the IFNAR1 chain of type I interferon receptor. J. Biol. Chem. *285*, 2318–2325.

Bigay, J., and Antonny, B. (2012). Curvature, Lipid Packing, and Electrostatics of Membrane Organelles: Defining Cellular Territories in Determining Specificity. Dev.

Cell *23*, 886–895.

Blouin, C.M., Le Lay, S., Lasnier, F., Dugail, I., and Hajduch, E. (2008). Regulated association of caveolins to lipid droplets during differentiation of 3T3-L1 adipocytes.

Biochem. Biophys. Res. Commun. *376*, 331–335.

Blouin, C.M., Hamon, Y., Gonnord, P., Boularan, C., Kagan, J., Viaris de Lesegno, C., Ruez, R., Mailfert, S., Bertaux, N., Loew, D., et al. (2016). Glycosylation-Dependent IFNGamma-R Partitioning in Lipid and Actin Nanodomains Is Critical for JAK Activation. Cell *166*, 920–934.

Brierley, M.M., and Fish, E.N. (2002). Review: IFN-alpha/beta receptor interactions to biologic outcomes: understanding the circuitry. J. Interferon Cytokine Res. *22*, 835–845.

Bromberg, J.F., Wrzeszczynska, M.H., Devgan, G., Zhao, Y., Pestell, R.G., Albanese, C., and Darnell, J.E.J. (1999). Stat3 as an oncogene. Cell *98*, 295–303.

Bucci, M., Gratton, J.P., Rudic, R.D., Acevedo, L., Roviezzo, F., Cirino, G., and Sessa, W.C. (2000). In vivo delivery of the caveolin-1 scaffolding domain inhibits nitric oxide synthesis and reduces inflammation. Nat. Med. *6*, 1362–1367.

Buchert, M., Burns, C.J., and Ernst, M. (2016). Targeting JAK kinase in solid tumors: emerging opportunities and challenges. Oncogene *35*, 939–951.

Burgener, R., Wolf, M., Ganz, T., and Baggiolini, M. (1990). Purification and characterization of a major phosphatidylserine-binding phosphoprotein from human platelets. Biochem. J. *269*, 729–734.

Butcher, D., Alliston, T., and Weaver, V.M. (2009). A tense situation: forcing tumour progression. *9*, 108–122.

Byrne, D.P., Dart, C., and Rigden, D.J. (2012). Evaluating Caveolin Interactions: Do Proteins Interact with the Caveolin Scaffolding Domain through a Widespread Aromatic Residue-Rich Motif? PLoS One *7*.

Caffarel, M.M., Zaragoza, R., Pensa, S., Li, J., Green, A.R., and Watson, C.J. (2012). Constitutive activation of JAK2 in mammary epithelium elevates Stat5 signalling, promotes alveologenesis and resistance to cell death, and contributes to tumourigenesis. Cell Death Differ. *19*, 511–522.

Cai, C., Weisleder, N., Ko, J.-K., Komazaki, S., Sunada, Y., Nishi, M., Takeshima, H., and Ma, J. (2009). Membrane repair defects in muscular dystrophy are linked to altered interaction between MG53, caveolin-3, and dysferlin. J. Biol. Chem. *284*, 15894–15902.

Cajean-Feroldi, C., Nosal, F., Nardeux, P.C., Gallet, X., Guymarho, J., Baychelier, F., Sempe, P., Tovey, M.G., Escary, J.-L., and Eid, P. (2004). Identification of residues of the IFNAR1 chain of the type I human interferon receptor critical for ligand binding

and biological activity. Biochemistry *43*, 12498–12512.
Cao, H., Alston, L., Ruschman, J., and Hegele, R.A. (2008). Heterozygous CAV1 frameshift mutations (MIM 601047) in patients with atypical partial lipodystrophy and hypertriglyceridemia. Lipids Health Dis. *7*, 3.

Capanni, C., Sabatelli, P., Mattioli, E., Ognibene, A., Columbaro, M., Lattanzi, G., Merlini, L., Minetti, C., Maraldi, N.M., and Squarzoni, S. (2003). Dysferlin in a hyperCKaemic patient with caveolin 3 mutation and in C2C12 cells after p38 MAP kinase inhibition. Exp. Mol. Med. *35*, 538–544.

Casanova, J.-L., Holland, S.M., and Notarangelo, L.D. (2012). Inborn errors of human JAKs and STATs. Immunity *36*, 515–528.

Cecelja, M., and Chowienczyk, P. (2009). Dissociation of aortic pulse wave velocity with risk factors for cardiovascular disease other than hypertension: a systematic review. Hypertens. (Dallas, Tex. 1979) *54*, 1328–1336.

Chan, S.R., Vermi, W., Luo, J., Lucini, L., Rickert, C., Fowler, A.M., Lonardi, S., Arthur, C., Young, L.J., Levy, D.E., et al. (2012). STAT1-deficient mice spontaneously develop estrogen receptor alpha-positive luminal mammary carcinomas. Breast Cancer Res. *14*, R16.

Chang, S.-F., Chang, C.A., Lee, D.-Y., Lee, P.-L., Yeh, Y.-M., Yeh, C.-R., Cheng, C.-K., Chien, S., and Chiu, J.-J. (2008). Tumor cell cycle arrest induced by shear stress: Roles of integrins and Smad. Proc. Natl. Acad. Sci. *105*, 3927–3932.

Charpin, C., Secq, V., Giusiano, S., Carpentier, S., Andrac, L., Lavaut, M.-N., Allasia, C., Bonnier, P., and Garcia, S. (2009). A signature predictive of disease outcome in breast carcinomas, identified by quantitative immunocytochemical assays. Int. J. Cancer *124*, 2124–2134.

Chaturvedi, R.R., Herron, T., Simmons, R., Shore, D., Kumar, P., Sethia, B., Chua, F., Vassiliadis, E., and Kentish, J.C. (2010). Passive stiffness of myocardium from congenital heart disease and implications for diastole. Circulation *121*, 979–988.

Chaudhary, N., Gomez, G.A., Howes, M.T., Lo, H.P., McMahon, K.A., Rae, J.A., Schieber, N.L., Hill, M.M., Gaus, K., Yap, A.S., et al. (2014). Endocytic Crosstalk: Cavins, Caveolins, and Caveolae Regulate Clathrin-Independent Endocytosis. PLoS Biol. *12*.

Cheng, J.P.X., and Nichols, B.J. (2016). Caveolae: One Function or Many? Trends Cell Biol. *26*, 177–189.

Cheng, J.P.X., Mendoza-Topaz, C., Howard, G., Chadwick, J., Shvets, E., Cowburn, A.S., Dunmore, B.J., Crosby, A., Morrell, N.W., and Nichols, B.J. (2015). Caveolae protect endothelial cells from membrane rupture during increased cardiac output. J. Cell Biol. *211*, 53–61.

Chmiest, D., Sharma, N., Zanin, N., Viaris de Lesegno, C., Shafaq-Zadah, M., Sibut, V., Dingli, F., Hupé, P., Wilmes, S., Piehler, J., et al. (2016). Spatiotemporal control

of interferon-induced JAK/STAT signalling and gene transcription by the retromer complex. Nat. Commun. *7*, 13476.

Cohen, A.W., Razani, B., Wang, X.B., Combs, T.P., Williams, T.M., Scherer, P.E., and Lisanti, M.P. (2003). Caveolin-1-deficient mice show insulin resistance and defective insulin receptor protein expression in adipose tissue. Am. J. Physiol. Cell Physiol. *285*, C222-35.

Cohen, B., Novick, D., Barak, S., and Rubinstein, M. (1995). Ligand-induced association of the type I interferon receptor components. Mol. Cell. Biol. *15*, 4208–4214.

Collins, B.M., Davis, M.J., Hancock, J.F., and Parton, R.G. (2012). Structure-Based Reassessment of the Caveolin Signaling Model: Do Caveolae Regulate Signaling through Caveolin-Protein Interactions? Dev. Cell *23*, 11–20.

Constantinescu, S.N., Croze, E., Wang, C., Murti, A., Basu, L., Mullersman, J.E., and Pfeffer, L.M. (1994). Role of interferon alpha/beta receptor chain 1 in the structure and transmembrane signaling of the interferon alpha/beta receptor complex. Proc. Natl. Acad. Sci. U. S. A. *91*, 9602–9606.

Coste, B., Mathur, J., Schmidt, M., Earley, T.J., Ranade, S., Petrus, M.J., Dubin, A.E., and Patapoutian, A. (2011). Piezo1 and Piezo2 are essential components of distinct mechanically-activated cation channels. *330*, 55–60.

Cotarla, I., Ren, S., Zhang, Y., Gehan, E., Singh, B., and Furth, P.A. (2004). Stat5a is tyrosine phosphorylated and nuclear localized in a high proportion of human breast cancers. Int. J. Cancer *108*, 665–671.

Couet, J., Li, S., Okamoto, T., Ikezu, T., and Lisanti, M.P. (1997a). Identification of peptide and protein ligands for the caveolin- scaffolding domain. Implications for the interaction of caveolin with caveolae-associated proteins. J. Biol. Chem. *272*, 6525–6533.

Couet, J., Sargiacomo, M., and Lisanti, M.P. (1997b). Interaction of a receptor tyrosine kinase, EGF-R, with caveolins. Caveolin binding negatively regulates tyrosine and serine/threonine kinase activities. J. Biol. Chem. *272*, 30429–30438.

Darnell, J.E.J., Kerr, I.M., and Stark, G.R. (1994). Jak-STAT pathways and transcriptional activation in response to IFNs and other extracellular signaling proteins. Science *264*, 1415–1421.

Das, K., Lewis, R.Y., Scherer, P.E., and Lisanti, M.P. (1999). The membrane-spanning domains of caveolins-1 and -2 mediate the formation of caveolin hetero-oligomers. Implications for the assembly of caveolae membranes in vivo. J. Biol. Chem. *274*, 18721–18728.

David, M., Chen, H.E., Goelz, S., Larner, A.C., and Neel, B.G. (1995). Differential regulation of the alpha/beta interferon-stimulated Jak/Stat pathway by the SH2 domain-containing tyrosine phosphatase SHPTP1. Mol. Cell. Biol. *15*, 7050–7058.

Davidson, S., McCabe, T.M., Crotta, S., Gad, H.H., Hessel, E.M., Beinke, S., Hartmann, R., and Wack, A. (2016). IFNlambda is a potent anti-influenza therapeutic without the inflammatory side effects of IFNalpha treatment. EMBO Mol. Med. *8*, 1099–1112.

DeLoach, S.S., and Townsend, R.R. (2008). Vascular Stiffness: Its measurement and significance for epidemiologic and outcome studies. Clin. J. Am. Soc. Nephrol. *3*, 184–192.

Desmedt, C., Haibe-Kains, B., Wirapati, P., Buyse, M., Larsimont, D., Bontempi, G., Delorenzi, M., Piccart, M., and Sotiriou, C. (2008). Biological processes associated with breast cancer clinical outcome depend on the molecular subtypes. Clin. Cancer Res. *14*, 5158–5165.

Dewulf, M., Köster, D., Sinha, B., Lesegno, C.V. De, Chambon, V., Bigot, A., Tardif, N., Johannes, L., Nassoy, P., Butler-browne, G., et al. (2018). Lack of functional caveolae in Cav3 mutated human dystrophic myotubes results in deficient mechanoprotection and IL6/STAT3 mechanosignaling. Melissa.

Diaz, N., Minton, S., Cox, C., Bowman, T., Gritsko, T., Garcia, R., Eweis, I., Wloch, M., Livingston, S., Seijo, E., et al. (2006). Activation of stat3 in primary tumors from high-risk breast cancer patients is associated with elevated levels of activated SRC and survivin expression. Clin. Cancer Res. *12*, 20–28.

Dietzen, D.J., Hastings, W.R., and Lublin, D.M. (1995). Caveolin is palmitoylated on multiple cysteine residues. Palmitoylation is not necessary for localization of caveolin to caveolae. J. Biol. Chem. *270*, 6838–6842.

Ding, X., Boney-montoya, J., Owen, B.M., Bookout, A.L., Coate, C., Mangelsdorf, D.J., and Kliewer, S.A. (2013). Balancing forces: architectural control of mechanotransduction. *16*, 387–393.

Drab, M., Verkade, P., Elger, M., Kasper, M., Lohn, M., Lauterbach, B., Menne, J., Lindschau, C., Mende, F., Luft, F.C., et al. (2001). Loss of caveolae, vascular dysfunction, and pulmonary defects in caveolin-1 gene-disrupted mice. Science *293*, 2449–2452.

Dulhunty, A.F., and Franzini-Armstrong, C. (1975). The relative contributions of the folds and caveolae to the surface membrane of frog skeletal muscle fibres at different sarcomere lengths. 513–539.

Dupont, S., Morsut, L., Aragona, M., Enzo, E., Giulitti, S., Cordenonsi, M., Zanconato, F., Le Digabel, J., Forcato, M., Bicciato, S., et al. (2011). Role of YAP/TAZ in mechanotransduction. Nature *474*, 179–183.

Egeblad, M., Rasch, M.G., and Weaver, V.M. (2010). Dynamic interplay between the collagen scaffold and tumor evolution. Curr. Opin. Cell Biol. *22*, 697–706.

Elosegui-Artola, A., Andreu, I., Beedle, A.E.M., Lezamiz, A., Uroz, M., Kosmalska,

A.J., Oria, R., Kechagia, J.Z., Rico-Lastres, P., Le Roux, A.-L., et al. (2017). Force Triggers YAP Nuclear Entry by Regulating Transport across Nuclear Pores. Cell *171*, 1397–1410.e14.

Elsasser, T.H., Kahl, S., Li, C.J., Sartin, J.L., Garrett, W.M., and Rodrigo, J. (2007). Caveolae nitration of Janus kinase-2 at the 1007Y- 1008Y site: Coordinating inflammatory response and metabolic hormone readjustment within the somatotropic axis. Endocrinology *148*, 3803–3813.

Endo, T.A., Masuhara, M., Yokouchi, M., Suzuki, R., Sakamoto, H., Mitsui, K., Matsumoto, A., Tanimura, S., Ohtsubo, M., Misawa, H., et al. (1997). A new protein containing an SH2 domain that inhibits JAK kinases. Nature *387*, 921–924.

Engel, S., Heger, T., Mancini, R., Herzog, F., Kartenbeck, J., Hayer, A., and Helenius, A. (2011). Role of endosomes in simian virus 40 entry and infection. J. Virol. *85*, 4198–4211.

Engelman, J.A., Wykoff, C.C., Yasuhara, S., Song, K.S., Okamoto, T., and Lisanti, M.P. (1997). Recombinant expression of caveolin-1 in oncogenically transformed cells abrogates anchorage-independent growth. J. Biol. Chem. *272*, 16374–16381.

Engler, A.J., Sen, S., Sweeney, H.L., and Discher, D.E. (2006). Matrix Elasticity Directs Stem Cell Lineage Specification. Cell *126*, 677–689.

Engler, A.J., Carag-krieger, C., Johnson, C.P., Raab, M., Tang, H., Speicher, D.W., Sanger, J.W., Sanger, J.M., and Discher, E. (2008). Elasticity : Scar-Like Rigidity Inhibits Beating. *121*, 3794–3802.

Epand, R.M., Sayer, B.G., and Epand, R.F. (2005). Caveolin scaffolding region and cholesterol-rich domains in membranes. J. Mol. Biol. *345*, 339–350.
Evans, E.A., and Calderwood, D.A. (2007). Forces and bond dynamics in cell adhesion. Science *316*, 1148–1153.

Fabry, B., Maksym, G.N., Butler, J.P., Glogauer, M., Navajas, D., and Fredberg, J.J. (2001). Scaling the microrheology of living cells. Phys. Rev. Lett. *87*, 148102.

Feng, J., Witthuhn, B.A., Matsuda, T., Kohlhuber, F., Kerr, I.M., and Ihle, J.N. (1997). Activation of Jak2 catalytic activity requires phosphorylation of Y1007 in the kinase activation loop. Mol. Cell. Biol. *17*, 2497–2501.

Fernandez-Hernando, C., Yu, J., Davalos, A., Prendergast, J., and Sessa, W.C. (2010). Endothelial-specific overexpression of caveolin-1 accelerates atherosclerosis in apolipoprotein E-deficient mice. Am. J. Pathol. *177*, 998–1003.

Finer, J.T., Simmons, R.M., and Spudich, J.A. (1994). Single myosin molecule mechanics: Piconewton forces and nanometre steps. Nature *368*, 113–119.

Firmbach-Kraft, I., Byers, M., Shows, T., Dalla-Favera, R., and Krolewski, J.J. (1990). tyk2, prototype of a novel class of non-receptor tyrosine kinase genes. Oncogene *5*, 1329–1336.

Fra, A.M., Williamson, E., Simons, K., and Parton, R.G. (1995). De novo formation of caveolae in lymphocytes by expression of VIP21-caveolin. Proc. Natl. Acad. Sci. U. S. A. *92*, 8655–8659.

Francois-Newton, V., Magno de Freitas Almeida, G., Payelle-Brogard, B., Monneron, D., Pichard-Garcia, L., Piehler, J., Pellegrini, S., and Uze, G. (2011). USP18-based negative feedback control is induced by type I and type III interferons and specifically inactivates interferon alpha response. PLoS One *6*, e22200.

Francois-Newton, V., Livingstone, M., Payelle-Brogard, B., Uze, G., and Pellegrini, S. (2012). USP18 establishes the transcriptional and anti-proliferative interferon alpha/beta differential. Biochem. J. *446*, 509–516.

Fujimoto, T. (1993). Calcium pump of the plasma membrane is localized in caveolae. J. Cell Biol. *120*, 1147–1157.

Fujimoto, T., Kogo, H., Ishiguro, K., Tauchi, K., and Nomura, R. (2001). Caveolin-2 is targeted to lipid droplets, a new “membrane domain” in the cell. J. Cell Biol. *152*, 1079–1085.

Furqan, M., Akinleye, A., Mukhi, N., Mittal, V., Chen, Y., and Liu, D. (2013). STAT inhibitors for cancer therapy. J. Hematol. Oncol. *6*, 90.

Galbiati, F., Volonte, D., Engelman, J.A., Watanabe, G., Burk, R., Pestell, R.G., and Lisanti, M.P. (1998). Targeted downregulation of caveolin-1 is sufficient to drive cell transformation and hyperactivate the p42/44 MAP kinase cascade. EMBO J. *17*, 6633–6648.

Galbiati, F., Engelman, J.A., Volonte, D., Zhang, X.L., Minetti, C., Li, M., Hou, H.J., Kneitz, B., Edelmann, W., and Lisanti, M.P. (2001). Caveolin-3 null mice show a loss of caveolae, changes in the microdomain distribution of the dystrophin-glycoprotein complex, and t-tubule abnormalities. J. Biol. Chem. *276*, 21425–21433.

Galbraith, C.G., Yamada, K.M., and Sheetz, M.P. (2002). The relationship between force and focal complex development. J. Cell Biol. *159*, 695–705.

Gambin, Y., Ariotti, N., McMahon, K.-A., Bastiani, M., Sierecki, E., Kovtun, O., Polinkovsky, M.E., Magenau, A., Jung, W., Okano, S., et al. (2014). Single-molecule analysis reveals self assembly and nanoscale segregation of two distinct cavin subcomplexes on caveolae. Elife *3*, e01434.

Gangadharan, V., Nohe, A., Caplan, J., Czymmek, K., and Duncan, R.L. (2015). Caveolin-1 regulates P2X7 receptor signaling in osteoblasts. Am. J. Physiol. Cell Physiol. *308*, C41-50.

Garcia-Cardena, G. (1997). Dissecting the Interaction between Nitric Oxide Synthase (NOS) and Caveolin. functional significance of the nos caveolin binding domain in vivo. J. Biol. Chem. *272*, 25437–25440.
Garcia, J., Bagwell, J., Njaine, B., Norman, J., Levic, D.S., Wopat, S., Miller, S.E.,

nLiu, X., Locasale, J.W., Stainier, D.Y.R., et al. (2017). Sheath Cell Invasion and Trans-differentiation Repair Mechanical Damage Caused by Loss of Caveolae in the Zebrafish Notochord. Curr. Biol. *27*, 1982–1989.e3.

Gavutis, M., Lata, S., Lamken, P., Muller, P., and Piehler, J. (2005). Lateral ligand-receptor interactions on membranes probed by simultaneous fluorescence-interference detection. Biophys. J. *88*, 4289–4302.

Gazzerro, E., Sotgia, F., Bruno, C., Lisanti, M.P., and Minetti, C. (2010). Caveolinopathies: from the biology of caveolin-3 to human diseases. Eur. J. Hum. Genet. *18*, 137–145.

Gazziola, C., Cordani, N., Carta, S., De Lorenzo, E., Colombatti, A., and Perris, R. (2005). The relative endogenous expression levels of the IFNAR2 isoforms influence the cytostatic and pro-apoptotic effect of IFNalpha on pleomorphic sarcoma cells. Int. J. Oncol. *26*, 129–140.

Gervasio, O.L., Phillips, W.D., Cole, L., and Allen, D.G. (2011). Caveolae respond to cell stretch and contribute to stretch-induced signaling. J. Cell Sci. *124*, 3581–3590.

Ghislain, J., Lingwood, C.A., and Fish, E.N. (1994). Evidence for glycosphingolipid modification of the type 1 IFN receptor. J. Immunol. *153*, 3655–3663.

Ghitescu, L., Fixman, A., Simionescu, M., and Simionescu, N. (1986). Specific binding sites for albumin restricted to plasmalemmal vesicles of continuous capillary endothelium: receptor-mediated transcytosis. J. Cell Biol. *102*, 1304–1311.

Glenney, J.R., and Soppet, D. (1992). Sequence and expression of caveolin, a protein component of caveolae plasma membrane domains phosphorylated on tyrosine in Rous sarcoma virus-transformed fibroblasts. Proc. Natl. Acad. Sci. U. S. A. *89*, 10517–10521.

Goetz, J.G., Lajoie, P., Wiseman, S.M., and Nabi, I.R. (2008). Caveolin-1 in tumor progression: The good, the bad and the ugly. Cancer Metastasis Rev. *27*, 715–735.

Goetz, J.G., Minguet, S., Navarro-Lerida, I., Lazcano, J.J., Samaniego, R., Calvo, E., Tello, M., Osteso-Ibanez, T., Pellinen, T., Echarri, A., et al. (2011). Biomechanical remodeling of the microenvironment by stromal caveolin-1 favors tumor invasion and metastasis. Cell *146*, 148–163.

Gonnord, P., Blouin, C.M., and Lamaze, C. (2012). Membrane trafficking and signaling: Two sides of the same coin. Semin. Cell Dev. Biol. *23*, 154–164.

Grashoff, C., Hoffman, B.D., Brenner, M.D., Zhou, R., Parsons, M., Yang, M.T., Mclean, M.A., Sligar, S.G., S, C., Ha, T., et al. (2011). Regulation of Focal Adhesion Dynamics. *466*, 263–266.

Gresser, I., and Belardelli, F. (2002). Endogenous type I interferons as a defense against tumors. Cytokine Growth Factor Rev. *13*, 111–118.

Guilluy, C., Osborne, L.D., Van Landeghem, L., Sharek, L., Superfine, R., Garcia-Mata, R., and Burridge, K. (2014). Isolated nuclei adapt to force and reveal a mechanotransduction pathway in the nucleus. Nat. Cell Biol. *16*, 376–381.

Guo, Y., Yang, L., Haught, K., and Scarlata, S. (2015). Osmotic stress reduces Ca^{2+} signals through deformation of caveolae. J. Biol. Chem. *290*, 16698–16707.

Gustincich, S., and Schneider, C. (1993). Serum deprivation response gene is induced by serum starvation but not by contact inhibition. Cell Growth Differ. *4*, 753–760.

Haan, C., Kreis, S., Margue, C., and Behrmann, I. (2006). Jaks and cytokine receptors--an intimate relationship. Biochem. Pharmacol. *72*, 1538–1546.

Han, F., Gu, D., Chen, Q., and Zhu, H. (2009). Caveolin-1 acts as a tumor suppressor by down-regulating epidermal growth factor receptor-mitogen-activated protein kinase signaling pathway in pancreatic carcinoma cell lines. Pancreas *38*, 766–774.

Hansen, C.G., and Nichols, B.J. (2010). Exploring the caves: cavins, caveolins and caveolae. Trends Cell Biol. *20*, 177–186.

Hansen, C., Bright, N., Howard, G., and Nichols, B.J. (2009). SDPR induces membrane curvature and functions in the formation of caveolae. Nat. Cell Biol. *11*.

Hansen, C.G., Howard, G., and Nichols, B.J. (2011). Pacsin 2 is recruited to caveolae and functions in caveolar biogenesis. J. Cell Sci. *124*, 2777–2785.

Hansen, C.G., Shvets, E., Howard, G., Riento, K., and Nichols, B.J. (2013). Deletion of cavin genes reveals tissue-specific mechanisms for morphogenesis of endothelial caveolae. Nat. Commun. *4*, 1813–1831.

Haricharan, S., and Li, Y. (2014). STAT signaling in mammary gland differentiation, cell survival and tumorigenesis. Mol. Cell. Endocrinol. *382*, 560–569.

Harris, A.K., Wild, P., Stopak, D., Series, N., and Apr, N. (2008). Silicone Rubber Substrata : A New Wrinkle in the Study of Cell Locomotion Silicone Rubber Substrata : A New Wrinkle in the Study of Cell Locomotion. *208*, 177–179.

Harunaga, J.S., and Yamada, K.M. (2011). Cell-matrix adhesions in 3D. Matrix Biol. *30*, 363–368.

Hayashi, K., Matsuda, S., Machida, K., Yamamoto, T., Fukuda, Y., Nimura, Y., Hayakawa, T., and Hamaguchi, M. (2001). Invasion activating caveolin-1 mutation in human scirrhous breast cancers. Cancer Res. *61*, 2361–2364.

Hayashi, Y.K., Matsuda, C., Ogawa, M., Goto, K., Tominaga, K., Mitsuhashi, S., Park, Y.-E., Nonaka, I., Hino-Fukuyo, N., Haginoya, K., et al. (2009). Human PTRF mutations cause secondary deficiency of caveolins resulting in muscular dystrophy

with generalized lipodystrophy. J. Clin. Invest. *119*, 2623–2633.
Hayer, A., Stoeber, M., Ritz, D., Engel, S., Meyer, H.H., and Helenius, A. (2010a). Caveolin-1 is ubiquitinated and targeted to intralumenal vesicles in endolysosomes for degradation. J. Cell Biol. *191*, 615–629.

Hayer, A., Stoeber, M., Bissig, C., and Helenius, A. (2010b). Biogenesis of caveolae: stepwise assembly of large caveolin and cavin complexes. Traffic *11*, 361–382.
Hernandez-Deviez, D.J., Martin, S., Laval, S.H., Lo, H.P., Cooper, S.T., North, K.N.,

Bushby, K., and Parton, R.G. (2006). Aberrant dysferlin trafficking in cells lacking caveolin or expressing dystrophy mutants of caveolin-3. Hum. Mol. Genet. *15*, 129–142.

Hernandez, V.J., Weng, J., Ly, P., Pompey, S., Dong, H., Mishra, L., Schwarz, M., Anderson, R.G.W., and Michaely, P. (2013). Cavin-3 dictates the balance between ERK and Akt signaling. Elife *2013*, 1–26.

Hill, M.M., Bastiani, M., Luetterforst, R., Kirkham, M., Kirkham, A., Nixon, S.J., Walser, P., Abankwa, D., Oorschot, V.M.J., Martin, S., et al. (2008). PTRF-Cavin, a Conserved Cytoplasmic Protein Required for Caveola Formation and Function. Cell *132*, 113–124.

Hirama, T., Das, R., Yang, Y., Ferguson, C., Won, A., Yip, C.M., Kay, J.G., Grinstein, S., Parton, R.G., and Fairn, G.D. (2017). Phosphatidylserine dictates the assembly and dynamics of caveolae in the plasma membrane. J. Biol. Chem. *292*, 14292–14307.

Hoop, C.L., Sivanandam, V.N., Kodali, R., Srnec, M.N., and van der Wel, P.C.A. (2012). structural characterization of the caveolin scaffolding domain in association with cholesterol-rich membranes. *51*, 90–99.

Hu, J.K.H., Du, W., Shelton, S.J., Oldham, M.C., DiPersio, C.M., and Klein, O.D. (2017). An FAK-YAP-mTOR Signaling Axis Regulates Stem Cell-Based Tissue Renewal in Mice. Cell Stem Cell *21*, 91–106.e6.

Hughes, K., and Watson, C.J. (2012). The spectrum of STAT functions in mammary gland development. JAK-STAT *1*, 151–158.

Hynes, N.E., and Watson, C.J. (2010). Mammary gland growth factors: roles in normal development and in cancer. Cold Spring Harb. Perspect. Biol. *2*, a003186.
Igaz, P., Toth, S., and Falus, A. (2001). Biological and clinical significance of the JAK-STAT pathway; lessons from knockout mice. Inflamm. Res. *50*, 435–441.

Iliopoulos, D., Jaeger, S.A., Hirsch, H.A., Bulyk, M.L., and Struhl, K. (2010). STAT3 activation of miR-21 and miR-181b-1 via PTEN and CYLD are part of the epigenetic switch linking inflammation to cancer. Mol. Cell *39*, 493–506.

Ingber, D.E. (2006). Cellular mechanotransduction: putting all the pieces together again. FASEB J. *20*, 1230–1232.

Irianto, J., Swift, J., Martins, R.P., McPhail, G.D., Knight, M.M., Discher, D.E., and Lee, D.A. (2013). Osmotic challenge drives rapid and reversible chromatin condensation in chondrocytes. Biophys. J. *104*, 759–769.

Isaacs, A., and Lindenmann, J. (1957). Virus interference. I. The interferon. Proc. R. Soc. London. Ser. B, Biol. Sci. *147*, 258–267.

Isshiki, M., and Anderson, R.G.W. (2003). Function of caveolae in Ca2+ entry and Ca2+-dependent signal transduction. Traffic *4*, 717–723.

Itano, N., Okamoto, S. -i., Zhang, D., Lipton, S.A., and Ruoslahti, E. (2003). Cell spreading controls endoplasmic and nuclear calcium: A physical gene regulation pathway from the cell surface to the nucleus. Proc. Natl. Acad. Sci. *100*, 5181–5186.

Iwabuchi, K., Handa, K., and Hakomori, S. (1998). Separation of “glycosphingolipid signaling domain” from caveolin-containing membrane fraction in mouse melanoma B16 cells and its role in cell adhesion coupled with signaling. J. Biol. Chem. *273*, 33766–33773.

Izumi, Y., Hirai, S. i, Tamai, Y., Fujise-Matsuoka, A., Nishimura, Y., and Ohno, S. (1997). A protein kinase Cdelta-binding protein SRBC whose expression is induced by serum starvation. J. Biol. Chem. *272*, 7381–7389.

Jaitin, D.A., Roisman, L.C., Jaks, E., Gavutis, M., Piehler, J., Van der Heyden, J., Uze, G., and Schreiber, G. (2006). Inquiring into the differential action of interferons (IFNs): an IFN-alpha2 mutant with enhanced affinity to IFNAR1 is functionally similar to IFN-beta. Mol. Cell. Biol. *26*, 1888–1897.

Janmey, P.A., and Miller, R.T. (2011). Mechanisms of mechanical signaling in development and disease. J. Cell Sci. *124*, 9–18.

Jansa, P., Burek, C., Sander, E.E., and Grummt, I. (2001). The transcript release factor PTRF augments ribosomal gene transcription by facilitating reinitiation of RNA polymerase I. Nucleic Acids Res. *29*, 423–429.

Jasmin, J.F., Mercier, I., Sotgia, F., and Lisanti, M.P. (2006). SOCS proteins and caveolin-1 as negative regulators of endocrine signaling. Trends Endocrinol. Metab. *17*, 150–158.

Jeong, E.G., Kim, M.S., Nam, H.K., Min, C.K., Lee, S., Chung, Y.J., Yoo, N.J., and Lee, S.H. (2008). Somatic mutations of JAK1 and JAK3 in acute leukemias and solid cancers. Clin. Cancer Res. *14*, 3716–3721.

Jiao, H., Berrada, K., Yang, W., Tabrizi, M., Platanias, L.C., and Yi, T. (1996). Direct association with and dephosphorylation of Jak2 kinase by the SH2-domain-containing protein tyrosine phosphatase SHP-1. Mol. Cell. Biol. *16*, 6985–6992.

Joshi, B., Bastiani, M., Strugnell, S.S., Boscher, C., Parton, R.G., and Nabi, I.R. (2012). Phosphocaveolin-1 is a mechanotransducer that induces caveola biogenesis

via Egr1 transcriptional regulation. J. Cell Biol. *199*, 425–435.

Jung, W., Sierecki, E., Bastiani, M., O'Carroll, A., Alexandrov, K., Rae, J., Johnston, W., Hunter, D.J.B., Ferguson, C., Gambin, Y., et al. (2018). Cell-free formation and interactome analysis of caveolae. J. Cell Biol. *217*, 2141–2165.

Kai, F., Laklai, H., and Weaver, V. (2016). Force Matters: Biomechanical Regulation of Cell Invasion and Migration in Disease. Trends Cell Biol. *xx*, 1–12.

Kandoth, C., McLellan, M.D., Xie, M., Zhang, Q., Mcmichael, J.F., Wyczalkowski, M.A., Wendl, M.C., Ley, T.J., Wilson, R.K., and Raphael, B.J. (2013). Mutational landscape and significance across 12 major cancer types. Nature *502*, 333–339.

Kaptein, A., Paillard, V., and Saunders, M. (1996). Dominant negative stat3 mutant inhibits interleukin-6-induced Jak-STAT signal transduction. J. Biol. Chem. *271*, 5961–5964.

Kawamura, M., McVicar, D.W., Johnston, J.A., Blake, T.B., Chen, Y.Q., Lal, B.K., Lloyd, A.R., Kelvin, D.J., Staples, J.E., and Ortaldo, J.R. (1994). Molecular cloning of L-JAK, a Janus family protein-tyrosine kinase expressed in natural killer cells and activated leukocytes. Proc. Natl. Acad. Sci. U. S. A. *91*, 6374–6378.

Kershaw, N.J., Murphy, J.M., Liau, N.P.D., Varghese, L.N., Laktyushin, A., Whitlock, E.L., Lucet, I.S., Nicola, N.A., and Babon, J.J. (2013a). SOCS3 binds specific receptor-JAK complexes to control cytokine signaling by direct kinase inhibition. Nat. Struct. Mol. Biol. *20*, 469–476.

Kershaw, N.J., Murphy, J.M., Lucet, I.S., Nicola, N.A., and Babon, J.J. (2013b). Regulation of Janus kinases by SOCS proteins. Biochem. Soc. Trans. *41*, 1042–1047.

Khater, I.M., Meng, F., Wong, T.H., Nabi, I.R., and Hamarneh, G. (2018). Super Resolution Network Analysis Defines the Molecular Architecture of Caveolae and Caveolin-1 Scaffolds. Sci. Rep. *8*, 9009.

Kim, C.A., Delepine, M., Boutet, E., El Mourabit, H., Le Lay, S., Meier, M., Nemani, M., Bridel, E., Leite, C.C., Bertola, D.R., et al. (2008). Association of a homozygous nonsense caveolin-1 mutation with Berardinelli-Seip congenital lipodystrophy. J. Clin. Endocrinol. Metab. *93*, 1129–1134.

Kirkham, M., Nixon, S.J., Howes, M.T., Abi-Rached, L., Wakeham, D.E., Hanzal-Bayer, M., Ferguson, C., Hill, M.M., Fernandez-Rojo, M., Brown, D. a, et al. (2008). Evolutionary analysis and molecular dissection of caveola biogenesis. J. Cell Sci. *121*, 2075–2086.

Kisseleva, T., Bhattacharya, S., Braunstein, J., and Schindler, C.W. (2002). Signaling through the JAK/STAT pathway, recent advances and future challenges. Gene *285*, 1–24.

Koromilas, A.E., and Sexl, V. (2013). The tumor suppressor function of STAT1 in

breast cancer. Jak-Stat *2*, e23353.

Kovtun, O., Tillu, V.A., Jung, W., Leneva, N., Ariotti, N., Chaudhary, N., Mandyam, R.A., Ferguson, C., Morgan, G.P., Johnston, W.A., et al. (2014). Structural insights into the organization of the cavin membrane coat complex. Dev. Cell *31*, 405–419.

Krolewski, J.J., Lee, R., Eddy, R., Shows, T.B., and Dalla-Favera, R. (1990). Identification and chromosomal mapping of new human tyrosine kinase genes. Oncogene *5*, 277–282.

Kruger, M., Kratchmarova, I., Blagoev, B., Tseng, Y.-H., Kahn, C.R., and Mann, M. (2008). Dissection of the insulin signaling pathway via quantitative phosphoproteomics. Proc. Natl. Acad. Sci. U. S. A. *105*, 2451–2456.

Kurzchalia, T. V, Dupree, P., Parton, R.G., Kellner, R., Virta, H., Lehnert, M., and Simons, K. (1992). VIP21, a 21-kD membrane protein is an integral component of trans-Golgi-network-derived transport vesicles. J. Cell Biol. *118*, 1003–1014.

Kwon, H., and Pak, Y. (2010). Prolonged tyrosine kinase activation of insulin receptor by pY27-caveolin-2. Biochem. Biophys. Res. Commun. *391*, 49–55.

Kwon, H., Jeong, K., Hwang, E.M., Park, J.Y., Hong, S.G., Choi, W.S., and Pak, Y. (2009). Caveolin-2 regulation of STAT3 transcriptional activation in response to insulin. Biochim. Biophys. Acta - Mol. Cell Res. *1793*, 1325–1333.

Kwon, H., Jeong, K., Hwang, E.M., Park, J.Y., and Pak, Y. (2011). A novel domain of caveolin-2 that controls nuclear targeting: Regulation of insulin-specific ERK activation and nuclear translocation by caveolin-2. J. Cell. Mol. Med. *15*, 888–908.

Kwon, H., Lee, J., Jeong, K., Jang, D., and Pak, Y. (2015). Fatty acylated caveolin-2 is a substrate of insulin receptor tyrosine kinase for insulin receptor substrate-1-directed signaling activation. Biochim. Biophys. Acta - Mol. Cell Res. *1853*, 1022–1034.

Lahtinen, U., Honsho, M., Parton, R.G., Simons, K., and Verkade, P. (2003). Involvement of caveolin-2 in caveolar biogenesis in MDCK cells. FEBS Lett. *538*, 85–88.

Laklai, H., Miroshnikova, Y.A., Pickup, M.W., Collisson, E.A., Kim, G.E., Barrett, A.S., Hill, R.C., Lakins, J.N., Schlaepfer, D.D., Mouw, J.K., et al. (2016). Genotype tunes pancreatic ductal adenocarcinoma tissue tension to induce matricellular fibrosis and tumor progression. Nat. Med. *22*, 497–505.

Lamar, J.M., Stern, P., Liu, H., Schindler, J.W., Jiang, Z.-G., and Hynes, R.O. (2012). The Hippo pathway target, YAP, promotes metastasis through its TEAD-interaction domain. Proc. Natl. Acad. Sci. *109*, E2441–E2450.

Lamaze, C., and Torrino, S. (2015). Caveolae and cancer: A new mechanical perspective. Biomed. J. *38*, 367–379.

Lamaze, C., Tardif, N., Dewulf, M., Vassilopoulos, S., and Blouin, C.M. (2017). The caveolae dress code: structure and signaling. Curr. Opin. Cell Biol. *47*, 117–125.

Lamken, P., Lata, S., Gavutis, M., and Piehler, J. (2004). Ligand-induced assembling of the type I interferon receptor on supported lipid bilayers. J. Mol. Biol. *341*, 303–318.
Lamken, P., Gavutis, M., Peters, I., Van der Heyden, J., Uze, G., and Piehler, J. (2005). Functional cartography of the ectodomain of the type I interferon receptor subunit ifnar1. J. Mol. Biol. *350*, 476–488.

Le Lan, C., Neumann, J.-M., and Jamin, N. (2006). Role of the membrane interface on the conformation of the caveolin scaffolding domain: a CD and NMR study. FEBS Lett. *580*, 5301–5305.

Langer, J.A., and Pestka, S. (1988). Interferon receptors. Immunol. Today *9*, 393–400.

Le Lay, S., Hajduch, E., Lindsay, M.R., Le Liepvre, X., Thiele, C., Ferre, P., Parton, R.G., Kurzchalia, T., Simons, K., and Dugail, I. (2006). Cholesterol-induced caveolin targeting to lipid droplets in adipocytes: a role for caveolar endocytosis. Traffic *7*, 549–561.

Leaman, D.W., Leung, S., Li, X., and Stark, G.R. (1996). Regulation of STAT-dependent pathways by growth factors and cytokines. FASEB J. Off. Publ. Fed. Am. Soc. Exp. Biol. *10*, 1578–1588.

Lee, J., and Glover, K.J. (2012). The transmembrane domain of caveolin-1 exhibits a helix-break-helix structure. Biochim. Biophys. Acta *1818*, 1158–1164.

Lee, J., C., C., B., Y., R., E., A., C.-G., K., H., J., X., and D., M. (2015). Tissue Transglutaminase Mediated Tumor-Stroma Interaction Promotes Pancreatic Cancer Progression. *179*, 95–105.

Leonard, W.J., and O'Shea, J.J. (1998). Jaks and STATs: biological implications. Annu. Rev. Immunol. *16*, 293–322.

Levental, I., Georges, P.C., and Janmey, P.A. (2007). Soft biological materials and their impact on cell function. Soft Matter *3*, 299–306.

Levental, K.R., Yu, H., Kass, L., Lakins, J.N., Erler, J.T., Fong, S.F.T., Csiszar, K., Giaccia, A., Yamauchi, M., Gasser, D.L., et al. (2009). Matrix Crosslinking Forces Tumor Progression by Enhancing Integrin signaling Kandice. *139*, 891–906.

Levy, D.E., and Darnell, J.E.J. (2002). Stats: transcriptional control and biological impact. Nat. Rev. Mol. Cell Biol. *3*, 651–662.

Li, C., Rezania, S., Kammerer, S., Sokolowski, A., Devaney, T., Gorischek, A., Jahn, S., Hackl, H., Groschner, K., Windpassinger, C., et al. (2015). Piezo1 forms mechanosensitive ion channels in the human MCF-7 breast cancer cell line. Sci. Rep. *5*, 1–9.

Li, Q., Bai, L., Liu, N., Wang, M., Liu, J.P., Liu, P., and Cong, Y.S. (2014). Increased polymerase I and transcript release factor (Cavin-1) expression attenuates platelet-derived growth factor receptor signalling in senescent human fibroblasts. Clin. Exp. Pharmacol. Physiol. *41*, 169–173.

Li, S., Okamoto, T., Chun, M., Sargiacomo, M., Casanova, J.E., Hansen, S.H., Nishimoto, I., and Lisanti, M.P. (1995). Evidence for a regulated interaction between heterotrimeric G proteins and caveolin. J. Biol. Chem. *270*, 15693–15701.

Li, S., Couet, J., and Lisanti, M.P. (1996). Src tyrosine kinases, Galpha subunits, and H-Ras share a common membrane-anchored scaffolding protein, caveolin. Caveolin binding negatively regulates the auto-activation of Src tyrosine kinases. J. Biol. Chem. *271*, 29182–29190.

Li, T., Sotgia, F., Vuolo, M.A., Li, M., Yang, W.C., Pestell, R.G., Sparano, J.A., and Lisanti, M.P. (2006). Caveolin-1 mutations in human breast cancer: functional association with estrogen receptor alpha-positive status. Am. J. Pathol. *168*, 1998–2013.

Lien, S.C., Chang, S.F., Lee, P.L., Wei, S.Y., Chang, M.D.T., Chang, J.Y., and Chiu, J.J. (2013). Mechanical regulation of cancer cell apoptosis and autophagy: Roles of bone morphogenetic protein receptor, Smad1/5, and p38 MAPK. Biochim. Biophys. Acta - Mol. Cell Res. *1833*, 3124–3133.

Lim, Y.W., Lo, H.P., Ferguson, C., Martel, N., Giacomotto, J., Gomez, G.A., Yap, A.S., Hall, T.E., and Parton, R.G. (2017). Caveolae Protect Notochord Cells against Catastrophic Mechanical Failure during Development. Curr. Biol. *27*, 1968–1981.e7.

Ling, L.E., Zafari, M., Reardon, D., Brickelmeier, M., Goelz, S.E., and Benjamin, C.D. (1995). Human type I interferon receptor, IFNAR, is a heavily glycosylated 120-130 kD membrane protein. J. Interferon Cytokine Res. *15*, 55–61.

Lisanti, M.P., Scherer, P.E., Tang, Z., and Sargiacomo, M. (1994). Caveolae, caveolin and caveolin-rich membrane domains: a signalling hypothesis. Trends Cell Biol. *4*, 231–235.

Lisanti, M.P., Tang, Z., Scherer, P.E., Kubler, E., Koleske, A.J., and Sargiacomo, M. (1995). Caveolae, transmembrane signalling and cellular transformation. Mol. Membr. Biol. *12*, 121–124.

Liu, B., Mink, S., Wong, K.A., Stein, N., Getman, C., Dempsey, P.W., Wu, H., and Shuai, K. (2004). PIAS1 selectively inhibits interferon-inducible genes and is important in innate immunity. Nat. Immunol. *5*, 891–898.

Liu, H., Yang, L., Zhang, Q., Mao, L., Jiang, H., and Yang, H. (2016). Probing the structure and dynamics of caveolin-1 in a caveolae-mimicking asymmetric lipid bilayer model. Eur. Biophys. J.

Liu, L., Brown, D., McKee, M., Lebrasseur, N.K., Yang, D., Albrecht, K.H., Ravid, K.,

and Pilch, P.F. (2008). Deletion of Cavin/PTRF causes global loss of caveolae, dyslipidemia, and glucose intolerance. Cell Metab. *8*, 310–317.

Liu, L., Hansen, C.G., Honeyman, B.J., Nichols, B.J., and Pilch, P.F. (2014). Cavin-3 knockout mice show that cavin-3 is not essential for caveolae formation, for maintenance of body composition, or for glucose tolerance. PLoS One *9*, e102935.

Llorente, A., de Marco, M.C., and Alonso, M.A. (2004). Caveolin-1 and MAL are located on prostasomes secreted by the prostate cancer PC-3 cell line. J. Cell Sci. *117*, 5343–5351.

Lo, H.P., Nixon, S.J., Hall, T.E., Cowling, B.S., Ferguson, C., Morgan, G.P., Schieber, N.L., Fernandez-Rojo, M.A., Bastiani, M., Floetenmeyer, M., et al. (2015). The caveolin-Cavin system plays a conserved and critical role in mechanoprotection of skeletal muscle. J. Cell Biol. *210*, 833–849.

Logozzi, M., De Milito, A., Lugini, L., Borghi, M., Calabro, L., Spada, M., Perdicchio, M., Marino, M.L., Federici, C., Iessi, E., et al. (2009). High levels of exosomes expressing CD63 and caveolin-1 in plasma of melanoma patients. PLoS One *4*, e5219.

Londos, C., Brasaemle, D.L., Schultz, C.J., Adler-Wailes, D.C., Levin, D.M., Kimmel, A.R., and Rondinone, C.M. (1999). On the control of lipolysis in adipocytes. Ann. N. Y. Acad. Sci. *892*, 155–168.

Low, B.C., Pan, C.Q., Shivashankar, G. V, Bershadsky, A., Sudol, M., and Sheetz, M. (2014). YAP/TAZ as mechanosensors and mechanotransducers in regulating organ size and tumor growth. FEBS Lett. *588*, 2663–2670.

Lu, P., Takai, K., Weaver, V.M., and Werb, Z. (2011). Extracellular matrix degradation and remodeling in development and disease. Cold Spring Harb Perspect Biol *3*, 1–24.

Ludwig, A., Howard, G., Mendoza-Topaz, C., Deerinck, T., Mackey, M., Sandin, S., Ellisman, M.H., and Nichols, B.J. (2013). Molecular composition and ultrastructure of the caveolar coat complex. PLoS Biol. *11*, e1001640.

Ludwig, A., Nichols, B.J., and Sandin, S. (2016). Architecture of the Caveolar Coat Complex. J. Cell Sci.

Lupardus, P.J., Ultsch, M., Wallweber, H., Bir Kohli, P., Johnson, A.R., and Eigenbrot, C. (2014). Structure of the pseudokinase-kinase domains from protein kinase TYK2 reveals a mechanism for Janus kinase (JAK) autoinhibition. Proc. Natl. Acad. Sci. U. S. A. *111*, 8025–8030.

Lutfalla, G., Holland, S.J., Cinato, E., Monneron, D., Reboul, J., Rogers, N.C., Smith, J.M., Stark, G.R., Gardiner, K., and Mogensen, K.E. (1995). Mutant U5A cells are complemented by an interferon-alpha beta receptor subunit generated by alternative processing of a new member of a cytokine receptor gene cluster. EMBO J. *14*, 5100–5108.

Macek Jilkova, Z., Lisowska, J., Manet, S., Verdier, C., Deplano, V., Geindreau, C., Faurobert, E., Albiges-Rizo, C., and Duperray, A. (2014). CCM proteins control endothelial beta1 integrin dependent response to shear stress. Biol. Open *3*, 1228–1235.

Malakhova, O.A., Kim, K. Il, Luo, J.-K., Zou, W., Kumar, K.G.S., Fuchs, S.Y., Shuai, K., and Zhang, D.-E. (2006). UBP43 is a novel regulator of interferon signaling independent of its ISG15 isopeptidase activity. EMBO J. *25*, 2358–2367.

Marchetti, M., Monier, M.-N., Fradagrada, A., Mitchell, K., Baychelier, F., Eid, P., Johannes, L., and Lamaze, C. (2006). Stat-mediated signaling induced by type I and type II interferons (IFNs) is differentially controlled through lipid microdomain association and clathrin-dependent endocytosis of IFN receptors. Mol. Biol. Cell *17*, 2896–2909.

Marijanovic, Z., Ragimbeau, J., Kumar, K.G.S., Fuchs, S.Y., and Pellegrini, S. (2006). TYK2 activity promotes ligand-induced IFNAR1 proteolysis. Biochem. J. *397*, 31–38.

Martinac, B. (2004). Mechanosensitive ion channels: molecules of mechanotransduction. J. Cell Sci. *117*, 2449–2460.

Martinac, B., and Hamill, O.P. (2002). Gramicidin A channels switch between stretch activation and stretch inactivation depending on bilayer thickness. Proc. Natl. Acad. Sci. U. S. A. *99*, 4308–4312.

McMahon, H.T., and Gallop, J.L. (2005). Membrane curvature and mechanisms of dynamic cell membrane remodelling. Nature *438*, 590–596.

McMahon, K.-A., Zajicek, H., Li, W.-P., Peyton, M.J., Minna, J.D., Hernandez, V.J., Luby-Phelps, K., and Anderson, R.G.W. (2009). SRBC/cavin-3 is a caveolin adapter protein that regulates caveolae function. EMBO J. *28*, 1001–1015.

Meng, F., Saxena, S., Liu, Y., Joshi, B., Wong, T.H., Shankar, J., Foster, L.J., Bernatchez, P., and Nabi, I.R. (2017). The phospho–caveolin-1 scaffolding domain dampens force fluctuations in focal adhesions and promotes cancer cell migration.

Mol. Biol. Cell *28*, 2190–2201.
Mertens, C., and Darnell, J.E.J. (2007). SnapShot: JAK-STAT signaling. Cell *131*, 612.

Meshulam, T., Simard, J.R., Wharton, J., Hamilton, J.A., and Pilch, P.F. (2006). Role of caveolin-1 and cholesterol in transmembrane fatty acid movement. Biochemistry *45*, 2882–2893.

Meyer, T., Marg, A., Lemke, P., Wiesner, B., and Vinkemeier, U. (2003). DNA binding controls inactivation and nuclear accumulation of the transcription factor Stat1. Genes Dev. *17*, 1992–2005.

Mineo, C., Ying, Y.S., Chapline, C., Jaken, S., and Anderson, R.G. (1998). Targeting of protein kinase Calpha to caveolae. J. Cell Biol. *141*, 601–610.

Mohan, J., Moren, B., Larsson, E., Holst, M.R., and Lundmark, R. (2015). Cavin3 interacts with cavin1 and caveolin1 to increase surface dynamics of caveolae. J. Cell Sci. *128*, 979–991.

Monier, S., Parton, R.G., Vogel, F., Behlke, J., Henske, A., and Kurzchalia, T. V (1995). VIP21-caveolin, a membrane protein constituent of the caveolar coat, oligomerizes in vivo and in vitro. Mol. Biol. Cell *6*, 911–927.

Monier, S., Dietzen, D.J., Hastings, W.R., Lublin, D.M., and Kurzchalia, T. V (1996). Oligomerization of VIP21-caveolin in vitro is stabilized by long chain fatty acylation or cholesterol. FEBS Lett. *388*, 143–149.

Montel, F., Delarue, M., Elgeti, J., Malaquin, L., Basan, M., Risler, T., Cabane, B., Vignjevic, D., Prost, J., Cappello, G., et al. (2011). Stress clamp experiments on multicellular tumor spheroids. Phys. Rev. Lett. *107*, 188102.

Montesano, R., Roth, J., Robert, A., and Orci, L. (1982). Non-coated membrane invaginations are involved in binding and internalization of cholera and tetanus toxins. Nature *296*, 651–653.

Moon, H., Lee, C.S., Inder, K.L., Sharma, S., Choi, E., Black, D.M., Lê Cao, K., Winterford, C., Coward, J.I., Ling, M.T., et al. (2013). PTRF/cavin-1 neutralizes non-caveolar caveolin-1 microdomains in prostate cancer. Oncogene 1–10.

Morén, B., Shah, C., Howes, M.T., Schieber, N.L., McMahon, H.T., Parton, R.G., Daumke, O., and Lundmark, R. (2012). EHD2 regulates caveolar dynamics via ATP-driven targeting and oligomerization. Mol. Biol. Cell *23*, 1316–1329.

Mosqueira, D., Pagliari, S., Uto, K., Ebara, M., Romanazzo, S., Escobedo-Lucea, C., Nakanishi, J., Taniguchi, A., Franzese, O., Di Nardo, P., et al. (2014). Hippo pathway effectors control cardiac progenitor cell fate by acting as dynamic sensors of substrate mechanics and nanostructure. ACS Nano *8*, 2033–2047.

Mouw, J.K., Yui, Y., Damiano, L., Bainer, R.O., Lakins, J.N., Acerbi, I., Ou, G., Wijekoon, A.C., Levental, K.R., Gilbert, P.M., et al. (2014). Tissue mechanics modulate microRNA-dependent PTEN expression to regulate malignant progression. *20*, 360–367.

Mrkonjic, S., Destaing, O., and Albiges-Rizo, C. (2017). Mechanotransduction pulls the strings of matrix degradation at invadosome. Matrix Biol. *57–58*, 190–203.

Mundy, D.I., Li, W.P., Luby-Phelps, K., and Anderson, R.G.W. (2012). Caveolin targeting to late endosome/lysosomal membranes is induced by perturbations of lysosomal pH and cholesterol content. Mol. Biol. Cell *23*, 864–880.

Murata, M., Peränen, J., Schreiner, R., Wieland, F., Kurzchalia, T. V, and Simons, K. (1995). VIP21/caveolin is a cholesterol-binding protein. Proc. Natl. Acad. Sci. U. S. A.

92, 10339–10343.

Murata, T., Lin, M.I., Stan, R. V., Bauer, P.M., Yu, J., and Sessa, W.C. (2007). Genetic evidence supporting caveolae microdomain regulation of calcium entry in endothelial cells. J. Biol. Chem. *282*, 16631–16643.

Myers, M.P., Andersen, J.N., Cheng, A., Tremblay, M.L., Horvath, C.M., Parisien, J.P., Salmeen, A., Barford, D., and Tonks, N.K. (2001). TYK2 and JAK2 are substrates of protein-tyrosine phosphatase 1B. J. Biol. Chem. *276*, 47771–47774.

Na, S., Collin, O., Chowdhury, F., Tay, B., Ouyang, M., Wang, Y., and Wang, N. (2008). Rapid signal transduction in living cells is a unique feature of mechanotransduction. Proc. Natl. Acad. Sci. *105*, 6626–6631.

Nabi, I.R. (2009). Cavin fever: Regulating caveolae. Nat. Cell Biol. *11*, 789–791.
Naka, T., Narazaki, M., Hirata, M., Matsumoto, T., Minamoto, S., Aono, A., Nishimoto, N., Kajita, T., Taga, T., Yoshizaki, K., et al. (1997). Structure and function of a new STAT-induced STAT inhibitor. Nature *387*, 924–929.

Nassoy, P., and Lamaze, C. (2012). Stressing caveolae new role in cell mechanics. Trends Cell Biol. *22*, 381–389.

Ng, C.T., Sullivan, B.M., Teijaro, J.R., Lee, A.M., Welch, M., Rice, S., Sheehan, K.C.F., Schreiber, R.D., and Oldstone, M.B.A. (2015). Blockade of interferon Beta, but not interferon alpha, signaling controls persistent viral infection. Cell Host Microbe *17*, 653–661.

Nichols, B.J. (2002). A distinct class of endosome mediates clathrin-independent endocytosis to the Golgi complex. Nat. Cell Biol. *4*, 374–378.

Niwa, H., Burdon, T., Chambers, I., and Smith, A. (1998). Self-renewal of pluripotent embryonic stem cells is mediated via activation of STAT3. Genes Dev. *12*, 2048–2060.

Novick, D., Cohen, B., and Rubinstein, M. (1994). The human interferon alpha/beta receptor: characterization and molecular cloning. Cell *77*, 391–400.

Nystrom, F.H., Chen, H., Cong, L.N., Li, Y., and Quon, M.J. (1999). Caveolin-1 interacts with the insulin receptor and can differentially modulate insulin signaling in transfected Cos-7 cells and rat adipose cells. Mol. Endocrinol. *13*, 2013–2024.

O'Shea, J.J., Gadina, M., and Schreiber, R.D. (2002). Cytokine signaling in 2002: new surprises in the Jak/Stat pathway. Cell *109 Suppl*, S121-31.

O'Shea, J.J., Schwartz, D.M., Villarino, A. V, Gadina, M., Iain, B., and Laurence, A. (2015). The JAK-STAT Pathway: Impact on Human Disease and Therapeutic Intervention. 311–328.

Ogata, T., Ueyama, T., Isodono, K., Tagawa, M., Takehara, N., Kawashima, T.,

Harada, K., Takahashi, T., Shioi, T., Matsubara, H., et al. (2008). MURC, a muscle-restricted coiled-coil protein that modulates the Rho/ROCK pathway, induces cardiac dysfunction and conduction disturbance. Mol. Cell. Biol. *28*, 3424–3436.

Oh, P., McIntosh, D.P., and Schnitzer, J.E. (1998). Dynamin at the neck of caveolae mediates their budding to form transport vesicles by GTP-driven fission from the plasma membrane of endothelium. J. Cell Biol. *141*, 101–114.

Okamoto, T., Schlegel, a, Scherer, P.E., and Lisanti, M.P. (1998). Caveolins, a family of scaffolding proteins for organizing "preassembled signaling complexes" at the plasma membrane. J Biol Chem *273*, 5419–5422.
Onck, P.R., Koeman, T., van Dillen, T., and van der Giessen, E. (2005). Alternative explanation of stiffening in cross-linked semiflexible networks. Phys. Rev. Lett. *95*, 178102.

Orlandi, P.A., and Fishman, P.H. (1998). Filipin-dependent inhibition of cholera toxin: evidence for toxin internalization and activation through caveolae-like domains. J. Cell Biol. *141*, 905–915.

Orr, A.W., Helmke, B.P., Blackman, B.R., and Schwartz, M.A. (2006). Mechanisms of mechanotransduction. Dev. Cell *10*, 11–20.

Ortegren, U., Karlsson, M., Blazic, N., Blomqvist, M., Nystrom, F.H., Gustavsson, J., Fredman, P., and Stralfors, P. (2004). Lipids and glycosphingolipids in caveolae and surrounding plasma membrane of primary rat adipocytes. Eur. J. Biochem. *271*, 2028–2036.

Ost, A., Ortegren, U., Gustavsson, J., Nystrom, F.H., and Stralfors, P. (2005). Triacylglycerol is synthesized in a specific subclass of caveolae in primary adipocytes. J. Biol. Chem. *280*, 5–8.

Ostermeyer, A.G., Paci, J.M., Zeng, Y., Lublin, D.M., Munro, S., and Brown, D.A. (2001). Accumulation of caveolin in the endoplasmic reticulum redirects the protein to lipid storage droplets. J. Cell Biol. *152*, 1071–1078.

Pagano, R.E. (2003). Endocytic trafficking of glycosphingolipids in sphingolipid storage diseases. Philos. Trans. R. Soc. Lond. B. Biol. Sci. *358*, 885–891.

Palade, G.E. (1953). The fine structure of blood capillaries. J. Appl. Phys. *24*, 1424.
Panciera, T., Azzolin, L., Cordenonsi, M., and Piccolo, S. (2017). Mechanobiology of YAP and TAZ in physiology and disease. Nat. Rev. Mol. Cell Biol. *18*, 758–770.

Pardo-Pastor, C., Rubio-Moscardo, F., Vogel-Gonzalez, M., Serra, S.A., Afthinos, A., Mrkonjic, S., Destaing, O., Abenza, J.F., Fernandez-Fernandez, J.M., Trepat, X., et al. (2018). Piezo2 channel regulates RhoA and actin cytoskeleton to promote cell mechanobiological responses. Proc. Natl. Acad. Sci. U. S. A. *115*, 1925–1930.

Parton, R.G., and del Pozo, M. a (2013). Caveolae as plasma membrane sensors, protectors and organizers. Nat. Rev. Mol. Cell Biol. *14*, 98–112.

Parton, R.G., and Simons, K. (2007). The multiple faces of caveolae. Nat. Rev. Mol. Cell Biol. *8*, 185–194.

Parton, R.G., Hanzal-Bayer, M., and Hancock, J.F. (2006). Biogenesis of caveolae: a structural model for caveolin-induced domain formation. J. Cell Sci. *119*, 787–796.

Patel, H.H., Murray, F., and Insel, P.A. (2008). Caveolae as organizers of pharmacologically relevant signal transduction molecules. Annu. Rev. Pharmacol. Toxicol. *48*, 359–391.

Paty, D.W., and Li, D.K. (1993). Interferon beta-1b is effective in relapsing-remitting multiple sclerosis. II. MRI analysis results of a multicenter, randomized, double-blind, placebo-controlled trial. UBC MS/MRI Study Group and the IFNB Multiple Sclerosis Study Group. Neurology *43*, 662–667.

Pelham, R.J., and Wang, Y.L. (1998). Cell locomotion and focal adhesions are regulated by the mechanical properties of the substrate. Biol. Bull. *194*, 348–350.

Pelkmans, L., and Zerial, M. (2005). Kinase-regulated quantal assemblies and kiss-and-run recycling of caveolae. Nature *436*, 128–133.

Pelkmans, L., Kartenbeck, J., and Helenius, A. (2001). Caveolar endocytosis of simian virus 40 reveals a new two-step vesicular-transport pathway to the ER. Nat. Cell Biol. *3*, 473–483.

Pelkmans, L., Puntener, D., and Helenius, A. (2002). Local actin polymerization and dynamin recruitment in SV40-induced internalization of caveolae. Science *296*, 535–539.

Pestka, S., Krause, C.D., and Walter, M.R. (2004). Interferons, interferon-like cytokines, and their receptors. Immunol. Rev. *202*, 8–32.

Peters-Golden, M., and Brock, T.G. (2001). Intracellular compartmentalization of leukotriene synthesis: Unexpected nuclear secrets. FEBS Lett. *487*, 323–326.

Pfeffer, L.M., Dinarello, C.A., Herberman, R.B., Williams, B.R., Borden, E.C., Bordens, R., Walter, M.R., Nagabhushan, T.L., Trotta, P.P., and Pestka, S. (1998). Biological properties of recombinant alpha-interferons: 40th anniversary of the discovery of interferons. Cancer Res. *58*, 2489–2499.

Piehler, J., Thomas, C., Christopher Garcia, K., and Schreiber, G. (2012). Structural and dynamic determinants of type I interferon receptor assembly and their functional interpretation. Immunol. Rev. *250*, 317–334.

Platanias, L.C. (2005). Mechanisms of type-I- and type-II-interferon-mediated signalling. Nat. Rev. Immunol. *5*, 375–386.

Platanias, L.C., Uddin, S., and Colamonici, O.R. (1994). Tyrosine phosphorylation of the alpha and beta subunits of the type I interferon receptor. Interferon-beta

selectively induces tyrosine phosphorylation of an alpha subunit-associated protein. J. Biol. Chem. *269*, 17761–17764.

Pol, A., Luetterforst, R., Lindsay, M., Heino, S., Ikonen, E., and Parton, R.G. (2001). A caveolin dominant negative mutant associates with lipid bodies and induces intracellular cholesterol imbalance. J. Cell Biol. *152*, 1057–1070.

Pol, A., Martin, S., Fernandez, M.A., Ingelmo-Torres, M., Ferguson, C., Enrich, C., and Parton, R.G. (2005). Cholesterol and fatty acids regulate dynamic caveolin trafficking through the Golgi complex and between the cell surface and lipid bodies. Mol. Biol. Cell *16*, 2091–2105.

Prescott, L., and Brightman, M.W. (1976). The sarcolemma of Aplysia smooth muscle in freeze-fracture preparations. Tissue Cell *8*, 241–258.

Prosperini, L., Mancinelli, C.R., Pozzilli, C., Grasso, M.G., Clemenzi, A., Collorone, S., Pontecorvo, S., Francia, A., Villani, V., Koudriavtseva, T., et al. (2014). From high- to low-frequency administered interferon-beta for multiple sclerosis: a multicenter study. Eur. Neurol. *71*, 233–241.

Raab, M., Gentili, M., Belly, H. De, Thiam, H., Vargas, P., Jimenez, A.J., Lautenschlaeger, F., Voituriez, R., Manel, N., and Piel, M. (2016). ESCRT III repairs nuclear envelope ruptures during cell migration to limit DNA damage and cell death. *352*, 359–363.

Rao, M., and Mayor, S. (2014). Active organization of membrane constituents in living cells. Curr. Opin. Cell Biol. *29*, 126–132.

Razani, B., Engelman, J.A., Wang, X.B., Schubert, W., Zhang, X.L., Marks, C.B., Macaluso, F., Russell, R.G., Li, M., Pestell, R.G., et al. (2001). Caveolin-1 null mice are viable but show evidence of hyperproliferative and vascular abnormalities. J. Biol. Chem. *276*, 38121–38138.

Razani, B., Woodman, S.E., and Lisanti, M.P. (2002a). Caveolae: from cell biology to animal physiology. Pharmacol. Rev. *54*, 431–467.

Razani, B., Wang, X.B., Engelman, J.A., Battista, M., Lagaud, G., Zhang, X.L., Kneitz, B., Hou, H.J., Christ, G.J., Edelmann, W., et al. (2002b). Caveolin-2-deficient mice show evidence of severe pulmonary dysfunction without disruption of caveolae. Mol. Cell. Biol. *22*, 2329–2344.

del Rio, A., Perez-Jimenez, R., Liu, R., Roca-Cusachs, P., Fernandez, J.M., and Sheetz, M.P. (2009). Stretching single talin rod molecules activates vinculin binding. Science *323*, 638–641.

Rizwan Siddiqui, M., Komarova, Y.A., Vogel, S.M., Gao, X., Bonini, M.G., Rajasingh, J., Zhao, Y.Y., Brovkovych, V., and Malik, A.B. (2011). Caveolin-1-eNOS signaling promotes p190RhoGAP-A nitration and endothelial permeability. J. Cell Biol. *193*, 841–850.

Root, K.T., Plucinsky, S.M., and Glover, K.J. (2015). Recent Progress in the Topology, Structure, and Oligomerization of Caveolin: A Building Block of Caveolae (Elsevier Ltd).

Rothberg, K.G., Ying, Y.S., Kamen, B.A., and Anderson, R.G. (1990). Cholesterol controls the clustering of the glycophospholipid-anchored membrane receptor for 5-methyltetrahydrofolate. J. Cell Biol. *111*, 2931–2938.

Rothberg, K.G., Heuser, J.E., Donzell, W.C., Ying, Y.S., Glenney, J.R., and Anderson, R.G. (1992). Caveolin, a protein component of caveolae membrane coats. Cell *68*, 673–682.

du Roure, O., Saez, A., Buguin, A., Austin, R.H., Chavrier, P., Silberzan, P., and Ladoux, B. (2005). Force mapping in epithelial cell migration. Proc. Natl. Acad. Sci. U. S. A. *102*, 2390–2395.

Saharinen, P., and Silvennoinen, O. (2002). The pseudokinase domain is required for suppression of basal activity of Jak2 and Jak3 tyrosine kinases and for cytokine-inducible activation of signal transduction. J. Biol. Chem. *277*, 47954–47963.

Saharinen, P., Takaluoma, K., and Silvennoinen, O. (2000). Regulation of the Jak2 tyrosine kinase by its pseudokinase domain. Mol. Cell. Biol. *20*, 3387–3395.

Santini, S.M., Di Pucchio, T., Lapenta, C., Parlato, S., Logozzi, M., and Belardelli, F. (2002). The natural alliance between type I interferon and dendritic cells and its role in linking innate and adaptive immunity. J. Interferon Cytokine Res. *22*, 1071–1080.

Sargiacomo, M., Sudol, M., Tang, Z., and Lisanti, M.P. (1993). Signal transducing molecules and glycosyl-phosphatidylinositol-linked proteins form a caveolin-rich insoluble complex in MDCK cells. J. Cell Biol. *122*, 789–807.

Sargiacomo, M., Scherer, P.E., Tang, Z., Kubler, E., Song, K.S., Sanders, M.C., and Lisanti, M.P. (1995). Oligomeric structure of caveolin: implications for caveolae membrane organization. Proc. Natl. Acad. Sci. *92*, 9407–9411.

Sawada, Y., Tamada, M., Dubin-Thaler, B.J., Cherniavskaya, O., Sakai, R., Tanaka, S., and Sheetz, M.P. (2006). Force Sensing by Extension of the Src Family Kinase Substrate, p130Cas. Cell *127*, 1015–1026.

Scherer, P.E., Okamoto, T., Chun, M., Nishimoto, I., Lodish, H.F., and Lisanti, M.P. (1996). Identification, sequence, and expression of caveolin-2 defines a caveolin gene family. Proc. Natl. Acad. Sci. U. S. A. *93*, 131–135.

Scherer, P.E., Lewis, R.Y., Volonte, D., Engelman, J.A., Galbiati, F., Couet, J., Kohtz, D.S., van Donselaar, E., Peters, P., and Lisanti, M.P. (1997). Cell-type and tissue-specific expression of caveolin-2. Caveolins 1 and 2 co-localize and form a stable hetero-oligomeric complex in vivo. J. Biol. Chem. *272*, 29337–29346.

Schlegel, A., and Lisanti, M.P. (2000). A molecular dissection of caveolin-1 membrane attachment and oligomerization. Two separate regions of the caveolin-1

C-terminal domain mediate membrane binding and oligomer/oligomer interactions in vivo. J. Biol. Chem. *275*, 21605–21617.

Schlegel, A., Schwab, R.B., Scherer, P.E., and Lisanti, M.P. (1999). A role for the caveolin scaffolding domain in mediating the membrane attachment of caveolin-1. The caveolin scaffolding domain is both necessary and sufficient for membrane binding in vitro. J. Biol. Chem. *274*, 22660–22667.

Schlegel, A., Arvan, P., and Lisanti, M.P. (2001). Caveolin-1 binding to endoplasmic reticulum membranes and entry into the regulated secretory pathway are regulated by serine phosphorylation. Protein sorting at the level of the endoplasmic reticulum. J. Biol. Chem. *276*, 4398–4408.

Schrauwen, I., Szelinger, S., Siniard, A.L., Kurdoglu, A., Corneveaux, J.J., Malenica, I., Richholt, R., Van Camp, G., De Both, M., Swaminathan, S., et al. (2015). A Frame-Shift Mutation in CAV1 Is Associated with a Severe Neonatal Progeroid and Lipodystrophy Syndrome. PLoS One *10*, e0131797.

Schreiber, G. (2017). The molecular basis for differential type I interferon signaling. J. Biol. Chem. *292*, 7285–7294.

Schreiber, G., and Piehler, J. (2015). The molecular basis for functional plasticity in type I interferon signaling. Trends Immunol. *36*, 139–149.

Senju, Y., and Suetsugu, S. (2015). Possible regulation of caveolar endocytosis and flattening by phosphorylation of F-BAR domain protein PACSIN2/Syndapin II. Bioarchitecture *5*, 70–77.

Senju, Y., Itoh, Y., Takano, K., Hamada, S., and Suetsugu, S. (2011). Essential role of PACSIN2/syndapin-II in caveolae membrane sculpting. J. Cell Sci. *124*, 2032–2040.

Senju, Y., Rosenbaum, E., Shah, C., Hamada-Nakahara, S., Itoh, Y., Yamamoto, K., Hanawa-Suetsugu, K., Daumke, O., and Suetsugu, S. (2015). Phosphorylation of PACSIN2 by protein kinase C triggers the removal of caveolae from the plasma membrane. J. Cell Sci. *128*, 2766–2780.

Shajahan, A.N., Dobbin, Z.C., Hickman, F.E., Dakshanamurthy, S., and Clarke, R. (2012). Tyrosine-phosphorylated caveolin-1 (Tyr-14) increases sensitivity to paclitaxel by inhibiting BCL2 and BCLxL proteins via c-Jun N-terminal Kinase (JNK). J. Biol. Chem. *287*, 17682–17692.

Sharma, D.K., Choudhury, A., Singh, R.D., Wheatley, C.L., Marks, D.L., and Pagano, R.E. (2003). Glycosphingolipids internalized via caveolar-related endocytosis rapidly merge with the clathrin pathway in early endosomes and form microdomains for recycling. J. Biol. Chem. *278*, 7564–7572.

Shimoda, K., Kato, K., Aoki, K., Matsuda, T., Miyamoto, a, Shibamori, M.,

Yamashita, M., Numata, a, Takase, K., Kobayashi, S., et al. (2000). Tyk2 plays a

restricted role in IFN alpha signaling, although it is required for IL-12-mediated T cell function. Immunity *13*, 561–571.

Shvets, E., Bitsikas, V., Howard, G., Hansen, C.G., and Nichols, B.J. (2015). Dynamic caveolae exclude bulk membrane proteins and are required for sorting of excess glycosphingolipids. Nat. Commun. *6*, 6867.

Simoncic, P.D., Lee-Loy, A., Barber, D.L., Tremblay, M.L., and McGlade, C.J. (2002). The T cell protein tyrosine phosphatase is a negative regulator of janus family kinases 1 and 3. Curr. Biol. *12*, 446–453.

Simons, K., and Ikonen, E. (1997). Functional rafts in cell membranes. Nature *387*, 569–572.

Simons, K., and Sampaio, J.L. (2011). Membrane organization and lipid rafts. Cold Spring Harb. Perspect. Biol. *3*, a004697.

Sinha, B., Köster, D., Ruez, R., Gonnord, P., Bastiani, M., Abankwa, D., Stan, R. V., Butler-Browne, G., Vedie, B., Johannes, L., et al. (2011). Cells respond to mechanical stress by rapid disassembly of caveolae. Cell *144*, 402–413.

Song, K.S., Tang, Z., Li, S., and Lisanti, M.P. (1997). Mutational analysis of the properties of caveolin-1. A novel role for the C-terminal domain in mediating homo-typic caveolin-caveolin interactions. J. Biol. Chem. *272*, 4398–4403.

Sonnino, S., and Prinetti, A. (2009). Sphingolipids and membrane environments for caveolin. FEBS Lett. *583*, 597–606.

Sowa, G., Pypaert, M., Fulton, D., and Sessa, W.C. (2003). The phosphorylation of caveolin-2 on serines 23 and 36 modulates caveolin-1-dependent caveolae formation. Proc. Natl. Acad. Sci. U. S. A. *100*, 6511–6516.

Starr, R., Willson, T.A., Viney, E.M., Murray, L.J., Rayner, J.R., Jenkins, B.J., Gonda, T.J., Alexander, W.S., Metcalf, D., Nicola, N.A., et al. (1997). A family of cytokine-inducible inhibitors of signalling. Nature *387*, 917–921.

Stoeber, M., Stoeck, I.K., Hänni, C., Bleck, C.K.E., Balistreri, G., and Helenius, A. (2012). Oligomers of the ATPase EHD2 confine caveolae to the plasma membrane through association with actin. EMBO J. *31*, 2350–2364.

Stoeber, M., Schellenberger, P., Siebert, C.A., Leyrat, C., Helenius, A., and Grünewald, K. (2016). Model for the architecture of caveolae based on a flexible, net-like assembly of Cavin1 and Caveolin discs. Proc. Natl. Acad. Sci. U. S. A. 201616838.

Stoppani, E., Rossi, S., Meacci, E., Penna, F., Costelli, P., Bellucci, A., Faggi, F., Maiolo, D., Monti, E., and Fanzani, A. (2011). Point mutated caveolin-3 form (P104L) impairs myoblast differentiation via Akt and p38 signalling reduction, leading to an immature cell signature. Biochim. Biophys. Acta *1812*, 468–479.

Taira, J., Sugishima, M., Kida, Y., Oda, E., Noguchi, M., and Higashimoto, Y. (2011). Caveolin-1 is a competitive inhibitor of heme oxygenase-1 (HO-1) with heme: identification of a minimum sequence in caveolin-1 for binding to HO-1. Biochemistry *50*, 6824–6831.

Tachikawa, M., Morone, N., Senju, Y., Sugiura, T., Hanawa-Suetsugu, K., Mochizuki, A., and Suetsugu, S. (2017). Measurement of caveolin-1 densities in the cell membrane for quantification of caveolar deformation after exposure to hypotonic membrane tension. Sci. Rep. *7*, 7794.

Taki, S. (2002). Type I interferons and autoimmunity: lessons from the clinic and from IRF-2-deficient mice. Cytokine Growth Factor Rev. *13*, 379–391.

Tang, Z., Scherer, P.E., Okamoto, T., Song, K., Chu, C., Kohtz, D.S., Nishimoto, I., Lodish, H.F., and Lisanti, M.P. (1996). Molecular cloning of caveolin-3, a novel member of the caveolin gene family expressed predominantly in muscle. J. Biol. Chem. *271*, 2255–2261.

Taniguchi, K., Wu, L., Grivennikov, S.I., Jong, P.R. De, Yu, F., Wang, K., Ho, S.B., Boland, B.S., John, T., Sandborn, W.J., et al. (2015). A gp130-Src-YAP Module Links Inflammation to Epithelial Regeneration. *519*, 57–62.

Thiele, C., Hannah, M.J., Fahrenholz, F., and Huttner, W.B. (2000). Cholesterol binds to synaptophysin and is required for biogenesis of synaptic vesicles. Nat. Cell Biol. *2*, 42–49.

Thomsen, P., Roepstorff, K., Stahlhut, M., and van Deurs, B. (2002). Caveolae are highly immobile plasma membrane microdomains, which are not involved in constitutive endocytic trafficking. Mol. Biol. Cell *13*, 238–250.

Toms, A. V, Deshpande, A., McNally, R., Jeong, Y., Rogers, J.M., Kim, C.U., Gruner, S.M., Ficarro, S.B., Marto, J.A., Sattler, M., et al. (2013). Structure of a pseudokinase-domain switch that controls oncogenic activation of Jak kinases. Nat. Struct. Mol. Biol. *20*, 1221–1223.

Torgersen, M.L., Skretting, G., van Deurs, B., and Sandvig, K. (2001). Internalization of cholera toxin by different endocytic mechanisms. J. Cell Sci. *114*, 3737–3747.

Torrino, S., Wei-Wei, S., Blouin, C.M., Grassart, A., Köster, D., Fuhrmann, L., Vacher, S., Valades-Cruz, C.A., Chambon, V., Johannes, L., et al. (2018). EHD2 is a mechanotransducer connecting caveolae dynamics with gene transcription. In press.

Totta, P., Gionfra, F., Busonero, C., and Acconcia, F. (2016). Modulation of 17β-Estradiol Signaling on Cellular Proliferation by Caveolin-2. J. Cell. Physiol. *231*, 1219–1225.

Tran, D., Carpentier, J.L., Sawano, F., Gorden, P., and Orci, L. (1987). Ligands internalized through coated or noncoated invaginations follow a common intracellular pathway. Proc. Natl. Acad. Sci. U. S. A. *84*, 7957–7961.

Trane, A.E., Pavlov, D., Sharma, A., Saqib, U., Lau, K., Van Petegem, F., Minshall, R.D., Roman, L.J., and Bernatchez, P.N. (2014). Deciphering the binding of Caveolin-1 to client protein endothelial nitric-oxide synthase (eNOS): Scaffolding subdomain identification, interaction modeling, and biological significance. J. Biol. Chem. *289*, 13273–13283.

Trimmer, C., Sotgia, F., Whitaker-Menezes, D., Balliet, R.M., Eaton, G., Martinez-Outschoorn, U.E., Pavlides, S., Howell, A., Iozzo, R. V, Pestell, R.G., et al. (2011). Caveolin-1 and mitochondrial SOD2 (MnSOD) function as tumor suppressors in the stromal microenvironment: a new genetically tractable model for human cancer associated fibroblasts. Cancer Biol. Ther. *11*, 383–394.

Di Trolio, R., Simeone, E., Di Lorenzo, G., Buonerba, C., and Ascierto, P.A. (2015). The use of interferon in melanoma patients: a systematic review. Cytokine Growth Factor Rev. *26*, 203–212.

Tsuyada, A., Chow, A., Wu, J., Somlo, G., Chu, P., Loera, S., Luu, T., Li, A.X., Wu, X., Ye, W., et al. (2012). CCL2 mediates cross-talk between cancer cells and stromal fibroblasts that regulates breast cancer stem cells. Cancer Res. *72*, 2768–2779.

Ungureanu, D., Wu, J., Pekkala, T., Niranjan, Y., Young, C., Jensen, O.N., Xu, C.-F., Neubert, T.A., Skoda, R.C., Hubbard, S.R., et al. (2011). The pseudokinase domain of JAK2 is a dual-specificity protein kinase that negatively regulates cytokine signaling. Nat. Struct. Mol. Biol. *18*, 971–976.

Uze, G., Lutfalla, G., and Gresser, I. (1990). Genetic transfer of a functional human interferon alpha receptor into mouse cells: cloning and expression of its cDNA. Cell *60*, 225–234.

Vasile, E., Simionescu, M., and Simionescu, N. (1983). Visualization of the binding, endocytosis, and transcytosis of low-density lipoprotein in the arterial endothelium in situ. J. Cell Biol. *96*, 1677–1689.

Velazquez, L., Mogensen, K.E., Barbieri, G., Fellous, M., Uze, G., and Pellegrini, S. (1995). Distinct domains of the protein tyrosine kinase tyk2 required for binding of interferon-alpha/beta and for signal transduction. J. Biol. Chem. *270*, 3327–3334.

Villarino, A. V, Kanno, Y., and Shea, J.J.O. (2017). Mechanisms and consequences of Jak – STAT signaling in the immune system. *18*.

Vinten, J., Voldstedlund, M., Clausen, H., Christiansen, K., Carlsen, J., and Tranum-Jensen, J. (2001). A 60-kDa protein abundant in adipocyte caveolae. Cell Tissue Res. *305*, 99–106.

Vinten, J., Johnsen, A.H., Roepstorff, P., Harpoth, J., and Tranum-Jensen, J. (2005). Identification of a major protein on the cytosolic face of caveolae. Biochim. Biophys. Acta *1717*, 34–40.

Vogel, V., and Sheetz, M.P. (2009). Cell fate regulation by coupling mechanical

cycles to biochemical signaling pathways. Curr. Opin. Cell Biol. *21*, 38–46.

Volonte, D., McTiernan, C.F., Drab, M., Kasper, M., and Galbiati, F. (2008). Caveolin-1 and caveolin-3 form heterooligomeric complexes in atrial cardiac myocytes that are required for doxorubicin-induced apoptosis. Am. J. Physiol. Heart Circ. Physiol. *294*, H392-401.

Wallweber, H.J.A., Tam, C., Franke, Y., Starovasnik, M.A., and Lupardus, P.J. (2014). Structural basis of recognition of interferon-alpha receptor by tyrosine kinase 2. Nat. Struct. Mol. Biol. *21*, 443–448.

Walser, P.J., Ariotti, N., Howes, M., Ferguson, C., Webb, R., Schwudke, D., Leneva, N., Cho, K.-J., Cooper, L., Rae, J., et al. (2012). Constitutive formation of caveolae in a bacterium. Cell *150*, 752–763.

Wanaski, S.P., Ng, B.K., and Glaser, M. (2003). Caveolin scaffolding region and the membrane binding region of SRC form lateral membrane domains. Biochemistry *42*, 42–56.

Way, M., and Parton, R.G. (1995). M-caveolin, a muscle-specific caveolin-related protein. FEBS Lett. *376*, 108–112.

Weaver, V.M., Petersen, O.W., Wang, F., Larabell, C.A., Briand, P., Damsky, C., and Bissell, M.J. (1997). Reversion of the malignant phenotype of human breast cells in three-dimensional culture and in vivo by integrin blocking antibodies. J. Cell Biol. *137*, 231–245.

de Weerd, N.A., Samarajiwa, S.A., and Hertzog, P.J. (2007). Type I interferon receptors: biochemistry and biological functions. J. Biol. Chem. *282*, 20053–20057.

Wei, S.C., Fattet, L., Tsai, J.H., Guo, Y., Pai, V.H., Majeski, H.E., Chen, A.C., Sah, R.L., Taylor, S.S., Engler, A.J., et al. (2015a). Matrix stiffness drives epithelial-mesenchymal transition and tumour metastasis through a TWIST1-G3BP2 mechanotransduction pathway. Nat. Cell Biol. *17*, 678–688.

Wei, Z., Zou, X., Wang, H., Lei, J., Wu, Y., and Liao, K. (2015b). The N-terminal leucine-zipper motif in PTRF/cavin-1 is essential and sufficient for its caveolae-association. Biochem. Biophys. Res. Commun. *456*, 750–756.

Weichselbaum, R.R., Ishwaran, H., Yoon, T., Nuyten, D.S.A., Baker, S.W., Khodarev, N., Su, A.W., Shaikh, A.Y., Roach, P., Kreike, B., et al. (2008). An interferon-related gene signature for DNA damage resistance is a predictive marker for chemotherapy and radiation for breast cancer. Proc. Natl. Acad. Sci. U. S. A. *105*, 18490–18495.

Weiss, N., Couchoux, H., Legrand, C., Berthier, C., Allard, B., and Jacquemond, V. (2008). Expression of the muscular dystrophy-associated caveolin-3(P104L) mutant in adult mouse skeletal muscle specifically alters the Ca(2+) channel function of the dihydropyridine receptor. Pflugers Arch. *457*, 361–375.

Wilks, A.F. (1989). Two putative protein-tyrosine kinases identified by application of the polymerase chain reaction. Proc. Natl. Acad. Sci. U. S. A. *86*, 1603–1607.

Wilks, A.F. (2008). The JAK kinases: Not just another kinase drug discovery target. Semin. Cell Dev. Biol. *19*, 319–328.

Wilks, A.F., Harpur, A.G., Kurban, R.R., Ralph, S.J., Zurcher, G., and Ziemiecki, A. (1991). Two novel protein-tyrosine kinases, each with a second phosphotransferase-related catalytic domain, define a new class of protein kinase. Mol. Cell. Biol. *11*, 2057–2065.

Williams, T.M., and Lisanti, M.P. (2005). Caveolin-1 in oncogenic transformation, cancer, and metastasis. Am. J. Physiol. Cell Physiol. *288*, C494-506.

Williams, J.J.L., Alotaiq, N., Mullen, W., Burchmore, R., Liu, L., Baillie, G.S., Schaper, F., Pilch, P.F., and Palmer, T.M. (2018). Interaction of suppressor of cytokine signalling 3 with cavin-1 links SOCS3 function and cavin-1 stability. Nat. Commun. *9*, 168.

Williams, T.M., Hassan, G.S., Li, J., Cohen, A.W., Medina, F., Frank, P.G., Pestell, R.G., Di Vizio, D., Loda, M., and Lisanti, M.P. (2005). Caveolin-1 promotes tumor progression in an autochthonous mouse model of prostate cancer: genetic ablation of Cav-1 delays advanced prostate tumor development in tramp mice. J. Biol. Chem. *280*, 25134–25145.

Willis, A.L., Sabeh, F., Li, X.Y., and Weiss, S.J. (2013). Extracellular matrix determinants and the regulation of cancer cell invasion stratagems. J. Microsc. *251*, 250–260.

Wilmes, S., Beutel, O., Li, Z., Francois-Newton, V., Richter, C.P., Janning, D., Kroll, C., Hanhart, P., Hotte, K., You, C., et al. (2015). Receptor dimerization dynamics as a regulatory valve for plasticity of type I interferon signaling. J. Cell Biol. *209*, 579–593.

Winer, J.P., Oake, S., and Janmey, P.A. (2009). Non-linear elasticity of extracellular matrices enables contractile cells to communicate local position and orientation. PLoS One *4*.

Witkiewicz, A.K., Dasgupta, A., Sotgia, F., Mercier, I., Pestell, R.G., Sabel, M., Kleer, C.G., Brody, J.R., and Lisanti, M.P. (2009). An absence of stromal caveolin-1 expression predicts early tumor recurrence and poor clinical outcome in human breast cancers. Am. J. Pathol. *174*, 2023–2034.

Woodman, S.E., Ashton, A.W., Schubert, W., Lee, H., Williams, T.M., Medina, F.A., Wyckoff, J.B., Combs, T.P., and Lisanti, M.P. (2003). Caveolin-1 knockout mice show an impaired angiogenic response to exogenous stimuli. Am. J. Pathol. *162*, 2059–2068.

Wu, J., Lewis, A., and Grandi, J. (2017). Touch, Tension, and Transduction – the Function and Regulation of Piezo Ion Channels. *2*, 147–185.

Yamada, E. (1955). The fine structure of the gall bladder epithelium of the mouse. J. Biophys. Biochem. Cytol. *1*, 445–458.

Yamamoto, M., Toya, Y., Schwencke, C., Lisanti, M.P., Myers, M.G.J., and Ishikawa, Y. (1998). Caveolin is an activator of insulin receptor signaling. J. Biol. Chem. *273*, 26962–26968.

Yamaoka, K., Saharinen, P., Pesu, M., Holt, V.E.T. 3rd, Silvennoinen, O., and O'Shea, J.J. (2004). The Janus kinases (Jaks). Genome Biol. *5*, 253.

Yang, J., Liao, D., Chen, C., Liu, Y., Chuang, T.-H., Xiang, R., Markowitz, D., Reisfeld, R.A., and Luo, Y. (2013). Tumor-associated macrophages regulate murine breast cancer stem cells through a novel paracrine EGFR/Stat3/Sox-2 signaling pathway. Stem Cells *31*, 248–258.

Yang, L., and Scarlata, S. (2017). Super-resolution visualization of caveola deformation in response to osmotic stress. J. Biol. Chem. *292*, 3779–3788.

Yasukawa, H., Misawa, H., Sakamoto, H., Masuhara, M., Sasaki, A., Wakioka, T., Ohtsuka, S., Imaizumi, T., Matsuda, T., Ihle, J.N., et al. (1999). The JAK-binding protein JAB inhibits Janus tyrosine kinase activity through binding in the activation loop. EMBO J. *18*, 1309–1320.

Yetter, A., Uddin, S., Krolewski, J.J., Jiao, H., Yi, T., and Platanias, L.C. (1995). Association of the interferon-dependent tyrosine kinase Tyk-2 with the hematopoietic cell phosphatase. J. Biol. Chem. *270*, 18179–18182.

Yeow, I., Howard, G., Chadwick, J., Mendoza-Topaz, C., Hansen, C.G., Nichols, B.J., and Shvets, E. (2017). EHD Proteins Cooperate to Generate Caveolar Clusters and to Maintain Caveolae during Repeated Mechanical Stress. Curr. Biol. *27*, 2951–2962.e5.

Yin, H., Wang, M.D., Svoboda, K., Landick, R., Block, S.M., and Gelles, J. (1995). Transcription Against an Applied Force. *270*, 1653–1657.

Yu, J., Bergaya, S., Murata, T., Alp, I.F., Bauer, M.P., Lin, M.I., Drab, M., Kurzchalia, T. V, Stan, R. V, and Sessa, W.C. (2006). Direct evidence for the role of caveolin-1 and caveolae in mechanotransduction and remodeling of blood vessels. J. Clin. Invest. *116*, 1284–1291.

Zheng, H., Qian, J., Varghese, B., Baker, D.P., and Fuchs, S. (2011). Ligand-stimulated downregulation of the alpha interferon receptor: role of protein kinase D2. Mol. Cell. Biol. *31*, 710–720.

Zhong, Z., Wen, Z., and Darnell, J.E.J. (1994). Stat3 and Stat4: members of the family of signal transducers and activators of transcription. Proc. Natl. Acad. Sci. U. S. A. *91*, 4806–4810.

- ANNEX 1-

Materials and methods of the discussion

Cell culture

All cells were grown at 37°C under 5% of CO2. HS578T, MDA-MB-231 cells were grown in DMEM GlutaMAX (Gibco, Life Technologies) supplemented with 10% FCS (Gibco, Life Technologies), 5 mM pyruvate (Gibco, Life Technologies) and 1% penicillin-streptomycin (Gibco, Life Technologies). MCF10A cells were grown in DMEM GlutaMAX (Gibco, Life Technologies) supplemented with 5% (v/v) horse serum; 20 ng/mL EGF; 100 ng/mL CTx; 0.01mg/mL human insulin; 500 ng/mL hydrochortisone. WT MLEC cells were cultured in Enothelial Balal Medium (EBM2) from Lonza supplemented with 15% Hyclone FCS, 4mM glutamine, 5mM sodium pyruvate, 0,01 % penicillin streptomycin (v/v), 0.04% hydrocortisone (v/v), 0.4% hEGF-B (v/v), 0.1% VEGF (v/v), 0.1% R3-IGF-1 (v/v), 0.1% ascorbic acid (v/v), 0.1% hEGF (v/v), 0.1% GA-1000 (v/v), 0.1% heparin (v/v) (EGM2 singlequote, Lonza).

Antibodies and reagents.

Mouse anti-αTubulin (Sigma-Aldrich, clone B512, T5168, 1/1000 for WB); mouse anti-chlatrin heavy chain (BD Transduction, 610500, 1/5000 for WB) rabbit anti-caveolin-1 (Cell Signaling 3238S, 1/1000 for WB); mouse anti-caveolin-1 (BD Transduction, 610407, 10µg/condition for IP); mouse anti-STAT3 (Cell signaling, clone 124H6, 9139, 1/1000 for WB); rabbit anti-pSTAT3 (Cell signaling, clone D3A7 9145, 1/1000 for WB); rabbit anti-STAT1 (Cell signaling, 9172, 1/1000 for WB); mouse anti-pSTAT1 (Cell Signaling, 9167, 1/1000 for WB); rabbit anti-JAK1 (Cell Signaling, 3332S, 1/1000 for WB); rabbit anti-phosphoTyrosine (Santa Cruz, sc-7020, 1/1000 for WB).

Immunoblotting.

Cells were lysed in sample buffer (62.5 mM Tris/HCl ph 6.0, 2% SDS (v/v), 10% glycerol (v/v), 40 mM dithiothreitol and 0.03% phenol red (w/v)). Lysates were analyzed by SDS-PAGE and Western blot analysis and immunoblotted with the indicated primary antibodies and horseradish peroxydase-conjugated secondary antibodies. Chemiluminescence signal was revealed using Pierce™ ECL Western Blotting Substrate, SuperSignal West Dura Extended Duration Substrate or SuperSignal West Femto Substrate (Thermo Scientific Life Technologies).

Acquisitions were performed with the ChemiDoc MP Imaging System (BioRad). Samples for the detection of phospho and non-phospho proteins were loaded on two different gels. The ratio of the signal detection for targeted protein/loading control was determined for each membrane. The overall ratio of (phosphoprotein/loading control)/(protein/loading control) was determined.

Compression

Multicellular spheroids are formed in 48-well plates using a classical agarose cushion protocol. When the MCS is formed, Dextran (molecular mass ¼ 100 kDa; Sigma-Aldrich, St. Louis, MO) is added to the culture medium to exert mechanical stress, as previously described in Montel et al., 2011 at a concentration of 55 g/L to exert 5 kPa, and 80 g/L to exert 10 kPa.

RNA silencing

Cav1 knock down in MCF10A cells was achieved using smart pool siRNA from Eurogentec: 5'-GCAAAUACGUAGACUCGGA55-3'; 5'-GCAGUUGUACCAUGCAUUA55-3'; 5'-CUAAACACCUCAACGAUGA55-3'. Cells were transfected using OzBiosciences SilenceMag Magnetofection™ according to manufcturer's protocol. Control siRNA (QIAGEN, 1022076) was used at the same concentration and served as reference point.

Co-immunoprecipitations.

Cells were lysed in 1% NP-40 in TNE (10 mM Tris/HCl pH 7.5, 150 mM NaCl, 0.5 mM EDTA) with protease inhibitors cocktail (Roche) for 30 min at 4°C. Cleared lysates (16,000g, 10 min, 4°C) were incubated overnight at 4°C under rotation with 1 µg/ml of the indicated antibody followed by incubation for 1 hour with 25 µl of protein A/G magnetic beads (Thermo Scientific) in the case of endogenous proteins. In the case of tagged proteins, 25 µl GFP-Trap or RFP-Trap beads (Chromotek) were used. After 3 washes in TNE, immunoprecipitated beads were eluted following the manufacturers' instructions.

Osmotic shock

For osmotic shock, cells were seeded 24h before experiment, then complete media was replaced by 30 mOsm media (10% media and 90% H_2O), cells were immediately lysed or hypo-osmmotic media was replaced by normal iso-osmotic media (recovery) before lysis.

- ANNEX 2 -

Available online at www.sciencedirect.com

ScienceDirect

Current Opinion in Cell Biology

The caveolae dress code: structure and signaling

Christophe Lamaze[1], Nicolas Tardif[1], Melissa Dewulf[1], Stéphane Vassilopoulos[2] and Cédric M Blouin[1]

Abstract

Over the past decade, interest in caveolae biology has peaked. These small bulb-shaped plasma membrane invaginations of 50–80 nm diameter present in most cell types have been upgraded from simple membrane structures to a more complex bona fide organelle. However, although caveolae are involved in several essential cellular functions and pathologies, the underlying molecular mechanisms remain poorly defined. Following the identification of caveolins and cavins as the main caveolae constituents, recent studies have brought new insight into their structural organization as a coat. In this review, we discuss how these new data on caveolae can be integrated in the context of their role in signaling and pathophysiology.

Addresses

[1] Institut Curie – Centre de Recherche, PSL Research University, CNRS UMR3666, INSERM U1143, Membrane Dynamics and Mechanics of Intracellular Signaling Laboratory, 75248 Paris cedex 05, France

[2] Inserm/UPMC UMR_S974, Institut de Myologie, Paris, France

Corresponding authors: Lamaze, Christophe (christophe.lamaze@curie.fr), Blouin, Cédric M (cedric.blouin@curie.fr)

Current Opinion in Cell Biology 2017, **47**:117–125

This review comes from a themed issue on **Cell organelles**

Edited by **Bruno Antonny** and **Catherine Rabouille**

http://dx.doi.org/10.1016/j.ceb.2017.02.014

The caveola robe

Caveolins

It took almost 40 years after caveolae were first visualized by electron microscopy (EM) in the 1950s to identify the caveolar protein components [1,2]. Caveolin-1 (Cav1) was identified in 1992 [3,4] followed by the two others homologues caveolin-2 (Cav2) [5] and the muscle specific caveolin-3 (Cav3) [6,7]. The three caveolin isoforms contain a family signature constituted by a single stretch of eight amino acids ^{68}FEDVIAEP^{75} localized in the N-terminal cytosolic oligomerization domain (Figure 1a) [7].

Cavins

Although Cav1 and Cav3 were initially thought to be necessary and sufficient for caveolae morphogenesis [8], several studies in the past decade have uncovered additional constituents. Thus, the identification of the cavin protein family brought precious insights into caveolae ultrastructure and assembly opening new avenues for better understanding the cellular functions of this intriguing organelle. The assembly of a *bona fide* caveola requires both Cav1 and cavin-1 (also called PTRF) [9,10]. In mammals, cavin-2 (SDPR), cavin-3 (SRBC) and the muscle-restricted cavin-4 (MURC) complete this four-member family, which has emerged as essential to caveolae formation and functions (Figure 1b) [11–13].

Purified cavins when added on phosphatidylserine (PS) enriched liposomes or when overexpressed in mammalian cells induce membrane tubulation, leading to the assumption that cavins may play a role in the initiation of the caveola invagination [11,14,15••]. Accordingly, cavin-1 depletion results in loss of caveolae while caveolae are not morphologically detectable in the prostate cancer PC3 cell line and in the nematode *Caenorhabditis elegans*, which both express Cav1 but not cavin-1 [9,16]. Nevertheless, it was reported that caveolae could be assembled in *Escherichia coli* independently from cavin-1 [17].

Accessory proteins

Several non-essential proteins have also been involved in caveolae biogenesis. PACSIN-2, also called Syndapin2, is the only F-BAR protein representative, proteins regulating membrane curvature, that has been involved in caveolae morphology [18,19]. The dynamin-2 GTPase and the dynamin-like ATPase EHD2 have been localized at the neck of caveolae [20,21]. EHD2 has been shown to stabilize caveolae by controlling their dynamics and association with the actin cytoskeleton [22]. Dynamin-2 however is not present in all caveolae and whether it plays a role in caveolae scission similarly to its classical role in clathrin-dependent endocytosis remains to be established.

A tailored coat

Caveolins bind lipids and organize membrane nanodomains

The assembly process is initiated by the export of caveolin-enriched vesicles from the Golgi apparatus to the plasma membrane [23]. Little is known about this first step except for a critical role of lipids and particularly cholesterol, which is essential for both caveolin oligomerization at the Golgi apparatus and caveola invagination at the plasma membrane [3]. Cav1 binds cholesterol with a

Figure 1

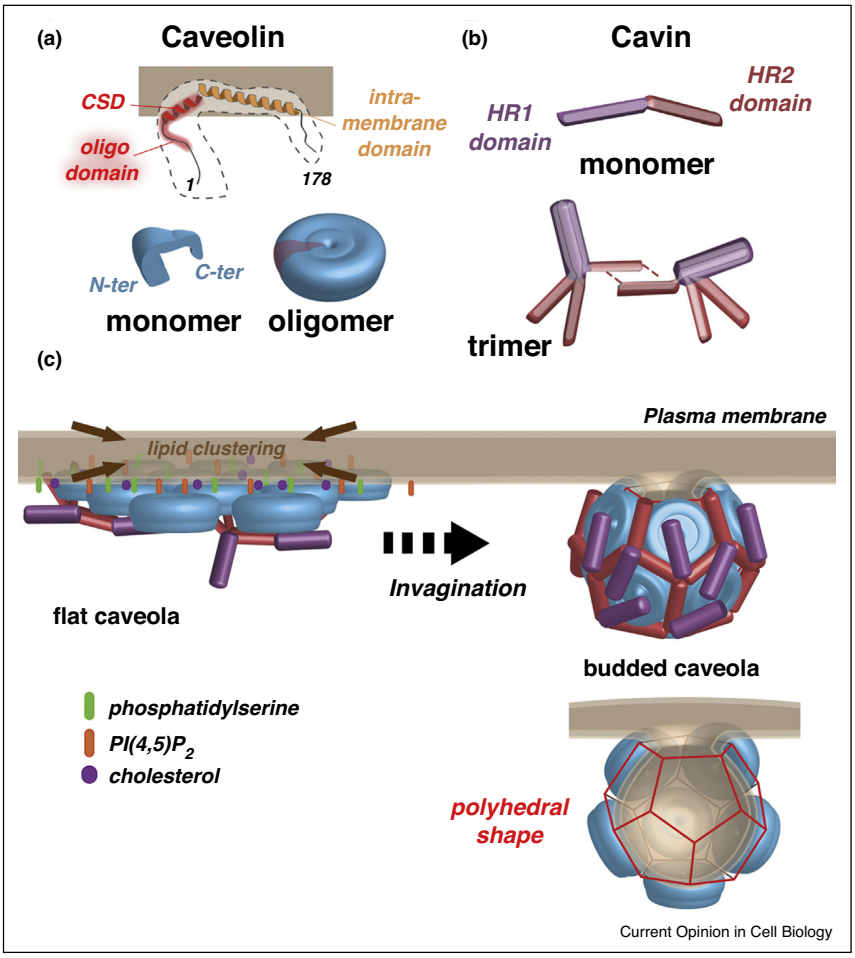

Putative model of caveolar coat assembly and organization.
(a) Schematic model of Cav1 topology. Cav1 is inserted into the plasma membrane through the caveolin scaffolding domain (CSD; red), an amphipathic helix part of the oligomerization domain (diffuse red), and through a second amphipathic helix, the intra-membrane domain (orange). Based on Cav3 ternary structure [108], Cav1 monomers may assemble as a disk-shaped oligomer with the C-terminal part oriented toward the center. **(b)** Cavin monomers exhibit two helical rich domains, HR1 and HR2, that may form coil-coiled structures [14]. Cavins, through interaction with the HR1 domain, can form trimers consisting of either three cavin-1 or two cavin-1 associated with one cavin-2 or one cavin-3 protein. The cavin-1 isoform could be responsible for a more complex assembly through the coiled-coil domain 2 (cc2) sequence in the HR2 domain [15]. **(c)** At the plasma membrane, Cav1 oligomers cluster specific lipids such as cholesterol, $PI(4,5)P_2$ and phosphatidyl serine involved in the recruitment of cavin trimers. This is followed by caveola invagination, a process not completely understood. It has been recently suggested that the overall architecture of the caveolar coat made of caveolins and cavins would best fit with a polyhedron structure [15,30]. In this model, Cav1 oligomers position on each pentagonal face and cavin complexes align with the vertices and cover the Cav1 oligomers.

1:1 stoichiometry [24,25], probably through a cholesterol recognition/interaction amino acid consensus (CRAC) motif (^{94}VTKYWFYR^{101}) located in the vicinity of the plasma membrane [26]. Caveolin oligomers trigger the clustering of specific lipids thereby constructing specialized lipid nanodomains at the plasma membrane [27]. They include sphingolipids (sphingomyelin, GD3 and GM1 gangliosides), phospholipids such as PS and phosphoinositides such as phosphatidylinositol (4,5)-bisphosphate ($PI(4,5)P_2$).

Cavins are recruited to caveolin-induced lipid nanodomains

Interestingly, PS and $PI(4,5)P_2$ were recently involved in caveola formation through electrostatic interactions between the negatively charged headgroups and two specific domains of cavins (HR1 & HR2) [9,12,14,15••,28]. Thus, cytosolic cavins form higher-order heterotrimers consisting of either three cavin-1 or two cavin-1 with one cavin-2 or one cavin-3, through their HR1/cc1 coiled-coil domain, that further polymerize

upon association with assembling caveolae (Figure 1c) [14,21,29].

Flat versus curved: the interplay between caveolins and cavins

At the plasma membrane cavins and caveolins invariably form characteristic stripes surrounded by a proteinaceous crescent made of globular proteins whose identity remains elusive (Figure 2). To date, it is still unclear whether caveolae assemble as flat structures that will then bud inward and produce the typical stable cup-shaped caveolae or if pre-formed caveolae emanating from intracellular compartments most likely the trans-Golgi network fuse with the plasma membrane.

Recent EM and X-Ray crystallography studies revealed that the characteristic striated coat that is observed on the outer cytoplasmic side of caveolae may be organized by cavins rather than caveolin oligomers alone as originally proposed [14,15••,21,29,30••]. These striations are observable on deep etch electron micrographs of caveolae presenting various degrees of invagination from flat to fully budded (Figure 2).

Figure 2

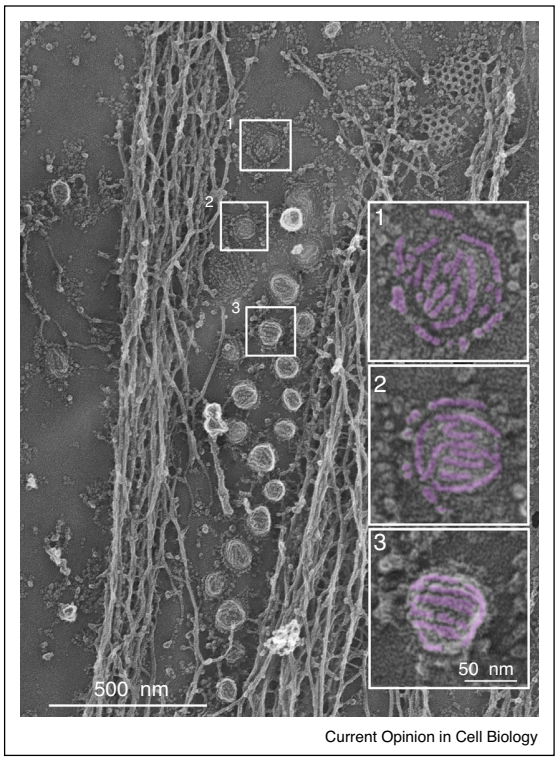

Visualization of the caveolar coat at the plasma membrane of myotubes.
Survey view of the cytoplasmic surface of an unroofed mouse myotube presenting caveolae at the plasma membrane. Different types of caveolae structures are apparent, ranging from flat (1), circular (2), to fully budded (3). Scale bar: 500 nm. Scale bar in insets: 50 nm.

It has been estimated that 150–200 Cav1 monomers associate with 50–60 cavins (≈15–20 trimers) to form a caveola [15••,21,29,31]. The overall architecture of caveolae was recently proposed to fit with a polyhedron most likely a dodecahedron structure formed by cavin complexes aligned with the vertices but also covering the caveolin oligomers positioned on each pentagonal face (Figure 1c) [15••,30••]. It is however difficult to visualize a dodecahedron organization when observing caveolae *en face* on deep-etch electron micrographs, and further efforts will be needed to validate this model with proteins which have been purified from more physiological systems than insect cells and bacteria.

Signaling regulation through direct interaction with Cav1

Over the years, caveolae have been associated with various physiological and pathological contexts in relation with their cellular functions in lipid homeostasis, signal transduction, endocytosis and transcytosis. If some debate still exists [32], early consensus suggested that caveolae could regulate cellular signaling by organizing specific signaling platforms at the plasma membrane [33].

Thus, a broad variety of growth factor and signaling receptors, kinases, enzymes and other signaling molecules have been localized into caveolae and/or co-immunoprecipitated with Cav1 including but not limited to eNOS [34], the insulin [35], EGF [36], TGF-β [37•] and P2X7 [38] receptors, Src tyrosine kinase [39], H-Ras and K-Ras [40], the heme oxygenase [41]. Caveolae have also been associated with *bona fide* mechanosignaling pathways including MAP kinase, Akt, Src kinases, Rho and Rac small GTPases [42].

The central role of the caveolin scaffolding domain

A first study identified a domain responsible for the direct regulation of heterotrimeric G proteins by Cav1 [43]. This interaction was further confirmed for H-Ras, the Src and Fyn tyrosine kinases, and the endothelial nitric oxide synthase eNOS [35,40,41].

This specific feature of Cav1 resides in a particular α-helical domain (residues 82–101) called the caveolin scaffolding domain (CSD) so named because it is also required for Cav1 oligomerization. The CSD is localized on the N-terminal part but its relative position to the plasma membrane remains unclear. The CSD would exert an inhibitory role on signaling effectors by binding directly to a putative corresponding caveolin binding motif (CBM) identified in several of these effectors [35,40,41,44,49]. Indeed, biochemical studies on eNOS revealed the critical role of the CSD phenylalanine residue 92, which, by extending its lateral chain, allows to

reach the hydrophobic pocket of eNOS to inhibit its catalytic activity [44,45]. A similar example was provided by the heme oxygenase 1 whose activity is inhibited through direct binding between its CBM domain and the CSD [41]. Furthermore, a small CSD-mimicking peptide inhibits eNOS activity whereas the corresponding mutated peptide increases eNOS activity most likely by competing with endogenous Cav1, which suggests a direct Cav1-CSD mediated inhibitory effect [46].

Controversy on CSD accessibility

However, new studies have recently undermined the model of signaling regulation through direct CBM/CSD interaction. The CBM motif was found to be poorly discriminative as it is also found in species such as *Saccharomyces cerevisiae* that do not express caveolins. No particular enrichment in proteins with the CBM sequence was found in the Cav1 interactome and the structural analysis of different CBM domains revealed that this domain was likely to be buried inside the proteins and therefore not readily available for interacting with the CSD [47,48]. Likewise, the CSD would also be an amphipathic helix and thus partially embedded inside the plasma membrane hence not accessible [49].

Alternative mechanisms could also be considered. Thus, a new study proposed that the CSD is a dynamic structure that can be either fully helical or partly unstructured, which may change its accessibility [50•]. Furthermore, the conformation of Cav1 could vary with the oligomerization state and the organization of the caveola components (cavin isoforms or lipids). In this context, mechanical stress by promoting the release of Cav1 from disassembled caveolae [51] could not only control the ratio of caveolar vs. free Cav1 but also the accessibility to its CSD.

Yet the mechanisms controlling the reversibility of these interactions, a key parameter in signaling, remain to be explored. In this context, the post-translational modifications of Cav1 may be particularly relevant. Phosphorylation on Cav1 Ser 80 would result in a more versatile topology exposing the CSD because of charge repulsion between the inner leaflet of the plasma membrane and the phosphorylated residue [52]. A similar mechanism was proposed for Cav1 Tyr 14 phosphorylation that would form a stable structure facilitating binding to the CSD [53]. Cav1 Tyr 14 phosphorylation was also shown to prevent the direct binding of Cav1 on Egr1 [54]. Whether Cav1/Egr1 interaction occurs through the CSD is however unknown.

Indirect regulation of signaling by caveolae

Through caveolae

In addition to the direct inhibitory effect of Cav1 on signaling effectors, caveolae can also indirectly modulate intracellular signaling. Caveolae interact with the actin cytoskeleton and contribute to lipid sorting and delivery to the plasma membrane through their enrichment in glycosphingolipids and cholesterol [55]. Caveolae can thus modulate the nanoscale plasma membrane organization, a key parameter in transmembrane receptor activation [56]. Once again this process could also be actively controlled by caveolae dynamics in response to mechanical strains [51,57]. In this regard, stretch-induced caveolae disassembly led to the redistribution of Cav1 and sphingolipids at the plasma membrane together with c-Src activation [58]. Furthermore, Cav1 depletion led to perturbations in Ras spatial nano-organization and signaling through changes in lipid composition and PS distribution [59•]. In agreement with the localization of calcium pumps in caveolae [60], the mechanical disassembly of caveolae led to reduced Ca^{2+} responses through changes in $G\alpha_q$/Cav1 association [58,61]. Finally, as for clathrin-mediated endocytosis, caveolae endocytosis, while limited under resting conditions, might also contribute to the endosomal control of signaling by delivering activated receptors to this compartment [62].

Through Cav2

The role of Cav2, which is not required for caveolae formation, remains enigmatic. Cav2 expression is required for activating the estrogen receptor α by 17β-oestradiol [63]. The insulin signaling pathway can be regulated by Cav2 fatty acylation and phosphorylation, two successive post-translational modifications that prevent the interaction of the SOCS3 phosphatase with the insulin receptor allowing the activation of IRS-1 (Insulin Receptor Substrate-1) and the nuclear translocation of activated STAT3 [64–66]. Cav2 was allegedly reported to mediate signaling from the plasma membrane to the nucleus, as phospho-ERK nuclear translocation induced by insulin relied on Cav2 ^{154}SSV^{156} C-terminal sequence [67].

Through cavins

Finally, the recently identified cavins may also contribute to caveolae signaling. Cavin-1 being essential to caveolae assembly, it controls the number of functional caveolae and thereby the localization of activated receptors in these structures [68,69]. Cavin-3 mediates ERK activation by anchoring caveolae to the plasma membrane via myosin-1c [70] and regulates their dynamics [71•]. Likewise CAVIN-1/-2/-3 KO mice display a certain degree of heterogeneity among endothelial caveolae depending on tissues and cavin-2 expression [72].

Caveolinopathies

Because of the multiple functions of caveolae and their impact on signaling, it is not unexpected that several pathologies have been associated with caveolae dysfunction. With the notable exception of neurons and lymphocytes, caveolae are ubiquitously found in most cells and are particularly enriched in adipocytes, endothelial and

muscle cells. Accordingly, mutations or deregulation of caveolae components expression have been associated with lipodystrophy, vascular dysfunction, musculopathies [73] or cancer [74]. It is certainly no coincidence that, all chronically experience mechanical forces in their environment [1,51,75,76]. Whether these diseases can be related to defects in caveolae mechanosensing and mechanotransduction remains however to be tested.

Lipodystrophy

In mice, Cav1 or cavin-1 deficiency leads to a similar lipodystrophic phenotype consisting in important loss of fat mass associated with hypertriglyceridemia [10,77]. A p.Glu38X stop codon CAV1 homozygous mutation resulting in caveolae loss was first identified in a patient suffering from Berardinelli-Seip congenital lipodystrophy [78] followed by the identification in lipodystophic patients of a homozygous frame shift mutation (c.696_697insC) in the PTRF gene coding for cavin-1 [79]. Other human mutations are found in Cav1 and cavin-1, including heterozygous frame shift mutations in the CAV1 gene (88delC and p.I134fsdelA-X137 in Ref. [80], p.Phe160X in Ref. [81•]) and a single deletion in PTRF gene (c.947delA in Ref. [82]), leading again to a similar phenotype. These studies and others emphasize the central role of caveolae in lipid metabolism. Lipodystrophy could be ascribed to the loss of caveolae-dependent lipid storage capacities by adipocytes as mice lacking Cav1 or cavin-1 remain lean under high fat diet [77,80,83]. Cav1 is found at the plasma membrane of adipocytes and at the surface of lipid droplets, the key lipid storage organelle [84]. Thus, the absence of Cav1 will affect both lipid uptake and associated caveolae-dependent signaling events together with lipid droplet composition [85,86]. Lipid uptake results also in rapid swelling of adipocytes, a mechanical stress that may require functional caveolae for efficient membrane mechanoprotection.

Vascular dysfunction

In addition to lipodystrophy, mice lacking Cav1 and cavin-1 experience vascular dysfunction [87–89]. Defects in stimulated contractility, myogenic tone and endothelium-dependent relaxation of arteries have been observed in CAV1 KO mice [87] that could be related to the control of NO and calcium signaling by Cav1 [90,91]. The phenotype of CAV2 KO mice, which still have caveolae, is surprisingly restricted to lung dysfunction through increased lung endothelial cell proliferation [92]. Again shear stress is intrinsically associated with endothelial cells in vessels and caveolae are likely to be involved in several shear-related functions [93].

Muscular dystrophies and cardiomyopathies

Mutations of muscle-specific Cav3, cavin-1 and cavin-4 have been associated with several forms of muscular dystrophies and cardiomyopathies [79,94]. The observed symptoms could be ascribed to several defects in muscle physiology. A lack of functional caveolae could lead to defective formation of the excitation contraction coupling machinery and disorganization of the T-tubule network [94,95]. It could also result in lipid homeostasis and mechanosensitivity defects upon muscle contraction, which in turn would directly affect the response of the sarcolemmal membrane to mechanical strains. Moreover, non-mutually exclusive caveolae-dependent defects have also been reported for signaling pathways important for muscle physiology such as those mediated by calcium, Akt or MAP kinases [96–98], or in the expression or localization of key proteins involved in membrane integrity or repair such as dysferlin [99], and also in mechanoprotection [51,100•].

Cancer

Several thousand studies have addressed the role of Cav1 in this broad-spectrum pathology that is cancer. Yet this role remains complex with studies describing Cav1 as a tumor suppressor and others as an oncogene. The nature of this role may vary with the type and stage of cancer [74] and is probably related to a deregulation of signaling pathways involved in tumor progression. The other components of caveolae have been less studied. In breast and prostate cancers [101,102], Cav2 expression was increased whereas cavins, with lower expression, were more likely to be tumor suppressors [68,103,104]. The role of caveolae in cancer should be reconsidered through their mechanosensing function as recent data have shed light on the key role of mechanical forces in tumor progression [105].

Other pathologies including pulmonary arterial hypertension [106], fibrosis [87] or atherosclerosis [107] have also been associated with caveolae deficiency or deregulated Cav1 expression. These pathologies can also be analyzed in the context of mechanical dysfunction [32].

Conclusion and unresolved questions

Obviously more than 60 years after the first description of caveolae, many fundamental questions remain unanswered. It is intellectually challenging to reconcile the diversity of their cellular functions with a unique organelle that is mostly stable at the plasma membrane. The absence or deregulation of this ubiquitous organelle results likewise in a rather specific set of pathologies. A major unresolved question concerns the mechanisms by which caveolae can control so many signaling circuits. The recent structural description of the caveolar coat has been a major step forward that will allow to better understand how signaling effectors can associate with the different components of this compact structure. The resolution of the ternary structure of Cav1, as recently achieved for Cav3 [108], will bring new answers as well.

One could also speculate that the different Cav1 and cavin isoforms may assemble subpopulations of caveolae differing in their composition/structure thereby allowing customized signaling and local reactivity to mechanosensing in different cells and tissues. At the ultrastructural level, various degrees of caveolar invaginations can be observed (Figure 2). Whether these structures co-exist independently or are in dynamic exchange is unknown. It will be important to analyze the distribution of caveolin and cavin isoforms in these structures. Live cell imaging of caveolae with higher spatiotemporal resolution approaches such as super-resolution microscopy should also provide a better understanding of their significance [109••].

The rapid exchange of cavins and Cav1 from caveolae in response to mechanical constrains is potentially a new mechanism by which caveolae could control signaling in a highly dynamic and integrated manner [51,55,57,100,110•,111,112]. In this context, it is interesting that in most caveolae-associated pathologies, cells and tissues are subjected to increasing mechanical stress that may induce aberrant cellular mechanosignaling [105,113]. Thus, the miscellaneous functions of caveolae could be reunified through a central mechanoprotective role relying on mechanosensing and mechanosignaling. Thanks to the new conceptual and technological advances applied to caveolae biology during the past decade, we start to understand how this multifunctional organelle is capable of integrating and translating an array of various external stimuli into the regulation of distinct cellular functions. The next challenge is to translate this knowledge *in vivo* in order to design tailored therapeutics for treating caveolae-associated diseases.

Acknowledgements

The authors want to acknowledge the institutional support from the Institut Curie, INSERM, CNRS, and from Fondation de France, Agence Nationale de la Recherche (DECAV-RECAV ANR-14-CE09-0008-03), Marie Curie Actions - Networks for Initial Training (H2020-MSCA-ITN-2014) to C.L., and Young Researcher grant (ANR-14-CE12-0001-01) to S.V. C.M.B. was supported by a postdoctoral fellowship from Ligue Nationale contre le Cancer. N.T. and M.D. were respectively supported by PhD fellowships from French Ministry for Research and Association Française contre les Myopathies (AFM). The Lamaze team received support under the program "Investissements d'Avenir" launched by the French Government and implemented by ANR with the references Labex Cel- TisPhyBio ANR-10-LBX-0038 part of the IDEX Idex PSL ANR-10-IDEX-0001- 02 PSL. We would like to thank Robyn Roth and the Washington University Center for Cellular Imaging (St. Louis, MO) for their assistance with freeze-etching and electron microscopy acquisition. We are also grateful to Michael Barnes for carefully reading the manuscript.

References and recommended reading

Papers of particular interest, published within the period of review, have been highlighted as:

- • of special interest
- •• of outstanding interest

1. Palade GE: **The fine structure of blood capillaries**. *J. Appl. Phys.* 1953, **24**:1424.

2. Yamada E: **The fine structure of the gall bladder epithelium of the mouse**. *J. Biophys. Biochem. Cytol.* 1955, **1**:445-458.

3. Rothberg KG, Heuser JE, Donzell WC, Ying YS, Glenney JR, Anderson RG: **Caveolin, a protein component of caveolae membrane coats**. *Cell* 1992, **68**:673-682.

4. Kurzchalia TV, Dupree P, Parton RG, Kellner R, Virta H, Lehnert M, Simons K: **VIP21, a 21-kD membrane protein is an integral component of trans-Golgi-network-derived transport vesicles**. *J. Cell Biol.* 1992, **118**:1003-1014.

5. Scherer PE, Okamoto T, Chun M, Nishimoto I, Lodish HF, Lisanti MP: **Identification, sequence, and expression of caveolin-2 defines a caveolin gene family**. *Proc. Natl. Acad. Sci. U. S. A.* 1996, **93**:131-135.

6. Way M, Parton RG: **M-caveolin, a muscle-specific caveolin-related protein**. *FEBS Lett.* 1995, **376**:108-112.

7. Tang Z, Scherer PE, Okamoto T, Song K, Chu C, Kohtz DS, Nishimoto I, Lodish HF, Lisanti MP: **Molecular cloning of caveolin-3, a novel member of the caveolin gene family expressed predominantly in muscle**. *J. Biol. Chem.* 1996, **271**:2255-2261.

8. Fra AM, Williamson E, Simons K, Parton RG: **De novo formation of caveolae in lymphocytes by expression of VIP21-caveolin**. *Proc. Natl. Acad. Sci. U. S. A.* 1995, **92**:8655-8659.

9. Hill MM, Bastiani M, Luetterforst R, Kirkham M, Kirkham A, Nixon SJ, Walser P, Abankwa D, Oorschot VMJ, Martin S *et al.*: **PTRF-Cavin, a conserved cytoplasmic protein required for caveola formation and function**. *Cell* 2008, **132**:113-124.

10. Liu L, Brown D, McKee M, Lebrasseur NK, Yang D, Albrecht KH, Ravid K, Pilch PF: **Deletion of Cavin/PTRF causes global loss of caveolae, dyslipidemia, and glucose intolerance**. *Cell Metab.* 2008, **8**:310-317.

11. Hansen C, Bright N, Howard G, Nichols BJ: **SDPR induces membrane curvature and functions in the formation of caveolae**. *Nat. Cell Biol.* 2009, **11**:807-814.

12. McMahon K-A, Zajicek H, Li W-P, Peyton MJ, Minna JD, Hernandez VJ, Luby-Phelps K, Anderson RGW: **SRBC/cavin-3 is a caveolin adapter protein that regulates caveolae function**. *EMBO J.* 2009, **28**:1001-1015.

13. Bastiani M, Liu L, Hill MM, Jedrychowski MP, Nixon SJ, Lo HP, Abankwa D, Luetterforst R, Fernandez-Rojo M, Breen MR *et al.*: **MURC/Cavin-4 and cavin family members form tissue-specific caveolar complexes**. *J. Cell Biol.* 2009, **185**:1259-1273.

14. Kovtun O, Tillu VA, Jung W, Leneva N, Ariotti N, Chaudhary N, Mandyam RA, Ferguson C, Morgan GP, Johnston WA *et al.*: **Structural Insights into the organization of the cavin membrane coat complex**. *Dev. Cell* 2014, **31**:405-419.

15. •• Stoeber M, Schellenberger P, Siebert CA, Leyrat C, Helenius A, Grünewald K: **Model for the architecture of caveolae based on a flexible, net-like assembly of Cavin1 and Caveolin discs**. *Proc. Natl. Acad. Sci. U. S. A.* 2016, **113**:E8069-E8078 http://dx.doi.org/10.1073/pnas.1616838113.
With Ref. [30], first description of the structural basis of the caveolar coat organization with 15 nm-wide circular Cav1 oligomers on each face of a dodecahedron.

16. Tang Z, Okamoto T, Boontrakulpoontawee P, Katada T, Otsuka AJ, Lisanti MP: **Identification, sequence, and expression of an invertebrate caveolin gene family from the nematode Caenorhabditis elegans. Implications for the molecular evolution of mammalian caveolin genes**. *J. Biol. Chem.* 1997, **272**:2437-2445.

17. Walser PJJ, Ariotti N, Howes M, Ferguson C, Webb R, Schwudke D, Leneva N, Cho K-J, Cooper L, Rae J *et al.*: **Constitutive formation of caveolae in a bacterium**. *Cell* 2012, **150**:752-763.

18. Senju Y, Itoh Y, Takano K, Hamada S, Suetsugu S: **Essential role of PACSIN2/syndapin-II in caveolae membrane sculpting**. *J. Cell Sci.* 2011, **124**:2032-2040.

19. Hansen CG, Howard G, Nichols BJ: **Pacsin 2 is recruited to caveolae and functions in caveolar biogenesis**. *J. Cell Sci.* 2011, **124**:2777-2785.

20. Oh P, McIntosh DP, Schnitzer JE: **Dynamin at the neck of caveolae mediates their budding to form transport vesicles by GTP-driven fission from the plasma membrane of endothelium**. *J. Cell Biol.* 1998, **141**:101-114.

21. Ludwig A, Howard G, Mendoza-Topaz C, Deerinck T, Mackey M, Sandin S, Ellisman MH, Nichols BJ: **Molecular composition and ultrastructure of the caveolar coat complex**. *PLoS Biol.* 2013, **11**:e1001640.

22. Stoeber M, Stoeck IK, Hänni C, Bleck CKE, Balistreri G, Helenius A: **Oligomers of the ATPase EHD2 confine caveolae to the plasma membrane through association with actin**. *EMBO J.* 2012, **31**:2350-2364.

23. Hayer A, Stoeber M, Bissig C, Helenius A: **Biogenesis of caveolae: stepwise assembly of large caveolin and cavin complexes**. *Traffic* 2010, **11**:361-382.

24. Murata M, Peränen J, Schreiner R, Wieland F, Kurzchalia TV, Simons K: **VIP21/caveolin is a cholesterol-binding protein**. *Proc. Natl. Acad. Sci. U. S. A.* 1995, **92**:10339-10343.

25. Thiele C, Hannah MJ, Fahrenholz F, Huttner WB: **Cholesterol binds to synaptophysin and is required for biogenesis of synaptic vesicles**. *Nat. Cell Biol.* 2000, **2**:42-49.

26. Epand RM, Sayer BG, Epand RF: **Caveolin scaffolding region and cholesterol-rich domains in membranes**. *J. Mol. Biol.* 2005, **345**:339-350.

27. Sonnino S, Prinetti A: **Sphingolipids and membrane environments for caveolin**. *FEBS Lett.* 2009, **583**:597-606.

28. Burgener R, Wolf M, Ganz T, Baggiolini M: **Purification and characterization of a major phosphatidylserine-binding phosphoprotein from human platelets**. *Biochem. J.* 1990, **269**:729-734.

29. Gambin Y, Ariotti N, McMahon K-AK, Bastiani M, Sierecki E, Kovtun O, Polinkovsky ME, Magenau A, Jung W, Okano S *et al.*: **Single-molecule analysis reveals self assembly and nanoscale segregation of two distinct cavin subcomplexes on caveolae**. *Elife* 2014, **3**:e01434.

30. •• Ludwig A, Nichols BJ, Sandin S: **Architecture of the caveolar coat complex**. *J. Cell Sci.* 2016, **129**:3077-3083.
3D cryo-electron microscopy study that first describes, with [15], the organization of the polyhedral Cav1 oligomers coated with cavin filaments.

31. Pelkmans L, Zerial M: **Kinase-regulated quantal assemblies and kiss-and-run recycling of caveolae**. *Nature* 2005, **436**:128-133.

32. Cheng JPX, Nichols BJ: **Caveolae: one function or many?** *Trends Cell. Biol.* 2016, **26**:177-189.

33. Simons K, Toomre D: **Lipid rafts and signal transduction**. *Nat. Rev. Mol. Cell Biol.* 2000, **1**:31-39.

34. García-Cardeña G, Martasek P, Masters BS, Skidd PM, Couet J, Li S, Lisanti MP, Sessa WC: **Dissecting the interaction between nitric oxide synthase (NOS) and caveolin:Functional significance of the nos caveolin binding domain in vivo**. *J. Biol. Chem.* 1997, **272**:25437-25440.

35. Nystrom FH, Chen H, Cong LN, Li Y, Quon MJ: **Caveolin-1 interacts with the insulin receptor and can differentially modulate insulin signaling in transfected Cos-7 cells and rat adipose cells**. *Mol. Endocrinol.* 1999, **13**:2013-2024.

36. Couet J, Sargiacomo M, Lisanti MP: **Interaction of a receptor tyrosine kinase, EGF-R, with caveolins:Caveolin binding negatively regulates tyrosine and serine/threonine kinase activities**. *J. Biol. Chem.* 1997, **272**:30429-30438.

37. • Strippoli R, Loureiro J, Moreno V, Benedicto I, Pérez ML, Barreiro O, Pellinen T, Minguet S, Foronda M, Teresa M *et al.*: **Caveolin-1 deficiency induces a MEK-ERK1/2- Snail-1-dependent epithelial-mesenchymal transition and fibrosis during peritoneal dialysis**. *EMBO Mol. Med.* 2015, **7**:102-123.
This study shows that epithelial-mesenchymal transition and fibrosis induced through chronic exposure to hypotonic shock during repeated peritoneal dialysis are more pronounced in CAV1$^{-/-}$ mice. These results provide another illustration of the mechanoprotective role of caveolae *in vivo.*

38. Gangadharan V, Nohe A, Caplan J, Czymmek K, Duncan RL: **Caveolin-1 regulates P2 × 7 receptor signaling in osteoblasts**. *Am. J. Physiol. Cell Physiol.* 2015, **308**:C41-50.

39. Li S, Couet J, Lisanti MP: **Src tyrosine kinases, Galpha subunits, and H-Ras share a common membrane-anchored scaffolding protein, caveolin**. *J. Biol. Chem.* 1996, **271**:29182-29190.

40. Song KS, Shengwen Li, Okamoto T, Quilliam LA, Sargiacomo M, Lisanti MP: **Co-purification and direct interaction of Ras with caveolin, an integral membrane protein of caveolae microdomains. Detergent-free purification of caveolae microdomains**. *J. Biol. Chem.* 1996, **271**:9690-9697.

41. Taira J, Sugishima M, Kida Y, Oda E, Noguchi M, Higashimoto Y: **Caveolin-1 is a competitive inhibitor of heme oxygenase-1 (HO-1) with heme: identification of a minimum sequence in caveolin-1 for binding to HO-1**. *Biochemistry* 2011, **50**:6824-6831.

42. Parton RG, Simons K: **The multiple faces of caveolae**. *Nat. Rev. Mol. Cell Biol.* 2007, **8**:185-194.

43. Li S, Okamoto T, Chun M, Sargiacomo M, Casanova JE, Hansen SH, Nishimoto I, Lisanti MP: **Evidence for a regulated interaction between heterotrimeric G proteins and caveolin**. *J. Biol. Chem.* 1995, **270**:15693-15701.

44. Bernatchez PN, Bauer PM, Yu J, Prendergast JS, He P, Sessa WC: **Dissecting the molecular control of endothelial NO synthase by caveolin-1 using cell-permeable peptides**. *Proc. Natl. Acad. Sci. U. S. A.* 2005, **102**:761-766.

45. Trane AE, Pavlov D, Sharma A, Saqib U, Lau K, Van Petegem F, Minshall RD, Roman LJ, Bernatchez PN: **Deciphering the binding of Caveolin-1 to client protein endothelial nitric-oxide synthase (eNOS): scaffolding subdomain identification, interaction modeling, and biological significance**. *J. Biol. Chem.* 2014, **289**:13273-13283.

46. Bernatchez P, Sharma A, Bauer PM, Marin E, Sessa WC: **A noninhbitory mutant of the caveolin1 scaffolding domain enhances eNOS-derived NO synthesis and vasodilation in mice**. *J. Clin. Invest.* 2011, **121**:3747-3755.

47. Collins BM, Davis MJ, Hancock JF, Parton RG: **Structure-based reassessment of the caveolin signaling model: do caveolae regulate signaling through caveolin-protein interactions?** *Dev. Cell* 2012, **23**:11-20.

48. Byrne DP, Dart C, Rigden DJ: **Evaluating caveolin interactions: do proteins interact with the caveolin scaffolding domain through a widespread aromatic residue-rich motif?** *PLoS One* 2012, **7**:e44879.

49. Kirkham M, Nixon SJ, Howes MT, Abi-Rached L, Wakeham DE, Hanzal-Bayer M, Ferguson C, Hill MM, Fernandez-Rojo M, Brown Da *et al.*: **Evolutionary analysis and molecular dissection of caveola biogenesis**. *J. Cell Sci.* 2008, **121**:2075-2086.

50. • Liu H, Yang L, Zhang Q, Mao L, Jiang H, Yang H: **Probing the structure and dynamics of caveolin-1 in a caveolae-mimicking asymmetric lipid bilayer model**. *Eur. Biophys. J.* 2016, **45**:511-521.
By performing molecular dynamic simulation, this study provides new clues on Cav1 plasma membrane embedding through 82- > 136 amino acids. It opens new possibilities for Cav1 CSD accessibility and interaction with signaling effectors.

51. Sinha B, Köster D, Ruez R, Gonnord P, Bastiani M, Abankwa D, Stan RV, Butler-Browne G, Vedie B, Johannes L *et al.*: **Cells respond to mechanical stress by rapid disassembly of caveolae**. *Cell* 2011, **144**:402-413.

52. Ariotti N, Rae J, Leneva N, Ferguson C, Loo D, Okano S, Hill MM, Walser P, Collins BM, Parton RG: **Molecular characterization of caveolin-induced membrane curvature**. *J. Biol. Chem.* 2015, **290**:24875-24890.

53. Shajahan AN, Dobbin ZC, Hickman FE, Dakshanamurthy S, Clarke R: **Tyrosine-phosphorylated caveolin-1 (Tyr-14) increases sensitivity to paclitaxel by inhibiting BCL2 and**

BCLxL proteins via c-Jun N-terminal kinase (JNK). *J. Biol. Chem.* 2012, **287**:17682-17692.

54. Joshi B, Bastiani M, Strugnell SS, Boscher C, Parton RG, Nabi IR: **Phosphocaveolin-1 is a mechanotransducer that induces caveola biogenesis via Egr1 transcriptional regulation**. *J. Cell Biol.* 2012, **199**:425-435.

55. Echarri A, Del Pozo MA: **Caveolae—mechanosensitive membrane invaginations linked to actin filaments**. *J. Cell Sci.* 2015, **128**:2747-2758.

56. Blouin CM, Hamon Y, Gonnord P, Boularan C, Kagan J, Viaris de Lesegno C, Ruez R, Mailfert S, Bertaux N, Loew D *et al.*: **Glycosylation-dependent IFN-γR partitioning in lipid and actin nanodomains is critical for JAK activation**. *Cell* 2016, **166**:920-934.

57. Nassoy P, Lamaze C: **Stressing caveolae new role in cell mechanics**. *Trends Cell. Biol.* 2012, **22**:381-389.

58. Gervasio OL, Phillips WD, Cole L, Allen DG: **Caveolae respond to cell stretch and contribute to stretch-induced signaling**. *J. Cell Sci.* 2011, **124**:3581-3590.

59. • Ariotti N, Fernández-Rojo MA, Zhou Y, Hill MM, Rodkey TL, Inder KL, Tanner LB, Wenk MR, Hancock JF, Parton RG: **Caveolae regulate the nanoscale organization of the plasma membrane to remotely control Ras signaling**. *J. Cell Biol.* 2014, **204**:777-792.
The core structural domain of Cav1 inserted in membrane and necessary for caveolae formation is defined from a bacterial expression system.

60. Fujimoto T: **Calcium pump of the plasma membrane is localized in caveolae**. *J. Cell Biol.* 1993, **120**:1147-1157.

61. Guo Y, Yang L, Haught K, Scarlata S: **Osmotic stress reduces Ca^{2+} signals through deformation of caveolae**. *J. Biol. Chem.* 2015, **290**:16698-16707.

62. Gonnord P, Blouin CM, Lamaze C: **Membrane trafficking and signaling: two sides of the same coin**. *Semin. Cell Dev. Biol.* 2012, **23**:154-164.

63. Totta P, Gionfra F, Busonero C, Acconcia F: **Modulation of 17β-estradiol signaling on cellular proliferation by caveolin-2**. *J. Cell Physiol.* 2016, **231**:1219-1225.

64. Kwon H, Jeong K, Hwang EM, Park J-YY, Hong S-GG, Choi W-SS, Pak Y: **Caveolin-2 regulation of STAT3 transcriptional activation in response to insulin**. *Biochim. Biophys. Acta* 2009, **1793**:1325-1333.

65. Kwon H, Pak Y: **Prolonged tyrosine kinase activation of insulin receptor by pY27-caveolin-2**. *Biochem. Biophys. Res. Commun.* 2010, **391**:49-55.

66. Kwon H, Lee J, Jeong K, Jang D, Pak Y: **Fatty acylated caveolin-2 is a substrate of insulin receptor tyrosine kinase for insulin receptor substrate-1-directed signaling activation**. *Biochim. Biophys. Acta Mol. Cell Res* 2015, **1853**:1022-1034.

67. Kwon H, Jeong K, Hwang EM, Park JY, Pak Y: **A novel domain of caveolin-2 that controls nuclear targeting: regulation of insulin-specific ERK activation and nuclear translocation by caveolin-2**. *J. Cell Mol. Med.* 2011, **15**:888-908.

68. Moon H, Lee CS, Inder KL, Sharma S, Choi E, Black DM, Lê Cao K, Winterford C, Coward JI, Ling MT *et al.*: **PTRF/cavin-1 neutralizes non-caveolar caveolin-1 microdomains in prostate cancer**. *Oncogene* 2013, **33**:3561-3570.

69. Li Q, Bai L, Liu N, Wang M, Liu JP, Liu P, Cong YS: **Increased polymerase I and transcript release factor (Cavin-1) expression attenuates platelet-derived growth factor receptor signalling in senescent human fibroblasts**. *Clin. Exp. Pharmacol. Physiol.* 2014, **41**:169-173.

70. Hernandez VJ, Weng J, Ly P, Pompey S, Dong H, Mishra L, Schwarz M, Anderson RGW, Michaely P: **Cavin-3 dictates the balance between ERK and Akt signaling**. *Elife* 2013, **2013**:1-26.

71. • Mohan J, Rn Moré NB, Larsson E, Holst MR, Lundmark R: **Cavin3 interacts with cavin1 and caveolin1 to increase surface dynamics of caveolae**. *J. Cell Sci.* 2015, **128**:979-991.
This paper shows cavin-specific functions as illustrated by cavin3 which regulates caveolae residency time at the plasma membrane.

72. Hansen CG, Shvets E, Howard G, Riento K, Nichols BJ: **Deletion of cavin genes reveals tissue-specific mechanisms for morphogenesis of endothelial caveolae**. *Nat. Commun.* 2013, **4**:1831.

73. Ariotti N, Parton RG: **SnapShot: Caveolae, Caveolins, and Cavins**. *Cell* 2013, **154** 704–704.e1.

74. Goetz JG, Lajoie P, Wiseman SM, Nabi IR: **Caveolin-1 in tumor progression: the good, the bad and the ugly**. *Cancer Metastasis Rev.* 2008, **27**:715-735.

75. Merrillees NC: **The fine structure of muscle spindles in the lumbrical muscles of the rat**. *J. Biophys. Biochem. Cytol.* 1960, **7**:725-742.

76. Scherer PE, Lisanti MP, Baldini G, Sargiacomo M, Mastick CC, Lodish HF: **Induction of caveolin during adipogenesis and association of GLUT4 with caveolin-rich vesicles**. *J. Cell Biol.* 1994, **127**:1233-1243.

77. Razani B, Combs TP, Wang XB, Frank PG, Park DS, Russell RG, Li M, Tang B, Jelicks LA, Scherer PE *et al.*: **Caveolin-1-deficient mice are lean, resistant to diet-induced obesity, and show hypertriglyceridemia with adipocyte abnormalities**. *J. Biol. Chem.* 2002, **277**:8635-8647.

78. Kim CA, Delépine M, Boutet E, El Mourabit H, Le Lay S, Meier M, Nemani M, Bridel E, Leite CC, Bertola DR *et al.*: **Association of a homozygous nonsense caveolin-1 mutation with berardinelli-seip congenital lipodystrophy**. *J. Clin. Endocrinol. Metab.* 2008, **93**:1129-1134.

79. Hayashi YK, Matsuda C, Ogawa M, Goto K, Tominaga K, Mitsuhashi S, Park Y-EYE, Nonaka I, Hino-Fukuyo N, Haginoya K *et al.*: **Human PTRF mutations cause secondary deficiency of caveolins resulting in muscular dystrophy with generalized lipodystrophy**. *J. Clin. Invest.* 2009, **119**:2623-2633.

80. Cao H, Alston L, Ruschman J, Hegele RA: **Heterozygous CAV1 frameshift mutations (MIM 601047) in patients with atypical partial lipodystrophy and hypertriglyceridemia**. *Lipids Heal. Dis* 2008, **7**:3.

81. • Schrauwen I, Szelinger S, Siniard AL, Kurdoglu A, Corneveaux JJ, Malenica I, Richholt R, Van Camp G, De Both M, Swaminathan S *et al.*: **A frame-shift mutation in CAV1 is associated with a severe neonatal progeroid and lipodystrophy syndrome**. *PLoS One* 2015, **10**:e0131797.
The second human heterozygous mutation described for CAV1 leading to partial loss of Cav1 and caveolae.

82. Ardissone A, Bragato C, Caffi L, Blasevich F, Maestrini S, Bianchi ML, Morandi L, Moroni I, Mora M: **Novel PTRF mutation in a child with mild myopathy and very mild congenital lipodystrophy**. *BMC Med. Genet.* 2013, **14**:89.

83. Ding S-Y, Lee M-J, Summer R, Liu L, Fried SK, Pilch PF: **Pleiotropic effects of cavin-1 deficiency on lipid metabolism**. *J. Biol. Chem.* 2014, **289**:8473-8483.

84. Blouin CM, Le Lay S, Lasnier F, Dugail I, Hajduch E: **Regulated association of caveolins to lipid droplets during differentiation of 3T3-L1 adipocytes**. *Biochem. Biophys. Res. Commun.* 2008, **376**:331-335.

85. Le Lay S, Hajduch E, Lindsay MR, Le Lièpvre X, Thiele C, Ferré P, Parton RG, Kurzchalia T, Simons K, Dugail I: **Cholesterol-induced caveolin targeting to lipid droplets in adipocytes: a role for caveolar endocytosis**. *Traffic* 2006, **7**:549-561.

86. Blouin CM, Le Lay S, Eberl AA, Köfeler HC, Guerrera IC, Klein C, Le Liepvre X, Lasnier F, Bourron O, Gautier JF *et al.*: **Lipid droplet analysis in caveolin-deficient adipocytes: alterations in surface phospholipid composition and maturation defects**. *J. Lipid Res.* 2010, **51**:945-956.

87. Drab M, Verkade P, Elger M, Kasper M, Lohn M, Lauterbach B, Menne J, Lindschau C, Mende F, Luft FC *et al.*: **Loss of caveolae, vascular dysfunction, and pulmonary defects in caveolin-1 gene-disrupted mice**. *Science* 2001, **293**:2449-2452.

88. Razani B, Engelman JA, Wang XB, Schubert W, Zhang XL, Marks CB, Macaluso F, Russell RG, Li M, Pestell RG *et al.*: **Caveolin-1 null mice are viable but show evidence of**

hyperproliferative and vascular abnormalities. *J. Biol. Chem.* 2001, **276**:38121-38138.

89. Karbalaei MS, Rippe C, Albinsson S, Ekman M, Mansten A, Uvelius B, Swärd K: **Impaired contractility and detrusor hypertrophy in cavin-1-deficient mice**. *Eur. J. Pharmacol.* 2012, **689**:179-185.

90. Bucci M, Gratton JP, Rudic RD, Acevedo L, Roviezzo F, Cirino G, Sessa WC: **In vivo delivery of the caveolin-1 scaffolding domain inhibits nitric oxide synthesis and reduces inflammation**. *Nat. Med.* 2000, **6**:1362-1367.

91. Isshiki M, Anderson RGW: **Function of caveolae in Ca^{2+} entry and Ca^{2+}-dependent signal transduction**. *Traffic* 2003, **4**:717-723.

92. Razani B, Wang XB, Engelman JA, Battista M, Lagaud G, Zhang XL, Kneitz B, Hou H, Christ GJ, Edelmann W *et al.*: **Caveolin-2-deficient mice show evidence of severe pulmonary dysfunction without disruption of caveolae**. *Mol. Cell Biol.* 2002, **22**:2329-2344.

93. Yu J, Bergaya S, Murata T, Alp IF, Bauer MP, Lin MI, Drab M, Kurzchalia TV, Stan RV, Sessa WC: **Direct evidence for the role of caveolin-1 and caveolae in mechanotransduction and remodeling of blood vessels**. *J. Clin. Invest.* 2006, **116**:1284-1291.

94. Gazzerro E, Sotgia F, Bruno C, Lisanti MP, Minetti C: **Caveolinopathies: from the biology of caveolin-3 to human diseases**. *Eur. J. Hum. Genet.* 2010, **18**:137-145.

95. Galbiati F, Engelman JA, Volonte D, Zhang XL, Minetti C, Li M, Hou H, Kneitz B, Edelmann W, Lisanti MP: **Caveolin-3 null mice show a loss of caveolae, changes in the microdomain distribution of the dystrophin-glycoprotein complex, and T-tubule abnormalities**. *J. Biol. Chem.* 2001, **276**:21425-21433.

96. Weiss N, Couchoux H, Legrand C, Berthier C, Allard B, Jacquemond V: **Expression of the muscular dystrophy-associated caveolin-3 P104L mutant in adult mouse skeletal muscle specifically alters the Ca^{2+} channel function of the dihydropyridine receptor**. *Eur. J. Physiol.* 2008, **457**:361-375.

97. Stoppani E, Rossi S, Meacci E, Penna F, Costelli P, Bellucci A, Faggi F, Maiolo D, Monti E, Fanzani A: **Point mutated caveolin-3 form (P104L) impairs myoblast differentiation via Akt and p38 signalling reduction, leading to an immature cell signature**. *Biochim. Biophys. Acta* 2010, **1812**:468-479.

98. Capanni C, Sabatelli P, Mattioli E, Ognibene A, Columbaro M, Lattanzi G, Merlini L, Minetti C, Maraldi NM, Squarzoni S: **Dysferlin in a hyperCKaemic patient with caveolin 3 mutation and in C2C12 cells after p38 MAP kinase inhibition**. *Exp. Mol. Med.* 2003, **35**:538-544.

99. Hernandez-Deviez DJ: **Aberrant dysferlin trafficking in cells lacking caveolin or expressing dystrophy mutants of caveolin-3**. *Hum. Mol. Genet.* 2005, **15**:129-142.

100. • Lo HP, Nixon SJ, Hall TE, Cowling BS, Ferguson C, Morgan GP, Schieber NL, Fernandez-Rojo MA, Bastiani M, Floetenmeyer M *et al.*: **The caveolin-Cavin system plays a conserved and critical role in mechanoprotection of skeletal muscle**. *J. Cell Biol.* 2015, **210**:833-849.
This paper shows that expression of a dominant active disease-associated Cav3 mutant in zebrafish embryo leads to compromised muscle plasma membrane integrity after intense muscular activity.

101. Savage K, Leung S, Todd SK, Brown LA, Jones RL, Robertson D, James M, Parry S, Rodrigues Pinilla SM, Huntsman D *et al.*: **Distribution and significance of caveolin 2 expression in normal breast and invasive breast cancer: an immunofluorescence and immunohistochemical analysis**. *Breast Cancer Res. Treat.* 2008, **110**:245-256.

102. Sugie S, Mukai S, Yamasaki K, Kamibeppu T, Tsukino H, Kamoto T: **Significant Association of Caveolin-1 and Caveolin-2 with Prostate Cancer Progression**. *Cancer Genom. Proteomics* 2015, **12**:391-396.

103. Bai L, Deng X, Li Q, Wang M, An WAD, Gao Z, Xie Y, Dai Y, Cong Y-S: **Down-regulation of the cavin family proteins in breast cancer**. *J. Cell Biochem.* 2012, **113**:322-328.

104. Nassar ZD, Hill MM, Parton RG, Parat M-O: **Caveola-forming proteins caveolin-1 and PTRF in prostate cancer**. *Nat. Rev. Urol.* 2013, **10**:529-536.

105. Lamaze C, Torrino S: **Caveolae and cancer: a new mechanical perspective**. *Biomed. J.* 2015, **38**:367.

106. Austin ED, Ma L, LeDuc C, Berman Rosenzweig E, Borczuk A, Phillips JA, Palomero T, Sumazin P, Kim HR, Talati MH *et al.*: **Whole exome sequencing to identify a novel gene (caveolin-1) associated with human pulmonary arterial hypertension**. *Circ. Cardiovasc. Genet.* 2012, **5**:336-343.

107. Frank PG: **Genetic ablation of caveolin-1 confers protection against atherosclerosis**. *Arterioscler. Thromb. Vasc. Biol.* 2004, **24**:98-105.

108. Whiteley G, Collins RF, Kitmitto A: **Characterization of the molecular architecture of human caveolin-3 and interaction with the skeletal muscle ryanodine receptor**. *J. Biol. Chem.* 2012, **287**:40302-40316.

109. •• Li D, Shao L, Chen B-C, Zhang X, Zhang M, Moses B, Milkie DE, Beach JR, Hammer JA, Pasham M *et al.*: **Extended-resolution structured illumination imaging of endocytic and cytoskeletal dynamics**. *Science* 2015, **349** aab3500.
First super-resolution imaging of Cav1 in living cells by nonlinear structured illumination microscopy revealing Cav1 ring-like structures in addition to classical individual caveolae at the plasma membrane.

110. • Cheng JPX, Mendoza-Topaz C, Howard G, Chadwick J, Shvets E, Cowburn AS, Dunmore BJ, Crosby A, Morrell NW, Nichols BJ: **Caveolae protect endothelial cells from membrane rupture during increased cardiac output**. *J. Cell Biol.* 2015, **211**:53-61.
This study suggests that mechanoprotection may occur*in vivo* through caveolae flattening as mice lacking CAV1 exhibit increased plasma membrane damages in cardiac and lung endothelial cells.

111. Goedicke-Fritz S, Kaistha A, Kacik M, Markert S, Hofmeister A, Busch C, Bänfer S, Jacob R, Grgic I, Hoyer J: **Evidence for functional and dynamic microcompartmentation of Cav-1/TRPV4/KCa in caveolae of endothelial cells**. *Eur. J. Cell Biol.* 2015, **94**:391-400.

112. Guo Y, Yang L, Haught K, Scarlata S: **Osmotic stress reduces Ca^{2+} signals through deformation of caveolae**. *J. Biol. Chem.* 2015, **290**:16698-16707.

113. Kai F, Laklai H, Weaver VM: **Force matters: biomechanical regulation of cell invasion and migration in disease**. *Trends Cell. Biol.* 2016, **26**:486-497.

- ANNEX 3 -

Dystrophy-associated caveolin-3 mutations reveal that caveolae couple IL6/STAT3 signaling with mechanosensing in human muscle cells

Melissa Dewulf[1], Darius Köster[2], Bidisha Sinha[3], Christine Viaris de Lesegno[1], Valérie Chambon[4], Anne Bigot[5], Nicolas Tardif[1], Ludger Johannes[4], Pierre Nassoy[6], Gillian Butler-Browne[5], Christophe Lamaze[1]* and Cedric M. Blouin[1]*

[1] Institut Curie – Centre de recherche, PSL Research University, Membrane dynamics and mechanics of intracellular signaling laboratory, CNRS UMR3666, INSERM U1143, Paris, France.
[2] Centre for mechanochemical cell biology, University of Warwick, Coventry, United Kingdom.
[3] Department of Biological Sciences, Indian Institute of Science Education and Research (IISER) Kolkata, Mohanpur, West Bengal, India.
[4] Institut Curie – centre de recherche, PSL Research University, Endocytic trafficking and intracellular delivery laboratory, CNRS UMR3666, INSERM U1143, Paris, France.
[5] Institut de Myologie, Sorbonne Universités, UPMC Université Paris 06, Thérapie des muscles striés laboratory, INSERM UMRS974, CNRS FRE3617, Paris, France.
[6] LP2N, CNRS UMR 5298, IOA, Institut d'Optique Graduate School, Université de Bordeaux, Talence, France.

* Co-last and corresponding authors: christophe.lamaze@curie.fr, cedric.blouin@curie.fr

Abstract

Caveolin-3 is the major structural protein of caveolae in muscle cells. Mutations in the *CAV3* gene cause different types of myopathies that are characterized by several defects altering membrane integrity and repair, expression of muscle proteins, and regulation of muscle signaling pathways. We show here that myotubes derived from patients bearing the *CAV3* P28L and R26Q mutations present a dramatic decrease of caveolae at the plasma membrane, which results in an abnormal response to mechanical stress. Mutant myotubes were unable to buffer the increase in membrane tension induced by mechanical stress. This resulted in impaired regulation of the IL6/STAT3 signaling pathway leading to IL6/STAT3 constitutive hyperactivation and increased expression of muscle related genes. These defects were fully reversed by reassembling a pool of functional caveolae through expression of wild type caveolin-3. Our study reveals that under mechanical stress

the regulation of mechanoprotection by caveolae is directly coupled with the regulation of IL6/STAT3 signaling in muscle cells and that this regulation is absent in muscle cells from Cav3-associated dystrophic patients.

Introduction

Caveolae are cup-shaped plasma membrane invaginations that were first observed in the 50's by Palade and Yamada on electron micrographs from vascular and gall bladder tissues[1,2]. Caveolae present a specific protein signature involving two main families of proteins, caveolins (caveolin-1, -2 and -3), and cavins (cavin-1, -2, -3 and -4)[3,4,5,6,7,8,9]. Caveolins and cavins are expressed in almost every cell type, except for caveolin-3 (Cav3) and cavin-4, whose expression is restricted to smooth and striated muscle cells[9,10]. Cav3, like Cav1 in non muscle cells, is necessary for the formation of caveolae at the plasma membrane of muscle cells[11].

Caveolae have long been associated with several important cellular functions including endocytosis, lipid metabolism and cell signaling, albeit with several persistent controversies[12,13]. More recently, a new function of caveolae was established as mechanosensors that play an essential role in cell mechanoprotection both *in vitro* and *in vivo*[14,15,16,17,18]. Mutations or abnormal expression of caveolae components have been associated with lipodystrophy, vascular dysfunction, cancer and muscle disorders[13,19]. The molecular mechanisms underlying caveolin-associated diseases are still poorly understood.

In this study, we explored the mechanical role of caveolae in human muscle cells and their possible deregulation in caveolinopathies, a family of muscle genetic disorders involving mutations in the *CAV3* gene. These diseases affect both cardiac and skeletal muscle tissues, and share common characteristics including mild muscle weakness, high levels of serum creatine kinase, variations in muscle fiber size and an increased number of central nuclei[20,21,22,23]. We focused our investigations on the human *CAV3* P28L mutation responsible for hyperCKemia[24], and *CAV3* R26Q, which is responsible for ripple muscle disease, hyperCKemia and limb-girdle disease 1C[25]. Studies with transgenic mice and zebrafish or cells overexpressing the Cav3 mutants have linked the P28L and R26Q *CAV3* mutations to deregulations in distinct signaling pathways[25,26], defects in membrane repair[27,28] and mechanoprotection of the muscle tissue[16]. Nevertheless, the role of the

caveolae mechanoresponse in human myotubes and its possible deregulation in dystrophy-associated Cav3 mutations have not yet been addressed.

We show here that the Cav3 P28L and Cav3 R26Q myotubes are unable to assemble sufficient amounts of functional caveolae at the plasma membrane, leading to a loss of membrane tension buffering and membrane integrity under mechanical stress. The absence of functional caveolae in mutant myotubes uncouples the regulation of IL6/STAT3 signaling with mechanical stress, which results in the constitutive hyperactivation of the IL6/STAT3 signaling pathway and the upregulation of several muscle related genes. Finally, the expression of WT Cav3 in mutant myotubes was sufficient to restore a functional pool of caveolae and to rescue the coupling of caveolae mechanosensing with IL6/STAT3 signaling. These results establish caveolae as central connecting devices that adapt intracellular signaling to mechanical cues in muscle cells. The loss of this function in Cav3-associated mutations may be responsible for some of the clinical symptoms described in human dystrophic patients.

Results

Drastic decrease in the number of caveolae at the plasma membrane of Cav3 mutant myotubes.

To address the impact of Cav3 mutations in human muscle disorders, we analyzed wild type (WT), Cav3 P28L and Cav3 R26Q myotubes derived from immortalized myoblasts, which were isolated from healthy or Cav3 mutant patients and differentiated for four days. The state of myotube differentiation was validated by the expression level of the differentiation marker MF-20 (myosin heavy chain) in all three cell lines (Supplementary Fig. 1a). We first analyzed the presence and the ultrastructure of caveolae at the plasma membrane of myotubes by electron microscopy. In WT myotubes, we observed numerous invaginated structures corresponding to *bona fide* caveolae i.e. characteristic 60-100 nm cup-shaped invaginations that were connected to the plasma membrane, or to larger vacuoles of variable size deeper inside the cell known as rosettes, and that could still be connected to the plasma membrane. In contrast, a lot less caveolae could be detected at the plasma membrane of mutant myotubes and very few, if any, large vacuolar structures were observed (Fig. 1a and 1b). While we could still visualize a

few caveolae in mutant myotubes, they were often grouped in the same area and large areas of plasma membrane were completely devoid of caveolae (not shown). Interestingly, we could observe, mainly in mutant myotubes, the presence of aberrant oversized caveolae (Fig. 1a).

This drastic decrease in caveolae number led us to investigate the localization of Cav3, which is required for caveolae assembly at the plasma membrane[11]. Immunoblot analysis showed a reduced expression of mutant Cav3 (P28L: - 50%; R26Q: - 51%) as compared to WT (Fig. 1c and 1d), with a shifted band for the R26Q mutant corresponding to the Cav3 mutant form, as reported previously[25]. Cav3 immunostaining revealed that WT Cav3 was mainly associated with the plasma membrane of myotubes and partially localized in the Golgi complex, defined by GM130 staining (Fig. 1e). In contrast, Cav3 strongly accumulated in the Golgi complex as shown by the colocalization with GM130 in the Cav3 P28L and R26Q myotubes, in agreement with earlier studies[25,26]. This indicates that the strong reduction in the number of caveolae present at the plasma membrane of the Cav3 mutant myotubes is a consequence of the abnormal retention of mutant Cav3 in the Golgi complex.

It was still possible that differentiated myotubes express Cav1, which could potentially participate to the formation of caveolae independently from Cav3. We therefore analyzed Cav1 expression in myotubes after four days of differentiation and found that Cav1 was indeed expressed to the same level in all three cell lines (Supplementary Fig. 1b). Cav1 colocalized perfectly with Cav3 at the plasma membrane and to a lesser extent at the Golgi complex in WT myotubes, whereas it was mainly present in the Golgi complex in Cav3 P28L and R26Q myotubes (Supplementary Fig. 1c). It indicates that Cav1 is likely to form hetero-oligomers with Cav3, and that the Cav3 P28L and R26Q mutants have a dominant effect on Cav1 localization.

Cav3 P28L and R26Q myotubes present major defects in membrane tension buffering and mechanoprotection.

To know whether the almost total absence of caveolae at the plasma membrane of mutant myotubes could induce defects in cell mechanoprotection, we first determined if the Cav3 P28L and R26Q myotubes could buffer the increase of membrane tension induced by mechanical stress. We thus applied a 45 mOsm

hypo-osmotic shock to myotubes aligned by micropatterning and we measured the apparent membrane tension before and after 5 min of hypo-osmotic shock using membrane nanotube pulling with optical tweezers as described[14]. As expected, hypo-osmotic shock led to myotube swelling in WT and Cav3 mutant cells. While the mutant myotubes showed no significant changes in membrane tension in resting condition (Fig. 2a), they showed a significant increase of membrane tension (P28L: 63% ± 7%; R26Q: 94% ± 11%) under 45 mOsm hypo-osmotic shock compared to WT myotubes (38% ± 9%) (Fig. 2b). These results clearly show that the Cav3 P28L and R26Q mutant myotubes have lost the ability to buffer membrane tension variations induced by mechanical stress.

We next tested whether the lack of membrane tension buffering could result in insufficient mechanoprotection and increased membrane fragility in mechanically challenged mutant myotubes. We designed an assay to quantify the percentage of cells that rupture their membrane under mechanical stress. To monitor membrane bursting, micropatterned myotubes were incubated with calcein-AM, a permeant green fluorescent dye that only becomes fluorescent inside the cell, and with the nucleus specific blue dye DAPI to specifically visualize differentiated myotubes by nuclei staining (Supplementary Fig. 2b). Live imaging was performed on myotubes subjected to a 30 mOsm hypo-osmotic shock for 10 min in the presence of propidium iodide (PI), a non-permeant red fluorescent dye that cannot enter cells with intact plasma membrane. The concomitant decrease of calcein-AM fluorescence and the appearance of PI fluorescence in the nucleus indicate a loss of membrane integrity (Fig. 2c). In comparison to WT myotubes, Cav3 mutant myotubes not only showed a higher percentage of burst cells after a 10 min hypo-osmotic shock (WT: 53% ± 3%; P28L: 78% ± 2%; R26Q: 89% ± 2%) but also a shorter time of resistance to membrane bursting (WT: 4.5 min ± 0.2, P28L: 2.1 min ± 0.1, R26Q: 2.7 min ± 0.2) (Fig. 2d). When we apply a milder hypo-osmotic shock (150 mOsm), for which no increase in membrane tension could be measured, the plasma membrane of all three cell lines remained intact after 10 min of shock (Supplementary Fig. 2b and 2c). We repeated these experiments in WT myotubes depleted for Cav3 and measured a percentage of burst cells that was similar to mutant myotubes (siCtl: 23% ± 1%, siCav3: 89% ± 1%) (Fig. 2e and 2f; Supplementary Fig. 2d). Likewise, Cav3 depleted myotubes showed a significantly faster time of bursting as compared to control myotubes (siCtl: 3.1 min ± 0.2, siCav3: 2.4 min ± 0.1) (Fig. 2e and 2f).

Together, our results demonstrate that the Cav3 P28L and R26Q mutant myotubes are unable to provide the mechanoprotection that is required to maintain the integrity of the myotube plasma membrane under mechanical stress and behave similarly to myotubes depleted for Cav3.

The IL6/STAT3 signaling pathway is constitutively hyperactivated in Cav3 P28L and R26Q mutant myotubes.

Considering the key role of caveolae and caveolin in intracellular signaling[12,13], we next investigated whether the loss of functional caveolae could impact some of the key signaling pathways in the muscle. We focused our analysis on the IL6/STAT3 signaling pathway that has been associated with satellite cell exhaustion and muscle wasting[29,30,31]. Furthermore, the IL6 signal transducer glycoprotein gp130, which, together with the IL6 receptor subunit, assemble the IL6 receptor, has been localized in caveolae in a myeloma cell line[32], suggesting a potential regulation of the IL6 signaling pathway by caveolae. IL6 binding to the IL6 receptor is classically followed by the activation of receptor-bound JAK1 and JAK2 kinases, which in turn phosphorylate the signal transducer and activator of transcription 3 (STAT3) that is then translocated as a dimer to the nucleus where it activates the transcription of IL6 sensitive genes[33].

We therefore monitored the level of STAT3 activation i.e. tyrosine (Tyr^{705}) phosphorylation (pSTAT3) in myotubes stimulated for 5 and 15 min with physiological concentrations of IL6 (Figure 3). At steady state, in the absence of IL6 stimulation, little tyrosine phosphorylation of STAT3, if any, could be detected in WT myotubes. In contrast, we found a substantially higher level of pSTAT3 in Cav3 P28L and R26Q mutant myotubes, even in the absence of IL6 stimulation. While IL6 stimulation led to increased levels of pSTAT3 in WT myotubes, we still observed higher levels of pSTAT3 in Cav3 P28L and R26Q mutant myotubes for similar times of IL6 stimulation (Fig. 3a and 3b). To rule out the possible contribution of undifferentiated myotubes in IL6 signaling, we investigated the nuclear translocation of pSTAT3 by immunofluorescence since differentiated myotubes are characterized by the presence of multiple nuclei (Fig. 3c and 3d). Again, we detected a significantly higher level of pSTAT3 in the nuclei of mutant myotubes as compared to WT at steady state. After 15 min of IL6 stimulation, mutant myotubes exhibited higher pSTAT3 nuclear translocation, although it was less pronounced in P28L mutants.

Altogether, these data reveal that the IL6/STAT3 signaling pathway is constitutively hyperactivated in the Cav3 P28L and R26Q mutant myotubes.

We next investigated whether the regulation of IL6/STAT3 signaling would require the presence of functional caveolae at the plasma membrane and thus the expression of Cav3. We therefore monitored the kinetics of STAT3 activation by IL6 in WT myotubes depleted for Cav3. Immunoblot analysis showed a hyperactivation of the IL6 pathway in Cav3 depleted myotubes with an overall activation of STAT3 (Fig. 3e and 3f). These results indicate that Cav3 is a negative regulator of the IL6/STAT3 pathway in healthy myotubes and that the depletion of Cav3 in WT myotubes reproduces the phenotype observed in the Cav3 mutants. It demonstrates that the absence of Cav3 and/or caveolae at the plasma membrane of mutant myotubes is responsible for the constitutive hyperactivation of the IL6/STAT3 signaling pathway.

STAT3 is a key transcription factor controlling the transcription of many downstream genes whose products mediate the pleiotropic effects of STAT3 in physiological and pathological contexts[34]. We therefore examined the consequences of the constitutive hyperactivation of the IL6/STAT3 pathway on gene expression. In the context of muscle disease, we investigated the transcription of muscle-related genes since STAT3 has been suggested to be involved in their regulation. We focused our analysis on the *SOCS3*, *MYH8*, *ACTC1* and *ACTN2* genes that are associated with muscle development and regeneration[31]. *SOCS3* serves also as a positive control, as it is transcribed upon STAT3 activation and its gene product SOCS3 is a major actor in the negative regulation of this pathway[33]. Using quantitative PCR, we found an increased transcription of *SOCS3*, *MYH8*, *ACTC1* and *ACTN2* genes (Fig. 3g). These data strongly suggest that the constitutive hyperactivation of STAT3 found in the Cav3 P28L and R26Q mutant myotubes is responsible for the deregulation of several genes involved in muscle pathophysiology.

IL6/STAT3 mechanosignaling is impaired in Cav3 P28L and R26Q mutant myotubes.

Although caveolae and caveolins have long been associated with signaling[12,13], the integration of this function with their role in mechanosensing has not yet been reported. We have proposed the hypothesis that the mechano-dependent cycle of

caveolae disassembly and reassembly could impact some of the caveolae-dependent signaling pathways[13,35]. We thus analyzed whether the regulation of the IL6/STAT3 pathway by caveolae could depend on mechanical stress. When myotubes were subjected to hypo-osmotic shock prior to IL6 stimulation, we observed a dramatic decrease of STAT3 activation (approx. 80%) in WT myotubes whereas no significant change was observed in Cav3 P28L and R26Q mutant myotubes (Fig. 4a and 4b). We also tested the effect of mechanical stretching on IL6/STAT3 signaling as this is more relevant to the nature of mechanical stress experienced by skeletal muscles during exercise. When we applied a 10% cyclic stretch at 0.5 Hz for 30 min to WT myotubes followed by IL6 stimulation, we also observed a drastic reduction of STAT3 activation, confirming that the IL6/STAT3 pathway is tightly regulated by mechanical stress in muscle cells (Supplementary Fig. 3).

We next determined whether the mechanical regulation of IL6 signaling required the presence of functional caveolae. We applied a hypo-osmotic shock to WT myotubes depleted of Cav3 and whereas no effect was observed at steady state, we found that STAT3 activation by IL6 was slightly decreased by mechanical stress (approx. 20%) in WT myotubes. More importantly no changes were observed in Cav3 depleted myotubes (Fig. 4c and 4d). The poor adhesion of Cav3 P28L and R26Q mutant myotubes on the stretching membrane did not allow us to confirm these data under cyclic stretching. Nevertheless, these results confirm that the IL6/STAT3 signaling pathway is negatively regulated by mechanical stress in myotubes and that this regulation is lost in the absence of functional caveolae as shown in Cav3 P28L and R26Q mutant myotubes and in WT myotubes depleted for Cav3.

Expression of WT Cav3 is sufficient to rescue a normal phenotype in Cav3 P28L myotubes.

Our experiments showing that the depletion of Cav3 in WT myotubes faithfully reproduces the mechanoprotection and signaling defects observed in P28L and R26Q myotubes, implies that the absence of Cav3 at the plasma membrane, as a result of its abnormal retention in the Golgi complex, is responsible for the observed phenotype. To validate this hypothesis, we generated stable WT and P28L myoblasts transduced either by GFP alone or by WT Cav3 tagged with GFP (Cav3-

GFP). Immunofluorescent microscopy confirmed that expressed Cav3-GFP was mainly localized at the plasma membrane and not retained at the Golgi complex in Cav3-GFP P28L myotubes (Fig. 5a and Supplementary Fig. 4a). We performed electron microscopy to see whether Cav3 WT expression would allow us to reconstitute a pool of structurally defined caveolae at the plasma membrane of Cav3 P28L myotubes expressing GFP or Cav3-GFP. While the plasma membrane of control GFP myotubes presented few, often isolated, caveolae structures, Cav3-GFP rescued myotubes presented a significantly higher number of *bona fide* caveolae, including larger vacuolar structures with connected caveolae i.e. rosettes (Fig. 5b and 5c), as classically observed in WT myotubes (Fig. 1c). These observations confirm that the decrease in the number of caveolae in Cav3 P28L myotubes is a direct consequence of the retention of Cav3 P28L in the Golgi complex.

Next, we examined whether the reconstitution of the caveolae reservoir at the plasma membrane of Cav3 P28L myotubes was sufficient to rescue the regulatory role of caveolae in mechanoprotection and IL6/STAT3 signaling. We therefore monitored the resistance to membrane bursting of GFP- and WT Cav3-GFP expressing P28L myotubes as described above. Notably, Cav3-GFP P28L myotubes showed a strong increase in the resistance to membrane bursting under hypo-osmotic shock as compared to GFP P28L myotubes (GFP: 49% ± 3%; Cav3-GFP: 18% ± 2%). It also took a significantly longer time for Cav3-GFP P28L myotubes to burst as compared to GFP P28L myotubes (GFP: 1.6 min ± 0.1; Cav3-GFP: 2.3 min ± 0.2) (Fig. 5d and 5e). Finally, we analyzed the regulation of the IL6/STAT3 pathway by monitoring STAT3 phosphorylation and nuclear translocation in GFP and Cav3-GFP expressing P28L myotubes. At steady state, we observed a significant decrease of pSTAT3 activation and nuclear translocation in Cav3-GFP P28L myotubes as compared to GFP P28L myotubes, indicating that the expression of Cav3 was sufficient to reduce the hyperactivation of STAT3 observed at steady state in Cav3 P28L myotubes (Fig. 5f and 5g). Upon IL6 stimulation, we measured a slightly decreased but not significant pSTAT3 nuclear translocation in Cav3-GFP P28L myotubes, similarly to what we observed when comparing WT to non-transduced Cav3 P28L myotubes (Fig. 3d and 5g). Interestingly, we also found that the expression of Cav3-GFP in WT myotubes led to a decrease of pSTAT3 activation and nuclear translocation at steady state as compared to non transduced WT myotubes (Supplementary Fig. 4c). Altogether, these results show that the

expression and localization of Cav3 at the plasma membrane of P28L myotubes is sufficient to restore membrane mechanoprotection and the regulation of IL6/STAT3 signaling by caveolae.

Discussion

In the present work, we investigated two aspects of caveolae that have been so far poorly characterized in human muscle cells. We first addressed the role of caveolae in mechanosensing and mechanoprotection, a new function of caveolae that has been recently established by several investigators in various cell types. When cells experience acute mechanical stress such as cell swelling or cell stretching, caveolae flatten out into the plasma membrane to provide extra membrane area and prevents membrane tension increase and membrane rupture[14,15,16,17,36]. In agreement with these studies, we found that the presence of functional caveolae was absolutely required to protect human myotubes against severe mechanical stress. Thus, the Cav3 P28L and R26Q mutant myotubes presented a major defect in mechanoprotection with a lack of membrane tension buffering and increased sensibility to membrane rupture. Whereas the mutant myotubes showed a dramatic decrease in the number of caveolae present at the plasma membrane, the expression of wild type Cav3 allowed to restore a number of caveolae sufficient to reinstall mechanoprotection. The depletion of Cav3 in healthy myotubes faithfully reproduced the phenotypes observed in Cav3 P28L and R26Q myotubes indicating that the retention of Cav3 in the Golgi complex is responsible for the absence of a functional reservoir of caveolae at the plasma membrane and thereby the lack of mechanoprotection in these mutants. Our finding that Cav3 P28L and R26Q myotubes still express caveolae at the plasma membrane, albeit to a much lesser extent, most likely indicates that this number is too low to assure an efficient mechanoprotection and/or that these caveolae are not fully functional as suggested by their aberrant size. It is tempting to speculate that the increased fragility of the mutant myotubes membrane could be related to the pathological phenotype reported in Cav3-related muscle dystrophies. We were however surprised that these defects were mainly observed when mutant myotubes were subjected to a severe hypo-osmotic shock. Mild hypo-osmotic shocks did not allow to reveal mechanoprotection defects in mutant myotubes. This is indeed in agreement with early electron microscopy studies showing that *Aplysia californica* smooth muscle and frog skeletal

muscle fibers must be stretched up to nonphysiological levels such as three times the *in situ* length in order to visualize the presence of flattened caveolae[37,38]. This is also consistent with the mild-to-moderate clinical symptoms described in these patients[39].

This incited us to explore other functions of caveolae that could also be deregulated by caveolae dysfunction in Cav3 mutant myotubes. We investigated the regulation of muscle cells signaling as several signaling defects have been described in muscle dystrophies and caveolae have long been associated with the regulation of intracellular signaling. Indeed, Cav3 has been involved in the regulation of distinct signaling pathways important for muscle function such as calcium homeostasis[40], the insulin/GLUT4/Akt pathway[41] or TrkA and EGFR signaling[26]. We focused our analysis on the interleukin-6 (IL6)/STAT3 signaling pathway which has been shown to play an essential role in muscle tissue homeostasis[42]. In addition, the IL6 pathway is tightly associated to mechanical stress in muscle cells as IL6 is secreted mostly during physical exercise[43]. Our data show for the first time a major deregulation of the IL6/STAT3 signaling pathway in the Cav3 mutant myotubes with a constitutive hyperactivation of STAT3 at steady state. This defect translated into increased STAT3 nuclear translocation and expression of *MYH8*, *SOCS3, ACTC1* and *ACTN2*, genes that are known to be regulated by STAT3 and that have been associated with muscle development and regeneration. As for the defects in mechanoprotection, the deregulation of the IL6/STAT3 signaling pathway could be reproduced by depleting healthy myotubes from Cav3, indicating that the absence of Cav-3 and/or caveolae was responsible for the hyperactivation of STAT3. More importantly, we observed that IL6/STAT3 signaling was regulated by mechanical stress in a Cav3-dependent manner in human myotubes. The regulation of IL6/STAT3 mechanosignaling by caveolae was lost in Cav3-mutant myotubes or when healthy myotubes were depleted of Cav3. Again, as observed for mechanoprotection, the regulation of IL6 signaling could be rescued in P28L Cav3 myotubes transduced by the WT form of Cav3, supporting the role of *bona fide* caveolae in the regulation of these two processes.

The first *CAV3* mutation associated with muscle disorders was described 20 years ago and today it has been extended to five distinct genetic disorders: rippling muscle disease (RMD), distal myopathies (DM), hyperCKemia (HCK), limb-girdle muscular dystrophy 1C (LGMD-1C), and familial hypertrophic cardiomyopathy

(HCM)[20,39]. Although many studies have addressed the role of these mutations in muscle damages, the underlying mechanisms remain poorly characterized. Cav3 has been involved in several aspects of muscle physiology including myoblast fusion[44] and T-tubules organization[45]. Moreover, Cav3 interacts with the dystrophin complex[46] and regulates the trafficking of dysferlin[47], two important muscle proteins whose expression and localization are deregulated in severe myopathies. It is therefore likely that the mechanisms by which Cav3 mutations are responsible for muscle dystrophies are multiple.

In conclusion, we describe a new mechanism by which the Cav3 mutations can be deleterious in human myotubes. We uncovered a new regulation of IL6/STAT3 signaling by caveolae under mechanical stress. Our findings revealed a striking similarity between the regulation of mechanoprotection and the control of IL6/STAT3 signaling by caveolae under mechanical stress. Our data confirm that the retention of Cav3 P28L and R26Q in the Golgi complex is responsible for the absence of functional and morphologically defined caveolae at the plasma membrane, which in turn results in deficient mechanoprotection and IL6/STAT3 mechanosignaling. The IL6/STAT3 pathway is tightly associated with the regulation of muscle mass and size[31,42]. It is likely that the alteration of mechanoprotection and muscle size, two critical parameters for general muscle homeostasis, are deleterious for muscle tissue integrity. It is therefore tempting to propose that the caveolae-dependent mechano-regulation of the IL6/STAT3 pathway that we have unraveled here is critical to couple the activation of the IL6/STAT3 pathway with the intensity of mechanical stress that myotubes constantly experience during their lifetime thereby preventing a chronic hyperactivation of IL6/STAT3, through a negative feedback loop, that would be otherwise pathological to muscle cells.

Methods

Cell lines. P28L and R26Q human myoblasts were immortalized by the platform for immortalization of human cells of the Institute of Myology as described in [48]. Briefly, myoblasts were transduced with lentiviral vectors encoding hTERT and cdk4 and containing puromycin (P28L) or puromycin and neomycin (R26Q) selection markers. Transduced cells were selected with puromycin (1 µg/ml) for 6 days (P28L) or with

puromycin (1 µg/ml) for 6 days and neomycin (1 mg/ml) for 10 days (R26Q). Cells were seeded at clonal density, and individual myogenic clones were isolated.
For caveolin-3 expression, immortalized WT and P28L myoblasts were transduced with lentiviral vectors expressing WT caveolin-3 and a GFP reporter gene (MOI 5). A GFP lentiviral vector was used as control (MOI 5).

Cell culture. All cells were grown at 37°C under 5% of CO_2. All myoblasts cell lines were cultured in Skeletal Muscle Cell Growth Medium (Promocell) supplemented with 20% FCS (Gibco, Life technologies), 50 µg/mL of fetuine, 10 ng/mL of epidermal growth factor, 1 ng/mL basic fibroblast growth factor, 10 µg/mL of insulin and 0.4 µ/mL of dexamethasone (Promocell). Prior to any cell seeding, surfaces (well, coverslip, patterned coverslips) are coated with 0.01% of matrigel (v/v) (Sigma) for 15 min at 37°C. For myoblast differentiation, confluent cells (80-100% confluency) are put in DMEM high-glucose Glutamax (Gibco, Life Technologies), supplemented with 0.1% of insulin (v/v) (Sigma) for 4 days.

Antibodies and reagents. Mouse anti-αTubulin (Sigma-Aldrich, clone B512, T5168, 1/1000 for WB); mouse anti-caveolin-3 (Santa Cruz, clone A3, sc-5310, 1/1000 for WB, 1/250 for IF); rabbit anti-caveolin-1 (Cell Signaling, 3238, 1/1000 for WB, 1/500 for IF); goat anti-GM130 (Santa Cruz, clone P-20, sc-16268, 1/50 for IF); mouse anti-MF20 (kind gift of Vincent Mouly, 1/100 for WB, 1/20 for IF); mouse anti-STAT3 (Cell Signaling, clone 124H6, 9139, 1/1000 for WB); rabbit anti-pSTAT3 (Cell Signaling, clone D3A7, 9145, 1/1000 for WB, 1/75 for IF); Secondary antibodies conjugated to Alexa FITC, Cy3, Cy5 or horseradish peroxidase (Beckman Coulter or Invitrogen). DAPI (Sigma-Aldrich).

RNA interference-mediated silencing. Myoblasts were transfected with small interfering RNAs (siRNAs) using HiPerFect (Qiagen) according to the manufacturer's instructions at days 0 and 2 of differentiation and were cultured in differentiation medium for a total of 4 days. Experiments were performed on validation of silencing efficiency by immunoblot analysis using specific antibodies and normalizing to the total level of tubulin used as loading controls. 20 nM of a pool of four siRNA targeting Cav3 were used (SI03068730, SI02625665, SI02625658 and SI00146188,

QIAGEN), Control siRNA (1022076, QIAGEN) was used at the same concentration and served as reference point.

Immunoblotting. Cells were lysed in sample buffer (62.5 mM Tris/HCl pH 6.0, 2% v/v SDS, 10% glycerol v/v, 40 mM dithiothreitol and 0.03% w/v phenol red). Lysates were analyzed by SDS–PAGE and Western blot analysis and immunoblotted with the indicated primary antibodies and horseradish peroxidase- conjugated secondary antibodies. Chemiluminescence signal was revealed using Pierce™ ECL Western Blotting Substrate**,** SuperSignal West Dura Extended Duration Substrate or SuperSignal West Femto Substrate (Thermo Scientific Life Technologies). Acquisition and quantification were performed with the ChemiDoc MP Imaging System (Bio-rad).

Immunofluorescence. Myoblasts were grown and differentiated on coverslips for 4 days. For Cav3, Cav1, MF-20, GM130 staining, cells are fixed with 4% PFA (v/v) (Sigma-Aldrich) for 10 min at RT, quenched in 50 mM NH_4Cl and then permeabilized with 0.2% BSA (v/v) and 0.05% saponin (v/v) (Sigma-Aldrich) in PBS for 20 min. Cells are incubated sequentially with indicated primary and fluorescence-conjugated secondary antibody in permeabilization buffer for 1h at RT. For pSTAT3 staining, cells are fixed and permeabilized with cold methanol for 15 min at -20°C. After washes with PBS 0.2% BSA (v/v), cells are incubated sequentially with indicated primary and fluorescence-conjugated secondary antibody in PBS 0.2% (v/v) for 1 h at RT. In both protocols, coverslips are mounted in Fluoromount-G mounting medium (eBioscience) supplemented with 2 µg/mL of DAPI (Sigma-Aldrich). Acquisition of images are done using a spinning disk microscope (inverted Spinning Disk Confocal Roper/Nikon; Camera: CCD 1392x1040 CoolSnap HQ2 ; objective : 60x CFI Plan Apo VC).

Electron microscopy. Epon embedding was used to preserve the integrity of cell structures. Myotubes were fixed sequentially for 1 h at room temperature with 1.25% glutaraldehyde in 0.1 M Na-Cacodylate and then overnight at 4°C.
Cells were washed extensively with 0.1 M Na-Cacodylate pH 7.2. Membrane fixation was performed for 1 h at room temperature with 1% OsO4 in 0.1 M Na-Cacodylate pH 7.2. Cells were dehydrated by incubation with aqueous solutions of ethanol at

increasing concentrations (50, 70, 90, then 100%, each for 10 min at RT). Embedding was finally performed in LX112 resin. Cells were infiltrated with a 1:1 LX112:ethanol solution, washed with LX112, and embedded overnight at 60°C in LX112 resin. Ultrathin 65 nm sections were sliced using a Leica UCT ultramicrotome and mounted on nickel formvar/ carbon-coated grids for observations. Contrast was obtained by incubation of the sections for 10 min in 4% uranyl acetate followed by 1 min in lead citrate.
Electron micrographs were acquired on a Tecnai Spirit electron microscope (FEI, Eindhoven, The Netherlands) equipped with a 4k CCD camera (EMSIS GmbH, Münster, Germany)

Micropatterning. 18 mm coverslips were micropatterned as described in (Carpi et al., 2011) using a photo-mask with lines of 10 µm of width, separated by 60 µm. In both force measurements and membrane bursting assay, myoblasts are plated at confluency on line micropatterns coverslips coated with 0.01% of matrigel (v/v) (Sigma) for 15 min at 37°C. Differentiation of myoblasts is achieved as described above in section *Cell culture*.

Force Measurements. Plasma membrane tethers were extracted from cells by a concanavalin A (Sigma-Aldrich) coated bead (3 µm in diameter, Polysciences) trapped in optical tweezers. The optical tweezers are made of a 1064 nm laser beam (ytterbium fiber laser, λ = 1064 nm, TEM 00, 5 W, IPG Photonics, Oxford, MA) expanded and steered (optics by Elliot Scientific, Harpenden, UK) in the back focal plane of the microscope objective (Apo-TIRF 100× NA 1.45, Nikon). The whole setup was mounted on a Nikon Eclipse-Ti inverted microscope. The sample was illuminated by transmitted light, and movies were acquired at 10 Hz with an EM-charge-coupled device camera (Andor iXon 897) driven by Micro-Manager. The fine movements and particularly the translational movement necessary to pull the membrane tether were performed using a custom-made stage mounted on a piezoelectric element (P753, Physik Instrumente, Karlsruhe, Germany) driven by a servo controller (E665, Physik Instrumente) and a function generator (Sony Tektronix AFG320).
Calibration was performed using an oscillatory modulation driven by a function generator and measuring the response of the bead to an oscillatory motion of the

stage. We measured k = 159 pN/µm. This relationship is linear in the laser power range used for the experiments (0.4–1.2 W).
The membrane tether was held at constant length to measure the static force. For measuring membrane tension changes due to hypo-osmotic shock, a first tether was first pulled at 300 mOsm (iso condition). A second tube was pulled on the same cell 5 min after diluting the medium with milliQ water to obtain 45 mOsm. The position of the bead used to compute tether forces was detected from the images using a custom ImageJ macro.

Membrane bursting assay. Line micropatterned myotubes are incubated in 5 µg/mL of calcein-AM (Life techonologies) and 50 µg/mL of DAPI (Sigma-Aldrich) for 15 min at 37°C in the dark. Medium was then switched back with differentiation medium to wash out the excess of calcein-AM. The medium is then switched again with a 30 mOsm hypo-osmotic shock medium obtained after a dilution of 10% medium and 90% H_2O, supplemented with 2 mg/mL of PI (Sigma). Immediately after medium switching, pictures are taken every minute for 10 min using a videomicroscope (Inverted microscope Nikon Ti-E, Camera: CCD 1392x1040 CoolSnap HQ2, objective: 10x CFI Fluor).

IL6 stimulation. Myotubes were starved 4 h by switching the differentiation medium to DMEM medium. In resting conditions, cells are then stimulated by switching the medium with DMEM with 0.2% BSA (w/v), supplemented with 10 ng/mL of human recombinant IL6 (R&D) for 0, 5 or 15 min at 37°C. For hypo-osmotic conditions, medium was first switched to 75% hypo-osmotic shock (25% DMEM, 75% H_2O) for 5 min and then switched to the same medium supplemented with 10 ng/mL of IL6 for 5 more minutes at 37°C. For stretching conditions, myoblasts were differentiated on fibronectin (Sigma-Aldrich) coated stretchable plates (Uniflex® culture plate, Flexcell International) and were then subjected or not to 30 min of cyclic stretch (10% elongation, 0.5 Hz), using the FX-4000T TM Tension Plus device (Flexcell International), followed or not by 5 min of 10 ng/mL IL6 stimulation. Cells are lysed and samples are analyzed by immunoblotting. For the analysis, pSTAT3 levels were quantified by calculating the ratio between pSTAT3 and STAT3, both normalized to Tubulin signal. For the analysis of pSTAT3 nuclear translocation, myotubes were differentiated on coverslips, stimulated with IL6 as described above for 0 min or 15

min and were then fixed for further immunofluorescence analysis. Quantification corresponds to the ratio between the mean pSTAT3 intensity in the nuclei on the one in the cytoplasm.

Quantitative PCR. Cells were lysed and RNA extraction was performed using an extraction kit (RNeasy Plus, Qiagen). Reverse-transcription reaction was performed with 1 µg of RNA per reaction, using high capacity cDNA reverse-transcritpion kit (Applied biosystem). qPCR was performed on 50 ng of cDNA for a reaction in a total volume of 20 µL, using Taqman Gene Expression Assays (*GAPDH*: Hs02786624_g1 ; *ACTC1*: Hs01109515_m1 ; *MYH8*: Hs00267293_m1 ; *SOCS3*: Hs02330328_s1, *ACTN2*: Hs00153809_m1, Applied biosystem) and a Lightcycler 480 Probes Master kit (Roche). Relative expression levels were calculated using $\Delta\Delta$CT method with fold changes calculated as $2^{-\Delta\Delta CT}$.

Statistical analyses

All analyses were performed using GraphPad Prism version 6.0 and 7.0, GraphPad Software, La Jolla California USA, www.graphpad.com. Two-tailed (paired or unpaired) t-test was used if comparing only two conditions. For comparing more than two conditions, Kurskal-Wallis test was used with Dunn's multiple comparison test (if comparing all conditions to the control condition). Significance of mean comparison is marked on the graphs by asterisks. Error bars denote SEM or SD.

Acknowledgments

We would like to thank Catherine Coirault and Stéphane Vassilopoulos, Nicolas Carpi and the laboratory of Bruno Goud for providing materials and/or expertise. We are grateful to Paolo Pierobon for help on the analysis of membrane tension measurements. The facilities as well as scientific and technical assistance from staff in the PICT-IBiSA/Nikon Imaging Centre at Institut Curie-CNRS and the France-BioImaging infrastructure (N°ANR-10-INSB-04) are acknowledged. The electron microscope facility was supported by the French National Research Agency through the "Investments for the Future" program (France-BioImaging, ANR-10-INSB-04). This work was supported by institutional grants from the Curie Institute, INSERM and CNRS, and by specific grants from Association Française contre les Myopathies

(AFM): CAV-MUT (17151) to M.D; CAV-STRESS-MUS (14266 to C.M.B and 14293 to C.L)

Author Contributions

M.D designed and performed the experiments, analyzed results and wrote the manuscript. D.K, B.S, C.V.L, V.C performed experiments or analysis. A.B, N.T, L.J, P.N, G.B.B provided technical support and conceptual advice. C.L and C.M.B supervised the project, designed experiments and wrote the manuscript.

Declaration

The authors declare no competing financial interest.

References

1. Palade, G. E. The fine structure of blood capillaries. *J. Appl. Phys.* **24,** 1424 (1953).
2. Yamada, E. The fine structure of the gall bladder epithelium of the mouse. *J. Biophys. Biochem. Cytol.* **1,** 117–122 (1955).
3. Aboulaich, N., Vainonen, J. P., Stralfors, P. & Vener, A. V. Vectorial proteomics reveal targeting, phosphorylation and specific fragmentation of polymerase I and transcript release factor (PTRF) at the surface of caveolae in human adipocytes. *Biochem. J.* **383,** 237–248 (2004).
4. Hansen, C. G., Howard, G. & Nichols, B. J. Pacsin 2 is recruited to caveolae and functions in caveolar biogenesis. *J. Cell Sci.* **124,** 2777–2785 (2011).
5. Hill, M. M. *et al.* PTRF-Cavin, a Conserved Cytoplasmic Protein Required for Caveola Formation and Function. *Cell* **132,** 113–124 (2008).
6. Morén, B. *et al.* EHD2 regulates caveolar dynamics via ATP-driven targeting and oligomerization. *Mol. Biol. Cell* **23,** 1316–1329 (2012).
7. Rothberg, K. G. *et al.* Caveolin, a protein component of caveolae membrane coats. *Cell* **68,** 673–682 (1992).
8. Scherer, P. E. *et al.* Identification, sequence, and expression of caveolin-2 defines a caveolin gene family. *Proc. Natl. Acad. Sci. U. S. A.* **93,** 131–135 (1996).
9. Way, M. & Parton, G. M-caveolin, a muscle-specific caveolin-related protein. *FEBS Lett.* **376,** 108–112 (1995).
10. Tagawa, M. *et al.* MURC, a muscle-restricted coiled-coil protein, is involved in the regulation of skeletal myogenesis. *Am. J. Physiol. Cell Physiol.* **295**, 490-498 (2008).
11. Minetti, C. *et al.* Impairment of Caveolae Formation and T-System

Disorganization in Human Muscular Dystrophy with Caveolin-3 Deficiency. *Am. J. Pathol.* **160,** 265–270 (2002).
12. Cheng, J. P. X. & Nichols, B. J. Caveolae: One Function or Many? *Trends Cell Biol.* **26,** 177–189 (2016).
13. Lamaze, C., Tardif, N., Dewulf, M., Vassilopoulos, S. & Blouin, M. C. The caveolae dress code: structure and signaling. *Curr. Opin. Cell Biol.* **47,** 117–125 (2017).
14. Sinha, B. *et al.* Cells Respond to Mechanical Stress by Rapid Disassembly of Caveolae. *Cell* **144,** 402–413 (2011).
15. Cheng, J. P. X. *et al.* Caveolae protect endothelial cells from membrane rupture during increased cardiac output. *J. Cell Biol.* **211,** 53–61 (2015).
16. Lo, H. P. *et al.* The caveolin-Cavin system plays a conserved and critical role in mechanoprotection of skeletal muscle. *J. Cell Biol.* **210,** 833–849 (2015).
17. Garcia, J. *et al.* Sheath Cell Invasion and Trans-differentiation Repair Mechanical Damage Caused by Loss of Caveolae in the Zebrafish Notochord. *Curr. Biol.* **27,** 1982–1989 (2017).
18. Lim, Y.-W. *et al.* Caveolae Protect Notochord Cells against Catastrophic Mechanical Failure during Development. *Curr. Biol.* **27,** 1968–1981 (2017).
19. Le Lay, S. & Kurzchalia, T. V. Getting rid of caveolins: Phenotypes of caveolin-deficient animals. *Biochim. Biophys. Acta.* **1746,** 322–333 (2005).
20. Minetti, C. *et al.* Mutations in the caveolin-3 gene cause autosomal dominant limb-girdle muscular dystrophy. *Nat. Genet.* **18,** 365–368 (1998).
21. Carbone, I. *et al.* Mutation in the CAV3 gene causes partial caveolin-3 deficiency and hyperCKemia. *Neurology* **54,** 1373–1376 (2000).
22. Betz, R. C. *et al.* Mutation in CAV3 cause mechanical hyperirritability of skeletal muscle in rippling muscle disease. *Nat. Genet.* **28,** 218–219 (2001).
23. Tateyama, M. *et al.* Mutation in the caveolin-3 gene causes a peculiar form of distal myopathy. *Neurology* **58,** 323–325 (2002).
24. Merlini, L. *et al.* Familial isolated hyperCKaemia associated with a new mutation in the caveolin-3 (CAV-3) gene. *J. Neurol. Neurosurg. Psychiatry* **73,** 65–67 (2002).
25. Sotgia, F. *et al.* Phenotypic behavior of caveolin-3 R26Q, a mutant associated with hyperCKemia, distal myopathy, and rippling muscle disease. *Am. J. Physiol. Cell Physiol.* **285,** 1150-1160 (2003).
26. Brauers, E. *et al.* Differential effects of myopathy-associated caveolin-3 mutants on growth factor signaling. *Am. J. Pathol.* **177,** 261–270 (2010).
27. Hernandez-Deviez, D. J. *et al.* Caveolin regulates endocytosis of the muscle repair protein, dysferlin. *J. Biol. Chem.* **283,** 6476–6488 (2008).
28. Cai, C. *et al.* Membrane repair defects in muscular dystrophy are linked to altered interaction between MG53, caveolin-3, and dysferlin. *J. Biol. Chem.* **284,** 15894–15902 (2009).
29. Tierney, M. T. *et al.* STAT3 signaling controls satellite cell expansion and skeletal muscle repair. *Nat. Med.* **20,** 1182–1186 (2014).
30. Price, F. D. *et al.* Inhibition of JAK-STAT signaling stimulates adult satellite cell function. *Nat. Med.* **20,** 1174–1181 (2014).
31. Bonetto, A. *et al.* STAT3 activation in skeletal muscle links muscle wasting and the acute phase response in cancer cachexia. *PLoS One* **6**, e22538 (2011).
32. Podar, K. *et al.* Essential role of caveolae in interleukin-6- and insulin-like growth factor I-triggered Akt-1-mediated survival of multiple myeloma cells. *J. Biol. Chem.* **278,** 5794–5801 (2003).

33. Heinrich, P. C. *et al.* Principles of interleukin (IL)-6-type cytokine signalling and its regulation. *Biochem. J.* **374,** 1–20 (2003).
34. Levy, D. E. & Lee, C. K. What does Stat3 do? *J. Clin. Invest.* **109,** 1143–1148 (2002).
35. Nassoy, P. & Lamaze, C. Stressing caveolae new role in cell mechanics. *Trends Cell Biol.* **22,** 381–389 (2012).
36. Lim, Y. W. *et al.* Caveolae Protect Notochord Cells against Catastrophic Mechanical Failure during Development. *Curr. Biol.* **27,** 1968–1981 (2017).
37. Prescott, L. & Brightman, M. W. The sarcolemma of Aplysia smooth muscle in freeze-fracture preparations. *Tissue Cell* **8,** 241–258 (1976).
38. Dulhunty, A. F. & Franzini-Armstrong, C. The relative contributions of the folds and caveolae to the surface membrane of frog skeletal muscle fibres at different sarcomere lengths. *J. Physiol.* **250,** 513–39 (1975).
39. Gazzerro, E., Sotgia, F., Bruno, C., Lisanti, M. P. & Minetti, C. Caveolinopathies: from the biology of caveolin-3 to human diseases. *Eur. J. Hum. Genet.* **18,** 137-145 (2010).
40. Weiss, N. *et al.* Expression of the muscular dystrophy-associated caveolin-3P104L mutant in adult mouse skeletal muscle specifically alters the Ca^{2+} channel function of the dihydropyridine receptor. *Eur. J. Physiol.* **457,** 361–375 (2008).
41. Fecchi, K., Volonte, D., Hezel, M. P., Schmeck, K. & Galbiati, F. Spatial and temporal regulation of GLUT4 translocation by flotillin-1 and caveolin-3 in skeletal muscle cells. *FASEB J.* **20,** 705–707 (2006).
42. Muñoz-Cánoves, P., Scheele, C., Pedersen, B. K. & Serrano, A. L. Interleukin-6 myokine signaling in skeletal muscle: A double-edged sword? *FEBS J.* **280,** 4131–4148 (2013).
43. Ostrowski, K., Rohde, T., Zacho, M., Asp, S. & Pedersen, B. Evidence that IL-6 is produced in skeletal muscle during intense long-term muscle activity. *J. Physiol.* **508,** 949–953 (1998).
44. Bjerregard, B., Ziomkiewicz, I., Schulz, A. & Larsson, L.-I. Syncytin-1 in differentiating human myoblasts: relationship to caveolin-3 and myogenin. *Cell Tissue Res.* **357,** 355–362 (2014)
45. Galbiati, F. *et al.* Caveolin-3 Null Mice Show a Loss of Caveolae, Changes in the Microdomain Distribution of the Dystrophin-Glycoprotein Complex, and T-tubule Abnormalities. *J. Biol. Chem.* **276,** 21425–21433 (2001).
46. Song, K. S. *et al.* Expression of caveolin-3 in skeletal, cardiac, and smooth muscle cells: Caveolin-3 is a component of the sarcolemma and co-fractionates with dystrophin and dystrophin-associated glycoproteins. *J. Biol. Chem.* **271,** 15160–15165 (1996).
47. Hernández-Deviez, D. J. *et al.* Aberrant dysferlin trafficking in cells lacking caveolin or expressing dystrophy mutants of caveolin-3. *Hum. Mol. Genet.* **15,** 129–142 (2006).
48. Mamchaoui, K. *et al.* Skeletal Muscle Immortalized pathological human myoblasts: towards a universal tool for the study of neuromuscular disorders Immortalized pathological human myoblasts: towards a universal tool for the study of neuromuscular disorders. *Skelet. Muscle* **1,** 34 (2011).
49. Carpi, N., Piel, M., Azioune, A. & Fink, J. Micropatterning on glass with deep UV. *Protoc. Exch.* (2011). doi:10.1038/protex.2011.238

Figure legends

Figure 1 | Characterization of caveolae and Cav3 expression in WT, Cav3 P28L and Cav3 R26Q myotubes. (**a**) Electron micrographs of WT, Cav3 P28L and Cav3 R26Q myotubes. Caveolae, interconnected caveolae and aberrant sized caveolae are indicated with black arrowheads, asterisks and white arrowheads, respectively. (**b**) Quantification of the number of caveolae / μm^2 in (**a**). (**c**) Immunoblot analysis of total levels of Cav3 in WT, Cav3 P28L and Cav3 R26Q differentiated myotubes. Tubulin serves as a loading control. (**d**) Quantification of the expression of Cav3 in (**c**) by calculating the ratio between Cav3 and tubulin expression. (**e**) Immunofluorescent labeling of Cav3 and GM130 in WT, Cav3 P28L or Cav3 R26Q myotubes analyzed by confocal microscopy. Arrows in inset indicate the plasma membrane and arrowheads indicate the Golgi complex. (**a**) Scale bar = 200 nm. Representative cells quantified in (**b**) (number of regions analyzed: WT = 115, P28L = 154, R26Q = 146; Total area screened: WT = 1140 μm^2, P28L = 1187 μm^2, R26Q = 1216 μm^2) (**d**) Quantification was done on 3 independent experiments (**e**) Scale bar = 10 µm. Reproducibility of experiments: (**a**) Representative cells. (**b**), (**c**) and (**d**) Representative data for 3 experiments. Mean value ± SEM. (**b, d**) Statistical analysis with a two-tailed unpaired t test, * P<0,05; *** P<0,0001.

Figure 2 | Cav3 P28L and Cav3 R26Q myotubes present major defects in membrane tension buffering and membrane integrity. (**a, b**) Membrane tension measurement analysis using optical tweezers and nanotube pulling on micropatterned WT, Cav3 P28L or Cav3 R26Q myotubes. Membrane tethers were pulled in the perpendicular axis of aligned myotubes after micropatterning in resting conditions and 5 min after a 45 mOsm hypo-osmotic shock (**a, b,** left panels). Membrane tension was analyzed in resting condition (**a,** right panel) and the difference of membrane tension before and after hypo-osmotic shock was calculated, reflecting the percentage of increase of membrane tension upon mechanical stress (**b,** right panel).

(**c, e**) Micropatterned WT, Cav3 P28L or Cav3 R26Q myotubes (**c**) or WT ctl (siCtl) and Cav3-depleted (siCav3) myotubes (**e**) were loaded with calcein-AM (green). The medium was switched with a 30 mOsm medium supplemented with propidium iodide (PI, red). Representative pictures were taken at the indicated times during hypo-osmotic shock. Arrows correspond to myotubes and asterisks correspond to burst myotubes. (**d, f**) Quantification of the percentage of burst myotubes (upper panel) and mean time of bursting in minutes (lower panel) in (**c**) and (**e**), respectively. (**a, b**) Scale bar = 5 µm. (**c, e**) Scale bar = 120 µm. Reproducibility of experiments: (**a**) Representative pictures and quantifications from 7 independent experiments (WT n=20, P28L n=23 and R26Q n=22) (**b**) Representative pictures and quantifications from 7 independent experiments (WT n=20, P28L n=27 and R26Q n=18). (**c**) Representative data of 3 independent experiments quantified in (**d)** (% burst cells: WT n=310, P28L n=299 and R26Q n=271; mean time of bursting: WT n=165, P28L n=233 and R26Q n=240). (**e**) Representative data of 3 independent experiments quantified in (**f**) (% burst cells: siCtl n=749 and siCav3 n=569; mean time of bursting: siCtl n=171 and siCav3 n=506). Mean value ± SD. (**a**, **b**) Statistical analyses were done using Kurskal-Wallis test. (**d**, **f**) Statistical analysis with two-tailed unpaired t test; * P<0,05; *** P<0,001.

Figure 3 | Constitutive hyperactivation of IL6/STAT3 signaling in Cav3 P28L and Cav3 R26Q myotubes. (**a**) Immunoblot analysis of pSTAT3 and STAT3 levels in WT, Cav3 P28L and Cav3 R26Q myotubes stimulated for the indicated times with 10 ng/mL IL6. Tubulin serves as a loading control. (**b**) Quantification of STAT3 activation of (**a**), corresponding to the ratio pSTAT3 on STAT3 total levels after normalization to tubulin levels. (**c**) Confocal microscopy of immunofluorescent pSTAT3 in WT, Cav3 P28L and Cav3 R26Q myotubes stimulated or not for 15 min with 10 ng/mL IL6. White dashed lines outline nucleus boundaries (**d**) Quantification of pSTAT3 nuclear translocation in (**c**) corresponding to nuclei/cytoplasm mean intensity ratio of pSTAT3. (**e**) Immunoblot analysis of pSTAT3 levels in WT ctl (siCtl) and Cav3-depleted (siCav3) myotubes stimulated for the indicated times with 10 ng/mL IL6. (**f**) Quantification of STAT3 activation in (**e**), corresponding to the ratio pSTAT3 on STAT3 total level after normalization with tubulin level. (**g**) Expression of STAT3 related genes: from left to right *SOCS3*, *MYH8*, *ACTC1* and *ACTN2* in WT, Cav3 P28L or Cav3 R26Q myotubes. (**c**) Scale bar = 10 µm. Reproducibility of

experiments: (**a**, **c** and **e**) Representative data. (**b**) Quantification was done on 4 independent experiments. (**d**) Quantification was done on 3 independent experiments (0 min: WT n=41, P28L n=25, R26Q n=21; 15 min: WT n=22, P28L n=30, R26Q n=30). (**f**) Quantification was done on 4 experiments. (**g**) Quantification was done on 5 (*SOCS3*), 8 (*MYH8*), 3 (*ACTC1*) and 7 (*ACTN2*) independent experiments. Mean value ± SEM. (**b**, **f**) Statistical analysis with two-tailed paired t test. (**d, g**) Statistical analysis with two-tailed unpaired t test * P<0,05; ** P<0,01; *** P<0,001; ns, non significant.

Figure 4 | IL6/STAT3 mechanosignaling is impaired in Cav3 P28L and R26Q myotubes. (**a, c**) Immunoblot analysis of pSTAT3 and STAT3 levels in WT, Cav3 P28L and Cav3 R26Q myotubes. (**a**) WT ctl (siCtl) or Cav3-depleted (siCav3) myotubes (**c**) subjected or not to a 75 mOsm hypo-osmotic shock (Hypo-Osm) for 10 min, followed by stimulation or not with 10 ng/mL IL6 for 5 min. Tubulin serves as loading control. (**b, d**) Quantification of STAT3 activation in (**a**) and (**c**) respectively, corresponding to the ratio pSTAT3 on STAT3 total level after normalization to tubulin level.
Reproducibility of experiments: (**a, c**) Representative data. (**b**) Quantification was done on 5 and 3 independent experiments for WT and mutants respectively. (**d**) Quantification was done on 4 independent experiments. Mean value ± SEM. (**b, d**) Statistical analysis with two-tailed paired t test; * P<0,05; ** P<0,01; ns, non significant.

Figure 5 | Expression of WT Cav3 rescues a normal phenotype in Cav3 P28L and R26Q myotubes.
(**a**) Immunofluorescent labeling of Cav3 and Golgi marker GM130 in Cav3 P28L GFP and P28L Cav3-GFP transduced myotubes analyzed by confocal microscopy. Arrows in inset indicate the plasma membrane and arrowheads indicate the Golgi complex. (**b**) Electron micrographs of Cav3 P28L GFP and P28L Cav3-GFP transduced myotubes. Caveolae and interconnected caveolae are indicated with arrowheads and asterisks, respectively. (**c**) Quantification of the number of caveolae/ μm^2 (left panel) and the total number of caveolae in (b) (right panel). (**d**) Micropatterned Cav3 P28L GFP and P28L Cav3-GFP transduced myotubes were

loaded with calcein-AM (green). The medium was switched with a 30 mOsm medium supplemented with propidium iodide (PI, red). Representative pictures were taken at the indicated times during hypo-osmotic shock. Arrows correspond to myotubes and asterisks correspond to burst myotubes. (**e**) Quantification of the percentage of burst myotubes (upper panel) and mean time of bursting in minutes (lower panel) in (**d**). (**f**) Confocal microscopy of immunofluorescent pSTAT3 in Cav3 P28L GFP or P28L Cav3-GFP transduced myotubes stimulated or not for 15 min with 10 ng/mL IL6. White dashed lines outline nucleus boundaries (g) Quantification of pSTAT3 nuclear translocation in (**f**) corresponding to nuclei/cytoplasm mean intensity ratio of pSTAT3. (**a**) Scale bar = 10 µm. (**b**) Scale bar = 200 nm. (**d**) Scale bar = 120 µm. (**f**) Scale bar = 10 µm. Reproducibility of experiments: (**a**) Representative pictures of 3 experiments. (**b**) Representative pictures quantified in (**c**) (number of analyzed regions: P28L GFP = 169, P28L Cav3-GFP = 182; Total screened area: P28L GFP = 1405 μm^2, P28L Cav3-GFP = 1349 μm^2) (**d**) Show representative data of 3 experiments quantified in (**e**) (% burst cells: GFP n=353 and Cav3-GFP n=358; time of burst: GFP n=175 and Cav3-GFP n=65). (**f**) Show representative data of 3 experiments quantified in (**g**) (control: GFP n=33 and Cav3-GFP n=42; 15 min: GFP n=14 and Cav3-GFP n=13). Mean value ± SEM. (**c**), (**e**) and (**g**) Statistical analysis with a two-tailed unpaired t test; ** P<0,01; *** P<0,0001; ns, non significant.

Figure 1. ***Dewulf et al.***

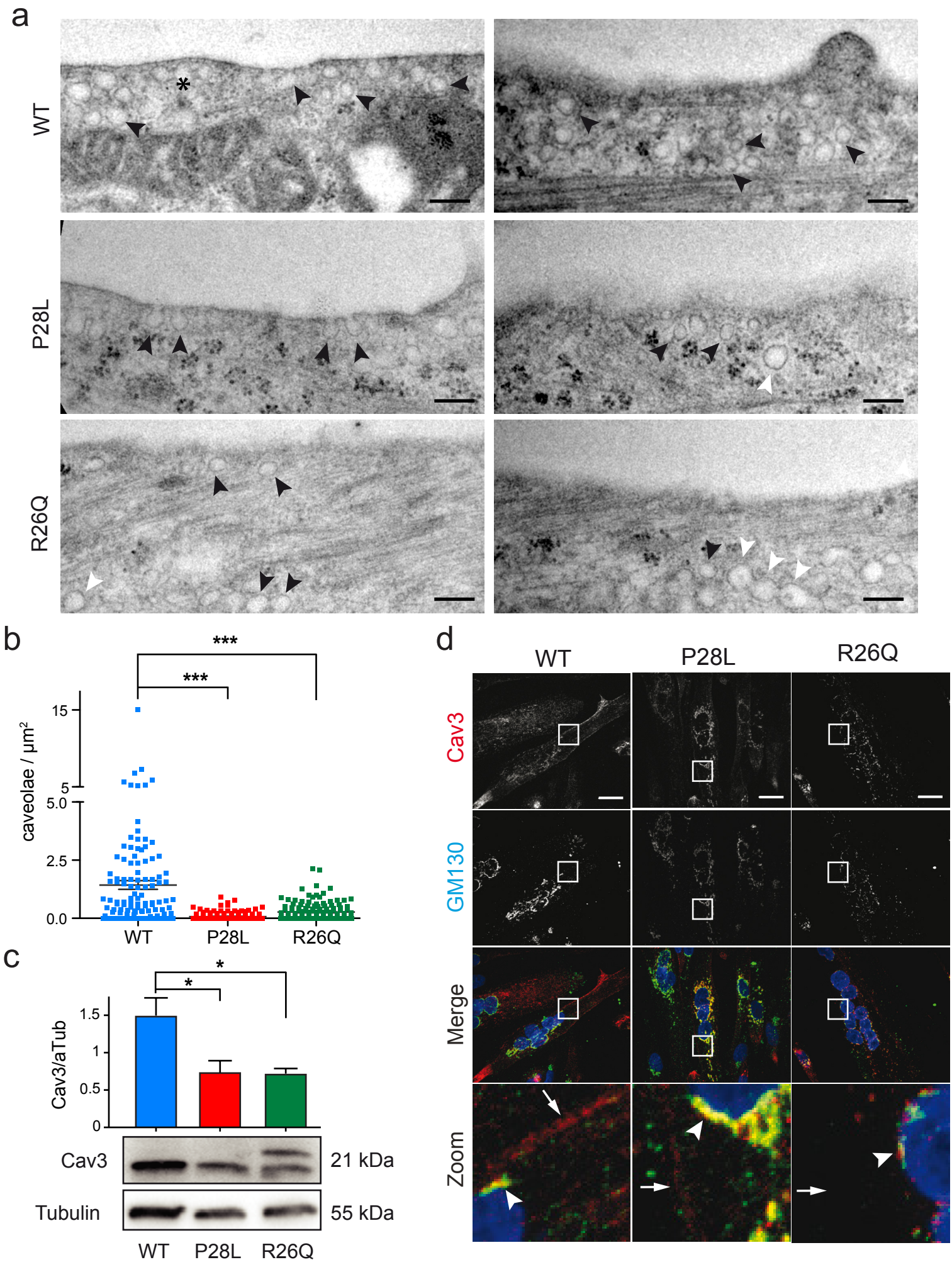

Figure 2. *Dewulf et al.*

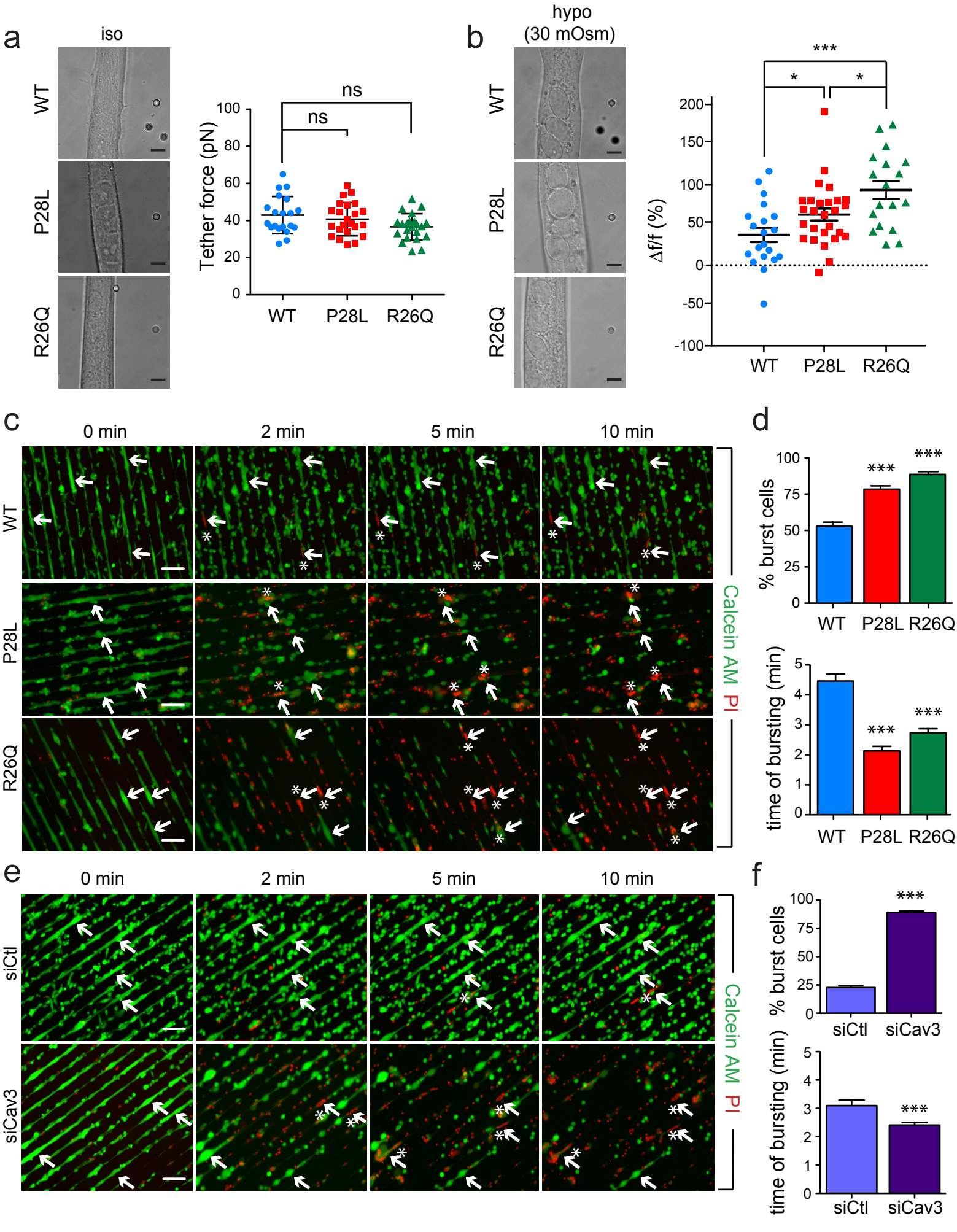

Figure 3. *Dewulf et al.*

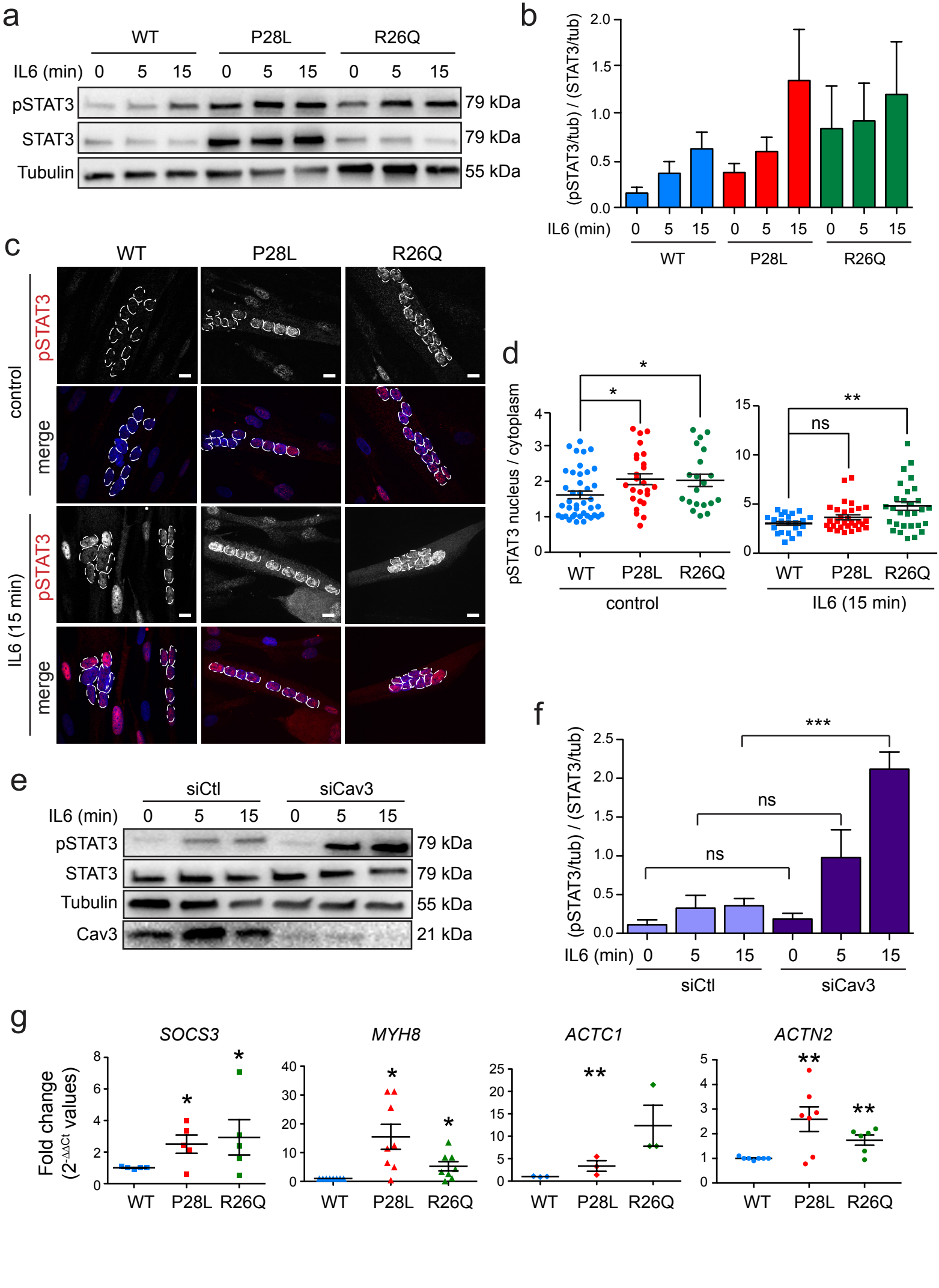

Figure 4. ***Dewulf et al.***

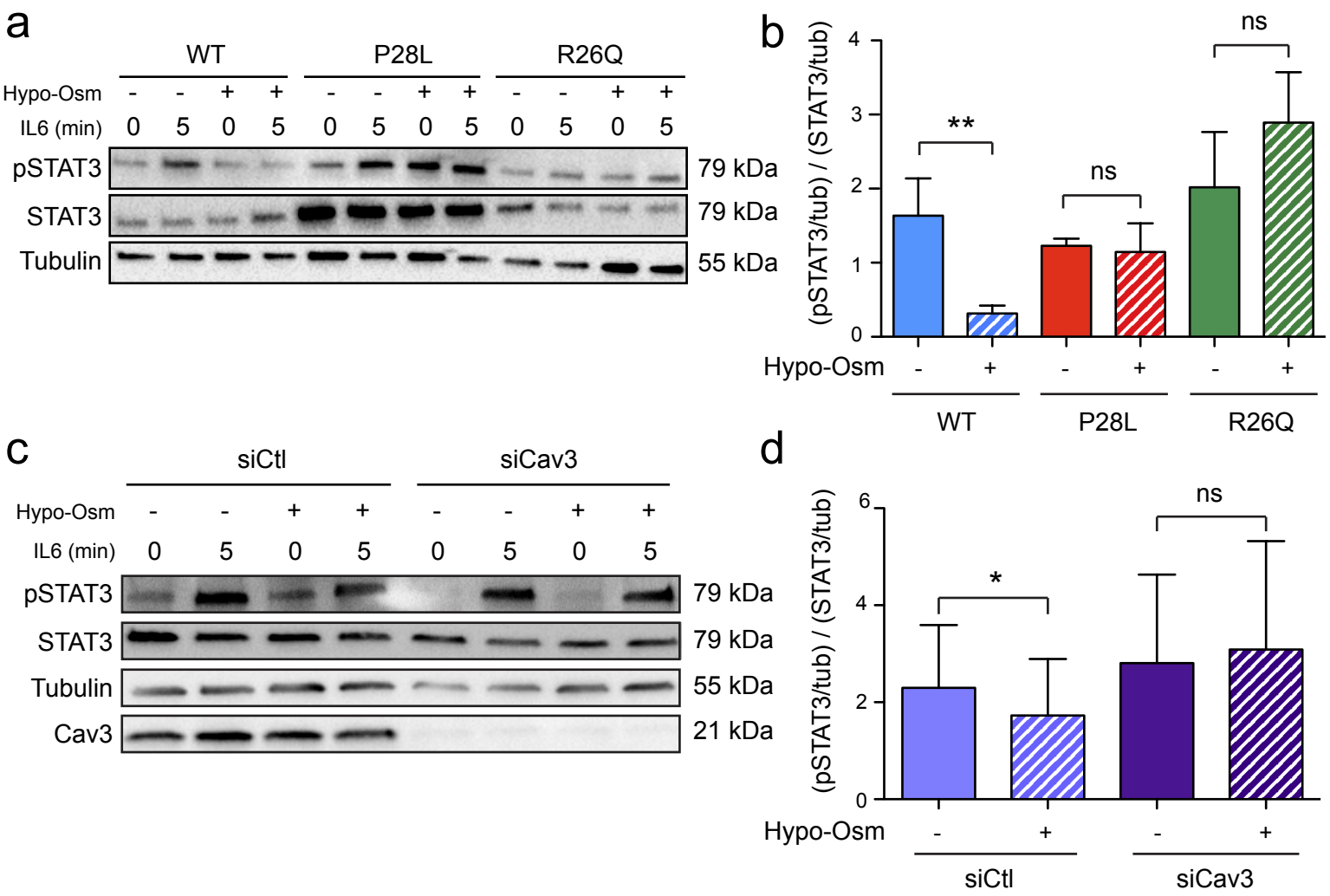

Figure 5. *Dewulf et al.*

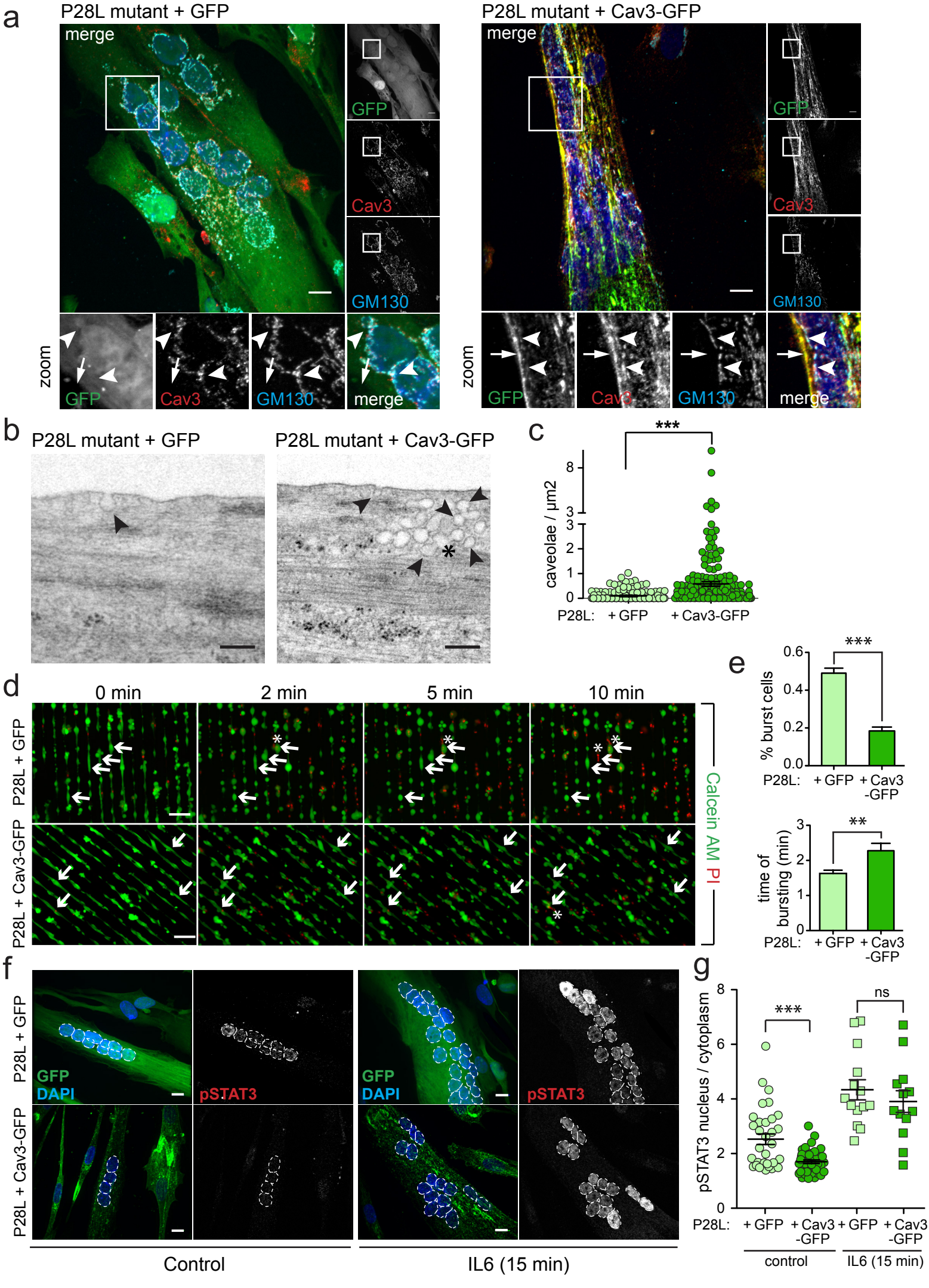

Supplementary figure legends

Supplementary figure 1 | MF20 and Cav1 expression in WT, Cav3 P28L and R26Q myotubes. (**a, b**) Immunoblot analysis of total levels of MF20 (**a**) and Cav1 (**b**) in WT, Cav3 P28L and Cav3 R26Q myotubes. Tubulin serves as a loading control. (**c**) Cav3, Cav1 and Golgi marker GM130 immunofluorescence were analyzed by confocal microscopy in WT, Cav3 P28L and Cav3 R26Q myotubes. (**a**), (**b**) and (**c**) Representative data for 3 experiments. (**c**) Scale bar = 10 µm.

Supplementary figure 2 | Efficient membrane tension buffering and mechanoprotection in Cav3 P28L and Cav3 R26Q myotubes under mild hypo-osmotic shock. (**a**) Calcein-AM and DAPI fluorescence of WT, Cav3 P28L and Cav3 R26Q myotubes prior to hypo-osmotic shock in the membrane bursting assay described in **Figure 2c**. Insets show DAPI in myotubes indicated with arrows in **Figure 2c**. (**b**) Micropatterned WT, Cav3 P28L and Cav3 R26Q myotubes were loaded with calcein-AM (green). The medium was switched to a 150 mOsm medium supplemented with propidium iodide (PI, red). Representative pictures were taken at the indicated times during hypo-osmotic shock. Arrows correspond to myotubes and asterisks correspond to burst myotubes. (**c**) Membrane tension measurement analysis using optical tweezers and nanotube pulling on micropatterned WT, Cav3 P28L and Cav3 R26Q myotubes. Membrane tethers were pulled in the perpendicular axis of myotubes after micropatterning in resting conditions and 5 min after a 150 mOsm hypo-osmotic shock (upper panel). Membrane tension was analyzed in resting condition (lower panel, left) and the difference of membrane tension before and after hypo-osmotic shock was calculated, reflecting the percentage of increase of membrane tension upon mechanical stress (lower panel, right) (**d**) Immunoblot analysis of Cav3 depletion in **Figure 2e**. (**a, b**) Scale bar = 120 µm. (**c**) Scale bar = 5µm Reproducibility of experiments: (**c**) Quantifications were done on 5 independent experiments (WT n=17, P28L n=16, R26Q n=14). Mean value ± SD. Statistical analyses were done using Kruskal-Wallis test; ns, non significant.

Supplementary figure 3 | IL6/STAT3 signaling in WT myotubes under cyclic stretch. (**a**) Immunoblot analysis of pSTAT3 and STAT3 levels in WT myotubes subjected or not to 30 min cyclic stretch. Myotubes were then stimulated or not with

10 ng/mL IL6 for 5 min. Tubulin serves as a loading control. (**b**) Quantification of STAT3 activation in (**a**) corresponding to the ratio pSTAT3 on STAT3 total levels after normalization to tubulin levels. Reproducibility of experiments: (**b**) Quantification was done on 3 experiments. Mean value ± SEM. Statistical analyses were done using two-tailed paired t test; * P<0,05.

Supplementary figure 4 | Effect of Cav3 expression in mechanoprotection and IL6 signaling in WT myotubes. (**a**) Immunofluorescent labeling of Cav3 and Golgi marker GM130 in WT GFP and WT Cav3-GFP transduced myotubes analyzed by confocal microscopy. Arrows and arrowheads in inset indicate the plasma membrane and the Golgi complex respectively. (**b**) Quantification of the percentage of burst myotubes after a 30 mOsm hypo-osmotic shock (left panel) and mean time of bursting in minutes (right panel) in (**a**). (**c**) Quantification of pSTAT3 nuclear translocation in WT GFP or WT Cav3-GFP transduced myotubes stimulated or not for 15 min with 10 ng/mL IL6, corresponding to nuclei/cytoplasm mean intensity ratio of pSTAT3. (**a**) Scale bar = 10 µm. Reproducibility of experiments: (**a**) Representative data from 3 independent experiments. (**b**) Quantification was done on 3 independent experiments (% burst: GFP n=714, Cav3-GFP n=610; time of burst: GFP n=80, Cav3-GFP n=171). (**c**) Quantification was done on 3 independent experiments (control: GFP n=16, Cav3-GFP n=21; 15 min: GFP n=16, Cav3-GFP n=21). (**b, c**) Statistical analyses were done using two-tailed unpaired t test; ***P<0,0001; *P<0,05; ns, non significant.

Supplementary figure 1. ***Dewulf et al.***

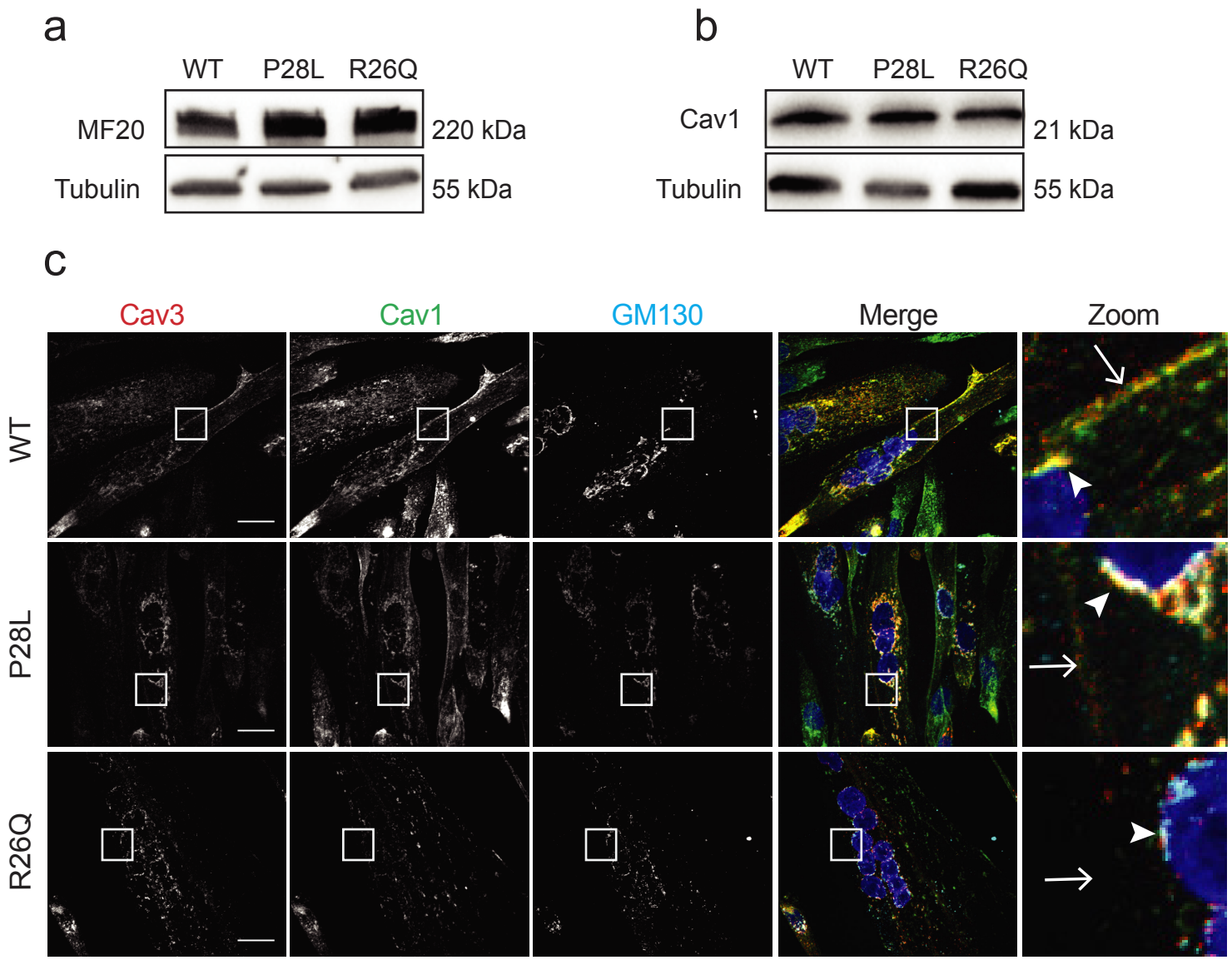

Supplementary figure 2. *Dewulf et al.*

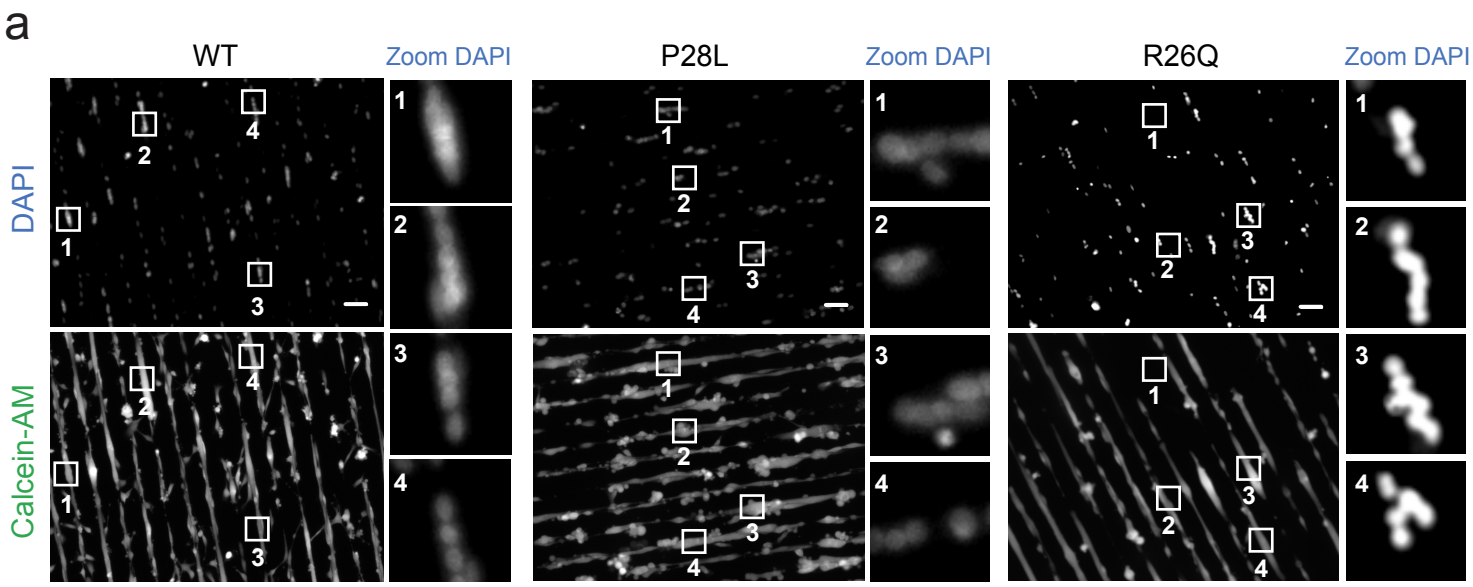

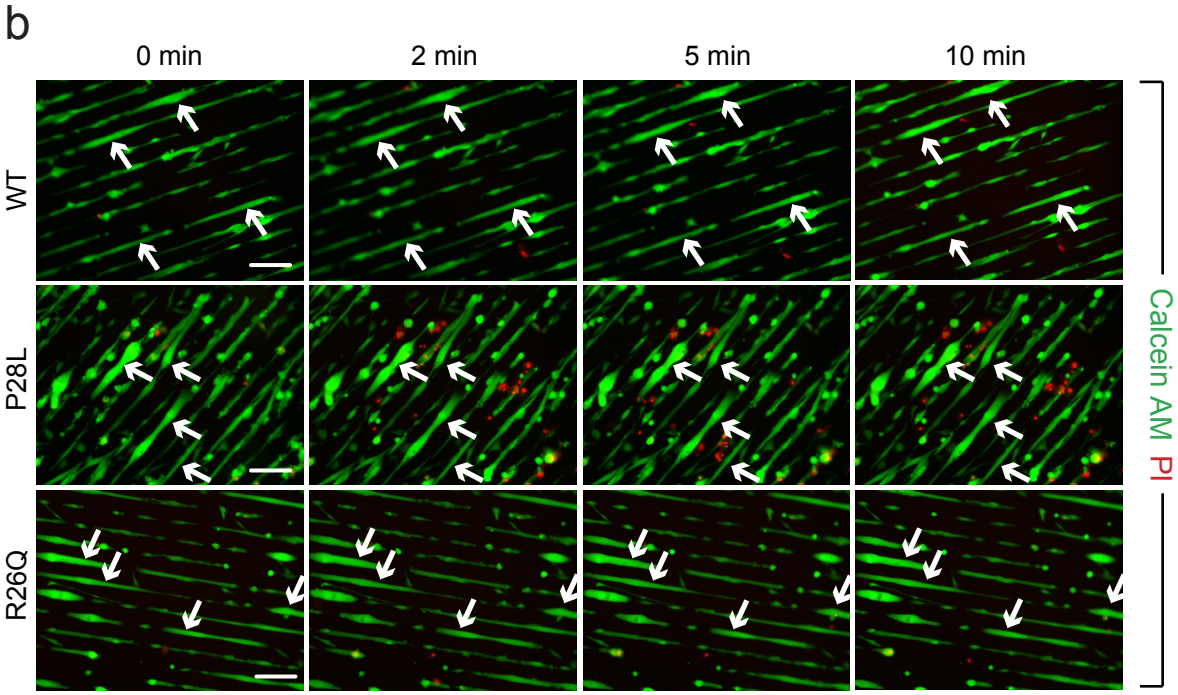

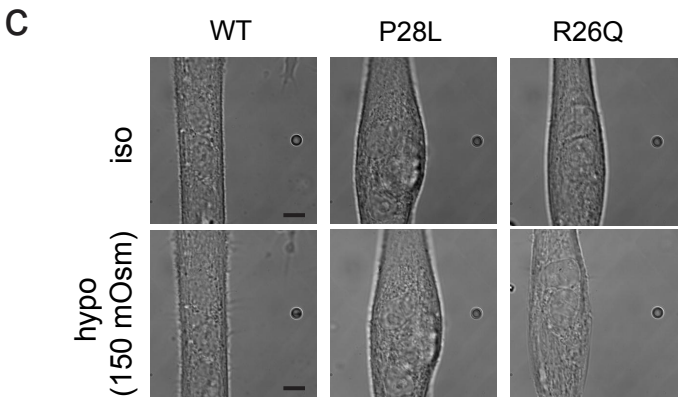

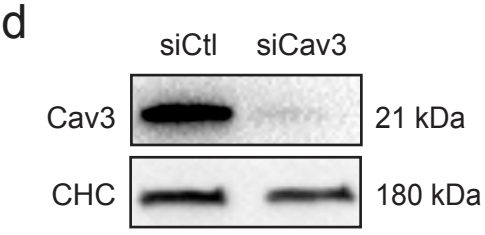

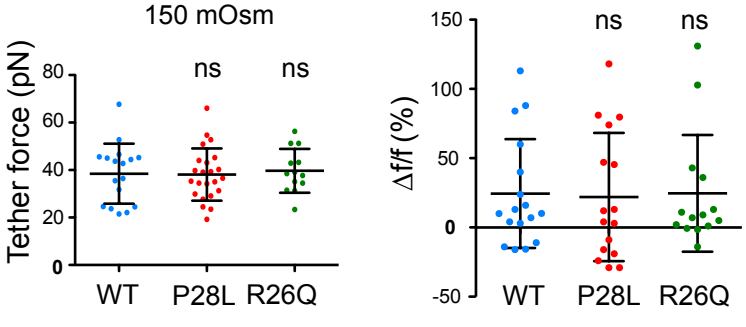

Supplementary figure 3. ***Dewulf et al.***

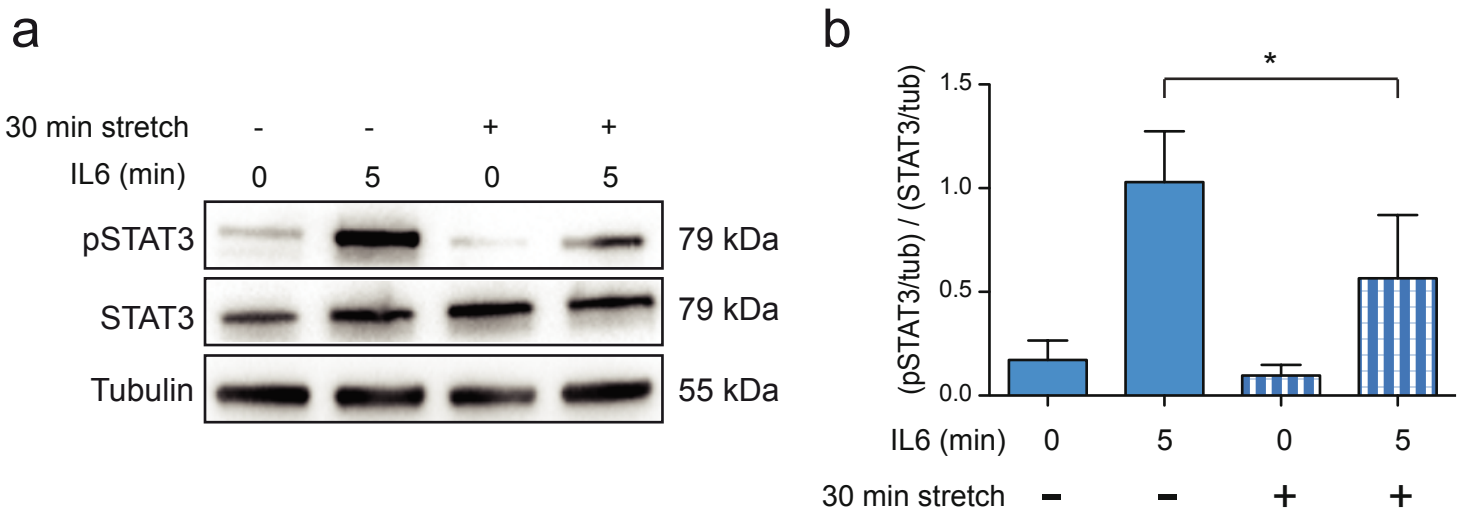

Supplementary figure 4. *Dewulf et al.*

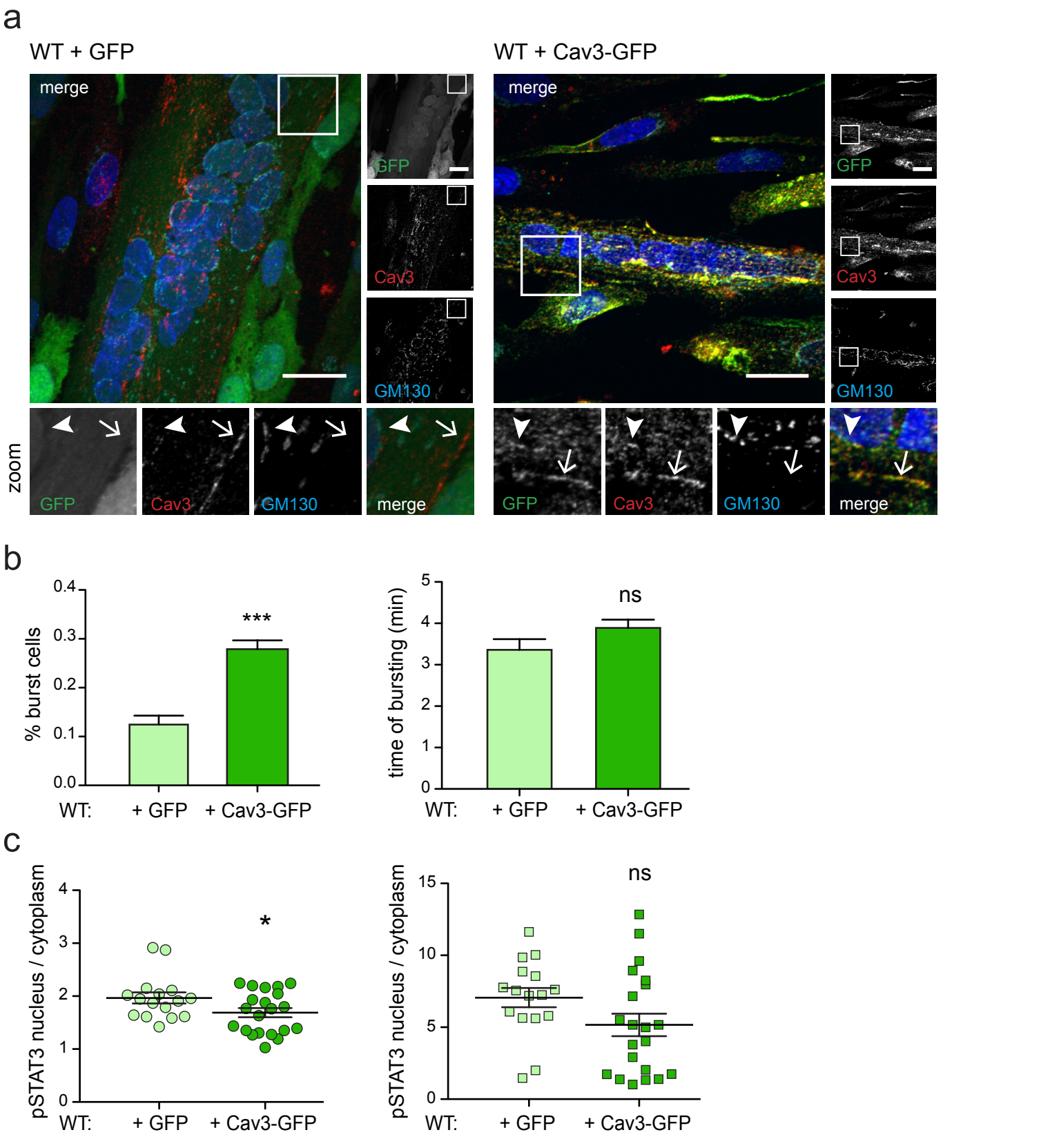

université PARIS-SACLAY
ÉCOLE DOCTORALE
Signalisation et réseaux intégratifs en biologie (BIOSIGNE)

Titre : Mécanosignalisation par les cavéoles : un rôle nouveau dans le contrôle de la signalisation JAK-STAT

Mots clés : mécanosignalisation ; mécanotransduction ; cavéoles ; JAK-STAT

Résumé : Les cavéoles sont des invaginations en forme de coupelle à la membrane plasmique. Ces organelles multifonctionnelles jouent entre autres, un rôle clé dans la mécano-protection et la signalisation cellulaire. En effet, les cavéoles ont la faculté de s'aplanir en réponse à l'augmentation de la tension membranaire, afin de protéger la cellule des contraintes mécaniques. Les cavéoles jouant un rôle clé dans la signalisation cellulaire, nous avions émis l'hypothèse que le cycle mécano-dépendent de désassemblage/réassemblage des cavéoles constitue un interrupteur mécanique de certaines voies de signalisation. Ce projet consiste à élucider le mécanisme moléculaire responsable du contrôle de la voie de signalisation JAK-STAT par la mécanique des cavéoles. Dans ces travaux, nous avons pu démontré que la cavéoline-1 (Cav1), un constitutant essentiel des cavéoles est libérée et devient hautement mobile au niveau de la membrane plasmique. Considérant les propriétés de signalisation de Cav1, Nous avons testé l'effet du désassemblage des cavéoles sur la signalisation cellulaire. Un criblage à haut débit, nous a permis identifié la voie de signalisation JAK- STAT stimulée par l'IFN-α comme voie modèle pour cette étude. En effet, la transduction du signal JAK-STAT induit par l'IFN-α est modulée par la mécanique des cavéoles. Afin de disséquer le mécanisme moléculaire responsable du contrôle de la signalisation JAK-STAT par la mécanique des cavéoles, nous avons déterminé le rôle de Cav1 dans ce contrôle. Nous avons observé que Cav1 est un régulateur négatif de la phosphorylation de STAT3 dépendante de la kinase JAK1. De plus, nous avons démontré que Cav1 interagit avec JAK1 en fonction de la tension membranaire. Nous avons également démontré que cette interaction Cav1-JAK1 fait intervenir le « scaffolding domain » de Cav1 (CSD), et que celui-ci est responsable de l'abolition de l'activité kinase de JAK1. Par conséquent, l'interaction de Cav1 avec JAK1 empêche l'activation de STAT3 par la kinase JAK1. Ces résultats démontrent que les cavéoles sont des organelles de mécano-signalisation, qui, lors d'un stress mécanique, libèrent de la Cav1 non cavéolaire capable d'inactiver la kinase JAK1, empêchant ainsi, la transduction du signal JAK-STAT.

Title : Mechanosignaling through cavolae : A new role for the control of JAK-STAT signaling

Keywords : Mechaosignaling ; Mechanotransduction ; Caveolae ; JAK-STAT

Abstract : Caveolae are small cup-shaped plasma membrane invaginations. These multifunctional organelles play a key role in cell mechanoprotection and cell signaling. Indeed our laboratory reported that caveolae have the ability to flatten out upon membrane tension increase, protecting cells from mechanical strains. Since caveolae play a key role in cell signaling we hypothesized that the mechano-dependent cycle of caveolae disassembly/reassembly may constitute a mechanical switch for signaling pathways. In this project, we elucidated the molecular mechanism underlying the control of JAK-STAT signaling by caveolae mechanics. We showed that caveolin-1 (Cav1), an essential caveolar component is released and become highly mobile at the plasma membrane under mechanical stress. Considering that caveolae are important signaling hubs at the plasma membrane, we addressed the effects of the mechanical release of Cav1 on cell signaling. Using high throughput screening, we identified the JAK-STAT signaling pathway as a candidate. To further dissect the molecular mechanism underlying the control of JAK-STAT signaling by caveolae mechanics, we addressed the role of Cav1 in the control of JAK-STAT signaling stimulated by IFN-α. We found that Cav1 was a specific negative regulator of the JAK1 dependent STAT3 phosphorylation. Furthermore, the level of Cav1 interaction with JAK1 depended on mechanical stress. We could show that Cav1-JAK1 interaction was mediated by the caveolin scaffolding domain (CSD), abolishing JAK1 kinase activity, hence, interfering with STAT3 activation upon IFN-α stimulation. Altogether our results show that caveolae are mechanosignaling organelles that disassemble under mechanical stress, releasing non-caveolar Cav1, which binds to the JAK1 kinase and inhibits its catalytic activity, preventing thereby JAK-STAT signal transduction.

Université Paris-Saclay
Espace Technologique / Immeuble Discovery
Route de l'Orme aux Merisiers RD 128 / 91190 Saint-Aubin, France